AD-A108 394 HARRIS CORP MELBOURNE FL GOVERNMENT COMMUNICATION SY--ETC F/G 17/2
FIBER OPTIC DATA BUS FOR THE AN/GYQ-21(V),(U)
JUN 81 R E DRAGOO, D B KIMSEY F30602-79-C-0218
UNCLASSIFIED RADC-TR-81-153 NL

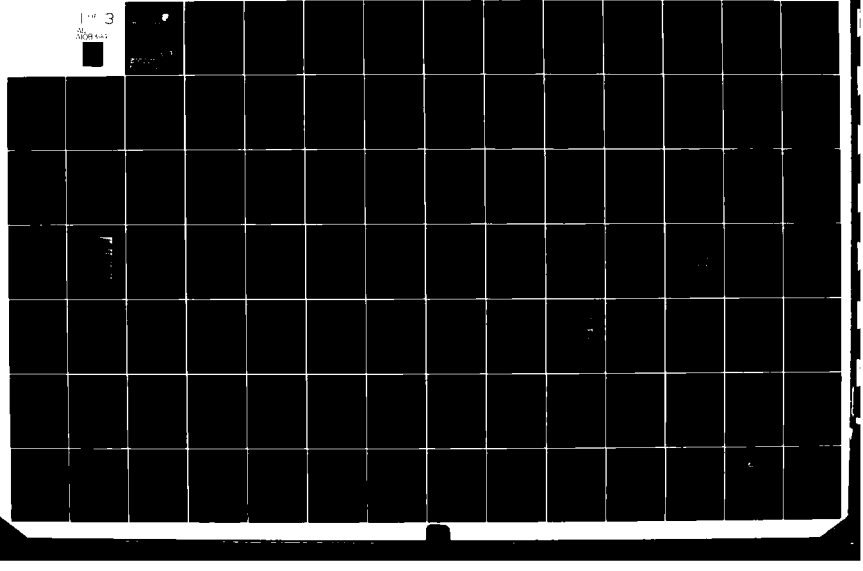

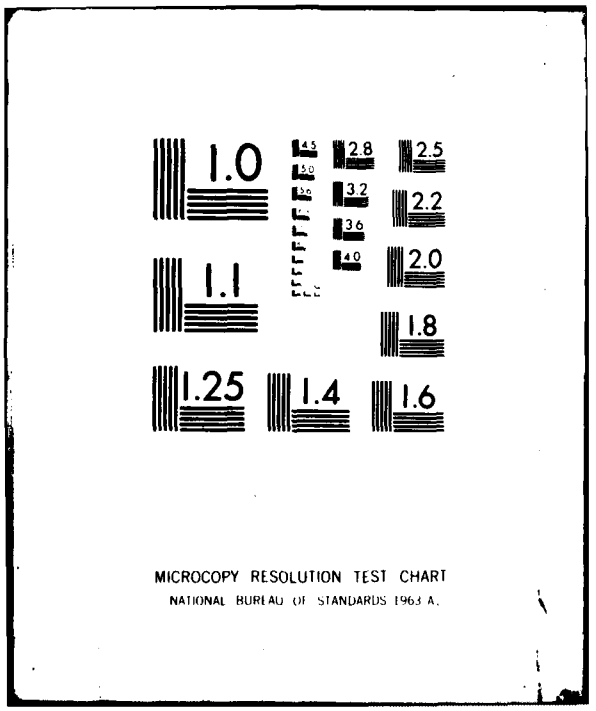
1.0
1.1
1.25
1.4
1.6
1.8
2.0
2.2
2.5
2.8
3.2
3.6
4.0
MICROCOPY RESOLUTION TEST CHART
NATIONAL BUREAU OF STANDARDS 1963 A.

LEVEL II

RADC-TR-81-153
Final Technical Report
June 1981

AD A108394

FIBER OPTIC DATA BUS FOR THE AN/GYQ-21(V)

Harris Corporation

R. E. Dragoo
D. B. Kinsey

ROME AIR DEVELOPMENT CENTER
Air Force Systems Command
Griffiss Air Force Base, New York 13441

This report has been released to the [illegible] Office of [illegible] and is releasable to the National Technical Information Service (NTIS). At NTIS it will be available to the general public, including foreign nations.

RADC-TR-65-133 has been reviewed and is approved for publication.

APPROVED: Paul Sirbak

PAUL SIRBAK
Project Engineer

APPROVED: Bruno Beek

BRUNO BEEK, Acting Technical Director
Communications and Control Division

FOR THE COMMANDER: John P. Huss

JOHN P. HUSS
Acting Chief, Plans Office

[redacted]

UNCLASSIFIED

SECURITY CLASSIFICATION OF THIS PAGE (When Data Entered)

REPORT DOCUMENTATION PAGE	READ INSTRUCTIONS BEFORE COMPLETING FORM
1. REPORT NUMBER: RADC-TR-81-153	2. GOVT ACCESSION NO.: AD A108 374
	3. RECIPIENT'S CATALOG NUMBER:
4. TITLE (and Subtitle): FIBER OPTIC DATA BUS FOR THE AN/GYQ-21(V)	5. TYPE OF REPORT & PERIOD COVERED: Final Technical Report 23 July 79 - 23 Oct 80
	6. PERFORMING ORG. REPORT NUMBER: N/A
7. AUTHOR(s): R. E. Dragoo D. B. Kimsey	8. CONTRACT OR GRANT NUMBER(s): F30602-79-C-0218
9. PERFORMING ORGANIZATION NAME AND ADDRESS: Harris Corporation Government Communications System Division Melbourne FL 32901	10. PROGRAM ELEMENT, PROJECT, TASK AREA & WORK UNIT NUMBERS: 62702F 45192126
11. CONTROLLING OFFICE NAME AND ADDRESS: Rome Air Development Center (DCCT) Griffiss AFB NY 13441	12. REPORT DATE: June 1981
	13. NUMBER OF PAGES: 261
14. MONITORING AGENCY NAME & ADDRESS(if different from Controlling Office): Same	15. SECURITY CLASS. (of this report): UNCLASSIFIED
	15a. DECLASSIFICATION/DOWNGRADING SCHEDULE: N/A

16. DISTRIBUTION STATEMENT (of this Report)
Approved for public release; distribution unlimited.

17. DISTRIBUTION STATEMENT (of the abstract entered in Block 20, if different from Report)
Same

18. SUPPLEMENTARY NOTES
RADC Project Engineer: Paul Sierak (RADC/DCCT)

19. KEY WORDS (Continue on reverse side if necessary and identify by block number)
Fiber Optics
Data Bus Communication
Local Area Networks
Data Transmission

20. ABSTRACT (Continue on reverse side if necessary and identify by block number)
This report describes the application of fiber optic bus technology to the AN/GYQ-21(V) system with the goal of providing for increased separation distances between peripherals and increased long distance data transfer rates. The ring network and the transmissive star network are described as implementable fiber optic busses which can provide for the following enhancements to the 21(V) system: increased separation distances up to 1 kilometer between peripherals and increased long distance data transfer rates up to 60 Mbps.

DD FORM 1 JAN 73 1473 EDITION OF 1 NOV 65 IS OBSOLETE

UNCLASSIFIED

SECURITY CLASSIFICATION OF THIS PAGE (When Data Entered)

TABLE OF CONTENTS

TABLE OF CONTENTS (Continued)

TABLE OF CONTENTS (Continued)

LIST OF ILLUSTRATIONS

LIST OF ILLUSTRATIONS (Continued)

LIST OF TABLES

1.0 INTRODUCTION

This study report addresses the design considerations of a multi-terminal fiber-optic data bus to support a variety of AN/GYQ-21(V) computer system configurations. The objective of the study is to recommend an optimal network configuration and establish a performance baseline for the recommended bus network. The study also addresses achievable fiber-optic receiver performance, optical components, optical modulation formats, and a reliability assessment.

The requirements established as design criteria for the bus were a maximum of 128 terminals, a worst case terminal-to-terminal separation of one kilometer (km), a maximum bus data rate of 60 Mb/s, with an average user input data rate of 1 Mb/s. A computer equipment temperature environment is anticipated, due to the type of equipment being supported.

Due to the diversity of configurations available with the AN/GYQ-21(V), a "standard" configuration is not available. The configuration determined for purposes of analyses within this report is a cluster of terminals, each cluster having a maximum of 31 terminals and one "gateway" terminal allowing access to other clusters.

The approach used in the study is to establish the receiver performance achievable. Given this receiver performance, a source coupled power is then ascertained to allow determination of the available loss budget. This loss budget is then allocated among the various loss contributors, dependent on the network configuration.

With the link fundamentals established, the next discussion centers on various protocol strategies that may be implemented with each network type. A review of optical modulation formats and their impact on optical receivers then is addressed, followed by a discussion of timing and synchronization.

With the control and protocol strategies of the various networks defined, a review of the feasibility of the architectures selected for further analysis is performed to ascertain the actual loss budgets, available link margin, and dynamic range issues. These same architectures are also reviewed from a reliability, availability, and maintainability aspect. The same architectures are also reviewed from a latency and efficiency aspect to establish a rank-ordering of the feasible architectures.

To complete the analysis of the viable architectures, a costing estimate was made using the RCA "PRICE" program to establish any cost advantage or disadvantage of any of the architectures. The PRICE program results are included for two architectures. The conclusions of the study and a summary of recommendations follows the PRICE program. A design summary concludes the report.

2.0 SYSTEM REQUIREMENTS AND EXECUTIVE SUMMARY

The AN/GYQ-21(V) study effort is targeted on supporting a variety of network configurations of the current AN/GYQ-21(V) computer network. The current system has limited geographic dispersion capabilities, with extended system lengths being achieved using 50 kb/s line rates. The use of a fiber-optic data bus to interconnect the peripherals allows extended distances (up to 1 km) and high data throughput rates.

2.1 System Requirements

The baseline network configuration assumed for purposes of the study effort was a maximum terminal-to-terminal separation of one kilometer and a maximum burst data rate of 60 Mb/s. An average bus efficiency of 50 percent is assumed, allowing a throughput rate of 30 Mb/s. Bus efficiencies of greater than 90 percent are achieved with selected protocols and the assumption of 50 percent is a conservative (low risk) design goal.

An uncorrected bit error rate on the bus of 1×10^{-9}, or better, was assumed for design purposes, allowing an undetected bit error rate of $< 1 \times 10^{-12}$ for simple error detection codes. More sophisticated error detecting codes can easily achieve undetected bit error rates of $< 1 \times 10^{-15}$, which is deemed suitable for computer requirements. Link margins are allowed in all cases to assure performance at raw bit error rates at $< 1 \times 10^{-14}$ under normal operating conditions.

The network was assumed to consist of a maximum of 128 terminals for discussion purposes. This 128 terminal maximum is not a "hard and fast" maximum, but only used to determine a baseline. The terminals are grouped in clusters of no more than 32, with clusters interconnected by "gateway" repeaters to achieve modular expansion capability.

The number of connectors per link is assumed to be a minimum of two, with four being required to interconnect terminals within two buildings (shelters, trucks, equipment clusters, etc.). Additional network constraints may require additional connectors. A temperature environment of that comparable to computer equipment was presumed, or an operating environment of 0^{o} C to 50^{o} C ambient temperature.

Storage temperature is not addressed, although not expected to impact the network design or component selection. Similarly, altitude and humidity are not anticipated to impact network design or performance. Shock and vibration are not treated, but should be reviewed carefully in any implementation program.

2.2 Executive Overview

The study report is divided into several major sections to partition the study into several parts. Section 3.0 addresses the fiber-optic components available and the receiver performance achievable with two specific designs. The development of the receiver noise analysis is thorough with the receiver performance determined in a general form based on component parameters. Available components are assumed with performance parameters based on those actually achieved to date. A receiver sensitivity is then determined and the results plotted in terms of noise bandwidth.

The receiver performance establishes the minimum optical power necessary as a function of noise bandwidth. The projected power for the 60 Mb/s data rate is -51.6 dBm (6.9 nanowatts, or nW, of optical power) for a bipolar input preamplifier using an avalanche photodiode gain of 20. Improvements on this sensitivity can be achieved by employing a Junction Field Effect Transistor (JFET) input (approximately 1 dB of improvement), or by raising the avalanche gain to 100 (approximately 3 dB of improvement). This minimum gain bipolar input is treated as a nominal worst case and is assumed as a baseline.

The receiver sensitivity sets the minimum power required. Given this "number", two courses are then available to the network designer: one may determine the source power available and thus the link loss budget, then allocating this loss budget among the various loss contributors; or one may total the loss contributors to determine the required source power. This second approach allows a comparison of various networks and by comparison with available sources determines whether the link may be "closed" (or is feasible) and is used in this report.

The logical next step is then to determine what the various optical loss contributors are and what source coupled powers are currently achievable. Source power is first determined, then the various loss contributors are discussed, including fiber losses, coupler and connector losses.

The ground work having been established for the optical and electro-optical components, the next discussion shifts to network configurations (or architectures) available to support the AN/GYQ-21(V) application. A review of ring networks, "T" networks, and star networks is addressed in terms of throughput, protocol, control schemes, and access methods.

Each of the network architectures are discussed in terms of the control schemes and protocol methodologies. Based on the analyses and discussion of network architectures tentative selection of the interlaced ring and passive star is made. A protocol selection is also made for each network type. These two approaches are the best candidates for further evaluation. These two candidates are further analyzed in terms of link data rates and network throughput. A final discussion of this section addresses various modulation schemes available for fiber-optic data buses.

The next section addresses the architecture feasibility of the two candidate approaches. Both architectures are analyzed from a loss budget point of view to determine network feasibility. The results of this analysis are that the interlaced ring and the star networks are both feasible with a slight complexity advantage accruing to the star network at the expense of slightly higher receiver design risk. Following the discussion of the link budgets is a discussion of component and network reliability. The star network enjoys a slight advantage in terms of network availability, but it is not significant. This section concludes with a review of network latency and efficiency. The ring network enjoys an advantage in terms of network latency.

With the conclusions of the technical merits of each of the network architectures in hand, the discussion turns to cost impacts. The various assemblies in each of the candidate architectures were assessed using the RCA PRICE program to project costs of the items in a production environment. The conclusions of this program were that the star network offered a slight cost advantage, but the advantage was not substantial.

The next discussion of the report distills each of the report sections and analyzes each of the networks against a set of criteria to lead to a preferred approach. The conclusion of this section is that the interlaced ring offers the least risk and would be selected for near term (less than approximately one year to delivery) equipment fabrication, while for longer term development the star network would be selected based on anticipated improvements and wider availability of star couplers.

The final section presents a design summary for the ring network in terms of performance criteria. A summary of each of the major elements of the BIU is presented and a brief discussion of a follow-on program structure presented.

3.0 FIBER-OPTIC COMPONENT ASSESSMENT

The analysis of the proposed fiber-optic data bus networks to support the AN/GYQ-21(V) interconnect requirements is divided into a number of discussion areas. To establish a baseline performance for all network configurations, the component limitations and the receiver performance attainable are first reviewed. The rationale for discussing receiver performance is to establish the minimum signal requirements (sensitivity). With this minimum sensitivity and the "source coupled power" the optical link loss budget may be formulated.

The receiver performance and the source coupled power are thus the determinants of the amount of optical loss between the transmitter (optical source) and the receiver (optical detector and associated preamplifier circuitry). The optical losses between the transmitter and the receiver are contributed by fiber, connectors, and any couplers in the link. Coupling losses between the source and the fiber and between the fiber and the detector are also included in the optical loss budget.

The receiver performance analysis is broken down into two sections, one section discussing field effect transistor (FET) input preamplifiers and the second section discussing bipolar junction transistor (BJT) input transistors. An overview discussion of avalanche photodiode (APD) detectors and PIN diode detectors is also reviewed as part of the receiver performance discussion. Source types, both light emitting diode (LED) and injection laser diode (ILD) sources, are discussed from a system viewpoint. Connector and coupler losses are discussed from a current achievability viewpoint. Similarly, fiber losses are discussed from both a requirements and availability viewpoint.

3.1 Receiver Performance

As introduced previously, the receiver performance determines the minimum optical power required to achieve a given system performance, usually stated as a bit error rate (BER) for digital systems. The receiver consists of some form of optical-to-electrical transducer, or detector, followed by amplification, timing regeneration, and data formatting. Only semiconductor detectors suitable for high rate transmission over single multimode optical fibers will be addressed. Therefore optical detectors such as photomultiplier tubes, p-n diodes, phototransistors and others not matched in responsivity or modulation rate can be eliminated. Devices which will be discussed as detectors include PIN and avalanche photodiodes.

A receiver in an optical cable system can be modelled as shown in Figure 3.1. An optical detector (photodiode) converts the received optical signal (pulses) to a signal photocurrent, i.e., which is applied to a preamplifier. The output of the preamplifier is input to a comparator circuit which compares the signal to a threshold level. If the signal exceeds the threshold the output is a pulse and if the signal is below threshold no pulse is output. In this manner a decision is made as to the presence of a data ONE or data ZERO in each time slot. These bit decisions are referred to as the "data estimate".

The receiver (preamplifier) design is impacted by the type of detector (PIN or avalanche) and the characteristics of the detector, such as the leakage currents, responsivity, junction capacitance and gain (if an avalanche photodiode is used). To provide a basis for the receiver analysis a review of photodetector parameters is appropriate. The next section discusses optical detectors in terms of what is currently available and what may be available in the near future. With an understanding of available detectors in hand, the receiver performance can then be addressed.

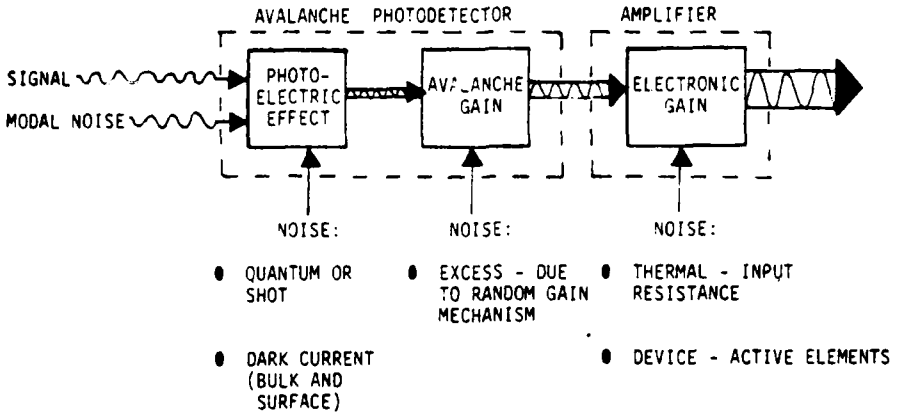

Figure 3.1. Block Diagram Showing Various Noise Sources at the Front End of an Optical Receiver

3.1.1 Optical Detectors

There are two semiconductor detector types, available to provide the optical-to-electrical energy conversion: the PIN detector, consisting of a doped "p" layer, an intrinsic layer, and a doped "n" layer of a base material (generally silicon); and the avalanche photodiode (APD), structured similarly to the PIN, but employing a high reverse bias to create multiple secondary electrons per incident photon.[1] The selection of a type detector impacts receiver design since it determines the signal input level into the receiver.

---

1 M. K. Barnoski, "Fundamentals of Optical Fiber Communications," Academic Press, 1976.

The generally accepted figure of merit for optical detectors is responsivity, given in amperes per incident watt of optical power (A/W). To convert this current source input to a signal voltage for succeeding stages, the preamplifier acts as a current-to-voltage converter, or transimpedance amplifier. The receiver preamplifier must be a low noise design to achieve maximum sensitivity. This low noise criteria is set by the signal currents generated by the optical detector.

The following are the important performance requirements for photodiodes:

- High response or sensitivity at the operating wavelengths. At present, the wavelengths of interest lie in the range 0.8-0.9 μm, where GaAlAs lasers and LED's have their emission lines. Future system operating wavelengths may shift to the 1.1-1.7 μm spectral region, where optical fibers have lower intrinsic optical loss and minimum material dispersion, as well as greater immunity to nuclear radiation effects.

- Sufficient bandwidth or speed of response to accommodate the information rate. Present systems can support signal rates to a few hundred megahertz, but future single-mode fiber systems may operate at multigigabit rates.

- Minimum additional noise introduced by the detector. Dark currents, leakage currents, and shunt conductances must be low and, if the detector is to provide internal gain, the gain mechanism should be as noise-free as possible.

- Low susceptibility of performance characteristics to change in ambient conditions. Sensitivity, noise, and internal gain of practical photodiodes all vary with ambient temperature. Compensation of temperature effects is essential in many applications.

Compatibility requirements involve considerations of the physical size of the detector, the coupling to the fiber and to the ensuing electronics, and the necessary power supply. The detector must be small so that it is easily packaged with other electronics and easily coupled to the fiber. It should not require excessive bias voltages or currents. Figure 3.1.1 provides a basic comparison of typical photodiode characteristics.[2]

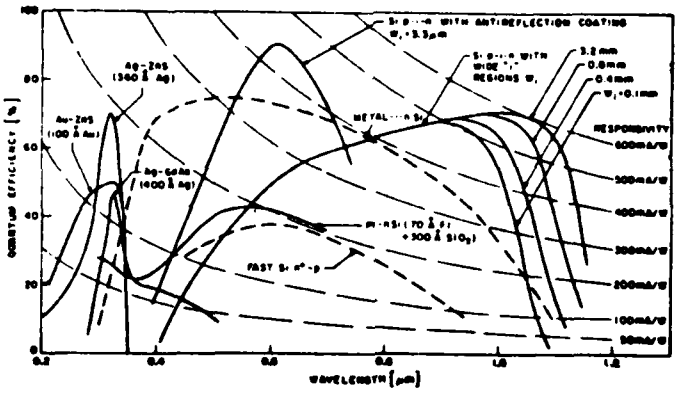

Figure 3.1.1. PIN Photodiode Responsivity Versus Wavelength

With these considerations in hand, a review of the PIN photodiodes and avalanche photodiodes is now addressed. The selection of a particular detector type is dependent on the receiver preamplifier design and the optical signal parameters; however the optimum photodetector from each group can be tentatively identified with some assumptions to be validated in the receiver discussion.

[2]P.W. Casper, "Optoelectronics and Interface Electronics", SPIE, Vol. 63, Guided Optical Communications (1975).

3.1.1.1 PIN Photodiodes

A typical reverse biased PIN junction features a depletion region containing a relatively high field and a diffusion region. The width of the depletion region (for fully depleted devices) is determined by doping and relates to the overall speed of the device. Basically when photons are absorbed, electrons from the valence band are excited into the conduction band and an electron-hole pair created. These photocarriers then travel at drift velocity (if under the influence of the depletion field) or diffusion velocity (if in the diffusion region). However, diffusion is much slower than drift and the device can be slow, suffering from a "long tail" response, for diodes having a wide diffusion region.

The depletion region is lengthened by decreased doping in the n-layer, thus minimizing diffusion velocity of carriers and increasing device response times. The practical device construction consists of a p-doped layer, very lightly doped n-layer and (for ohmic contact) a highly doped n-layer. This lightly doped n-region is the familiar intrinsic, or "I", layer of the PIN structure. Note that the addition of the highly n-doped layer does not defeat the purpose of the intrinsic layer because the high doping has very short carrier lifetimes, that is, the holes combine with electrons before reaching the depletion region and therefore do not effect a slow tail.

From the above discussion, it is clear that the speed of response of a photodiode combined with its output circuit is dependent on the following three parameters: (1) the RC time constant of the output circuit (including the photodiode capacitance), (2) the diffusion time of the photocarriers generated outside the depletion region, and (3) the transit time of the photocarriers in the depletion region.

In the PIN diode, there is often a trade-off between absorption efficiency (fraction of light absorbed) and speed of response. For high absorption efficiency, we desire a long absorption region. For fast speed, we require short drift times and thus, a short absorption region with high carrier velocities.

3.1.1.2 Avalanche Photodiodes (APD)

Consider an ideal photodiode in which every incident photon produces a photoelectron and at the wavelength of 1 μm the optical conversion efficiency, or responsivity, is about 0.6 to 0.8 ampere per incident optical watt. The most sensitive receivers operate at optical input levels of about a nanowatt. Thus, the photoelectron current is less than a nanoampere. Such small currents are very difficult to process electronically without adding excessive amplifier noise. Thus, it is desirable to use some mechanism to increase the photodiode output current before amplification by the preamplifier. Such a mechanism is avalanche gain. The next several paragraphs shall discuss the gain process within APDs and the systems applications where these devices are most beneficial.

When the electric field in the depletion region of a reverse-biased diode is sufficiently high (above 10^5 V/cm for Si), an electron or a hole can collide with a bound (valence) electron with sufficient energy to cause ionization, thereby creating an extra electron-hole pair. The additional carriers in turn can gain enough energy from the field to cause further impact ionization, until an avalanche of carriers has been produced. On the average, the total number of carrier pairs created is finite and is proportional to the number of injected (primary) carriers when the diode is biased below a certain (breakdown) voltage. Very high carrier multiplication or current gain is possible through this avalanche process even at microwave frequencies. The ionization rate, which is the average number of electron-hole pairs created by a carrier (electron or hole) per unit distance traveled, is a strong function of the electric field.

The result is an effective amplification of the photodiode output current for a given input optical power. This amplification is very useful, but the physical realization has some shortcomings when compared to what might be thought of an ideal electron multiplying mechanism. Such a mechanism would replace each hole-electron pair created by a photon with

exactly G secondary hole-electron pairs, i.e., the pair multiplication would be deterministic. In an actual avalanche photodiode, the multiplication is random, since the point of photon absorption and creation of the primary hole-electron pair is at some random coordinate in the high field region. Thus, each primary pair gets replaced by a random number of secondary pairs whose average number might be G (same as the ideal multiplier) but whose variance is large. This randomness, or "unpredictability" of the amplified current is a degradation which limits the sensitivity of an optical receiver below what it could be for an ideal multiplication device. This random process is treated as an "excess noise factor" and is modelled as an exponent. Proper device manufacturing can minimize this excess noise factor, with current technology supporting excess noise exponents of ~ 0.3.

The structure of avalanche diode may include a "guard ring." The purpose of this element is to prevent low breakdown voltages and excessive leakage at the junction edges, by lowering the fields in those regions. Most avalanche detectors available today are made of silicon. The best of these devices provide good multiplication statistics (for optical fiber receiver applications) and gains of a few hundred (enough for most fiber communication applications). In addition, with proper antireflection coatings, these detectors provide quantum efficiencies approaching the theoretical limit 100 percent.

In addition to good multiplication statistics, or low excess noise, speed of response is important in avalanche photodiodes. Like PIN diodes, initial (primary) hole electron pairs should be generated mostly in a region with sufficiently high drift field to bring the carriers to the high field (multiplication) region as quickly as possible. Carriers which are generated in very low field regions result in previously mentioned diffusion tails in the diode response. In practical diodes available today, the devices exhibit a trade-off between gain and bandwidth, or response speed. A gain-bandwidth product can be approximately ascribed to these devices which is on the order of 100 GHz.

Finally, before leaving the discussion on APD's it is important to mention a typical application problem with these devices. The constant-gain bias for avalanche devices is a very sensitive function of temperature (typically, 0.18 $V/^{o}$ C for the guard ring device and 1.8 $V/^{o}$ C for the "reach-through" device). Thus, for a dynamic thermal environment, temperature compensation must be included in bias supply designs.

These past two sections have dealt primarily with the basic properties associated with optical detection as applied to PIN and avalanche photodiodes. At this time, a summary of the implementation characteristics and state-of-the-art performance for each device is given:

- PIN detectors are well suited for many analog applications involving medium to high optical signal-to-noise (SNR) ratios. Although APD's are typically considered to provide an improvement in sensitivity (as much as 15 to 20 dB) over the PIN device, this is only true where the APD is operating well above the signal quantum noise limit (such as digital applications where SNR's are low but signal current shot noise is not the limiting noise factor). Thus for some applications the PIN may actually exceed the performance available from the APD.

- APD's support faster responses with bandwidths of approximately 800 MHz; however, PIN devices offer a very respectable 200-300 MHz and will not be excluded from consideration by bandwidth alone.

- Bias requirements are an important factor in device selection. Many manufacturers offer PIN photodetectors with low leakage currents (and therefore low noise) fully depleted at less than 20 Vdc bias. This is compared with APD bias voltages of 150 to 250 Vdc which also require temperature stabilization circuitry as previously mentioned.

- Finally, PIN devices can be normally designed with slightly larger active areas and can therefore easily accommodate output coupling to large core, large-NA optical fibers. Some single-fiber APD devices exhibit higher output loss because the surface area has been reduced to minimize leakage ("dark") currents generated through high bias voltages.

3.1.1.3 Detector Selection Criteria

The preceding discussion has outlined the operation of fiber-optic photodiodes as well as providing some insight into factors of selection for particular applications. At this time, additional details are given on desired device parameters for the AN/GYQ-21(V) system and how the environment affects performance in terms of sensitivity, degradation, etc.

Primary performance parameters for the system have been identified as:

- Modulation rate or bandwidth (response time)
- Sensitivity (responsivity and low noise)
- Reliability

Secondary characteristics include:

- Efficient coupling from fibers
- Bias requirements
- Environmental degradation

As previously suggested, the expected modulation rate has been established at ~60 Mb/s and, depending on modulation format, requires a minimum bandwidth of 35 to 70 MHz (system bandwidth ~ 30 MHz). PIN and avalanche photodiodes are typically well within this performance specification. Both devices can operate fully depleted to minimize capacitance effects associated with the receiver detector and impacting the receiver performance.

Photodiodes are available for operation over a finite range of optical wavelengths with maximum responsivity to optical energy determined by the material composition of the device. Figure 3.1.1.3 provides a typical plot of the more popular high speed photodiode responsivities as a function wavelength and material.[3] Note that silicon, the most popular material today, offers device quantum efficiencies of 0.8, which corresponds to a responsivity of 0.4 to 0.5 A/W in the 0.8-0.9 μm region. Silicon APD's are capable of meeting this performance. For longer wavelength operation (1.1 μm and greater), other materials are generally used (Ge, InGaAs) to provide a response characteristic which is optimized for this region.

In addition to high responsivity, a device's dark current will influence the signal sensitivity in terms of generated noise. The level of dark current is a function of material, active area, bias voltage and physical structure (guard rings mentioned earlier). Silicon technology is well established and offers good noise performance. Germanium (wavelengths of 1.1 μm) detectors have a higher dark currents (bulk and leakage) due to the narrower band gap material and less advanced surface passivation techniques. Various III-V semiconductor alloys are also being investigated for long wavelength operation and are attractive since the band gap (and thus responsivity) can be optimized by material composition.

[3] Op. Cit., Number 1

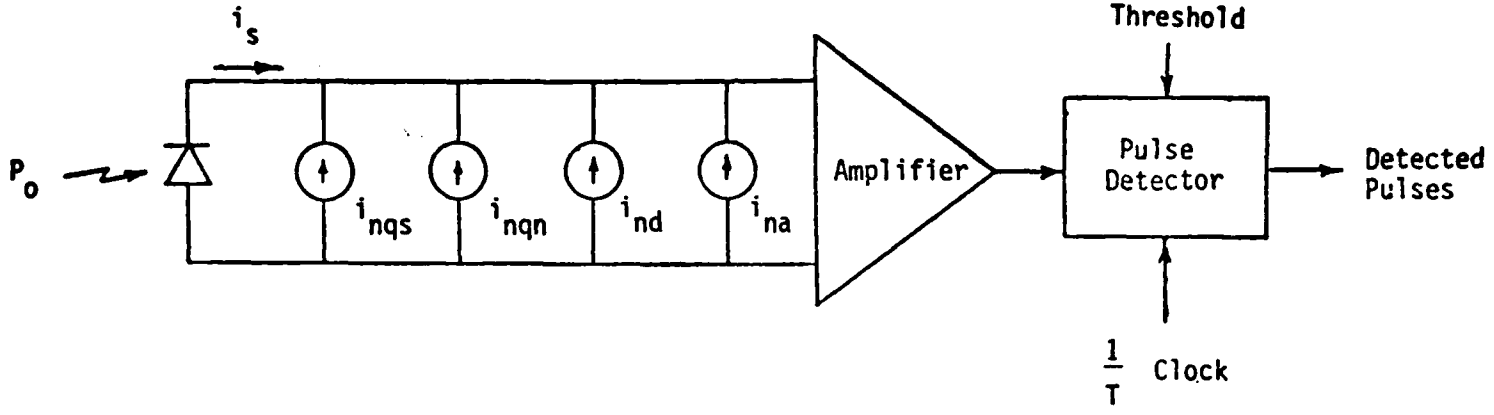

Figure 3.1.1.3. Receiver Model for Noise Analysis

The dark current is also a function of detector area which accounts for lower receiver noise levels in single fiber communications photodiodes. Development of fully depleted PIN diodes at low voltages (≤ 20 Vdc) offer attractive advantages in terms of dark current reduction without sacrificing speed. APD's, as discussed earlier, can achieve increased sensitivity through current multiplication, provided the signal is not signal quantum noise limited.

Since photodiodes are not subjected to high current densities, the lifetimes are very good with projections of $>10^6$ hours for PIN's and $\geq 10^5$ hours for APD's. The reduced lifetime associated with APD detectors is due to the high bias operating conditions. During the next few years, both device lifetimes are expected to exceed 10^6 hours.

The desire to minimize dark current through reduction in active area sometimes conflicts with the goal of full (but not excess) illumination area. For single fibers however, the output coupling loss from fiber to detector is primarily due to Fresnel reflections (~ 0.5 dB) and detector areas easily accommodate the small illumination patterns. This statement is typically true for both PIN and APD devices.

Environmental aspects of photodiode operation such as temperature and hermeticity do influence device selection, but temperature effects (increase in dark current at high temperature) are inherent properties of the material and common to both types of silicon devices. APD's do experience a change in gain due to shifts in avalanche breakdown voltage over temperature; however, proper bias stabilization circuitry can minimize these effects. Dark current is also impacted by temperature, due to the inverse exponential dependence on temperature characteristic of the diode equation. For wide temperature excursions active cooling may be considered to minimize dark current increases; however, for the "computer" environment anticipated, this requirement is avoided. PIN and APD devices use similar packaging styles and many manufacturers offer hermetically sealed devices.

Furthermore, since photodiodes are solid-state devices, problems associated with shock, vibration, and so forth, can be minimized through conventional MIL-STD packaging techniques.

Now that the basic operating factors for selection have been presented, it is appropriate to consider a device (or devices) most viable for the bus application. Tables 3.1.1.3-1 and 3.1.1.3-2 detail the specific characteristics for PIN and avalanche photodiodes, respectively. Receiver modules were also surveyed but are unsuitable except for specific application in nonstressed (temperature) environments, at relatively low data rates (< 25 Mb/s).

For both types of photodiodes, characteristics such as speed, responsivity, packaging, etc. are not sufficiently different between either type of high performance single fiber photodiode. Thus the primary consideration is sensitivity. Recalling that this application involves detection of high speed digital signals, it is felt that the selection of an APD can offer as much as 15 to 20 dB more received sensitivity and is therefore the recommended component. Several APD's are available to meet most of the requirements and are listed as follows:

- EMI GENCOM S30500 APD, low noise, moderate speed, good temperature range, hermetic seal, low responsivity
- RCA 30902E APD, low noise, high speed, moderate temperature range, hermetic seal, high responsivity
- NEC NDL 1202 APD, low noise, moderate speed, good temperature range, hermetic seal

In the event that future LED source powers attainable allow a PIN detector as a viable candidate then two devices are promising; (1) Hewlett Packard PIN photodiode, 5082-4204 and, (2) RCA PIN photodiode 30807E. This determination should be made during any fabrication of feasibility models.

Table 3.1.1.3-1. PIN Photodiode Matrix

MANUFACTURER AND MODEL	DETECTING AREA (mm^2)	BREAK-DOWN VOLTAGE (V)	PDBC (nA)	TEMP RANGE (°C)	RESPONSIVITY @ 830 nm (A/W)	QUANTUM EFF. (%)	V_{Bias} RECOMM. (V)	CAPACI-TANCE (pF)	tr (ns)	Id (nA)	NEP (w/√Hz)	HERMETIC	MIL SPEC	COMMENTS
AEG-TELEFUNKEN														
S168P	.25	32		-25 to 100	.5		5	5	10	1				
S178P		32		-25 to 80	.5		5	5	10	1				
CENTRONICS														
BPX 65	1	50	250	to 125		55		3.5	1	1	3.3E-14	Y	NO	
BPX 66	1	50	250	" "		55		3.5	.5	.15	1.3E-14	Y	NO	
OSD-1-3	1	100		-25 to 75		75		2	10	5	7E-14			
OSD-1-3 HSA	1	80		" "		65		8.5	1.5	5	" "			
EG & G														
FDD 100	5.1	125	200	-53 to 70	.62	93	90	8.5	1	90	2.9E-13	Y	NO	
FND 100	5.1	"	200	" "	.62	"	"	"	1	90	" "	Y		
FUJITSU														
FID08			50	-40 to 60		78	20	2		.3		Y		
HEWLETT-PACKARD														
5082-4207	.79	20	100	-55 to 125	.5		5 to 20	5.5	1	2.5	5.7E-14	Y	NO	Meets temp. requirement of MIL SPEC.
5082-4203	.2	50	100	" "	"		"	1.5	1	2	5.1E-14	Y	NO	Not formally qualified.
5082-4204	.2	20	"	" "	"		"	2	1	0.6	2.8E-14	Y	NO	"
5082-4[illegible]	.2	50	"	" "	"		"	2	1	5	8.1E-14	Y	NO	"
5082-4205	.05	50	50	" "	"		"	.7	1	.15	1.4E-14	Y	NO	"
MATH ASSOCIATES														
ES100	.2	25		-55 to 65	.42		25		5	.1	6E-15		NO	
ES102	.2	25		" "	.42		25		5	.1	2E-14		NO	
MERET														
MD31	.8	40		0 to 70	.65		40		3	20	2E-13	NO	NO	
MD32	4.5	40			.65		40		5	20	2E-13	NO	NO	

Table 3.1.1.3-1. PIN Photodiode Matrix (Continued)

MANUFACTURER AND MODEL	DETECTOR AREA (mm^2)	BREAK-DOWN VOLTAG (V)	PMAX (mW)	TEMP. RANGE (^{o}C)	RESPONSIVITY @ 830 nm (A/W)	QUANTUM EFF (%)	V_{BIAS} RECOMM. (V)	CAPACI-TANCE (pF)	tr (ns)	Id (nA)	N E P ($w/\sqrt{Hz}$)	H E R M E T I C	M I L S P E C	COMMENTS
NEC														
NDL2102	.03	30	100	-65 to 150	.40		10	2.5	1	10		YES	NO	
NDL2208	.5	30	100	-65 to 150	.57		10	5	10	100		YES	NO	Pigtail Available
NORTHERN TELECOM														
NT-D-5-1	.012	100		-40 to 80	.55	85	45	.6	3	1		NO	NO	
NT-D-5-2	.012	100		" "	"	"	"	"	"	"		"	"	Pigtail
RCA														
30900E	5	200		-40 to 80	.6	83	90	5	6	100	5E-13	YES	NO	
30807	.8	100	180	" "	"	"	45	2.5	3	10	1E-13	YES	NO	
30808	5	"		" "	"	"	"	6	5	30	1.5E-13	YES	NO	
30831	.2	"	45	" "	"	"	"	2	3	10	1E-13	YES	NO	
30920E		"		" "	"	"	"	2	3	5	1E-13	YES	NO	Pigtail, 250μm core fiber
SPECTRONICS														
SD-3478-001	2	150	200	-65 to 150	.5		100	4.4	1.1	1		YES	NO	
SD-3478-002	2	180		-65 to 150	.5			4.4	1.1	1		YES	NO	
SD-3322-002	-	30		-20 to 70	.25		14	2	1	1		YES	NO	Small junction volume device

Table 3.1.1.3-2. Avalanche Photodiodes Matrix

MANUFACTURER AND MODEL	DETECTOR AREA (mm^2)	BREAK-DOWN VOLTAGE (V)	TEMP. COEFF OF B.V.	OPERATING TEMP RANGE (°C)	RESPONSIVITY @ 830 nm (A/W)	QUANTUM EFF. (%)	V BIAS RECOMM. (V)	CAPACITANCE (pF)	GAIN-BW PRODUCT (GHz)	I_D (nA)	NOISE EQ POWER W/√Hz	NOISE FIGURE M²	MAX GAIN	HERMETIC	MIL SPEC	PIGTAIL	COMMENTS
AEG-TELEFUNKEN																	
S171P	.03	170	.2%/°C	-65 to 100		58		.85	200	1			1000	NO	NO	NO	
S177P		"	" "	-25 to 80		58		"	"	1			1000			Y	
EMI GENCOM																	
S30500	.2	220	.2V/°C	-70 to 125	18			5.5	.07	30	1E-13	2.4		Y	Y		Opt'l temp.monitor diode
S30502	.06	220	"	"	"			"	"	"	" "						
S30504	.008	90	"	"	24			"	"	2	6E-14	2.4		Y	Y	NO	
S30506	.06	260	"	"	18			"	"	20	1E-13	"		Y	Y	"	
S30508	4.9	530	"	"	-			-	"	1000	-	-		-	-	-	
S30510	.2	550	"	"	30			5	.035	200	5E-14	2.4		Y	Y	"	
S30512	.05	250	"	"	18			4	.07	20	1E-13	"		Y	Y	"	
FUJITSU																	
FPD080		155	.5%/°C	-40 to 60		68	150	1.5	.015	.3		.33		Y			
FPD080A		"	"	"		78	150	"	"	"		"		Y			
FPD081A		"	"	"		50	150	"	"	"		"		Y			
HITACHI																	
APD	.07	140	.5V/°C	-50 to 80		70		1.4	250	1		.32	1000			NO	
MITSUBISHI																	
PD1002	.03	150	.12%/°C	-40 to 80	.45	77	50	1.5	800	.3	1E-14	.25	1000	NO	NO	OPTION	
PD1005	.2	150	"	"	.45	"	50	5.5	300	.3	1E-14	"	"	NO	NO	"	
NEC																	
NDL 1202	.03	200		-65 to 150	.4	80	30	2	.035	1		.35		Y	NO	OPTION	
NDL 1102		130		" "	.43	65	30	2.5	.0035	1		.32		Y	NO	NO	630 nm
RCA																	
C 30817	.5	350		-40 to 70	75	85	Supplied	2	.02	50	1.5E-14		120	Y	NO		
C 30902E	.2	215		" "	77	77	w/Device	1.6	.11	15	3E-15		150	"	"		
C 30916E	1.77	350		" "	50	85	"	5	.007	200	2E-14		80	"	"		
C30904E	.2	"		" "	69	85	"	2	.02	50	1.3E-14		120	"	"		SMA CONNECTOR
C30906E	1.23	"		" "	46	85	"	3.5	.0093	100	2E-14		80	"	"		"
C30908E	.06	215		" "	77	77	"	1.6	.11	15	3.5E-14		150	"	"		"
C30921E	.05	215		" "	77	77	"	1.6	.11	15	" "		150				
NEBET	.8	280		0 to 70	30		250		.01	60				Y	N	N	

3.1.2 Receiver Performance Analysis

With the detector parameters reviewed, the combining of the detector and the preamplifier to determine the baseline receiver performance achievable is addressed. This receiver performance can be predicted from appropriate modelling of the preamplifier. Experimental verification of the receiver performance then validates the prediction.

With the basic parameters of the optical detector being the responsivity, given in amperes per incident watt of optical power (A/W), and the leakage current, the receiver performance necessary to meet the system requirements can be determined. The output of the detector acts as a current source, which must be converted to a signal voltage for succeeding stages. The preamplifier then must perform a current-to-voltage transformation, which can be accomplished with a transimpedance amplifier. The receiver preamplifier must be a low noise design to achieve maximum sensitivity. The three factors contributing to receiver noise, independent of receiver type, are discussed next.

A receiver in an optical cable system can be modelled as shown in Figure 3.1.1.3. A photodiode converts the received optical pulses to a signal photocurrent, i_s, which is applied to the input of a transimpedance amplifier. The amplifier output is operated on by a pulse comparator circuit which compares the signal to a threshold. If the signal exceeds the threshold, the comparator produces an output pulse; if the signal level is below threshold, no pulse is produced at the output of the comparator. In this manner, the pulse detector makes a decision concerning the presence or absence of a pulse during each time slot. Bit decisions are termed the "data estimate."

The signal from the photodetector is corrupted by several noise contributions, modeled here as current sources at the input to the amplifier. These noises are: shot noise in the signal photocurrent, i_{nqs}; shot noise contributed by the photodetector dark current, i_{nd}; shot noise of the nonsignal photocurrent, i_{nqn}; and thermal and shot noise in the amplifier, i_{na}. Photocurrent shot noise is generally referred to as quantum noise.

The signal and noise currents of the model may be expressed in terms of the photodetector and receiver parameters defined below.

P_{os} = optical signal power incident on photodetector during a pulse (W)

P_{on} = nonsignal (background or idle transmitter) optical power incident on photodetector (W)

r = unity gain responsivity of photodetector (A/W)

G = mean avalanche gain of photodetector

α = avalanche gain excess noise exponent

I_s = surface leakage component of photodetector dark current (A)

I_b = bulk leakage component of photodetector dark current (A)

B_n = noise-equivalent bandwidth of receiver (Hz)

The signal photocurrent is given by:

$$i_s = rGP_{os}$$

and the mean-square values of the noise currents are:[4]

$$i^2_{nqs} = 2qrG^{2+\alpha}P_{os}\,B_n, \text{ (signal quantum noise)}$$

$$i^2_{nqn} = 2qrG^{2+\alpha}\,P_{on}B_n, \text{ (nonsignal quantum noise)}$$

$$i^2_{nd} = 2q(I_s + G^{2+\alpha}I_b)B_n, \text{ (dark current noise)}$$

where q is the charge on an electron (1.6×10^{-19} C). Calculation of the amplifier noise contribution is addressed in the following sections. Except for their noise contributions which have already been included in the model, the dc values of the non-signal photocurrent and dark current do not enter into error probability calculations, which determine the receiver noise floor.

The receiver model presented here is generalized to include avalanche photodiode detectors and PIN photdiode detectors. If a PIN detector is used, the model is simplified to the extent that G is unity and a single quantity suffices to specify dark (leakage) current. As unity raised to any power remains unity, the excess noise exponent associated with avalanche gain can remain in the model for PIN detectors, without loss of generality.

[4]Hubbard, "Utilization of optical frequency carriers for low- and moderate-bandwidth channels", BSTJ, vol. 52, No. 5, May-June 1973, pp. 731-765.

Figure 3.1.2-1 illustrates that the detection process can be modelled as being summed at the input of a low-pass filter. The low-pass filter bandlimits the noise, noted as V_n. The bandlimited signal is applied to a comparator for level comparison against a threshold. Clock recovery circuitry is incorporated which extracts a clock estimate used to sample the data to determine when the data sample is to be compared to a threshold. The data decision is made at the output of the comparator and the clock estimate is used to clock this data to the output port timed to the clock estimate. This decision is then the data estimate.

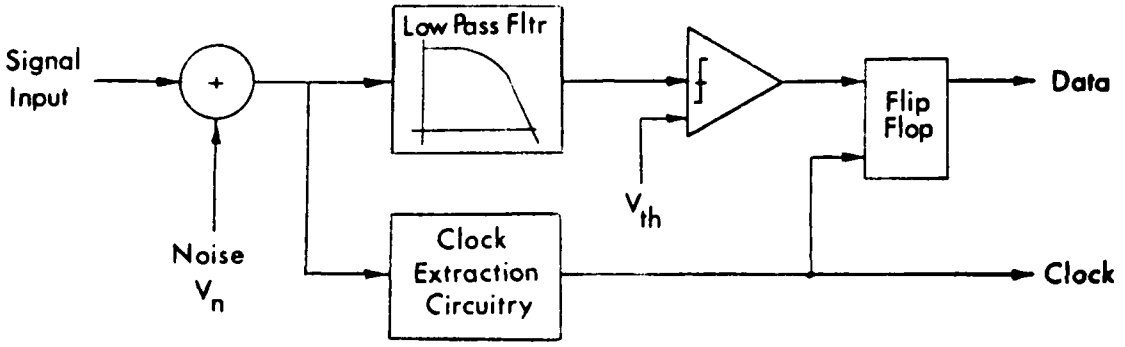

Figure 3.1.2-1. Signal Detection Model

To assess the bit error rate of a digital data stream, the probability of an error in a single bit decision is used. The probability of a bit-error is just the probability of an error in the pulse detection and decision processes. Two types of errors are possible in the detection of two level (binary) systems. The first type of error, termed a false alarm, results if the noise amplitude in the absence of a pulse is sufficient to exceed the threshold level at the decision instant. The second error type, referred to as a miss, occurs if the sum of the signal and noise amplitudes in the presence of a signal pulse is less than the threshold level at the decision instant.

These two types of errors can be combined to determine the probability of an error in the bit decision process. If the detection circuitry senses current voltage levels, the probability of a false alarm, P_f, and the probability of a miss, P_m, can be written as:

$$P_f = \int_{I_{Th}}^{\infty} f_a(i)\, di \tag{1}$$

$$P_m = \int_{-\infty}^{I_{th}} f_p(i)\, di \tag{1a}$$

where

I_{th} is the decision threshold current of the detection circuitry, in amperes (A)

$f_a(i)$ is the probability density function of the input referred noise current in the absence of a signal

and

$f_p(i)$ is the probability density function of the input referred noise current in the presence of a signal data pulse

It should be noted that in general the probability density functions in the presence and absence of a signal are not equal, since signal quantum noise is present with signal while a "no signal" condition possesses no signal quantum noise. If the bit statistics are such that ONE's and ZERO's are equally likely, the total pulse error probability, P_E, equivalent to the bit-error rate, is given as:

$$P_E = BER = \frac{1}{2}(P_f + P_m) \tag{2}$$

If the noise sources of the receiver are modelled as zero mean and Gaussian noise processes, then analytically tractable and reasonably accurate predictions of receiver performance can be made. With this assumption, the following formulae can be postulated for the probability density functions.

$$f_a(i) = \frac{1}{\sqrt{2\pi}\sigma_a} \exp-\left[i^2/2\sigma_a^2\right] \quad (3a)$$

$$f_p(i) = \frac{1}{\sqrt{2\pi}\sigma_p} \exp-\left[(i-I_{TH})^2/2\sigma_p^2\right] \quad (3b)$$

where

$f_a(i)$ is the probability density function of the preamplifier input-referred noise current in the absence of a pulse

$f_p(i)$ is the probability density function of the preamplifier input-referred noise current in the presence of a pulse.

and

σ_a and σ_p are the r.m.s. values of the input referred noise currents in the absence and presence of a pulse, respectively.

These r.m.s. noise current values, or standard deviations, σ_a and σ_p are definable in terms of the noise sources shown in Figure 3.1.1.3, and are:

$$\sigma_a = (i_{nqn}^2 + i_{nd}^2 + i_{na}^2)^{1/2} \quad (4a)$$

$$\sigma_p = (i_{nqs}^2 + i_{nqn}^2 + i_{nd}^2 + i_{na}^2)^{1/2} \quad (4b)$$

Note that the r.m.s. noise current value has a component directly related to the signal; i.e., the signal dependent quantum noise. Substituting these terms for signal absent and signal present into the assumed probability density functions and manipulating terms, we arrive at the following formulae:

$$P_f = \text{erfc} \left\{ \frac{I_{TH}}{\sigma_a} \right\} \quad (5a)$$

and

$$P_m = \text{erfc} \left\{ \frac{i_s - I_{TH}}{\sigma_p} \right\} \quad (5b)$$

where

$$\text{erfc} \left| x \right| = 1 - \text{erf} \left| x \right| \quad (6)$$

with

$$\text{erf} \left| x \right| = \frac{1}{2\pi} \int_x^\infty \exp - \left| y^2/2 \right| dy \quad (7)$$

The term, "erf $\left| x \right|$" is called the error function of x, and "erfc $\left| x \right|$" is called the complementary error function. The bit error rate (from equation (5)), is then:

$$BER = \frac{1}{2} \left[\text{erfc} \left| \frac{I_{TH}}{\sigma_a} \right| + \text{erfc} \left| \frac{i_s - I_{TH}}{\sigma_p} \right| \right] \quad (8)$$

It is possible to solve for a value of I_{TH} which minimizes the bit error rate; however, the result is unwieldy. To a good approximation the optimum decision threshold is that value of I_{TH} which makes P_m equal to P_f.[5] For this approximation, the optimum threshold, I_{THO}, is defined as:

$$I_{THO} = \left[\frac{\sigma_a}{\sigma_a + \sigma_p}\right] i_s \tag{9}$$

For this case the minimum error rate then becomes

$$BER = \text{erfc}\left\{\frac{i_s}{\sigma_a + \sigma_p}\right\} = \text{erfc}\left\{Q\right\} \tag{10}$$

For the case when the signal quantum noice (signal current shot noise) is negligible compared to other noise sources, the optimum threshold becomes one half the peak signal, since σ_a is then approximately equal to σ_p. It should be noted that signal quantum noise can generally be neglected for PIN detector input receivers. For receivers employing an avalanche photodiode the signal quantum noise cannot be neglected (generally) because of avalanche multiplication. In this case the optimum threshold is asymmetrical, with the degree of asymmetry being signal-dependent. The practicality of optimum thresholding in a large signal dynamic range environment (as may be encountered with a star coupled data bus) must be critically reviewed.

Substituting the signal and noise terms into equation (10), the following relationship results:

$$BER = \text{erfc}\left\{\frac{rGP_{os}}{\left[2qB_n\left(rG^2 + \alpha P_{os} + i'\right) + i_{na}{}^2 B_n\right]^{1/2} + \left[2qB_n i' + i_{na}{}^2 B_n\right]^{1/2}}\right\} \tag{11}$$

[5] Hubbard, "Utilization of Optical Frequency Carriers for Low and Moderate Bandwidth Channels, BSTJ, Vol 52, Number 5, May-June 1973, pp. 731-765.

where

$$i' = rG^{2+\alpha}P_{on} + I_s + G^{2+\alpha}I_b \qquad (11a)$$

Equation (11) indicates the dependence of BER optical power received during a pulse. A more useful equation can be arrived at by expressing the required optical power in terms of a specified bit error rate. Introduction of the intermediate parameter "Q" such that:

$$BER = \text{erfc}\left|Q\right| \qquad (12)$$

and some algebraic manipulation allows the required power to be expressed as:

$$P_{os} = \frac{2qQ^2G\,B_n}{r} + \frac{\sqrt{rB_n(G^{2+\alpha}rP_{on}+I_b + I_s) + i_{na}^2B_n}}{r} \qquad (13)$$

The value of "Q" can be determined from a plot of the BER versus the argument of the complementary error function, such as is shown in Figure 3.1.2-2.

This equation points out several quantities impacting the required power. These are the first term, constituting signal quantum noise, and the second term, comprised of dark current and amplifier noise contributions. The terms controllable by the designer in the equation are the noise bandwidth, B_n, the gain of the avalanche diode, G, and the input referred thermal and shot noise current of the preamplifier, i_{na}. To a lesser extent, the signal to noise ratio, Q^2, is controllable as a system requirement.

Although the noise bandwidth, B_n, and avalanche gain, G, are under the designer's control, maximizing system performance requires selection of optimum values for these parameters. The amplifier input referred noise (shot and thermal) have minimum values set, once a particular design and components are selected. The thermal and shot noise currents are related

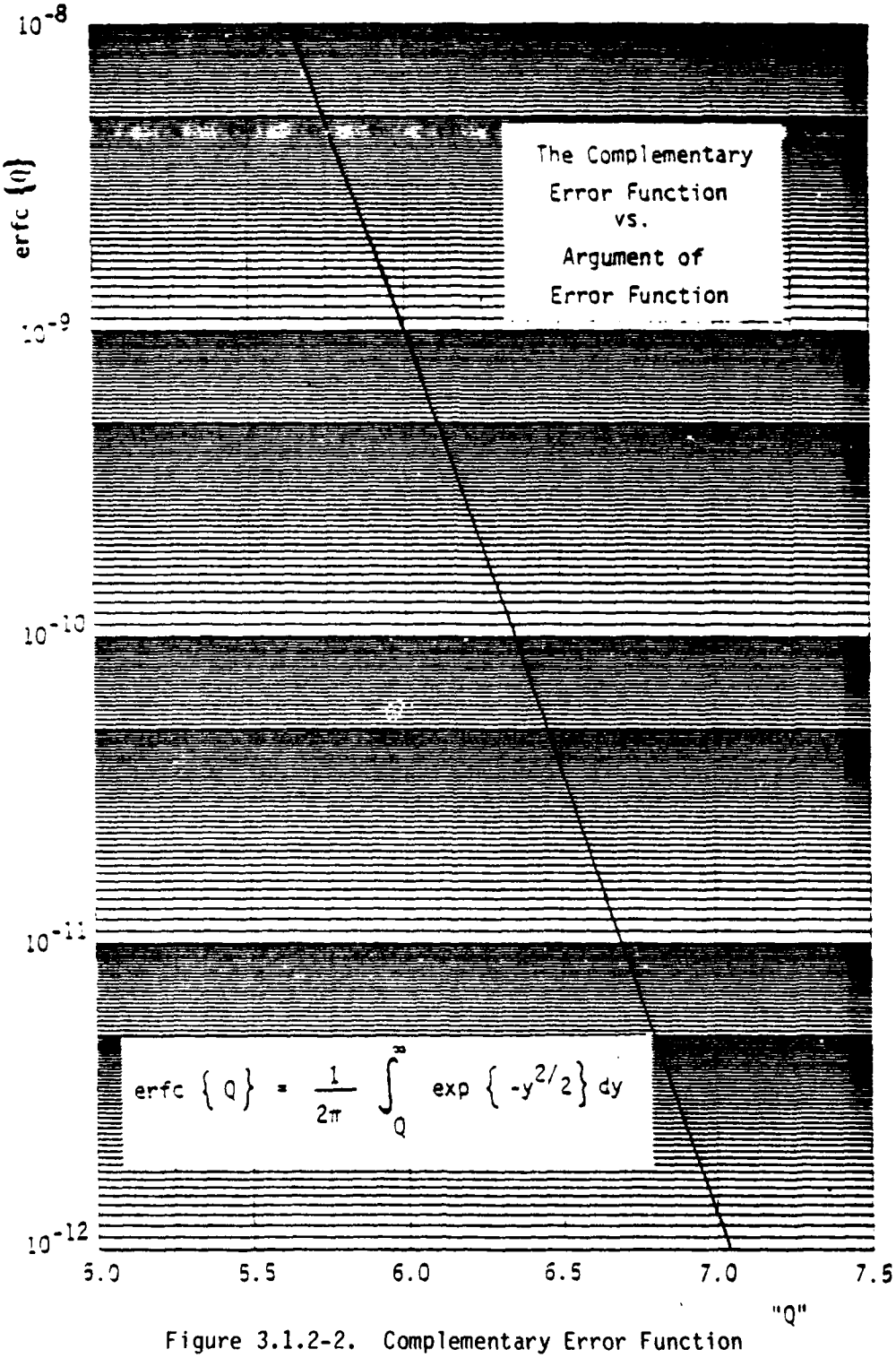

Figure 3.1.2-2. Complementary Error Function

to the input device selected. The thermal and shot noise currents are related to the input device (bipolar junction transistor, field effect transistor, or other input device), and these items will be discussed in the sections addressing transistor types.

Before reviewing the preamplifier performance a brief discussion of the gain available from avalanche detectors and the temperature dependence of the dark current is addressed. This brief discussion highlights a critical design criteria since the bulk leakage current exhibits a strong temperature dependence. This temperature dependence, like other diodes, is assumed to follow an approximate relationship of:[6]

$$I_b(T) = I_b(T_o)\, 2^{(T-T_o)/10} \tag{14}$$

where

$I_b(T)$ is the bulk leakage current in A, at temperature T, (in ^{o} K).

$I_b(T_o)$ is the bulk leakage current in A, at a known T_o (in ^{o} K).

T_o is the reference temperature, in ^{o} K.

and

T is the elevated operating temperature, in ^{o} K.

[6] W.E. Abare, R.E. Dragoo, and C.R. Patisaul, "Fiber-Optic Bus Receiver Requirements Study", Interim Technical Report Oct. 78-Jan. 79, AF Avionics Laboratory Contract #F33615-78-C-1561.

Since the bulk leakage current is multiplied by the gain of the device (raised to the 2 + α power), the APD detector is seen to be extremely sensitive to temperature. This is apparent from the plot of responsivity multiplied by gain versus reverse bias voltage for various temperatures for an RCA device #C30902E, reproduced as Figure 3.1.2-3. Note that for this plot the responsivity has been multiplied by the gain to preserve the "output amperes per input optical watt." The actual device responsivity must be divided by the avalanche gain to determine the normalized responsivity value used in equation (13). The design of a receiver to operate over even limited temperature ranges then must provide gain compensation circuitry.

3.1.2.1 Bipolar Junction Transistor Receiver

Several configurations of transistors are available for optical receivers. The noise model of Figure 3.1.1.3 indicates that the input from a biased photodiode can be treated as an ideal diode with several noise current sources corrupting the signal. Since the ideal diode is a current device the preamplifier must convert this signal current to a signal voltage for later stage amplification or other signal processing. One means of achieving the conversion of this signal current to a voltage is accomplished with a transimpedance (or transresistance) amplifier.

A transimpedance amplifier has a resistive feedback network and should be characterized by low noise, low distortion, and possess a flat frequency response. The flat frequency response may be accomplished by the use of negative feedback. Since the thermal noise of the amplifier is determined by the contributions of the feedback resistor, the biasing resistors, and the input capacitance, these noise sources must be minimized to achieve low noise performance. Additionally, since the noise is referred to the input, the input referred collector current shot noise must be combined with the base current shot noise when calculating noise contributions.

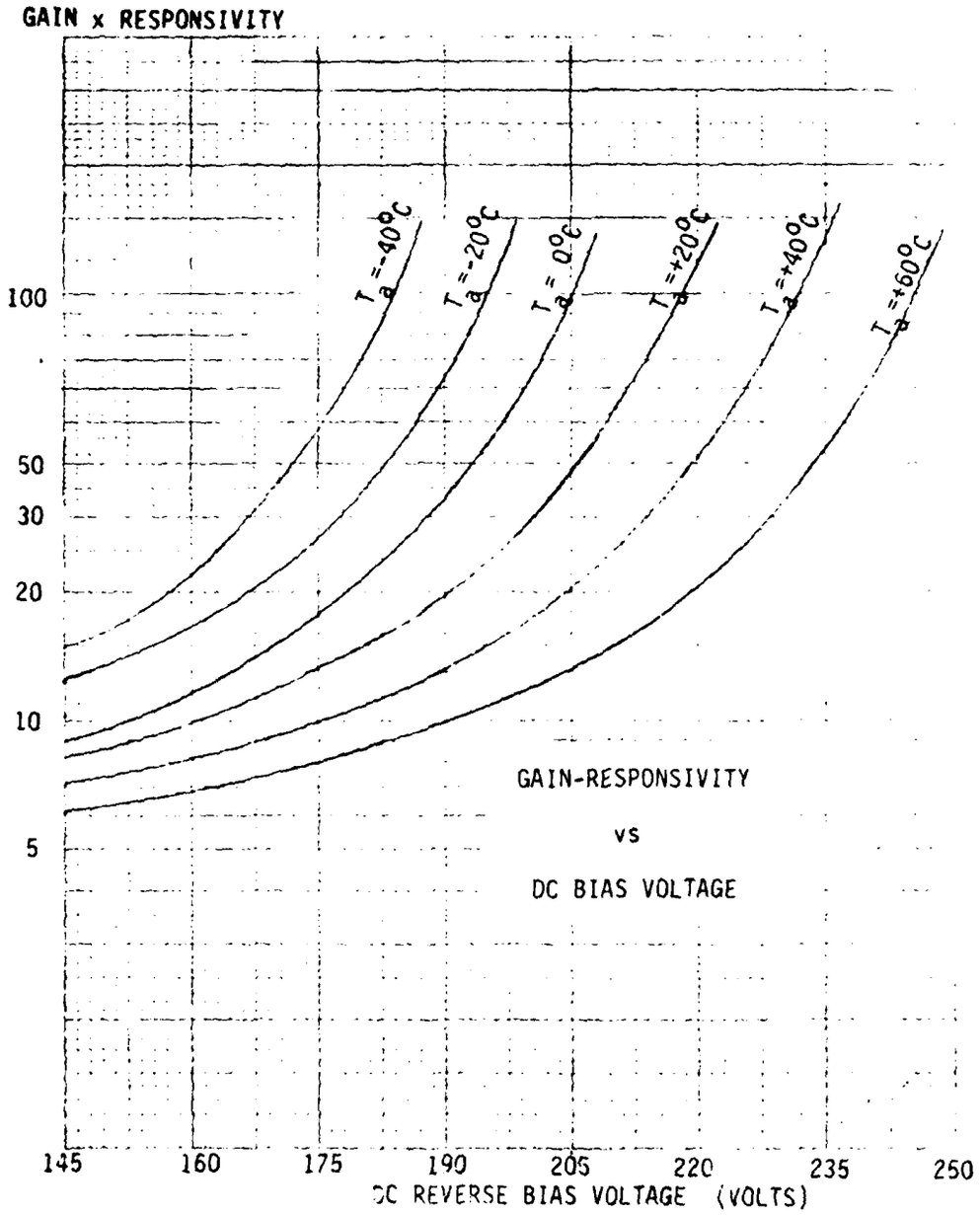

Figure 3.1.2-3. Plot of APD C0902E Gain vs. Bias Voltage for Various Temperatures

To determine the noise current spectral density (in $A/\sqrt{Hz}$) for a bipolar junction transistor (BJT) input preamplifier, the simplified transimpedance preamplifier schematic shown in Figure 3.1.2.1-1 will be used.[7]

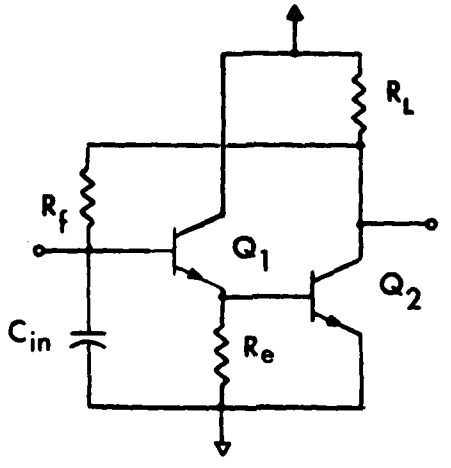

Figure 3.1.2.1-1. Simplified Schematic, Bipolar Junction Transistor Input Transimpedance Preamplifier

The noise model for the common emitter transistor is shown in Figure 3.1.2.1-2 and the equivalent input referred noise current spectral density may be expressed as:

$$\overline{i_{na}^2} = \left(S_b + S_{eb}\left(+\frac{S_c}{g_m^2}\right)\right)\left(\omega C_{in}\right)^2 \qquad (15)$$

or

$$\overline{i_{na}^2} = 2qI_b + \left(4kTr'_{bb} + \frac{2qI_c}{g_m^2}\right)(\omega C_{in})^2 \qquad (15a)$$

[7] W.T. Burton, Jr., R.R. Giri, and J.M. Mader, "Fiber-Optic Receiver Requirements Study", Interim Technical Report Jan. 79-May 79, AF Avionics Laboratory Contract #F33615-78-C-1561.

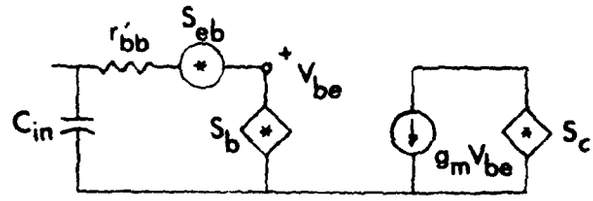

Figure 3.1.2.1-2. Noise Model for Common Emitter Bipolar Transistor

where terms are as defined in Figure 3.1.2.1-2 and, for a bipolar transistor:

$$I_b = \frac{I_E}{1 + h_{fe}} \simeq \frac{I_E}{h_{fe}} \tag{16}$$

$$I_E \simeq I_C \tag{17}$$

$$g_m = \frac{qI_E}{kT} \tag{18}$$

which leads to:

$$\overline{i_{na}^2} \simeq 2qI_b + \left(4kTr'_{bb} + \frac{2(kT)}{qI_E}^2\right)\left(\omega C_{in}\right)^2 \tag{14b}$$

where

i_{na} is the input referred noise current spectral density, in $A/\sqrt{Hz}$

I_b is the base current, in A

r'_{bb} is the base spreading resistance, in ohms

I_E is the emitter bias current, in A

and the other terms are as previously defined.

To determine the input referred amplifier noise current spectral density, the spectral density must be multiplied by the filter response and integrated across the bandwidth, then divided by the amplifier response or:

$$\overline{i_{na}^2} = \frac{\frac{1}{2\pi}\int_0^\infty S_{eg}\, F(\omega)\, d\omega}{\frac{1}{2\pi}\int_0^\infty F(\omega)\, d\omega} \tag{19}$$

where

i_{na}^2 is the mean squared input referred noise current spectral density in A^2/Hz, as previously defined.

$F(\omega)$ is the filter response, as a function of the radian frequency, ω, and the other terms are as previously defined.

Using the Butterworth filter response, due to its ease of mathematical manipulation, the filter response integrand is:

$$F(\omega) = \frac{1}{1 + \left(\frac{\omega}{\omega_0}\right)^{2n}} \tag{20}$$

where

ω_0 is the cutoff (half power) frequency filter

n is the order of the filter

and ω is the radian frequency at the point of interest.

Equation (19), with a filter response defined by (20), can be shown from an integral table to have the following form:

$$\int_0^\infty \frac{x^{m-1}\,dx}{1+x^p} = \frac{\pi}{p \sin\frac{m}{p}}, \quad 0<m<p \tag{21}$$

Finally, for a filter of order "n" and defining Γ_n and B_n as:

$$\Gamma_n = \frac{(2n)^2 \left[\sin\frac{\pi}{2n}\right]^3}{\pi^2 \sin\left(\frac{3\pi}{2n}\right)} \tag{22}$$

and

$$B_n = \frac{\pi f_o}{2n \sin\frac{\pi}{2n}} \tag{23}$$

where B_n is the noise bandwidth; the mean square noise current spectral density is

$$\overline{i_{na}^2} = 2q.\frac{I_E}{h_{fe}} + (2\pi C_{in})^2 \left\{ \frac{2(kT)^2}{qI_E} + 4kTr'_{bb} \right\} \Gamma_n \; B_n^2 \tag{24}$$

The above filter weighting factor has been computed for values of n, as shown in Table 3.1.2.1.

Table 3.1.2.1. Filter Weighting Factor

n	Γ_n
1	Undefined
2	0.81057
3	0.45595
4	0.39335
5	0.36956
10	0.34175
100	0.33342

Since the input referred noise current spectral density of the amplifier depends on the emitter bias current, an optimum value may be determined for minimal noise. This optimum value is determined by differentiating equation (24) with respect to I_E and setting the derivative equal to zero. This manipulation produces:

$$I_{E_{opt}} = \frac{2\pi kT\, C_{in}\, B_n}{q}\sqrt{\Gamma_n h_{fe}} \tag{25}$$

For this optimum emitter bias current the input referred mean square noise current spectral density can be computed as:

$$\overline{i_{na}^2} = 4\pi kT\, C_{in}\, B_n\sqrt{\frac{\Gamma_n}{h_{fe}}} + kT(2\pi C_{in})^2\Gamma_n\, B_n^2\left\{\frac{1}{C_{in}\, B_n\sqrt{\Gamma_n\, h_{fe}}} + 4r_{bb}'\right\} A^2/Hz \tag{26}$$

If the constants are inserted in the above equation and a third order filter response with absolute temperatures of 273^{0} K and 323^{0} K ($0\text{-}50^{0}$ C) are assumed, equation (26) can be plotted for various values of input capacitance, bandwidth and transistor parameters. These plots are shown in Figure 3.1.2.1-3 and include the variation of the small signal current gain (h_{fe}) with temperature.

The curves plotted in Figure 3.1.2.1-3 represent only the input referred noise spectral density of the preamplifier. To determine the optical signal power required this preamplifier noise must be combined with diode dark current shot noise and signal current shot noise (termed signal quantum noise). Additionally, the required bit error rate must be established, combined with the photodiode responsivity. These terms are combined in equation (13), introduced at the beginning of this discussion. Before calculating a minimum optical signal power requirement a review of comparative performance of the silicon junction field effect transistor (JFET) as the input transistor will establish a basis of comparison to select an optimal input transistor. This review of the JFET is addressed in the next section.

3.1.2.2 Junction Field Effect Transistor Receiver

The use of a silicon JFET as the input transistor to the preamplifier offers a high impedance input with low gate leakage current. A simplified schematic of a JFET input transimpedance preamplifier is shown in Figure 3.1.2.2-1.[8]

The noise model for the common source connected JFET is shown in Figure 3.1.2.2-2. The first stage is assumed to be the principal noise contributor.

[8] Ibid

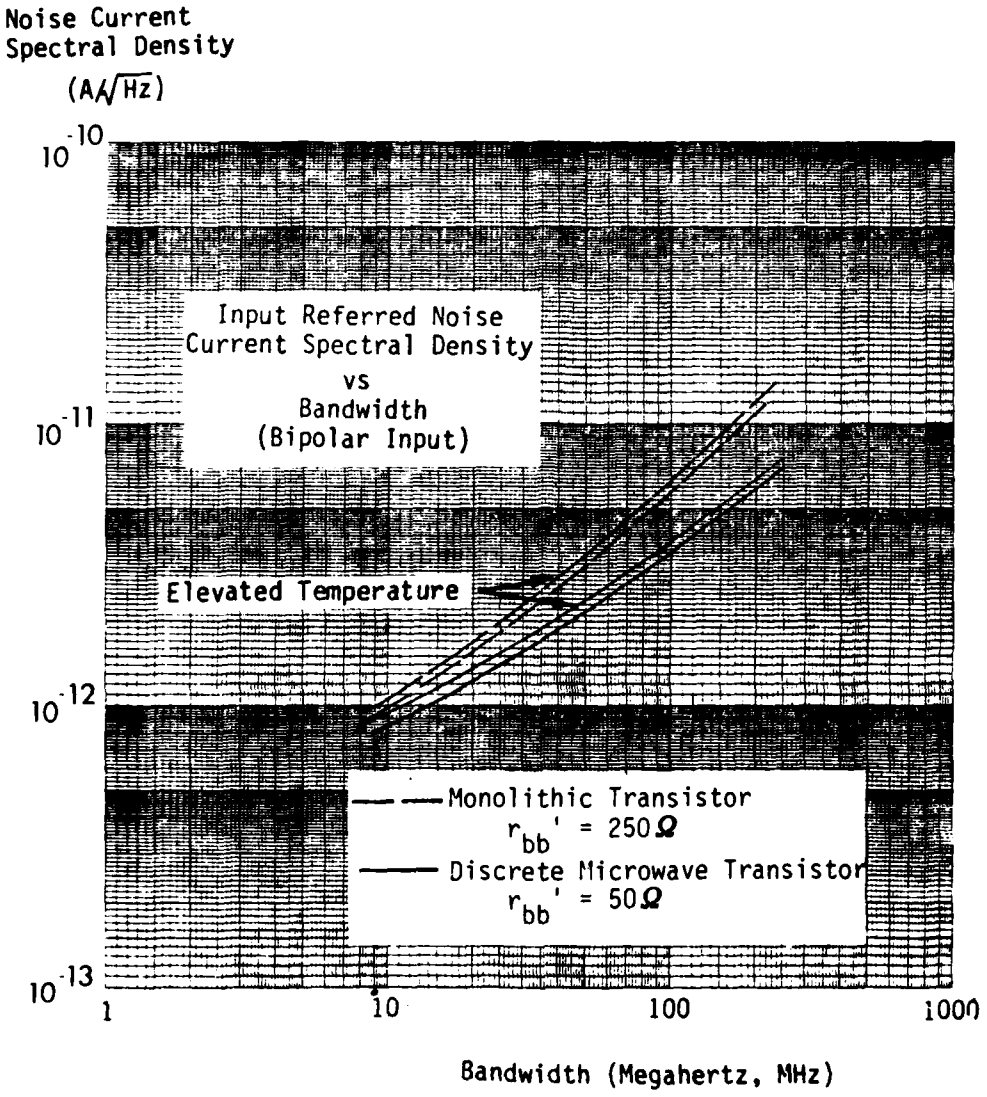

Figure 3.1.2.1-3. Bipolar Junction Transistor Input Referred Noise Current Spectral Density Versus Noise Bandwidth

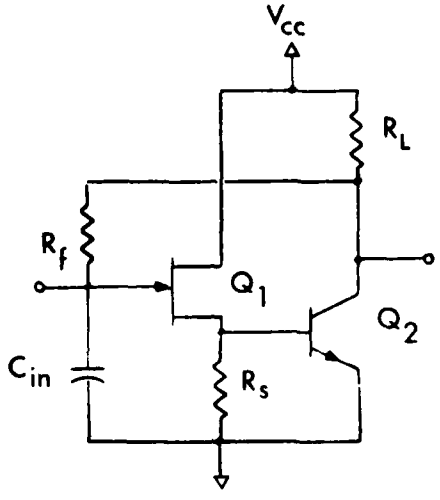

Figure 3.1.2.2-1. Simplified Schematic, Junction Field Effect Transistor Input Transimpedance Preamplifier

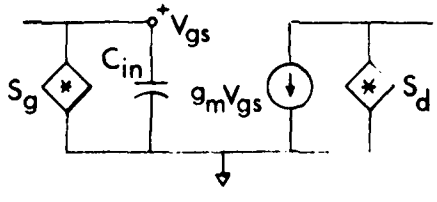

Figure 3.1.2.2-2. Noise Model for Common Source Junction Field Effect Transistor

To determine the input referred noise current spectral density, the noise current generator in the drain circuit must be reflected to the input of the JFET. This may be accomplished by placing an equivalent noise current generator in the gate to source path, as

$$I_d = g_m V_{gs} = \frac{I'_N g_m}{j\omega C_{in}} \tag{27}$$

where I_d is the drain current, in A

g_m is the transconductance of the JFET, in A/V, or Siemens (S)

V_{gs} is the gate to source voltage, in V

ω is the angular frequency, in rad/sec

C_{in} is the input capacitance, in F

and I'_N is the equivalent noise current in the gate circuit to reflect the drain current noise to the gate, in A

The equivalent input noise current spectral density can then be determined as:

$$S_{eq} = S_g + S_d \frac{(\omega C_{in})^2}{g_m^2} \tag{28}$$

or

$$S_{eq} = 2q\ I_g + \frac{4\ kT\omega^2\ C_{in}^2}{g_m}\left[\frac{2}{3} + \frac{2}{9}\left(\frac{C_{gs}}{C_{in}}\right)^2\right] \tag{28a}$$

Again, as was done in the case of the bipolar junction transistor, the input noise current is found by multiplying the equivalent input noise current spectral density by the filter transfer function and integrating over all frequencies, as (repeating equation (19))

$$\overline{i_{na}^2} = \frac{\frac{1}{2\pi}\int_0^\infty S_{eq}\ (\omega)\ F(\omega)\ d}{\frac{1}{2\pi}\int_0^\infty F(\omega)\ d\omega} \tag{19}$$

or, using a Butterworth filter response, and substituting the noise bandwidth into the equation:

$$\overline{i_{na}^2} = 2q\ I_g + \frac{16kT\ C_{in}^2}{g_m}\left[\frac{2}{3} + \frac{2}{9}\left(\frac{C_{gs}}{C_{in}}\right)^2\right]\frac{(2n)^2\left[\sin \pi/2n\right]^3}{\sin\left(\frac{3\pi}{2n}\right)}\ B_n^2 \tag{29}$$

Some simplification of equation (29) above can be achieved with the substitution of a constant reflecting the input capacitance, device parameters, and filter order. Similarly, the first term of equation (29) is generally several orders of magnitude less than the second term for ambient temperature environments of 0-50° C. With these simplifications equation (29) becomes:

$$\overline{i_{na}^2} \simeq \frac{4kT\ C_{in}^2\ B_n^2}{T\ g_m} \tag{29a}$$

where τ is defined as:

$$\frac{1}{\tau} = 4\left[\frac{2}{3} + \frac{2}{9}\left(\frac{C_{gs}}{C_{in}}\right)^2\right] \frac{(2n)^2 \left[\sin \frac{\pi}{2n}\right]^3}{\sin\left(\frac{3\pi}{2n}\right)} \qquad (30)$$

The value of τ is dependent on the filter type and order. To this point in the discussion, a Butterworth filter response has been assumed for simplicity of mathematics. Other filter response characteristics are available, including the Chebyshev and Bessel filter types. The other filter response characteristics are discussed in the next section. A plot of input referred noise current spectral density versus noise bandwidth then depends on the filter type. The filter selection for this and the bipolar input transistor are reviewed in the next discussion. For comparison purposes the noise bandwidth is used in three plots of noise current versus bandwidth.

A plot of i_{na}^2 against bandwidth for temperatures of 0^oC, 50^oC, and 85^o C using a 2N4417 JFET and an assumed C_{in} of 6 picofarads (pF) is shown in Figure 3.1.2.2-3. These three temperatures represent ambient temperatures of 0^o C (startup) 25^o C ambient (normal operation, or approximately 50^o C, junction temperature) and 50^o C ambient (85^o C junction temperature) such as might be encountered in the event of environmental conditioning failure. With this plot of the input noise current spectral density against bandwidth, a comparison can be made with a bipolar junction transistor to determine the better circuit. This is deferred until after a discussion of filter responses, undertaken next.

3.1.2.3 Filter Response Analysis

The previous discussions of the performance of bipolar junction transistor input and junction field effect transistor input preamplifiers employed a Butterworth filter response to bandlimit the noise for purposes of calculation. The noise bandwidth is determined once a specific filter

Figure 3.1.2.2-3. Input Referred Noise Current Spectral Density Versus Noise Bandwidth, JFET Input

type and order is selected. The filter "type" specifies the equation describing the response characteristic of filter, generally in the frequency domain. The filter must operate on the signal in the time domain however, necessitating a review of the filter response to time domain step functions.

Since most filter response characteristics are well documented in the frequency domain a translation back to the time domain yields the simplest technique of maximizing the benefit of the frequency domain characterization. As an example, the response of a Bessel filter to a rectangular pulse for various filter bandwidths (normalized to the pulse width) is shown in Figure 3.1.2.3-1. Inspecting Figure 3.1.2.3-1 indicates that the filter bandwidth affects both the output pulse rise time and peak amplitude. For narrow filter bandwidths, the pulse response does not reach the input pulse peak amplitude.

Although peak pulse amplitude is of concern from a peak signal to rms noise point of view, the noise bandwidth passed by the filter establishes the noise floor. The filter bandwidth should be adequate to pass the signal, but not so wide as to contribute excess noise. The bandwidth of three common filter types is shown in Table 3.1.2.3.[9]

From this table, it can be seen that the second order Butterworth filter has the lowest noise bandwidth to signal bandwidth (B_n/B_{3dB}) ratio for second order filters while the Chebyshev filter has the lowest B_n/B_{3dB} for 3rd order filters. Both the Butterworth and Chebyshev filter types exhibit "ringing," or overshoot, for a step response input. The Bessel filter response does not ring, but has a slightly larger noise bandwidth than either the Butterworth or Chebyshev filters. The filter response to a rectangular pulse for various filter bandwidths of a Butterworth filter is shown in Figure 3.1.2.3-2 and for a Chebyshev filter in Figure 3.1.2.3-3.

[9]Shelton and Adkins, "Noise Bandwidth of Common Filters," IEEE Trans on Communications Technology, Vol. COM-18, No. 6, December 1970, pp 828-830.

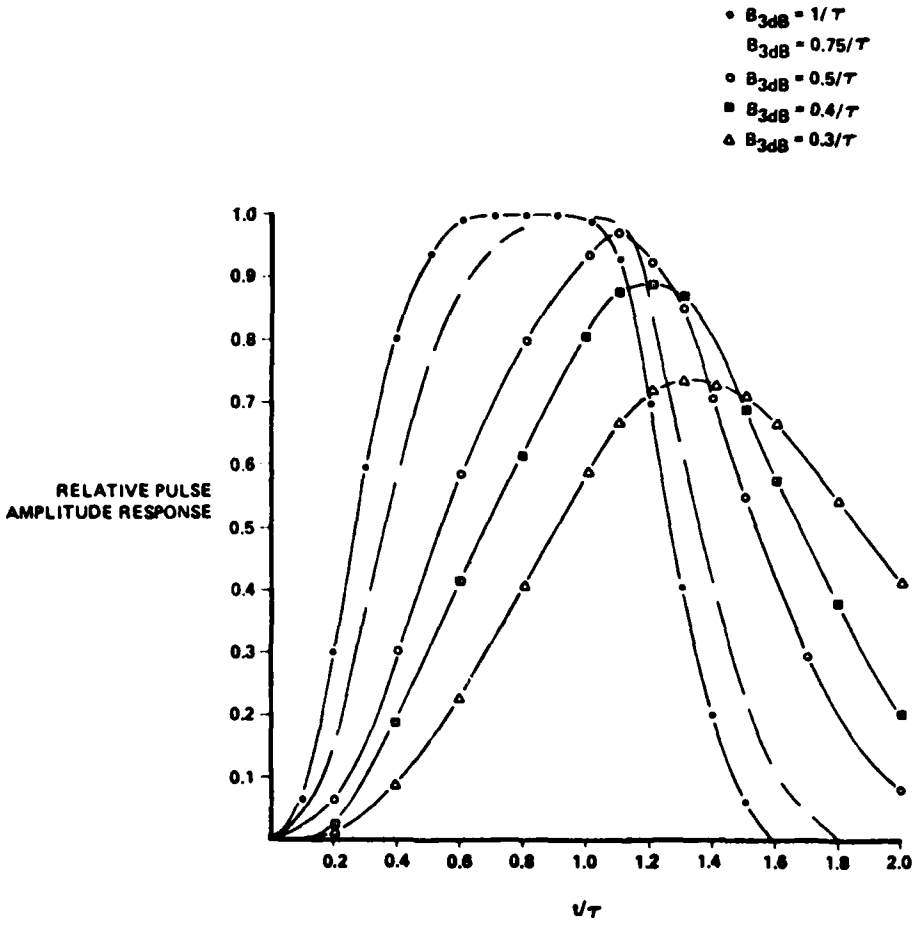

Figure 3.1.2.3-1. Response of Bessel Filter

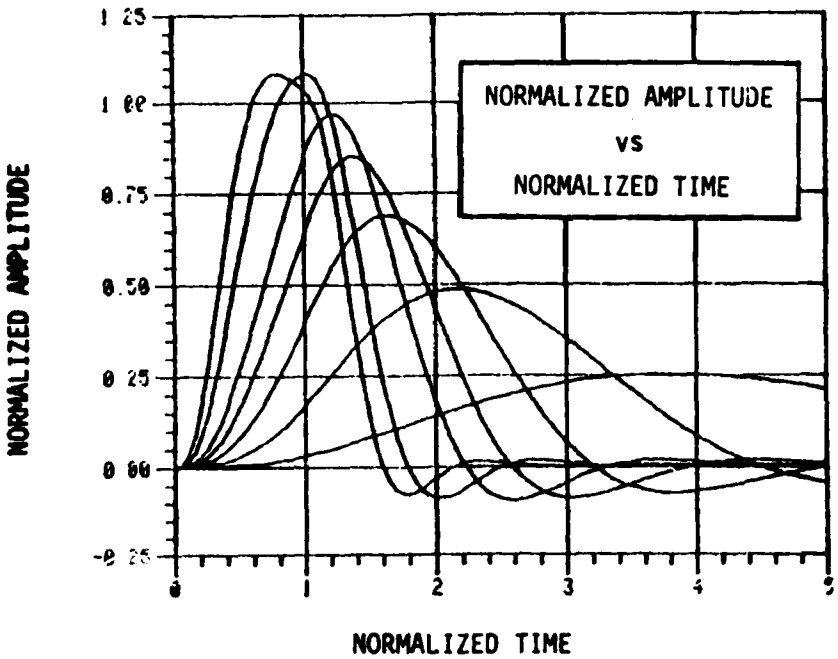

Figure 3.1.2.3-2. Butterworth Filter Step Response

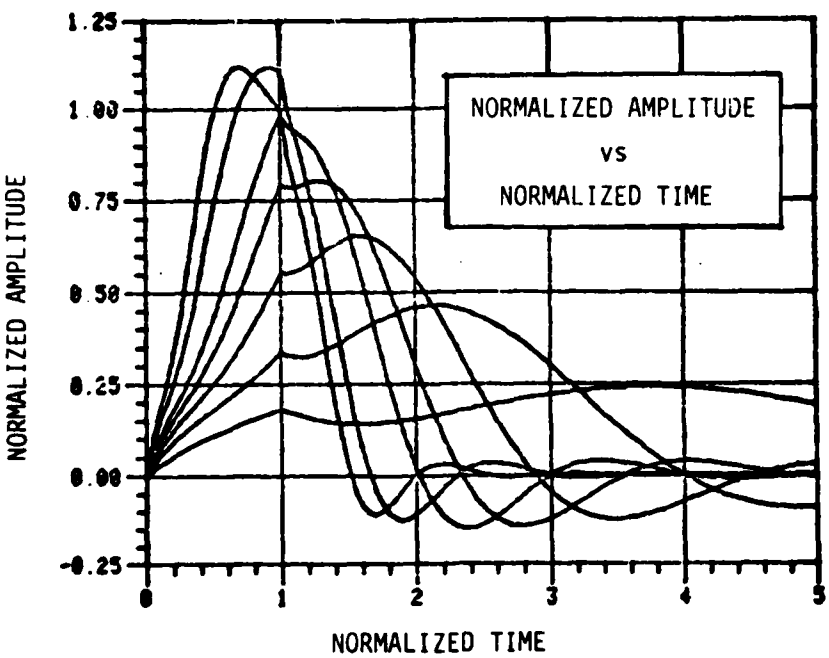

Figure 3.1.2.3-3. Chebyshev Filter Step Response

Table 3.1.2.3. Noise Bandwidths for Common Filter Types

Filter Type	Order	$B_{3\ dB}$**	B_N	$B_N/B_{3\ dB}$
Butterworth	1	1.00	1.571	1.571
	2	1.00	1.110	1.110
	3	1.00	1.045	1.045
Bessel	1	1.00	1.571	1.571
	2	1.36	1.571	1.155
	3	1.75	1.885	1.077
Inverse Chebyshev (.05 dB ripple)	1	2.86	4.495	1.572
	2	1.45	1.670	1.152
	3	1.17	1.165	1.004

* Stopband ripple set at 0.05 dB maximum
** Normalized bandwidth of 1 rad/sec compared to Butterworth filter

The Butterworth filter exhibits maximal flatness in the frequency domain.[10] As shown in Figure 3.1.2.3-2, the time domain response exhibits some overshoot (8% for a 3rd order filter response). The Bessel filter exhibits a maximally flat time delay in the frequency domain[11] (the equivalent response of the Butterworth filter with time delay substituted for attenuation), while the time domain response has essentially no overshoot, but exacts a penalty in the form of a slower rise time. The inverse Chebyshev filter frequency domain response exhibits the steepest attenuation slope (increase in attenuation per frequency interval), while the time domain response exhibits improved rise time (at the expense of larger overshoot) over the Butterworth filter for the same order filter response.

[10] L. Weinberg, "Network Analysis and Synthesis," McGraw-Hill 1962.
[11] Ibid

The "inverse Chebyshev" is the preferred Chebyshev filter for pulse data, since the response is monotonic in the (frequency domain) passband. The stopband is allowed to have "ripple," since it is outside the receiver bandwidth and does not affect the filter performance in the frequency band of interest. This filter response does exhibit some ringing in the time domain, much like the Butterworth response. The noise bandwidth of a third order Chebyshev can be treated the same as the "inverse Chebyshev," and the difference in noise bandwidth compared to the Butterworth response is negligible, for a given 3 dB bandwidth. Note that the 3 dB bandwidth of a Chebyshev filter is larger than the equivalent Butterworth filter response characteristic, allowing the 3 dB attenuation to be set lower for a Chebyshev type filter response than for a Butterworth response without additional degradation to the filter rise time.

For simplicity of calculations, the Butterworth response characteristic was used for derivations, with the noise bandwidth then modified per Table 3.1.2.3 to accommodate the Bessel filter bandwidths. The error induced by this manipulation is minimal and the derivations become much simpler and more tractable.

The noise bandwidth is thus seen to vary slightly with filter type selection. This noise bandwidth then influences the optical signal power required to achieve a given bit error rate ("Q"). For consistency, a Bessel filter response will be assumed for the remainder of the report, since the Bessel response offers linear phase delay at a slight penalty in noise bandwidth. Additionally, the Bessel filter offers significantly less (essentially zero) overshoot and ringing than either the Chebyshev or Butterworth filter responses. This lack of overshoot and ringing is of significant importance when employing a sampling technique to generate data estimates.

3.1.2.4 Performance Summary

A comparison of the mean amplifier noise current spectral densities between the JFET and BJT input preamplifiers is shown in Figure 3.1.2.4-1. From these plots it is seen that the BJT offers slightly improved performance at higher data rates over the 1 mS (mmho) transconductance JFET. The BJT base spreading resistance, r'_{bb}, and the JFET transconductance determine the predicted crossover point between the BJT and the JFET; however, parameter variations (including implementation losses such as a higher "C_{in}") can alter predicted performance. The expected base spreading resistance for both monolithic transistors (for integrated circuit receiver chips) and for discrete microwave transistors is shown in Figure 3.1.2.4-1.

For these values of noise current spectral density, the required power for a specified bandwidth can be plotted for each of the three cases, as shown in Figure 3.1.2.4-2. The JFET input with a transconductance of 4×10^{-3} Siemans offers the best predicted performance for lower data rates, while the discrete bipolar microwave transistor offers the best predicted performance for data rates of greater than $\sim$40 Mb/s.

Temperature also impacts the receiver preamplifier performance, with the JFET suffering slightly more since the transconductance varies over the temperature range approximately as:

$$g_m(T_e) = g_{mo}\left(\frac{T_e}{T_o}\right)^{-3/2} \qquad (31)$$

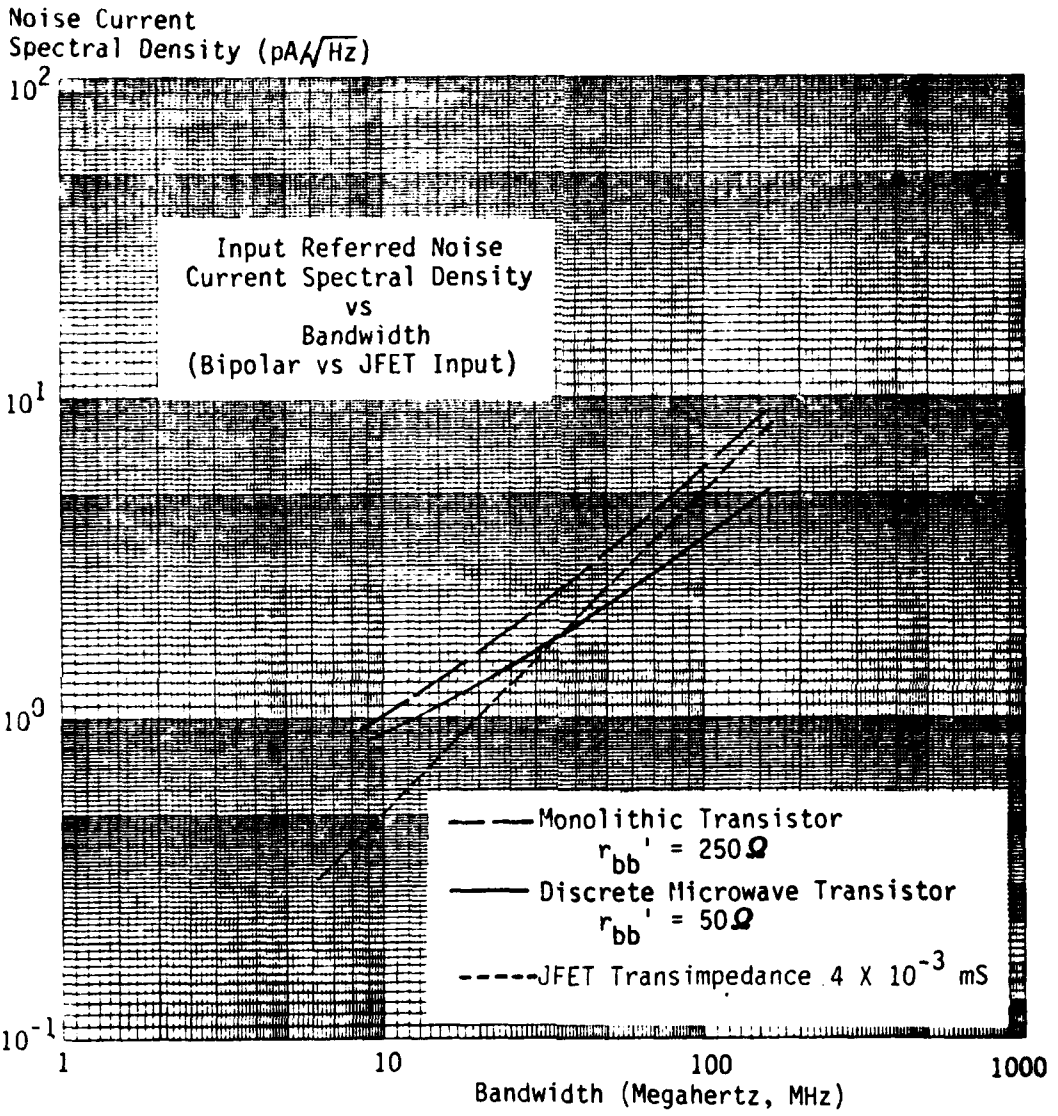

Figure 3.1.2.4-1. Bipolar Versus JFET Input Noise Current Spectral Density Versus Bandwidth

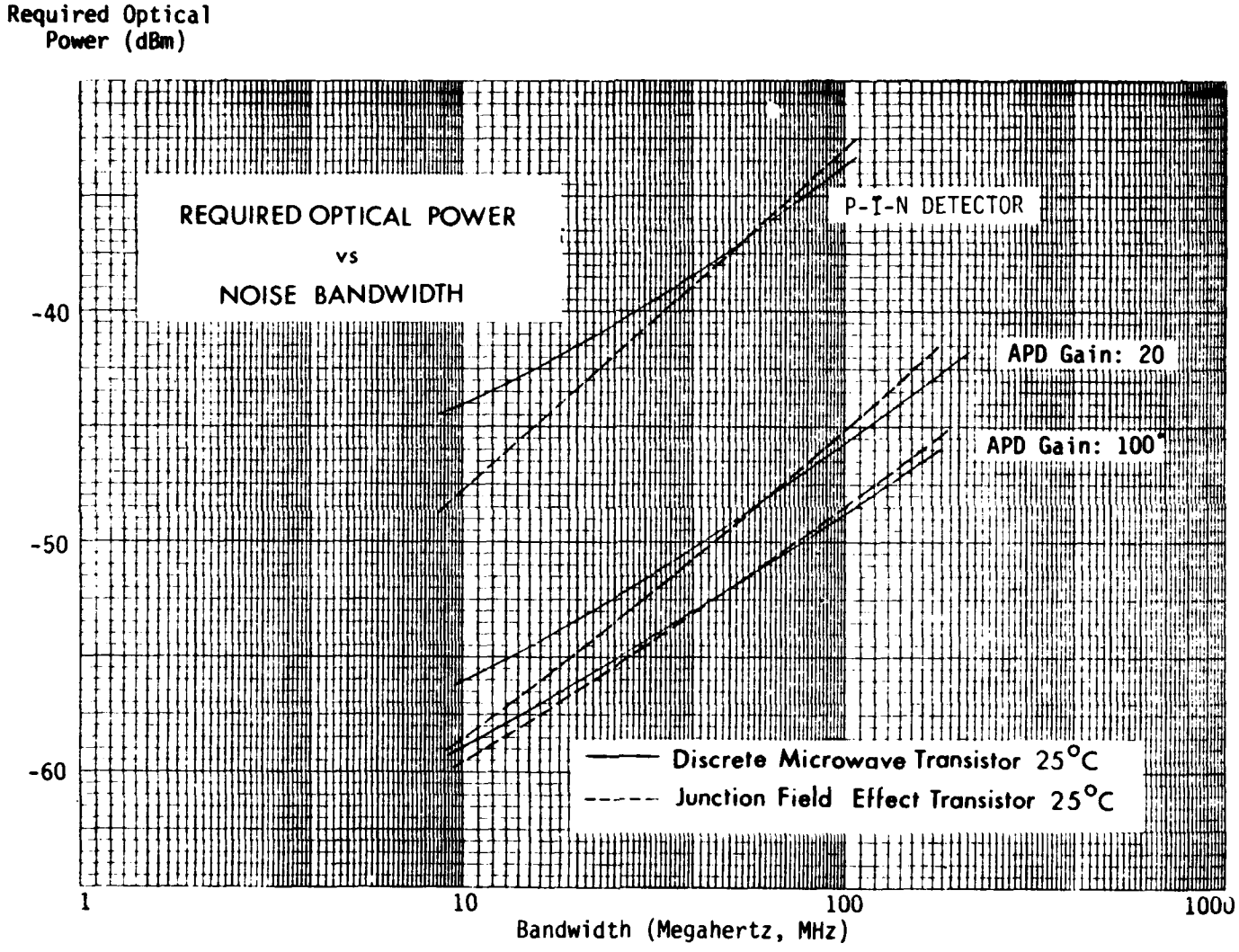

Figure 3.1.2.4-2. Required Optical Power Versus Noise Bandwidth

where $g_m(T)$ is the transconductance at elevated temperature "T_e", in A/V

g_{mo} is the transconductance at "T_o", in A/V

T_o is the ambient temperature at which g_{mo} is measured (27^o C), in ^{o} K,

and T_e is the elevated temperature, in ^{o} K

By comparison the bipolar junction transistor small signal current gain varies inversely with temperature as:

$$h_{fe}(T_e) = \frac{h_{fe}(T_o) \cdot T_o}{T_e} \qquad (32)$$

where $h_{fe}(T_e)$ is the short circuit current gain at the elevated temperature of the input transistor

$h_{fe}(T_o)$ is the short circuit current gain at an ambient temperature, T_o

T_o is the ambient temperature (assumed 300^o K), in ^{o} K

and T_e is the elevated temperature in ^{o} K

For the values of Figure 3.1.2.4-1, the noise current spectral density "crossover point" for the 4 mS transconductance JFET and the discrete microwave transistor moves from ~35 MHz to ~30 MHz for an increase in junction temperature from 50^{o} C to 85^{o} C.

These noise current spectral densities can be used to determine the required optical power and establish the receiver performance as indicated in Figure 3.1.2.4-2. The plots indicated in Figure 3.1.2.4-2 are predicated on the noise current spectral densities that have been established for both the JFET and BJT preamplifiers. The plots shown in Figure 3.1.2.4-2 indicate the required optical power for both PIN detectors and avalanche photodiode detectors. Two values of gain are plotted for the avalanche detector; 20 and 100. At a 60 Mb/s data rate an approximate 2 dB of improvement is achieved employing a gain of 100 in lieu of a gain of 20. The tradeoff is in temperature compensation circuitry complexity.

For any of the gain-detector combinations the JFET preamplifier offers a slight advantage in performance for the data rate envisioned at ambient temperatures of 25^{o} C (junction temperatures of 50^{o} C also). Raising the junction temperature to $+85^{o}$ C lowers the crossover point, but does not substantially raise the required power such that the BJT input would be the clear choice. The balance of this discussion will assume a JFET receiver for simplicity, recognizing that there is not a substantial performance differential.

3.2 Source Coupled Power Achievable

The previous discussion addressed the receiver performance attainable for current technology fiber-optic receivers. Given this receiver sensitivity and the source coupled power achievable, the link loss allowable can be determined. This section will address the source power achievable into an assumed fiber type, the fiber type being consistent with the direction now being followed in the draft MIL-STD-188-111.

Two broad factors impact source performance: communication performance, involving such characteristics as optical radiation risetime (or source bandwidth), coupled power, emission pattern, bias requirements, stabilization, etc.; and environmental performance, including temperature effects, shock, humidity, vibration and others. There is considerable interplay between these broad factors, such as temperature effects on coupled power and bias changes. Thus the partitioning of environmental performance identifies items such as temperature, humidity, altitude, etc. These effects, other than temperature, are considered as second order effects in this study, consistent with the computer equipment environment of the AN/GYQ-21(V).

Two general types of semiconductor optical sources are currently used with fiber-optic cable systems. These two source types are the light emitting diode (LED) and the injection laser diode (ILD). Both source types are available which operate with fiber systems in the 0.8-0.9 and 1.0-1.3 μm spectral regions. These two spectral regions correspond to low loss "windows" (spectral regions) of the fiber. The two source types present differing performance and design requirements, which are dependent on the system requirements. Each of these source types are addressed next.

3.2.1 Light Emitting Diodes

Basically, the types of LED's available for fiber-optic communications are surface emitters and edge emitters, where each type may be further subdivided according to material doping (GaAs, GaAs:Si, GaAs:Zn, GaAlAs) and chip construction (planar, dome, edge, etc.). Figure 3.2.1 provides a chart of the various characteristics of LED types. This chart does not reflect state of the art capabilities for double heterostructure (DH) devices such as the Burrus LED but it does provide a relative comparison of diode types and performance.

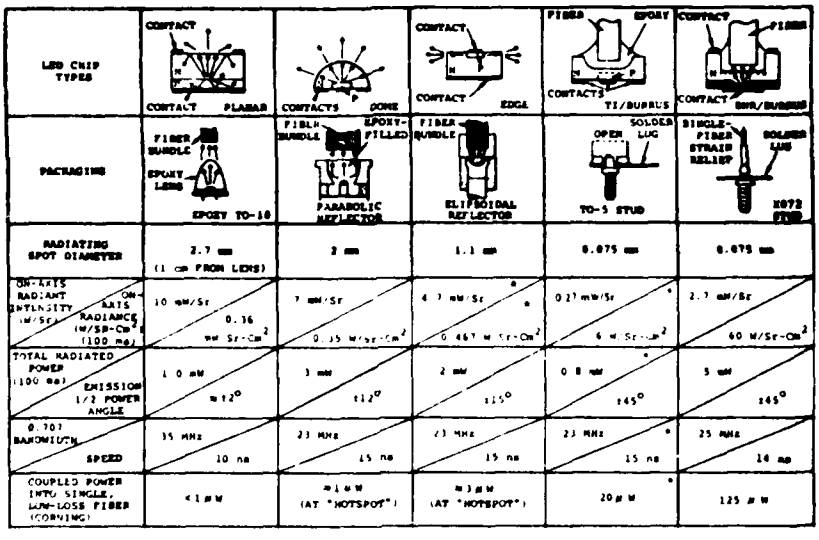

Figure 3.2.1. Typical LED Characteristics (Casper 1975)

For single fiber applications the heterostructure devices (Burrus and edge emitter) are typically most attractive because of several inherent characteristics:

- Increased conversion efficiency (greater electron confinement within the junction region)
- Because of less internal absorption the external efficiency is higher
- Decreased minority carrier lifetimes permit high modulation rates
- Structure promotes easy modification of operating wavelengths

The output of surface emitting Burrus devices is approximately Lambertian, that is, the surface radiance is constant in all directions, but maximum emission is perpendicular to the junction and falls off to the sides in proportion to the cosine of the viewing angle because the apparent area varies with this angle. The expected coupling of this output to the fiber depends upon the exact geometry and conditions, such as the LED emission pattern and radiance, fiber size and refractive index grading, effective NA of the fiber, relative area of the fiber core and LED emitting area, distance and alignment between the two, the medium between them, etc. However, a generalization of power coupling is that the amount of power coupled into a fiber is directly proportional to the radiance of the device. Thus, recalling Figure 3.2.1, it can be shown that although some devices (such as diffused GaAs) have high total output power, the emitting area is also quite large and is not suitable for single fibers.

As a point of reference, the literature[12] has reported coupling over 1 mW of optical power, at 0.8 microns (μm) into a low loss large core (115 μm) graded fiber with a 0.36 NA. The double heterostructure (DH) Burrus LED had an emitting area of 75 μm and delivered approximately 15 mW of optical power into free space. Similar LEDs have developed on U.S Air Force contracts which provide $\sim$1 mW of coupled power and have modulation rates of $\sim$200 Mb/s. These devices are qualified (to MIL-E-5400 Class II) for a wide range of temperatures and are hermetically sealed.

The discussion to this point has primarily dealt with the surface emitter, Burrus type device because of its availability and relatively good operating characteristics. The next few paragraphs shall briefly consider the second major type of LED, the edge emitter.

[12] O'Connor, P. B. et al, "Large Core High NA Fiber-Optic Data Link Applications", Electronic Letters: 13, 1977

An efficient edge-emitter LED emits part of its radiation in a relatively directed beam and thus has the advantage of improved efficiency in coupling light into a fiber. This is particularly important in coupling to a fiber with a small acceptance angle. The decrease in emission angle for this configuration is in the plane perpendicular to the junction, and it results from waveguiding effects of the heterostructure.

A reflector at one endface and an antireflection coating at the other assures that more of the propagating light is emitted at one endface. The emitted beam then is Lambertian with a half-power width of 120^{o} in the plane of the junction where there is no waveguide effect, but has been made as small as $25\text{-}35^{o}$ in the plane perpendicular to the junction by properly proportioning the waveguide.

A second advantage of this structure is that, as a result of the channeling of light to a very small endface by the waveguide, the effective radiance at this face can be very high. The value achieved to date is ~1500 W/cm^2-sr in an emitting area of 2-4 X 10^{-6} cm^2. This value is several times the 300 W/cm^2-sr achieved in air without antireflection coatings with a 15 μm diameter DH surface emitter and an order of magnitude greater than that reported for 50 μm diameter DH devices operated at one-half to two-thirds saturation (150-200 mA). With the aid of a lens at the end of the fiber (effective because the emitter area was smaller than the fiber cross section), 0.8 mW of optical power has been coupled into a 0.14NA, 90 μm core fiber from one of these edge emitters operating near diode saturation at 5.1 kA/cm^2. This is a coupling improvement of 7 dB compared to that expected from a purely Lambertian source.

On the basis of idealized assumptions, recent analysis has shown that an edge-emitter LED with a guiding region should be capable of coupling 7.5 times more power into a fiber than can a surface emitter of equal intrinsic radiance and active layer thickness. When more realistic assumptions are made, including, for example, the more difficult heat-sinking geometry of the edge emitter, this same analysis shows that the

expected advantage drops toward a factor of two for practical devices. However, for a variety of practical manufacturing and handling reasons, present day usage seems to favor surface emitters as incoherent sources for most systems and, as mentioned, recent Burrus devices offer both high coupled power and attractive modulation capabilities.

3.2.2 Injection Laser Diodes

The injection laser diode (ILD) is very similar in construction to the previously described double heterostructure edge emitters. Fabrication of the ILD chip is such that an optical cavity is typically formed through electron confinement and end facet reflection. (The end facet is typically cleaved to provide a "mirror" at each end of the pumping cavity for lasing.) This "optically resonant" cavity then provides stimulated emission above the device's threshold current. Note that LED's operate based on spontaneous emission whereas above threshold ILD's emit via stimulated mechanisms, the primary distinction being a much higher internal efficiency within and coherent emission from the ILD.

As the reader possibly suspects, for drive current below threshold (I_{th}), the ILD operates via spontaneous emission and is very similar to DH LED's. Similarly, because of like construction, most ILD's have an emission pattern as described earlier for the edge emitter. However, there is more waveguiding within the junction confinement region (to provide higher junction current densities) and the plane horizontal to the junction is less than Lambertian (reference Paragraph 3.2.1) yielding

better coupling efficiencies than even the edge emitter LED. As a point of comparison typical non-lensing coupling efficiencies for the DH LED's and ILD's are as shown in Table 3.2.2:

Table 3.2.2. Comparison of Coupling Losses

Device	Typical Coupling Loss	
	(50-85 μm Core)	(200 μm Core)
Burrus LED	15-20 dB	8-12 dB
Edge Emitter	8-12 dB	6-8 dB
ILD	3-6 dB	2-3 dB

Thus we see that although the larger core fiber (and typically higher NA) provides the greatest improvement for coupling to the Burrus device; the ILD remains the most efficient device with 50 percent or more coupled power. Note that due to the very small emission area and beam spread of the ILD, it is extremely efficient when terminated with large core fiber.

With the above in mind, the discussion shall proceed to factors considered in device selection.

3.2.3 Source Selection Criteria

The communication performance parameters which are most critical to the AN/GYQ-21(V) bus application are summarized as:

- Modulation rate of 60 Mb/s
- Coupled power - maximum achievable (discussed below)

- Reliability

- Spectral characteristics compatible with low loss fiber

To achieve the modulation requirements for rates of 60 Mb/s, the minimum bandwidths should be approximately 60 to 100 percent of this rate depending on modulation format (NRZ or RZ). Furthermore, to minimize system bandwidth reduction the modulation should be a factor 1.5 to 2 greater. Thus bandwidths are on the order of 90-120 MHz or more for RZ data, while for NRZ data the bandwidth requirement is on the order of 50-70 MHz.

Analysis on a previous program[13] has shown that the coupled power requirements are highly dependent on whether or not all worst-case conditions are imposed upon the link simultaneously. If an all worst case condition is potentially so, then to close the link other factors may be important (e.g., cooling source and detector) depending on the network configuration as well as environment. The power requirement shall be determined during later sections for each architecture being considered.

For ambient nonstressed environments, the lifetimes of devices are on the order of 10^5 hours or greater. LED's have, in the past, been considered as much more reliable than ILD's, however, recent developments in manufacturing technology and quality control promise ILD lifetimes projected in excess of 10^5 hours. Thus no distinction shall presently be made between high radiance LED and ILD sources solely on lifetime (later the discussion on temperature shall readdress the subject).

[13] Op. Cit, Number 6.

At this time, the environmental parameters shall be discussed. These are:

- Ambient temperature operation over 0^{o} C to $+50^{o}$ C as would be anticipated for a computer environment
- Packaging aspects

For the temperature environment above there are several considerations which bear further discussion in terms of device performance. Therefore, the following list is provided to summarize typical characteristics of LED's and ILD's over temperatures.

LED changes are as follows:

- Power output - reduced power (3-5 dB) at temperatures of 100 to 125^{o} C for constant bias
- Slight shift in center wavelength
- Gradual degradation in lifetime performance

The performance of an ILD is characterized by:

- Power output - significant change in output power may be seen since the threshold current level increases with rising temperature resulting in the loss of lasing action. Hence, some form of stabilization is required.
- Again slight shift in wavelength and spectral bandwidth. Most significant within dispersion limited systems.
- Catastrophic failure is typical of ILD's and is associated with threshold current level changes not accompanied with drive current reductions.

At low temperature, special precautions may be necessary to avoid end facet erosion (coating may avoid this problem). High temperature may cause failure of the junction due to thermal runaway. Furthermore, at junction temperatures of 60 to 70^{o} C the lifetime is reduced significantly due to permanent damage within the junction caused by formation of nonradiative centers. An ambient temperature of 50^{o} C coupled with a 20-25^{o} C thermal gradient between the package and ambient readily exceeds the 60 to 70^{o} C junction temperature.

Thus the selection of LED or ILD should seek to maximize the operating range of temperatures even with a relatively benign temperature environment. This objective is impacted by package design and active cooling. Although many sources can operate over the 0-50^{o} C (or "commercial") range of temperatures, the approach for selection shall be to consider manufacturer's stated range of operation as a guide and then during detailed analysis and design, determine special requirements (heat sinks, package design, cooling).

Packaging for both ILD and LED sources is a potential drawback, since many high performance sources are not provided in hermetic packages which readily accommodate various styles of connectors, fiber pigtails, active coolers, etc. Obviously the concern has been how to properly interface a pigtail fiber to the chip and maintain a seal through the package. Fortunately hermetically sealed sources do exist and as requirements increase more standardization will be seen. Other factors of the environment such as shock and vibration should not pose significant problems.

A few ILD manufacturers offer a packaging design which is hermetically sealed, has an integral fiber pigtail, optical feedback port and an internally mounted TE cooler. One such device supplied by General Optronics, contains an ILD which maintains linearity (i.e. "kinkfree" and constant slope curve) over a chip temperature of -40^{o} C to +60^{o} C. The cooler can provide an ambient-to-chip temperature differential of

approximately 40^{0} C as presently designed. Thus the maximum ambient temperature is approximately $+100^{0}$ C (chip at $+60^{0}$ C), well beyond the requirements of this program. Similarly, Hitachi and Laser Diode Laboratories are now also offering ILD packages with integral TE coolers, hermeticity, fiber pigtails, and an optical feedback port (back facet access).

One drawback to the ILD source is the presence of noise types not seen in LED systems. There are presently four identified noise types in laser driven single multimode fiber systems not associated with LED source driven systems. Three of these four noise types are of concern to this system. These three noise factors are laser noise, partition noise, and modal noise. The fourth noise type, delay noise, is of concern to very high data rate, (300 MHz) and long fiber (multikilometer) systems. The three noise types of concern are discussed in the following paragraphs.

The first noise type addressed is laser noise, which is defined as fluctuation of the total laser emission intensity. This noise is caused by a reflection of power back into the laser cavity, and is an external cavity effect. Transient thermal conditions on both the laser and the fiber affect the magnitude of this noise. The detected noise spectrum exhibits resonant peaks at intervals proportional to the distance to the reflection point, and reflected powers as low as 10^{-7} times the incident power[14] can affect primary emission intensity of the laser. For high data rates where the laser is not turned completely off during a "no signal" state, laser noise can dominate in either the LOW or HIGH state. Providing low loss connectors, especially at the source pigtail, alleviates this noise problem to some extent.

[14] E.J. Miskovic and P.W. Casper, "Noise Phenomena in High-Bit-Rate Fiber-Optic Systems, Proc of FOC-80, 14-16 Sep 80.

Partition noise from a laser requires a multimode emission from the laser, where the total emission intensity does not fluctuate, however the individual mode intensities fluctuate violently. Wavelength dependent losses from the fiber channel degrade the cavity mode intensity balance non-uniformly, and result in noisy pulses at the receiver. Single mode (CW) laser output can be driven into multimode emission with high speed modulation. This mode-hopping of the laser combined with thermal gradients, bias point changes of the laser, and wavelength dependent losses further aggravate the problem. Careful transmitter design is required to minimize environmental effects on the laser source.

Modal noise is fiber channel dependent, and requires some form of dynamic disturbance to the propagating modes. This dynamic disturbance can be a laser spectral instability, or some varying, mode-selective disturbance. This effect is primarily seen in the laser ON state. Some sources of modal noise are: differential thermal expansion or contraction coefficients, where the modal distribution changes with temperature changes; variation in the responsivity across the sensitive surface of a detector, coupled with mode pattern shifts; vibration of a fiber coupled with a varying misalignment of a connector in the vibration environment; or changes in the mode pattern emitted by the laser due to temperature gradient shifts, bias changes, aging, or other microscopic effects.

The effects of the above noise contributors are summarized for digital systems by stating that the eye diagram becomes more noisy in the ONE state, the eye closure worsens, the BER becomes highly data pattern dependent, and that more link margin may not help. To achieve higher tolerance of these noise types, the following example actions can be taken:

a. Lower the bit synchronizer (clock regeneration) detection threshold at the receiver to improve spectrum and modal noise tolerance.

b. Increase the bit synchronizer "Q" to improve receiver electrical noise immunity.

c. Lower the bit rate to improve noise tolerance to all sources.

d. Provide any repeaters with bit synchronizers.

This final paragraph shall present the survey data in tabular format for optical sources and briefly summarize those components which are most viable candidates for the AN/GYQ-21(V). Tables 3.2.3-1 and 3.2.3-2 provide information for LED and ILD source components. Based on previously discussed component criteria the following recommendations are presented.

The optical sources most promising for this application are:

- RCA C30133 GaAlAs DH LED
- Northern Telecom NT 40-3-15-2 GaAlAs DH LED
- Plessey HR982F GaAs:Zn Burrus LED
- Laser Diode Labs IRE 161 GaAlAs Burrus LED
- Fujitsu FLD080WA GaAlAs DH ILD
- General Optronics GOLH GaAlAs DH ILD and GOLS-1 DIP w/internal TE cooler
- NEC NDL3108P GaAlAs DH ILD

However, as mentioned, other devices being developed on DoD contracts should be closely monitored for application to any fabrication phase of this system. For example, the basic characteristics of the new Burrus LED (C0045) developed by Plessy under Air Force (AFAL) contract is also considered in the link budget calculations. This comment applies generally to all component areas.

Table 3.2.3-1. Light Emitting Diode Matrix

MANUFACTURER AND MODEL	DIODE TYPE	MATERIAL	I_{MAX} (mA)	RECOMMENDED CURRENT (mA)	POUT AT I_{RECOM} (mW)	B W or tr	λ (nm) (Δ λ)	EMISSION PATTERN	SOURCE SIZE	OPERATING TEMP (0^0C)	LIFE-TIME HOURS	HERMETIC	MIL SPEC	PACKAGE	COMMENTS
RCA															
C30119	DH	GaAlAs	200	200	.5	3 ns	850	LAMBERTAIN	25 μm	-40 to 90		NO	NO	STUD	
C30123	"	"	200	200	1	8 ns	830	"	62.5 μm	"		"	"	"	
C86011E	"	InGaAs	"	"	.2	10 ns	1060	"	"	"		"	"	"	
C30133	"	GaAlAs	"	"	.15	3 ns	820	PIGTAIL	DIAMETER	-40 to 60		"	"	"	Dupont 120 Pigtail
C86008E	"	"	"	"	.06	"	"	"	"	"		"	"	"	Siecor 1372
C86009E	"	"	"	"	.06	"	"	"	"	"		"	"	"	Siecor 112
C86013E	"	InGaAsP	"	"	.01	10 ns	1300	LAMBERTAIN	DIAMETER	-35 to 50		"	"	"	"
NORTHERN TELECOM															
NT40-3-10-2	DH	GaAlAs	300	150	22W/sr/cm^2	150 MHz	840(45)	LAMBERTAIN	75 μmDiam.	-40 to 85	10^5	NO	NO	STUD	
NT40-3-10-3	"	"	"	"	"	"	"	PIGTAIL	"	-40 to 85	"	"	"	"	Pigtail
NT40-3-15-2	"	"	"	"	33W/sr/cm^2	85 MHz	"	"	"	"	"	"	"	"	
NT40-3-15-3	DH	"	"	"		"	"	"	"	"	"	"	"	"	Pigtail
NT40-3-30-2	"	"	"	"		44 MHz	"	"	"	"	"	"	"	"	
NT40-3-30-3	"	"	"	"		"	"	"	"	"	"	"	"	"	Pigtail
SPECTRONICS															
SE-0352-003	Planer	GaAlAs	150	100	.2	12 ns	820(35)		PIGTAIL	-20 to 70	NO	NO	NO	To-46	Pigtail .3mA
SE-3352-003	"	"	"	100	.7	"	"	LAMBERTAIN	300 μm	"	"	"	"	To 5	
SE3353-001	"	"	"	100	1	"	"	22^0	Diameter 1140 μm Diameter	"	"	"	"	"	
VARIAN															
VLED106	DH	InGaAsP	100	50	.5	50 MHz	1060(65)			0 to 50	10^4	NO	NO		
VLED107	"	"	"	"	"	"	1270(90)			"	NO	NO	NO		
PLESSY															
HR103		InGaAs	300	300	10W/sr/cm^2	200MHz	1060(65)	LAMBERTAIN	50μmDia.	0 to 35		EPOXY		Stud	
HR952	Burrus	GaAs:Zn	"	"	15W/sr/cm^2	30MHz	900(30)	"	"	-40 to 125	10^5(10^{9*})	"	NO	"	
HR952F	"	"	"	"	.017	"	"	PIGTAIL	-	-2 to 50	"	"	"	"	Pigtail, .16 mA
HR953	"	"	"	"	30W/sr/cm^2	"	"	LAMBERTAIN	50μmDia.	-40 to 125	"	"	"	"	" "
HR953F	"	"	"	"	.035	"	"	PIGTAIL	-	-20 to 50	"	"	"	"	
HR954	"	"	"	"	40W/sr/cm^2	"	"	LAMBERTAIN	50μmDia.	-40 to 125	"	"	"	"	" "
HR954F	"	"	"	"	.06	"	"	PIGTAIL	-	-20 to 50	"	"	"	"	
HR982	"	"	"	"	17W/sr/cm^2	180MHz	"	LAMBERTAIN	50μmDia.	-40 to 125	"	"	"	"	" "
HR982F	"	"	"	"	.015	"	"	PIGTAIL	-	-20 to 50	"	"	"	"	

Table 3.2.3-1. Light Emitting Diode Matrix (Continued)

MANUFACTURER AND MODEL	DIODE TYPE	MATERIAL	I_{MAX} (mA)	RECOMMENDED CURRENT (mA)	POUT AT I_{RECOM} (mW)	B.W. or tr	λ (nm) (Δ λ)	EMISSION PATTERN	SOURCE SIZE	OPERATING TEMP (°C)	LIFE-TIME HOURS	HERMETIC	MIL SPEC	PACKAGE	COMMENTS
FUJITSU															
FED080FA	DH	AlGaAs	150	100	.25	60MHz	840(40)		PIGTAIL	-40 to 90					810 to 860 nm
HITACHI															
HLP-20	Dome	AlGaAs	250	200	20	12ns	840(30)	180°	600 µm DIAMETER	to 60°		NO	NO	SEVERAL	
HLP-30	"	"	"	"	30	"	"	"	" "	"		"	"	"	
HLP-40	"	"	"	"	40	"	"	"	" "	"		"	"	"	
HLP-50	"	"	"	"	50	"	"	"	" "	"		"	"	"	
HLP-60	"	"	"	"	60	"	"	"	" "	"		"	"	"	
LASER DIODE LABS															
IRE-150	MH	AlGaAs	150	100	1.5	7 ns	820(35)		230 µm	to 50		Y	NO	TO -5 TO -18	PIGTAIL AVAILABLE
IRE-151	MH	"	200	200	0.8	8 ns	"		230 µm	"		w/o			
IRE-152	MH	"	125	100	0.7	7 ns	"		150 µm	"		Pigtail			
									25 µm			"			
									100 µm			"			
IRE-161	MH	"	150	100	1.5	10 ns	870(45)		100 µm	-40to85		Y	"	TO -46	2nd HARMONIC -40dB
MATH ASSOCIATES															
E 1500			100	100	10	10 ns	890	40		-40 to 50		NO	NO	TO -18	PIGTAIL AVAILABLE
MITSUBISHI															
ME 1005	DH	AlGaAs-GaAs	75	50	1.5	50MHz	840(45)	40°		-40 to 100	Yes	NO	NO	LEADS	800 to 880 nm
ME 1013 C	"	"	"	"	"	"	"	"		"	"	"	"	"	"
ME 1203L, 1303L	"	"	100	"	"	"	"	"		"	"	"	"	STUD	
ME 1203F, 1303F	"	"	"	"	.03	"	"	"		-40 to 70	"	"	"	"	PIGTAIL
NEC															
NDL 4103	DH	AlGaAs	200	100	3	10ns	850(40)	LAMBERTAIN	60 µm Diameter	-30 to 80		Epoxy	NO	TO -18	
NDL 4103CP	"	"	"	"	.2	"	"	FIGTAIL	100 µm Dia.			"	NO		PIGTAIL
OD 8358						40MHz	850(45)	LAMB	100 µm Diameter					PANEL MOUNT	SMA CONNECTOR
ITT															
T-820	DH	GaAlAs	100	100	.04	15ns	840(40)	PIGTAIL	1µm x 70µm	-40 to 75		NO	NO	STUD	VARIOUS PIGTAILS AVAILABLE

Table 3.2.3-2. Injection Laser Diode Matrix

MANUFACTURER AND MODEL	DIODE TYPE*	MATERIAL	I MAX (MA)	I THRES HOLD (MA)	REC CURRENT (MA)	POUT AT I REC (MW)	B.W. OP tr	HARMONICS (dB)	λ (nm) (Δ λ)	EMMISSION PATTERN (DEGREES)	SOURCE SIZE (μm)	OPERATING TEMPERATURE RANGE (°C)	LIFETIME (HOURS)	HERMETIC	MIL SPEC	PACKAGE	COMMENTS
AEG - TELEFUNKEN																	
CQX-20		AlGaAs		200	300	5	1 ns		820 (2.5)	10 X 50						STUD	
FUJITSU																	
FLD080WA	DH	Al Ga As	200	120	155	8	1 ns		830 (1)	10 X 50		-40 to 70		YES	NO	STUD	BACK FACET MONITOR
GENERAL OPTRONICS																	
GOLS		GaAlAs	150	100	120	5	.7	2nd: -40 3rd: -50	830 (1)	10 X 45		-50 to 70	1E5	NO	NO	NONE	MOUNTED ON HEAT SINK, BUT NOT PACKAGED 800 to 870 nm AVAIL.
GOLH		"	150	100	120	5	.7	2nd: -40 3rd: -50	830 (1)	10 X 45		-50 to 70	1E5	YES		TO - 8	INTERNAL BIAS STABILIZATION CIRCUIT
GOLS-1 DIP		"	150	100	120	2.5	7	2nd: -40 3rd: -50	830 (1)	PIGTAIL		-50 to 70	1E5	NO	NO	DIP	GOLS DEVICE WITH TE COOLER IN DIP
HITACHI																	
HLP 1700	DH	Ga Al As		70	95	5	.5 ns		830 (1)	10 X 30		-40 to 50	1E5	NO	NO	SEVERAL	
HLP 1500	DH	Ga Al As		70	95	3	.5 ns		830 (1)	PIGTAIL		-40 to 50	1E5	NO	NO	SEVERAL	
HLP 2700	BH	Ga Al As		20	25	1.5	.5 ns		830 (1)	25 X 35		-40 to 50	1E5	NO	NO	SEVERAL	
HLP 2500	BH	Ga Al As		20	25	.8	.5 ns	-45	830 (1)	PIGTAIL		-40 to 50	1E5	NO	NO	SEVERAL	
HLP 3500	BH	Ga Al As		35	50	2	.5 ns	-50	830 (1)	PIGTAIL		-40 to 50	1E5	NO	NO	SEVERAL	
HLP 3700	BH	Ga Al As		35	50	6	.5 ns		830 (1)	25 X 35		-40 to 50	1E5	NO	NO	SEVERAL	
ITT																	
T-912	DH	Ga Al As	200	160	200	.5	1.5		840 (4)	PIGTAIL	1 m x 20 m	0 to 50		NO	NO	STUD	VARIOUS PIGTAIL AVAILABLE
LASER DIODE LABS																	
LCW-10	DH	Ga Al As	160	100	150	10	-1 ns		830 (2.5)	10 X 35	.2 x 7	0 to 60		NO	NO	STUD	800 nm to 900 nm AVAL
LCW-10F	DH	Ga Al As	160	100	150	1.5	-1 ns		830 (2.5)	PIGTAIL	.2 x 7	0 to 60		"	"	STUD	55 nm/125 nm PIGTAIL
SCW-20	DH	Ga Al As	110	60	85	7.5	-1 ns		830 (1)	10 X 35	.2 x 7	0 to 60		"	"	STUD	PIGTAIL AVAILABLE
MATH ASSOCIATES																	
E2000			300	200	300	7	.5 ns		820 (2.5)	7 X 7	16 x 16	-40 to 50	NO				
E2004			300	200	300	14	.5 ns		820 (2.5)	7 X 7		-40 to 50	NO				

* DH - DOUBLE HETEROSTRUCTURE BH - BURIED

Table 3.2.3-2. Injection Laser Diode Matrix (Continued)

MANUFACTURER AND MODEL	DIODE TYPE	MATERIAL	I MAX (MA)	I THRESHOLD (MA)	REC. CURRENT (MA)	POUT AT I REC. (MW)	G,W OR tr	HARMONICS (dB)	λ (nm) (Å)	EMISSION PATTERN (DEGREES)	SOURCE SIZE (μm)	OPERATING TEMPERATURE RANGE (°C)	LIFETIME (HOURS)	HERMETIC	MIL SPEC	PACKAGE	COMMENTS
MITSUBISHI																	
ML 2201	DH	Al Ga As/Ga As		30	40	3	26 Hz	- 50	830	10 X 40	2 x .4	-40 to 50	1E5	NO	NO	STUD	
ML 2205	DH	"		30	40	3	26 Hz	- 50	830	10 X 40	2 x .4	-40 to 50	1E5	NO	NO	STUD	
ML 2205F	DH	"		30	40	.7	26 Hz	- 50	830	10 X 40	2 x .4	-40 to 50	1E5	NO	NO	STUD	PIGTAIL
ML 2307	DH	"		30	40	3	26 Hz	- 50	830	10 X 40	2 x .4	-40 to 50	1E5	NO	NO	LEADS	
ML 7201X	DH	In Ga As P/In P		120	150	3	26 Hz		1300	10 X 40		-40 to 50	1E5	NO	NO	STUD	BACK FACET MONITOR AVAILABLE
NEC																	
NDL 3108	DH	Al Ga As	200	105	135	8	5 ns		830 (1.5)	10 X 40	.3x15	-40 to 65	10^5	YES	NO	STUD	MONITOR OUTPUT
NDL 3109P	DH	Al Ga As	200	105	135	2.5	.5 ns		830 (1.5)	10 X 40	3x15	-40 to 65	10^5	YES	NO	STUD	PIGTAIL, MONITOR OUTPUT
NDL 3205	DH	Al Ga As	150	65	90	5	.5 ns	- 30	860 (1)	10 X 30	0.5x2.5	-40 to 65	10^5	YES	NO	STUD	SINGLE MODE
NDL 3205 P	DH	Al Ga As	150	65	90	2	.5 ns	- 30	860 (1)	10 X 30	0.5x2.5	-40 to 65	10^5	YES	NO	STUD	PIGTAIL, SINGLE MODE
NORTHERN TELECOM																	
NTL-5 2	DH	Ga Al As	250	120	190	5	.2 ns		830 (3)	14 X 50		-40 to 85				STUD	
RCA																	
C 30127	DH	Ga Al As	400	250	300	10	1 ns		820	10 x 40	2 x 13	-35 to 50		NO	NO	STUD	
C 30130	DH	Ga Al As	400	250	300	10	1 ns		820	10 x 40	2 x 13	-35 to 50		NO	NO	STUD	
C 86000 E	DH	Ga Al As	200	75	100	7	1 ns		820	10 x 40	2 x 13	-35 to 50		NO	NO	STUD	
C 86014 E	DH	Ga Al As	150	75	100	7	1 ns		820	10 x 40	2 x 13	-35 to 50		NO	NO	STUD	
C 86002 E	DH	Ga Al As	300	175	200	1.5	1 ns		820		2 x 6	-35 to 50		NO	NO	STUD	PIGTAIL
C 96006 E	DH	Ga Al As	400	250	200	2	1 ns		820		100Dia	-35 to 50		NO	NO	STUD	PIGTAIL
C 96007 E	DH	Ga Al As	400	250	300	4	1 ns		820		200Dia	-35 to 50		NO	NO	STUD	PIGTAIL
C 86010 E	DH	Ga Al As	400	250	300	2	1 ns		820		62.5Dia	-35 to 50		NO	NO	STUD	PIGTAIL

3.3 Optical Fibers and Cables

A wide selection of optical fibers exist today, with various fiber types supporting various data rates (or signal bandwidths, for analog systems) and various link lengths. The AN/GYQ-21(V) application requires a bandwidth-length product of ~30 MHz-km. Unlike metallic cables, optical fibers exhibit linear dependence on length for a given bandwidth. Metallic cables exhibit an approximate square law dependence on length, i.e., bandwidth-length times length. Thus for high data rate systems optical fibers are attractive since doubling the link length merely halves the bandwidth of a given system.

Three basic types of optical fibers are available: the step index, multimode fiber; the graded index, multimode fiber; and the single mode (step index) fiber. Several types of step index fibers are available, including all plastic fiber, plastic clad silica (or PCS), and glass-on-glass step index fiber. Step index fibers are usually limited in bandwidth-length products to less than 10 MHz-km. The notable exceptions are the Japanese small core fibers (~25 μm core diameters) that support 25-50 MHz-km bandwidth-length products.

An alternative to step index fibers is graded index fibers which offer bandwidth-length products of 200 MHz-km to more than 1 GHz-km. Graded index fibers have smaller numerical apertures (NA) and couple less power from the source. The higher bandwidth-length products are only achievable with laser sources due to source linewidth and rise time considerations. Any of the graded index fibers will support the AN/GYQ-21(V) data bus network.

Another alternative to step index fibers is the "quasi-step" index fibers. These "quasi-step" fibers support bandwidths of 20-50 MHz in the lengths envisioned for the AN/GYQ-21(V) system requirements. These "quasi-step" fibers also have larger numerical apertures than the graded index fibers (NA ~0.3 vice ~0.25, or a 44 percent increase in coupled power).

These fibers are attractive for this application, since light emitting diode (LED) sources can couple significantly more power into quasi-step fibers than into graded index fibers. The use of LED sources, if feasible, is attractive since it avoids the problems of laser noise.

The cable selection criteria for the AN/GYQ-21(V) will consider the following:

- Large core and large NA (within the bandwidth limitations) to maximize the source coupled power
- Cable attenuation does not necessarily have to be ultra low, since cable losses of one kilometer are not significant.
- Rugged jacket and cable design

To evaluate cables with these selection criteria, first consider the available choices of optical cable. Basically, there are three families: 1) all plastic, 2) all glass and 3) plastic clad silica (PCS).

3.3.1 All Plastic Fiber

Desirable properties of all plastic fiber are large size, inherent freedom from fracture, easy to work with, inexpensive and so forth. However, these fibers are designed for very short distances ($\leq$10 m) since the losses are 500 to 1000 dB/km. Thus, even for the minimum link distances of 100 meters, the cable loss would be 50 to 100 dB. Therefore, based on loss alone, these fibers can be excluded. It should also be recognized that high temperatures also present an operational problem to some plastic fiber cable, although the anticipated 50^{o} C ambient is well within the limitations of plastic fibers.

3.3.2 All-Glass Fiber

The second cable to be considered consists of all-glass fibers and may be further subdivided into:

- Multimode step index - losses of 10 dB/km or less and bandwidths of 10 to 15 MHz-km are available. The use of "quasi-step" index fibers raises the attainable bandwidth length product to ~50 MHz-km. These fibers are evolving to meet many short distance light duty applications such as intrabuilding computer links. Reasonable coupling efficiencies are obtained through moderate core diameters (100-150 μm) and numerical apertures of 0.25 to 0.30. Also the all-glass construction offers good temperature performance.

- Single mode step index - designed for ultra low loss and maximum bandwidth operation (~1 dB/km, ~10 GHz-km). Small cores (5-10 μm) and low NA inhibit all but the most specialized optical sources in terms of efficient coupling. Also, these single mode cables place stringent manufacturing tolerances on connector designs to avoid high throughput losses. Recall that since this cable is aimed toward trunking, a minimum number of connectors (typically two) is required and higher termination losses can be tolerated. However, this is counterproductive in data bus applications.

- Multimode graded index - this fiber cable is presently the "practical substitute" for single-mode fiber. Attenuations of 5 dB/km and bandwidths of ~1 GHz-km are readily available. Core diameters are 50 to 65 μm with numerical apertures of ~0.20 available. For reasons similar to those cited above, graded index (GRIN) cables do not offer any advantages over multimode step index (or "quasi-step") fibers within the "local distribution environment" unless large bandwidths are required or a long drop is anticipated.

Thus for the all-glass fiber family the moderate sized fibers are the most attractive, with graded index fibers a possible second choice if adequate link margin is available.

3.3.3 Plastic Clad Silica Fiber

The third and final cable type employs the plastic clad silica (PCS) fiber which is usually composed of a core of pure fused silica and a polymer (or "plastic") cladding (normally silicone). PCS cables combine some of the more attractive characteristics of plastic fiber and glass "fat" fiber. Losses of 8-10 dB/km are readily available with NA's of 0.35 or greater depending on core size and cladding composition. The higher NA reduces practical bandwidths to ~20 MHz-km. To date the basic performance is comparable to that of the step indexed fibers; however, the advantage of PCS is the availability of larger core diameters (200-600 μm). It is appropriate to point out that PCS fiber cable does have its disadvantages such as: 1) more difficult to terminate because of soft silicone cladding, and 2) increased optical losses at low temperatures. Both of these factors shall be discussed next.

3.3.4 Temperature Performance of Plastic Clad Silica

Researchers have long known that plastic clad silica (PCS) offers attractive advantages over doped silica all-glass fibers. Unfortunately, PCS typically suffers increasing optical losses below -20° C to -30° C where the polymer cladding begins to increase in refractive index. At approximately -75° C the index of the cladding equals the core and waveguiding ceases (for all practical purposes).

For several years manufacturers have been trying to provide a polymer with the proper index of refraction which is basically stable at low temperature. Until recently, the hard cladding DuPont PIFAX S120 fiber cable offered the best temperature performance with losses of ~30 to 40 dB/km at -55° C. However, the intrinsic losses of the fiber are ~30 dB/km for a total (induced plus intrinsic) loss, due to temperature, of ~70 dB/km. This fiber is very attractive in terms of terminations since the cladding is a hard resin with hytrel coating that allows crimp-on or epoxy connectorization with good core/cladding concentricity.

Today two manufacturers (MAXLIGHT and Quartz Products Corp.) offer a low loss (≤8 dB/km) PCS fiber with low temperature-induced losses and in both cases the excess induced loss at -55° C is predicted to be less than 10 dB/km. Figure 3.3.4-1 shows a representative plot of fiber attenuation as a function of operating wavelength.

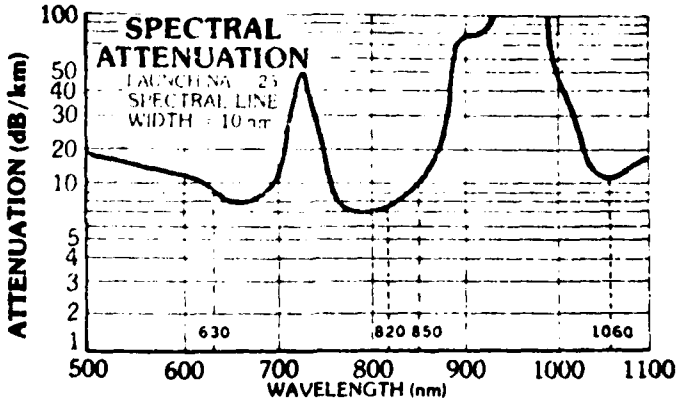

Figure 3.3.4-1. Plot of Fiber Attenuation Versus Wavelength

The KSC 200 fiber performance over temperature is shown in Figure 3.3.4-2. Thus, typical total losses are approximately 18 dB/km or less. The Cabled Fiber Matrix, Table 3.3.4-1, provides the basic characteristics of the above mentioned fibers together with other cable types as surveyed for the AN/GYQ-21(V) application.

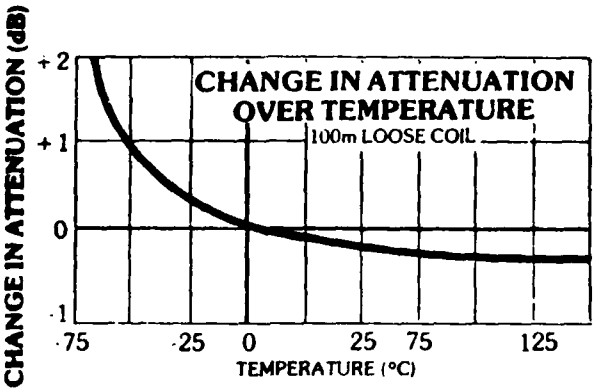

Figure 3.3.4-2. PCS Fiber Performance Over Temperature (MAXLIGHT KSC 200A)

Finally, a few brief comments on the mechanical aspects of fiber cable are appropriate. Such factors as temperature, shock, vibration, humidity, etc., all influence the cable construction. However, with a few special considerations (i.e., buffering, tensile stress during stranding, etc.), most fiber cable can be manufactured using conventional technology and materials to achieve tensile strength,* flame resistance, flexibility, etc., required for a military environment. As an example of cabling performance, consider the following description of a cable design developed for MAXLIGHT's 200 μm core PCS fiber to be used within a military environment.

*Fiber cables do typically employ nonmetallic strength members to maintain the "all dielectric" property of the cable.

Table 3.3.4-1. Fiber-Optic Cable Matrix

MANUFACTURER AND PART NUMBER	INTRINSIC LOSS (dB/km)	NUMERICAL APERTURE	CORE SIZE (CLAD SIZE) (μm)	BANDWIDTH OR DISPERSION	FIBER TYPE	FIBER MATERIALS CORE (CLAD)	CABLE MATERIALS	CABLE SIZE O.D. (mm)	CABLE WEIGHT (g/m)	CABLE TENSILE STRENGTH (kg) BEND RADIUS (cm)	OPERATING TEMPERATURE RANGE (°C)	MIL SPEC	CONNECTORS	COMMENTS
BELDEN														
225001	10 (820nm)	0.21	62.5 (125)	200 MHz-km	SG		KEVLAR, PVC	3.8	13.5	113 (3)				MULTI-FIBER CABLES AVAILABLE
220001	10 (850nm)	0.22	200 (400)	25 MHz-km	PCS	S (P)	KEVLAR, PVC	3.8	13.5	113 (3)				MULTI-FIBER CABLES AVAILABLE
221001	10 (850nm)	0.22	300 (440)	300 MHz-km	PCS	S (P)	KEVLAR, PVC	3.8	13.5	113 (3)				MULTI-FIBER CABLES AVAILABLE
CAMSTAR														
TIP-200	20 (810nm)	0.34	200 (280)	20 ns/km	PCS	S (P)	ARAMID FIBER, PVC	3	13	80 (4)	-20 to 55	NO	NO	MULTI-FIBER CABLES AVAILABLE
LIP-250	12 (810nm)	0.34	250 (325)	20 ns/km	PCS	S (P)	ARAMID FIBER, PVC	4	15	80 (4)	-10 to 30	NO	NO	MULTI-FIBER CABLES AVAILABLE
LIS-90	18 (930nm)	0.25	90 (125	15 ns/km	SS	S (DS)	ARAMID FIBER, PVC	4	15	80 (4)	-20 to 55	NO	NO	MULTI-FIBER CABLES AVAILABLE
LIS-100	18 (930nm)	0.25	100 (140)	15 ns/km	SS	S (DS)	ARAMID FIBER, PVC	4	15	80 (5)	-20 to 55	NO	NO	MULTI-FIBER CABLES AVAILABLE
DIG-062	12 (820nm)	0.21	62 (125)	800 MHz-km	SG	S (DS)	KEVLAR, PVC	4.5	18	40 (15)	-10 to 30	NO	NO	MULTI-FIBER CABLES AVAILABLE
DUPONT														
S-120	40 (790)	0.42	200 (600)	40 ns/km	PCS	S (P)	KEVLAR HYTEREL	2.4	4	65 (.15)		NO	YES	TWO FIBER CABLES ALSO AVAILABLE
S-120/TYPE 30	30 (820)	0.42	200 (600)	40 ns/km	PCS	S (P)	KEVLAR HYTEREL	2.4	6	65 (.15)	-53 to 75	NO	YES	TWO FIBER CABLES ALSO AVAILABLE
S-120/40C	40 (820)	0.42	200 (600)	40 ns/km	PCS	S (P)	HYTEREL	1.25	3	16 (.32)		NO	YES	TWO FIBER CABLES ALSO AVAILABLE
FIBER OPTIC CABLE														
01-1-10	20 (820nm)	0.25	125 (250)	30 ns/km	SS	S (DS)	HYTEREL			10 (2)				10 M LENGTHS

KEY: PCS: PLASTIC CLAD SILICA SG: GRADED SILICA SS: STEP INDEX SILICA S: SILICA DS: DOPED SILICA

Table 3.3.4-1. Fiber-Optic Cable Matrix (Continued)

MANUFACTURER AND PART NUMBER	INTRINSIC LOSS (dB/km)	NUMERICAL APERTURE	CORE SIZE (CLAD SIZE) (μm)	BANDWIDTH OR DISPERSION	FIBER TYPE	FIBER MATERIALS CORE (CLAD)	CABLE MATERIALS	CABLE SIZE O.D. (mm)	CABLE WEIGHT (g/m)	CABLE TENSILE STRENGTH (kg) BEND RADIUS	OPERATING TEMPERATURE RANGE (°C)	MIL. SPEC.	CONNECTORS *	COMMENTS
GALILEO														
4000-LC (S)	15 (820)	.4	204 (305)	10 MHz-km	PCS	S (P)	TEFZEL, KEVLAR	4.2	14.6	50 (1.9)	-55 to 150	NO	YES	Cable designs using Tefzel jacket and fiberglass strength member meet temperature requirements of MIL SPEC. Not formally qualified.
5000-1 (S)	7 (900)	.21	63 (125)	15 MHz-km	SS	S (DS)	TEFZEL, KEVLAR	4.2	14.6	50 (1.9)	-55 to 150	NO	YES	
5020 (S)	7 (900)	.25	125 (200)	13 MHz-km	SS	S (DS)	TEFZEL, KEVLAR	4.2	14.6	50 (1.9)	-55 to 150	NO	YES	
5050 (S)	7 (900)	.30	100 (140)	25 MHz-km	SG	S (DS)	TEFZEL, KEVLAR	4.2	14.6	50 (1.9)	-55 to 150	NO	YES	
6000-A1 (S)	3 (900)	.21	63 (125)	700 MHz-km	SG	S (DS)	TEFZEL, KEVLAR	4.2	14.6	50 (1.9)	-55 to 150	NO	YES	
6000-B1 (S)	5 (900)	.21	63 (125)	700 MHz-km	SG	S (DS)	TEFZEL, KEVLAR	4.2	14.6	50 (1.9)	-55 to 150	NO	YES	
GENERAL CABLE														
4400 (AT)	6 (820)	0.21	65 (125	400 MHz-km	SG	S (DS)	PVC	28	740	400 (3)	-20 to 60	NO	YES	1 to 24 FIBERS
4423	6 (820)	0.21	65 (125)	400 MHz-km	SG	S (DS)	PVC	13	82	45 (1.5)	-20 to 60	NO	YES	1 to 12 FIBERS
HEWLETT-PACKARD														
HPFBR 3001	10 (820)	.3	100 (140)	12 MHz-km	SS	S (DS)		2.5	7.7	30 (0.7)	0 to 70	NO	YES	100 M MAX LENGTH
NORTHERN TELECOM														
NTF-B-1	3.8 (840)	.22	95 (145	200 MHz-km	SG	DS (S)	A1 POLYETHELENE	6	30	30	-40 to 40			1 or 2 FIBERS
NTF-C-1	3.8 (840)	.22	95 (145)	200 MHz-km	SG	DS (S)	A1 POLYETHELENE STEEL	6	140	200	-40 to 40			1 or 2 FIBERS
OPTELECOM														
QK 101	15 (800)	.31	200 (600)	15 MHz-km	PCS	S (P)		3	18	40 (5)	0 to 55	NO	YES	
QK 101	10 (800)	.31	100	15 MHz-km	SG	S (DS)		3	13	45 (6)	-20 to 55	NO	YES	
QK 101	15 (800)	.31	200 (600)	15 MHz-km	PCS	S (P)		3.5	21	200 (10)	-10 to 55	NO	YES	

* Refers to availability of connectors from (or through) cable vendor.

Table 3.3.4-1. Fiber-Optic Cable Matrix (Continued)

MANUFACTURER & PART No.	INTRINSIC LOSS (dB/km)	NUMERICAL APERTURE	CORE SIZE (CLAD SIZE) (μm)	BANDWIDTH OR DISPERSION	FIBER TYPE	FIBER MATERIAL CORE (CLAD)	CABLE MATERIALS	CABLE SIZE OD (mm)	CABLE WEIGHT (kg/m)	CABLE STRENGTH (kg) BEND RADIUS (cm)	OPERATING TEMP RANGE (°C)	MIL SPEC	CONNECTORS *	COMMENTS
PILKINGTON														
204 205	20(900) "	.25 "	188 (244) 113 (140)		SS	S (DS)	Tefzel,PVC	1.5		1 b(7) 6(4)				
QUARTZ PRODUCTS														
QSF-A-125	8(850)	.22	125 (300)	30 MHz-km	PCS	S (P)	-				-55to106	NO	NO	Fiber only, cabled by
-200	"	"	200 (380)	25 MHz-km	"	"	-				"	NO	NO	Belden, Boston
-300	"	"	300 (440)	20 MHz-km	"	"	-				"	NO	NO	Insulated Wire and
-400	"	"	400 (550)	5 MHz-km	"	"	-				"	NO	NO	Cable Low Temp (55°) with
-600	"	"	600 (750)	9 MHz-km	"	"	-				"	NO	NO	Resin A
RANK OPTICS														
PCS 1	30 (820)	24	250	22 MHz-km	PCS	S (P)		1	12	10 (1)				
SUMITOMO														
FT	8 (830)	.25	150 (350)	15 ns/km	SS	S (S)				100(2.5)				
CT	12 (830)	.20	60 (150)	20 ns/km	SS	S (S)				100(2.5)				
THOMAS & BETTS														
TIS 1601	6	.2	50 (125)	300 MHz-km	SG	S (DS)	Acetal, Polyurethane	6		30 (H)	40 to 120		YES	
TIS 1501	6	.2	50 (125)	30 MHz-km	SS	S (DS)	" "	6		25 (8)	-40 to 120		"	
TAF P2200-01	25	.19	200 (400)	30 MHz-km	PCS		Tefzel	4.5		25 (8)	-40 to 120		"	
TIMES FIBER														
SZ-50	7 (820)	16	90 (125)	50 MHz-km	SS	S (DS)				91 (4)	-20 to 60	NO	YES	
GS-250	5 (820)	"	" "	250 MHz-km	SG	"				"	" "	"	"	
G6-600	6 (820)	"	" "	600 MHz-km	SG	"				"	" "	"	"	1 to 10 Fibers Per Cable
G7-250	7 (820)	"	" "	250 MHz-km	SG	"				"	" "	"	"	
G8-600	8 (820)	"	" "	600 MHz-km	SG	"				"	" "	"	"	
MARELCHT														
RSC 200A	7 (820)	36	200(300)	24MHz-km	PCS	S (P)	Custom	2.4	6	101 (.5)	-55to100 continuous	TESTING		Standard cable jacketing or UV inhibited and flame retardant. NA is for exit after 500 meters of fiber.
RSC 200B	8 (820)	36	200(300)	24MHz-km	PCS	S (P)	Custom	2.4	6	101 (5)	55to80			
BRAND-REX														
Type V	8 (850) 8 (850)	.22	200(380)	30MHz-km	PCS	S (P)	Custom							Custom designed cables with choice of PCS, SG, or SS fibers

* Refers to availability of connectors from (or through) cable vendor.

Table 3.3.4-1. Fiber-Optic Cable Matrix (Continued)

MANUFACTURER AND PART NO.	INTRINSIC LOSS (dB/km)	NUMERICAL APERTURE	CORE SIZE (CLAD SIZE) (μm)	BANDWIDTH OR DISPERSION	FIBER TYPE	FIBER MATERIAL CORE(CLAD)	CABLE MATERIALS	CABLE SIZE O.D. (mm)	CABLE WEIGHT (g/m)	CABLE TENSILE STRENGTH (kg)(BEND RADIUS)(cm)	OPERATING TEMP. RANGE (°C)	MIL SPEC	CONNECTORS *	COMMENTS
VALTEC														
PC08-02	15 (800)	.3	200 (325)	25MHz-km	PCS	SC(P)	KEVLAR, POLYURETHANE	6 x 9	43	50 (5)	-20 to 85	NO	YES	Medium duty cable data listed. Available in up to 6 fibe cable.
PC10-02	12 (800)	.3	250 (350)	25MHz-km	PCS	S (P)	"	6 x 9	"	50 (5)	-20 to 85	NO	YES	
MG05-02C	6 (800)	.3	625 (125)	200MHz-km	SG	DS (DS)	"	6 x 9	"	50 (5)	-20 to 85	NO	YES	
SIECOR														
142	10 (820)	.3	100 (140)	20MHz-km	SG	DS (DS)	HALAR, POLYURETHANE KEVLAR	4.8	24	40 (15)	-25 to 65	NO	YES	
112	10 (820)	.21	63 (125)	200MHz-km	SG	DS (DS)	"	4.8	24	40 (15)	-20 to 50	NO	YES	6 and 10 fiber cables available also.
122	6 (820)	.21	"	400MHz-km	SG	DS (DS)	"	4.8	24	40 (15)	-20 to 50	NO	YES	
LTT														
T 2501	10 (820)	.3	125 (300) and 200 (350)	30ns/km	PCS	S (P)	KEVLAR, POLYURETHANE	9	39	150 (5)	-55 to 85	NO	YES	Up to 19 fibers per cable. Choice of PCS, SG or SS fibers.
FORT														
TIS-LG	6 (820)	.2	50 (125)	300MHz-km	GS	S (S)	POLYURETHANE, HYTREL, PVC	6		25 (8)	-40 to 90	NO	YES	Other fiber/ combinations available
MVM-LS	10 (820)	.2	50 (125)	60 MHz-km	SS	S (S)	"	4.5		25 (8)	"	NO	YES	
TAF-PZ	25 (820)	19	200(400)	30 MHz-km	PCS	S (P)	TEFZEL, HYPREL HYTREL, PVC	4.5		25 (8)	-40 to 120	NO	YES	

* Refers to availability of connectors from (or through) cable vendor.

Typical cable designs may contain one or multiple fibers of various sizes within an overall sheath. The MAXLIGHT cable, for example, uses 200 micrometer optical fibers; each drawn from extremely pure fused silica and coated with RTV type silicone. The coating layer functions as an optical cladding and primary protection for the fiber as well as a protection against any roughness which may cause microbending. In addition, the coating must provide a plastic to glass interface with adequate humidity, radiation, and cold temperature performance. Although plastic clad fibers are not recommended for the AN/GYQ-21(V) application, it is instructive to review the mechanical performance parameters of the MAXLIGHT cable, since they are in consonance with military testing programs.

Each cladded fiber is jacketed with a "snug" ETFE jacket (see Figure 3.3.4-3). A loosely jacketed fiber slips easily inside the jacket causing spiralling of the fiber under load cycling and may be damaged or fractured if the jacket should be kinked by bending; however, the specific construction is usually application dependent. Most jacketing is designed to function under pressure, flexing tension, and through a wide range of environmental conditions, and provides protection of the fiber by the strength member, eliminating any large increase in attenuation under environmental stress conditions.

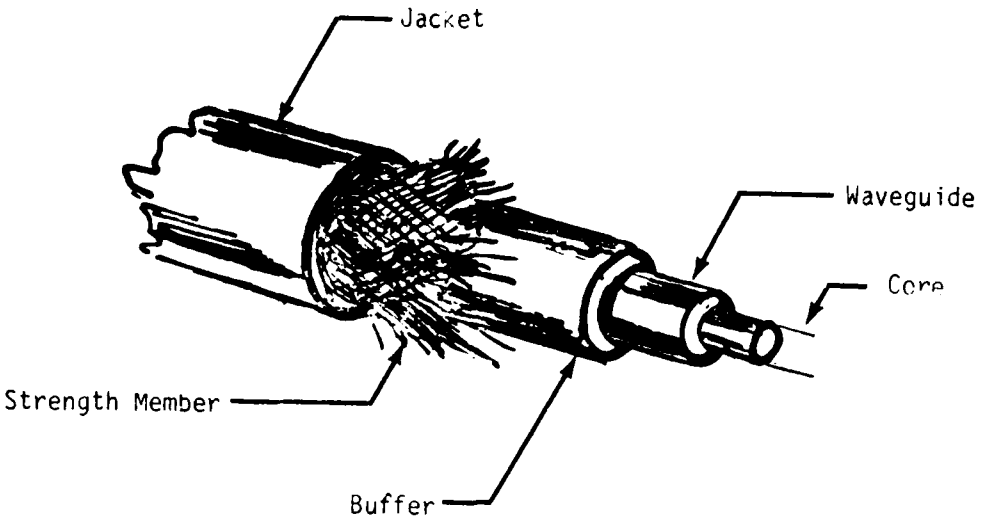

Figure 3.3.4-3. Rugged Cable Construction

Table 3.3.4-2 lists a summary of some of the test results generated on the individual sub-cables designed by MAXLIGHT:

Table 3.3.4-2. Mechanical Testing of Optical Cable

Test	Results
Humidity: MIL-STD-202 Modified Method 106, 10 Days (85° C, -10° C)	2.0 dB/km increase
Flexibility: DOD-STD-1678 Method 2010 except weight 2 kg	100,000 cycles Fiber and cable. No visible damage
Minimum Bend Radius	3.2 mm radius. 0.16 dB increase
Tensile	60 kg f
Temperature aging at 100° C Two 1 hour exposures	0.7 dB/km change
Cable Jacket Shrinkage	0.2% both ends, 1 meter length
Water Soak	3.0 dB/km increase

These cable test results may be taken as representative of other optical cable mechanical testing results. Plastic clad silica fibers do pose serious constraints on operation at low temperatures, however, the bandwidth requirement of the postulated AN/GYQ-21(V) network eliminates PCS from consideration. Additionally, termination considerations also must be addressed since maintaining concentric alignment of the cladding and core with soft cladding material represents a technical issue not laid to rest. These termination considerations are reviewed in Paragraph 3.4 for completeness.

Finally, it is important to consider the details of providing strength members within the optical cable. As mentioned, the strength member is typically a nonmetallic material to maintain the cable's all-dielectric characteristic. Two types of materials are typically used (1) Kevlar and (2) fiberglass. The actual construction techniques of cabling are usually applicable to any type of optical fiber cable; however, certain industry tests have indicated that cable performance varies with structure. For example, McDonnel Douglas has tested optical cabling and results indicate that under thermal shock conditions a fiberglass strength member is more desirable than Kevlar. The reason is that Kevlar has an opposite expansion coefficient to that of glass and under thermal shock the cable may fail. One cable structure, manufactured by Galite, uses a fiberglass strength member and has passed this particular thermal shock test without incident. Thus some consideration of cable design may be necessary by manufacturers when supplying fiber-optic cable for military systems where thermal shock conditions are anticipated (or possible).

AD-A108 394 HARRIS CORP MELBOURNE FL GOVERNMENT COMMUNICATION SY--ETC F/G 17/2
FIBER OPTIC DATA BUS FOR THE AN/GYQ-21(V),(U)
JUN 81 R E DRAGOO, D B KIMSEY F30602-79-C-0218
UNCLASSIFIED RADC-TR-81-153 NL

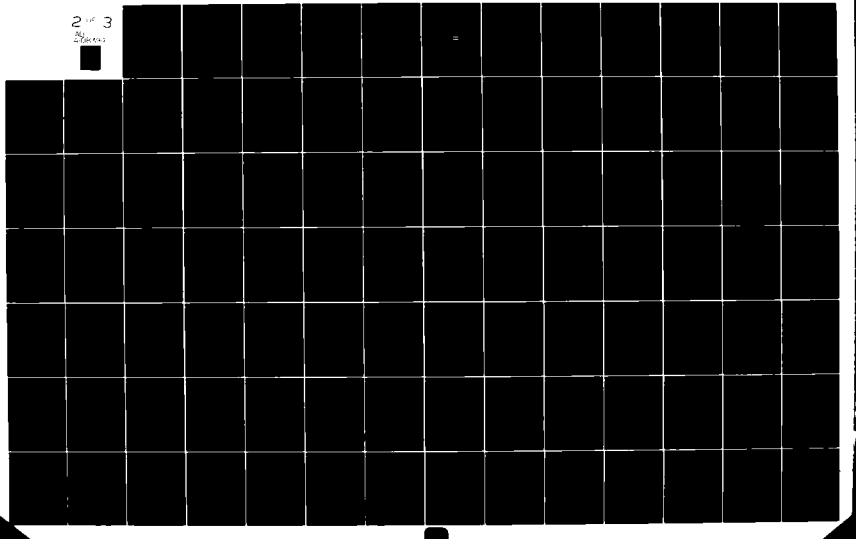

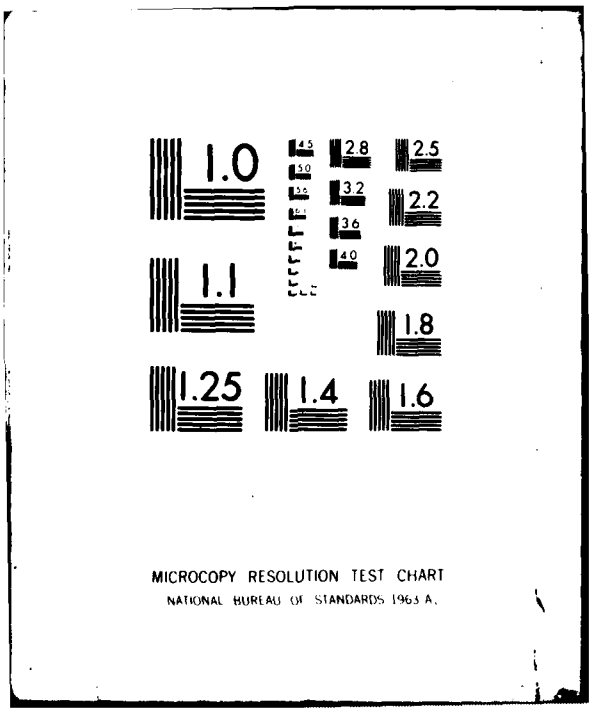
1.0
1.1
1.25
1.4
1.6
1.8
2.0
2.2
2.5
2.8
3.2
3.6
4.0
MICROCOPY RESOLUTION TEST CHART
NATIONAL BUREAU OF STANDARDS 1963 A.

3.3.5 Optical Cable Selection Criteria

The basic requirements of interest for optical cable may be summarized as:

- Minimum intrinsic loss with sufficient bandwidth
- Optimum coupling through selection of core size and numerical aperture (within bandwidth limitations)
- Minimum induced losses for operational environment
- Physical durability

Given a bandwidth requirement of the AN/GYQ-21(V) of ~30 MHz, (assuming a 60 Mb/s bus data rate and a 2 bit/Hertz encoding scheme - NRZ) the quasi-step index fibers appear as the most attractive. There are currently two manufacturers of this fiber type which can support a bandwidth of 30 MHz and an N.A. $\geq$0.3, and thus the potential fiber candidates can be limited to:

- Corning Short Distance Fiber (SDF), Type 1505
- Galite Type 5050 (screened)

If the bandwidth is relaxed to 25 MHz and the same numerical aperture requirement is maintained, several additional fibers can feasibly support the network. These additional fiber types are:

- MAXLIGHT Type KSC-200 A/B (PCS type fiber)
- Valtec Types PC-08/PC-10 (PCS type fibers)

The fibers can then be cabled to meet the ruggedization requirements necessary. The two glass-on-glass fibers (Corning Type 1505 and Galite Type 5050) offer the minimum program uncertainty from connectorization. The argument has been advanced that the "short links" to be employed for military systems should employ low loss cable. The fallacy of this argument is that the coupling losses encountered with low loss cables (with their attendant low numerical apertures) are substantially more than the gain in cable losses. Thus, the argument for low loss cables to support short distance links is not substantiated on inspection of the "overall" losses.

3.4 Optical Connectors, Splices, and Couplers

3.4.1 Connectors

A variety of optical connector styles exist today: each a result of attempts to provide a design which allows low loss (~1 dB) repeatable terminations and matings. Techniques differ in approaches to fiber preparation, alignment, strain relief, environmental stability, etc. Thus, all connectors do not mate with all cables and certainly are not interchangeable.

Most connectors employ precision machined contacts or ferrules which (depending on fiber type) may be crimped or epoxied directly to the cladding (or in some cases such as PCS, the core) of the fiber. If the fiber end preparation involves cleaving, then the ferrule is installed afterwards and completes the preparation. For fiber preparation using optical polishing, the ferrule is first installed and then the combination is polished to a smooth surface. In both cases the ferrules (or contacts) are then installed in a previously prepared back shell/strain relief assembly which constitutes a plug or receptacle depending on the manufacturer's design.

An alternate approach (used by Deutsch and TRW) is to use compression forces to secure the fiber without separate contacts or ferrules. This technique offers a fully reusable connector since ferrules are not replaced upon retermination.

Performance of the above connectors varies from 1 to 2 dB for most fiber diameters. This is typically the single most important performance parameter associated with optical connectors and includes repeatability over a large number of mating cycles.

The environmental aspects of optical connectors concern temperature induced changes in optical throughput, effects of humidity, corrosion and contaminants (dust, grease, or other). Fortunately, the conventional MIL-STD connector industry is well developed and by using similar materials to those in the electrical counterpart, manufacturers are producing optical connectors which promise the capability of passing military qualifications (i.e., Hughes, Amphenol) in the near term.

3.4.2 Splices

The two techniques presently used to perform splicing of optical fiber are mechanical splices and fusion splices. Mechanical splices offer somewhat simpler fabrication (less support equipment), albeit at some increase in optical loss. Fusion splices require some means of generating high temperatures and maintaining fiber-to-fiber alignment.

A mechanical splice generally utilizes alignment ferrules or sleeves to provide precision mechanical alignment and when properly positioned for minimum loss (~0.5 dB) the fibers are then typically secured with epoxy. Fusion splices are performed using an electric arc (or flame) to weld the fibers together when properly aligned. The arc is preferred since it constitutes a more controlled fusion method. Losses associated with fusion techniques are approximately half (0.25 dB) that of the mechanical approach.

3.4.2.1 Termination Techniques for Plastic Clad Silica Fiber

PCS fiber has established a rather well-known reputation for being difficult to terminate and maintain low connector throughput losses. Several factors contribute to these problems:

- Silicone cladding is typically soft and as such it is difficult to maintain core to cladding concentricity (key factor in connector loss).
- Silicone cladding does not bond securely to core, therefore installation of contacts and ferrules is difficult and the cladding tends to "flow".
- Core retains silicone deposit which resists epoxy bonding, unless thoroughly cleaned.

Manufacturers of fiber and connectors have been pursuing methods to termination of PCS with two generally applied approaches. However, as discussed later, a rather novel idea now offers a third approach.

The first approach is a buffer coating (Hytrel) of the silicone cladding which provides a tougher material for crimping a metal alignment contact. The contact is secured by compression (crimp) over several points on the fiber. This technique, although simple, does not preclude "pistoning" of the core within the contact or (for very soft cladding such as that required for low temperature and low loss) core/cladding deformity.

The second approach attempts to eliminate the above mentioned problems at the expense of additional fiber preparation. The process is called the cladding replacement method[15] and involves complete removal of cladding (and residue) from the core material. This bare core is then reclad (by dipping) with a harder material, such as OPTELECOM's cladding solution and (after curing) a contact may be crimped or epoxied to the newly added surface. A shortcoming of this approach as voiced by several connector and cable manufacturers is directly related to the cladding solution:

- Bonding to core is not very secure.
- Dipping process not well controlled since cladding thickness is a function of the number of successive dip operations and the solution's viscosity.
- Dipping process also may not yield core/cladding concentricity.

An alternative to the above technique still involves cladding replacement; however, the process is much more procedural and controlled. The following paragraphs describe this approach developed by Raychem Corporation for use with MAXLIGHT (subsidiary of Raychem) PCS cables.

The sleeve (called Fibersleeve^{TM}) is designed to contract upon the application of heat and bond directly to the glass surface once the buffer material has been removed. The sleeve assures a hard surface that can now be used for indexing in the connector ferrule. Once bonded into the ferrule the fiber can be polished using standard polishing methods. Cleaning of the fiber surface is an important operation to attain the maximum bond strength.

[15] Private conversation between S. Lang (Valtec) and R. Dragoo (Harris), May 1980.

The termination sleeve is made up of two concentric sleeves. The interface sleeve is made from a precision extrusion of a material that has an index of refraction similar to that used for the fiber buffer; thus losses are held to a minimum (approximately 0.3 dB). The outer sleeve is a precision extruded radiated heat-shrinkable material that is assembled with the interface sleeve. Figure 3.4.2.1 shows the installation procedure.

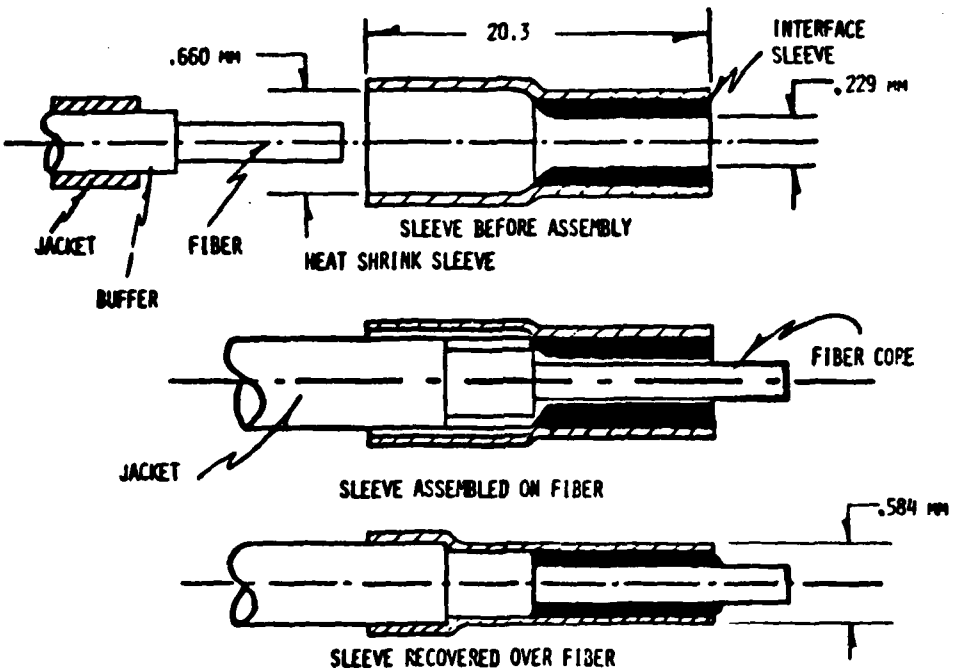

Figure 3.4.2.1. Composite Termination Sleeve

A number of different connectors can be used once the Fibersleeve^{TM} is installed. Because of the large outer diameter of the sleeve a large, straight bore design connector can be used. Examples of some of the usable connectors are those manufactured by Amphenol, Hewlett-Packard, Hughes, and AMP. Other connectors of similar design can likely be accommodated.

In the future, sleeve assemblies with the assembly procedure and tools can be supplied so that in-house or field installations can be made.

3.4.2.2 Optical Connector Selection Criteria

The criteria for selection of an optical connector consists of low loss and good environmental performance. Reviewing Table 3.4.2.2 shows that several connectors are available for the AN/GYQ-21(V) application (Amphenol/801, 905, 906, ITT/FOS; Hughes/Single or Multipin and ATI/SMA). Note however that the Hughes connector has a lower throughput loss of ~1 dB and also promises excellent environment performance due to its inherent capability for pressurization seals.

The recommended connectors for this application are:

- Hughes/Single or Multipin
- Amphenol/801 series

Both connectors have been designed with the goal of military qualification and therefore represent the most promising for harsh environmental conditions. The Hughes connector with the lowest quoted loss is the primary selection; however, an alternate choice at this time is the Amphenol 801 connector. Both connectors are designed with contacts and strain reliefs which accommodate various fiber types and sizes and cable constructions.

3.4.3 Optical Couplers

Coupler technology is very possibly the most immature component within fiber-optic communications. Early researchers developed several approaches to couplers but the basic design employed fiber bundles which are not considered for this application. There is presently much activity

Table 3.4.2.2. Fiber-Optic Connectors Matrix

MANUFACTURER & PART NO.	TYPE OF FIBER	FIBER SIZE	SPLICE, SOURCE DETECTOR FITTINGS	METAL CONNECTOR	CONNECTOR LOSS (dB)	OPERATING RANGE (°C)	MIL SPEC DESIGN	ALIGNMENT TOLERANCE RADIAL AXIAL ANGULAR	CABLES ACCOMMODATED MANUF.	CABLES ACCOMMODATED TYPE	END PREPARATION	COMMENTS
AMP												
OCS	MCS	102 μm to 406 μm	YES	NO	<2	-55 to 80	TESTING	.2 to 5mm GAP +10% FIB. DIAMETER 2°	DUPONT	P140,P140	POLISH	Multiple Fiber Connectors also available
Optimate	PCS,SG	125 μm to 1.91 mm	YES	NO	<2		TESTING		Belden Canstar Galileo H.P. ITT Pingkington VALTEC	225001 D1G-061 3000 LCMS 433 H20LR,75LR H20SR MD-M605	POLISH	
Amphenol												
905	PCS	.61 μm to 1.12 mm	YES	YES	3	-55 to 199	TESTING	30 μm GAP +13 μm -	Belden Canstar Dupont Galite ITT Siecor	220012,221001 226001,225001 D1S,D1G P740,P140R 1000,2000,3000 5000,5020 T400,202,322 112,122,133, 142,155,212, 222	POLISH	Not formally qualified. Single channel
906	S,G	125 μm to 245 μm	YES	YES	2	-55 to 199	TESTING	5 μm + 13 μm 1°	TimesFiber Valtec	GP1/G5-400,201, 045,6A,5A PC05,PC10,MG05	POLISH	
801	PCS,SG	55μm to 1.14mm	NO	YES	2	"	TESTING				POLISH	Not formally qualified. Multi-channel
Canon ITT												
FOS	Single	85 μm to 265 μm	YES	YES	2	-55 to 125	NO	0 GAP 51 μm 1°		All cables up to 4mm diameter	POLISH	Terminating tools available.
FOT	Single	85 μm to 265 μm	YES	YES	2	-55 to 125	NO				POLISH	For protected environments
FOR	Single	85 μm to 265 μm	YES	YES	2		NO			All cables up to 4mm diameter	POLISH	Also for bundle fibers
Deutsch												
DM	SG	62.5 μm	YES	YES	1	-55 to 90	NO		Siecor	{62.5 m core 125 m cladding}	CLEAVE	

Table 3.4.2.2. Fiber-Optic Connectors Matrix (Continued)

MANUFACTURER & PART NO.	TYPE OF FIBER	FIBER SIZE	SPLICE, SOURCE & DETECTOR FITTINGS	METAL CONNECTOR	CONNECTOR LOSS (dB)	OPERATING RANGE (°C)	MIL SPEC	ALIGNMENT TOLERANCE RADIAL AXIAL ANGULAR	CABLES ACCOMMODATED MANUF.	CABLES ACCOMMODATED TYPE	END PREPA-RATION	COMMENTS
Hughes 1093-7025	SP, SG	110 µm to 250µm	YES	YES	1	-55 to 125	YES	Spring load contact		Custom Fitted	POLISH/ CLEAVE	Can be combined with electrical connectors Inherent pressurization seals.
Northern Telecom C-20	Single	100 µm to 125 µm	NO	YES	1				Northern Telecom		POLISH	Sold only with factory termination
Stecor	SG	62.5 µm	YES	YES	1		NO		Stecor		POLISH	
Trompeter TPS	Single	300µm to 1100µm	YES	YES	2		NO	0 GAP		Custom Fitted	CLEAVE	Bayonet Type
SMA			-	-	2		NO	-			CLEAVE	SMA Threaded Type
TRW-Cinch Optalign	Single	90µm to 140µm	YES	YES	1	to85	YES		Stecor		CLEAVE	
Light Line	Single			YES	2						POLISH	
RADIALL SMA	SP, SG	200µm to 600µm	YES	YES	2	-25 to 125	NO	Spring load contact		Custom Fitted	CLEAVE	Crimp contacts
ATI SMA	SP, SG	125µm to 400µm	YES	YES	2	-55to125	YES	Spring load contact		Custom Fitted	CLEAVE	Crimp contacts

within the fiber-optic community which is aimed toward developing multiport and directional (or "T")couplers which use single fiber technology and do not introduce prohibitive characteristics such as:

- Excess implementation losses
- Significant port-to-port variation (primarily for star couplers)
- Low directivity/port isolation (directional couplers)

Several manufacturers do offer star and "T" couplers however they remain plagued with the above mentioned characteristics. These problems describe the performance characteristics that are normally considered for coupler selection and the general status. Manufacturing Methods and Technology (MMT) contracts presently being performed, are primarily concerned with optimizing present coupler performance and developing packaging which can be effectively used in military environments. Other research and development by commercial companies (e.g., Xerox[16] and NTT[17]) is directed toward unstressed environments such as "Office of the Future" where optical performance such as minimum excess loss and port to port variations are criteria more important than environmental survivability.

Of the devices surveyed, typically all employ passive optics to accomplish distribution or drop/add capability. One manufacturer offers an "active coupler" which is all electronic (combination of devices operating as dual source/ detector and electrical taps); however, the device is limited to speeds of a few hundred kilobits/sec and is unsuitable for this application.

---

[16] E.G. Rawson and M.D. Bailey, "Bitaper Star Couplers With Up to 100 Fiber Channels," Elect Letters, 5 July 1979, pp 432-433

[17] K. Nosu and R. Watanabe, "Slab Waveguide Star Coupler for Multimode Optical Fibers," Elect Letters, 17 July 1980, pp 608-609

As part of this study effort Harris fabricated several biconically tapered fused star couplers to evaluate the achievable performance. Several fiber types were employed to ascertain the performance attainable from each. The best performance achieved was with a 50 μm core graded index fiber supplied by Valtec. Three 10 fiber star couplers were successfully fabricated employing the techniques outlined in Appendix A. Based on results achieved with these couplers, it can be postulated that implementation losses of 2.5 dB are readily achieved and port-to-port variations of $\pm$0.5 dB can be achieved ($\pm$0.6 dB achieved with these rudimentary models).

A logical extension of the coupler fabrication effort is to fabricate a coupler, separate the two taper sections, and install a repeater between the two sections. This approach has not been reported to date and deserves further investigation.

Temperature performance is not typically available for couplers. NRL does have an MMT contract with ITT for development of MIL qualified couplers (star and "T") which promise to significantly advance component utilization.[18] Design objectives are $\leq$2 dB excess loss, $\leq$0.5 dB port-to-port variation for transmissive star couplers (8x8, 16x16, and 32x32 configurations) utilizing all glass "fat" fiber (100 μm core). The devices shall be packaged to survive both temperature extremes and shock, vibration, etc. Test data indicates that low temperature operation does not pose a problem, however, at high temperatures (80^{o} C and greater) care must be taken to ensure that the fabrication materials, such as epoxies, do not degrade.[19]

---

[18] Private Communications between J. Wyatt (Harris) and Dr. G. Bickel (ITT) February 1980.

[19] R.E. Dragoo, J.C. Wyatt, and D.M. Thomas, "NAVELEX Fiber-Optic Study," Contract Number N00039-79-C-0412.

3.4.3.1 Coupler Selection Criteria

At this time, a specific type of coupler is not specified because the bus networking tradeoffs have not been considered. Thus a star coupler and "T" coupler are identified. Referring to Table 3.4.3.1 shows that the selection of couplers is limited by virtue of available devices. Therefore several manufacturer's devices and rationale for consideration shall be presented.

Selection of a star coupler should include as primary:

- Harris - good performance, various core sizes, development item.
- ITT - good performance, large core, under contract for development of MIL qualified device under MMT.

Alternates include:[20]

- Amphenol
- Spectronics

Similarly, for the "T" coupler, candidates are:

- ITT - large core fibers, presently under development on MMT
- CANSTAR - large core fibers

---

[20] J.R. Baird, "Optoelectronic Aspects of Avionics Systems II, Contract Number AFAL-TR-314, May 1975.

Table 3.4.3.1. Optical Couplers Matrix

MANUFACTURER AND MODEL NO.	TYPE	NUMBER OF PORTS	FIBER SIZE	INSERTION LOSS (dB)	PORT-TO-PORT VARIATION (dB)	MAXIMUM RATIO (dB)	COMMENTS
Amphenol							
909-117	Star	32	100 to 125 μm	4.4	1.5	0	
Canstar							
TC3	Directional	3	65.5 to	1	.7	11.8	50 dB Directivity
TC4	Star	4	250 μm	1	.7		"
NEC							
OD 8601	Star	3	50 to	2	2	20	Less variation with
OD 8602	Star	4	100 μm	2	2	20	Lower splitting ratio
OD 8603	Star	3		1.5	2	20	Pigtail
OD 8604	Star	4		1.5	2	20	"
OD8663 A1	Wave-length Division Multiplexer	5	50 μm	2.5			
OD8663 A2		5	50 μm	3.5			
OD8683 B1		5	50 μm	3.5			
OD8683 B2		5	50 μm	4.5			
Harris	Biconically Tapered Star	10	Various	2.5	0.6	20	Development Item
Spectronics							
SPX 3613	Star	8,16 or 32	100 μm	4.2	2	0	0 to 70°C Operation

Table 3.4.3.1. Optical Coupler Matrix (Continued)

MANUFACTURER AND MODEL NO.	TYPE	NUMBER OF PORTS	FIBER SIZE	INSERTION LOSS (dB)	PORT-TO-PORT VARIATION (dB)	MAXIMUM RATIO (dB)	COMMENTS
IEI							
T-760	Transmission Star	2 to 32	55μm to 203μm	4	1	0	
T-767	Reflective Star	3 to 32	100μm to 127μm	4	1	0	
T-778	Directional TEE	3	55μm to 203μm	1	1	14	
T-782	Directional TEE	3	55μm to 127μm	1	1		Pin Detector
T-788	Wavelength Division Multiplexer	3	55μm	3	-	-	

3.4.4 Summary

The discussion of optical components in terms of their capability to support the AN/GYQ-21(V) system indicate the technology is sufficient to meet the requirements of the system. The development status of optical connectors indicates that near term realization of tactical field connectors is expected. For the relatively benign environment of the AN/GYQ-21(V) system several ruggedized connectors are presently available to support the network.

The area of optical fibers indicates that several fibers can support the requirements, and several alternatives are also available, if the link requirements can be relaxed. The implementation risk of any development program can, therefore, be arbitrarily reduced by relaxation of the requirements. Fiber-optic cables are currently being developed to meet tactical field requirements and support of the AN/GYQ-21(V) system in a tactical environment is feasible.

Optical couplers are the least developed area of components. Several "T" couplers are available on the commercial market, while star couplers remain a laboratory development item. Several manufacturing methods and technology (MMT) contracts have been released, but devices resulting from these contracts have not been released yet.

4.0 ALTERNATE FIBER-OPTIC BUS DESIGNS

The limiting factor in extending a processor's bus over large distances is propagation delay time. A handshake between the processor and a peripheral is required for every datum transferred on the bus. Such a handshake requires a round trip delay, thus the time for one bus transaction can be no shorter than the round trip delay on the bus. For bus distances of one kilometer, therefore, a bus transaction requires at least $\frac{2 \times 1 \text{ km}}{2 \times 10^5 \text{ km/sec}} = 10\ \mu\text{sec}$. Given a 16-bit data item, the maximum transmission rate for this case is $\frac{16 \text{ bits}}{10\ \mu\text{sec}} = 1.6$ Mb/s.

Since the time required for a handshake is fixed for a given separation, the only way to improve throughput is to transfer a larger number of bits per handshake. To solve this problem, packet communication systems have been developed over the past decade. The particular application of packet communications to a number of processors and peripherals with separation of a few kilometers is referred to as a Local Area Network[21]. Interest in Local Area Networks has mushroomed in recent years. In 1979, two conferences on Local Area Networks were held: the 4th Conference on Local Computer Networks cosponsored by IEEE and the University of Minnesota, and the Local Area Communications Network Symposium sponsored by the National Bureau of Standards and the Mitre Corporation. These conferences have now become regular annual events, and other more general conferences, such as COMPCON, have included sessions dedicated to Local Networks.

The AN/GYQ-2(V) Local Network must provide a common interconnect for one or more Digital Equipment Corporation (DEC) processors and a number of peripherals. The processors and peripherals connect to the network through a Bus Interface Unit (BIU) as shown in Figure 4.0. The BIU "back-end" provides a UNIBUS compatible interface to each processor, or

[21] D.D. Clark, K.T. Pogran, and D.P. Reed, "An Introduction to Local Area Networks", Proceedings of the IEEE, Vol. 66, No. 11, Nov. 1978, 1497-1517.

cluster of peripherals. The BIU "front-end" provides an interface to the network, and interacts with the other BIU's in the system to coordinate the sharing of the common interconnect.

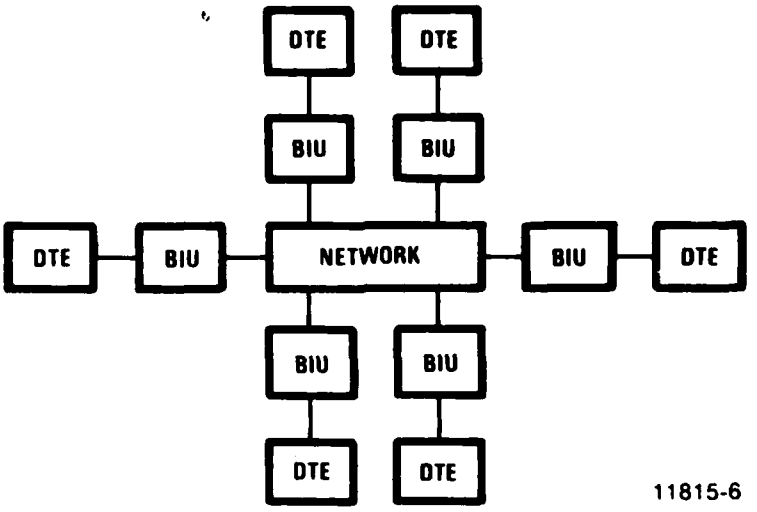

Figure 4.0. Function of Bus Interface Unit

A local Area Network is to be contrasted with a Long Haul Network, such as ARPANET, which connects processors over large geographic areas using a variety of connecting media. Long Haul Networks use a point-to-point store-and-forward scheme, whereby packets travel from the source node to the destination node via a path dynamically determined by the routing algorithm. Such schemes are unnecessarily complex for the Local Network and present untolerable store-and-forward delays.

The network architectures which are appropriate to the Local Network can generally be classified as the ring and the multiaccess bus. These two broad categories will be discussed in the following paragraphs.

4.1 Ring Architecture

The ring architecture connects the BIU's in a closed loop with a simple point-to-point link between BIU's. Data is circulated around the ring from a source BIU to a destination BIU. Each BIU in the ring has the option of retransmitting the data it is receiving, or "breaking" the ring to transmit its own data. The BIU is not required to store an entire packet (received from the upstream BIU) before forwarding it. The amount of storage required in each BIU is equal to the number of bits the BIU must modify (for control purposes) before retransmitting, and depends on the control structure in use.

4.1.1 Ring Control Schemes

The simplest control structure for a ring employs a circulating frame format divided into slots with each slot dedicated to a particular BIU. The frame format must be generated by a central control node. In this fixed bandwidth synchronous time division multiplexing scheme, the system bandwidth must be sized to equal the sum of the data rates of the individual users. Users with higher data rates may be given larger slots, or a larger number of slots, than lower rate users. Such dedicated slot schemes have been analyzed by Chu and Konheim[22], and Kosovych[23].

[22] W.W. Chu and A.G. Konheim "On the Analysis and Modeling of a Class of Computer Communications Systems," IEEE Transactions on Communications, Vol. COM-20, No. 3, June 1972, pp. 645-660.

[23] D.S. Kosovych, "Fixed Assignment Access Techniques," IEEE Transactions on Communications, Vol. COM-26, No. 9, Sept. 1978, pp. 1370-1376.

4.1.1.1 Reservation Systems

In a computer network, the users are generally intermittent and the aggregate data rate seldom approaches the sum of the individual user rates. Under the fixed bandwidth per user scheme, the system bandwidth must be designed to equal the sum of the individual rates resulting in a higher-than-desirable bandwidth, most of which would be unused at any point in time.

By using a reservation system, the system bandwidth can be chosen to be less than that required if all devices were simultaneously communicating. Bandwidth under a reservation scheme is assigned to users on an as-needed basis by a controller. The total system bandwidth is chosen so as to make the probability of overload arbitrarily small.

A reservation-type fiber-optic ring has been developed on an Independent Research and Development project at Harris GCSD and is being incorporated in the SDHS weather terminal for the US Air Force. This ring operates like a large circular shift register of approximately 50,000 bytes in length. A small portion of this register resides in each BIU, with the remainder of the storage in the Bus Control Unit (BCU). A frame structure of 50,000 bytes is circulated in the ring. This frame structure consists of a set of small slots with each slot dedicated to a BIU, and a set of large message-carrying slots which are undedicated. When a BIU has data to transmit, it places a request in its dedicated slot which is eventually received by the BCU. The BCU acts upon this request by granting an information slot to the BIU as soon as one is available. This control scheme may be viewed as consisting of two channels; a time-division multiplexed reservation channel, and a demand-assigned information channel.

The ring just described was optimized for high volume imagery transfer, and is not particularly suited to the 21(V) interconnect problem. Although a high efficiency is achieved, the waiting time (latency) for such a reservation-type ring can be rather long. Another criticism of reservation systems is the dependence on a centralized controller which becomes a single point of failure.

4.1.1.2 Distributed Control Systems

Most Local Networks reported in the literature have been designed with distributed control for reliability reasons. There are generally three distributed control schemes for use in the ring network.

A strategy of rotating slots was originally proposed by Pierce[24]. This scheme is not totally distributed, since a centralized device must generate a skeleton frame consisting of empty slots. Any BIU detecting a passing empty slot may place a message in it, tag it for a given destination, and mark it full. As the destination reads the data from the slot, it marks the slot empty. This strategy is vulnerable to an addressing fault, wherein the destination fails to remove the message and mark the slot empty either because a bit error altered the destination address, or because of a failure in the destination BIU. Such a fault results in a full slot circulating endlessly unless a fault monitoring and housecleaning function is included in a centralized device. A further disadvantage of the Pierce loop is that when variable-length messages are placed in fixed-size slots, some wasted bandwidth is inevitable.

Despite these disadvantages, the simplicity of the approach is appealing. The Spider Network[25] at Bell Laboratories uses the rotating slot approach and has enjoyed success since its inception in 1972. The Cambridge Ring[26] also uses a system of rotating slots.

---

[24] J.R. Pierce, "Network for Block Switching of Data," BSTJ, Vol. 51, pp. 1133-1143, July/August, 1972.

[25] A. Fraser, "A Virtual Channel Network," Datamation, February, 1975, pp. 51-56.

[26] A. Hopper, "Data Ring at Computer Laboratory, University of Cambridge," in Computer Science and Technology: Local Area Networking, Washington, D.C., Nat. Bur. Stand., NBS Special Publ. 500-31, August 22-23, 1977, pp. 11-16.

The control scheme of Farmer and Newhall[27] employs a circulating control token. Under normal conditions, only one token is circulating at a time. Any BIU, upon detecting the passing token, may change it into a message separator, transmit a message, and reinsert the control token after the message. The passage of the token from one BIU to the next is equivalent to a round robin poll of the BIU's to determine if they have a message to transmit, but eliminates the transit time associated with a central polling approach.

The DCS at the University of California at Irvine (also called Irvine Ring)[28] implements the control token method with an 8-bit token identical to the flag character used in bit-oriented protocols such as ADCCP, SDCC, and HDLC. This token (01111110) is prevented from appearing in the data stream by zero-insertion logic which inserts a zero following any occurence of five consecutive ones. This excludes six consecutive ones (and thus the token) from the data stream. Zero deletion logic in the receiver removes every zero which follows five consecutive ones.

The amount of storage required in each BIU is determined by the number of bits which must be modified before retransmission. Since the destination is not required to remove messages, the only amount of storage required is that necessary to change the control token into a message separator. The Irvine scheme performs this transformation by complementing the last bit of the token, thus only requiring one bit of delay through the BIU. For a large number of closely spaced BIU's, this savings in delay through a BIU significantly improves latency and efficiency of the ring over methods which require more storage.

---

[27] W.D. Farmer and E.E. Newhall, "An Experimental Distributed Switching System to Handle Bursty Computer Traffic," Proc. ACM Symp. Data Comm., pp. 1-33, October, 1969.

[28] D.J. Farber, "A Ring Network," Datamation, February, 1975, pp. 44-46.

Other advantages of the control token method are immediately obvious. Unlike the Pierce loop, which requires a centralized BIU to generate a skeleton frame, the control token method can be made completely distributed. Generation of the initial token, as well as fault correction, can be a cooperative effort amount the BIU's as discussed below. The control token method does not suffer the penalty of having to fit variable length messages into a series of fixed-length slots.

Finally, the addressing fault problem discussed above does not apply to this control method, since a message does not "freeze up" a portion of the bandwidth and does not have to be deleted by the destination. Messages appended after the token will eventually overwrite older messages with no regard for their presence. A message which is longer than the round trip delay will, in fact, overwrite itself. But in all cases, the destination has the opportunity to read the message before it is overwritten.

The major difficulty with this method is that of token maintenance. Initially, and any time a token is destroyed by a bit error, a new token must be generated. Further, if a token is accidentally created by a bit error, such a token must be eliminated. A scheme has been implemented[29] which uses the BIU's in a cooperative manner to generate new tokens and delete extraneous ones, thus obviating the need for a centralized control node. This ring system is called Ringnet, and is a commercial product of Prime Computer, Inc. Operating at a signalling rate of 10 Mb/s, Ringnet achieves an effective 8 Mb/s data rate through a 4-out-of-5 encoding scheme which insures the uniqueness of control characters.

[29] R.L. Gordon, W.W. Farr, and P. Levine, "Ringnet: A Packet Switched Local Network with Decentralized Control," 4th Conf. on Local Computer Networks, Minneapolis, Oct. 1979, pp. 13-19.

The third distributed control method for rings is the register insertion method of Hafner, et.al.[30]. Like the control token method, register insertion can be totally distributed. A BIU, upon detecting a passing message separator, may begin transmitting a message whether or not another message follows on the ring. While the BIU is shifting its message out, it must provide storage for data that is entering from upstream. Stated equivalently, the BIU places its message in a shift register, waits until a message separator appears on the ring, breaks the ring, ties the two ends of the broken ring to the two ends of the shift register, thus forming a larger ring, and shifts the message out while data from upstream enters the shift register.

The message journeys around the ring, being read but not deleted by the destination, until it returns to the shift register. Only then does the source BIU remove the register (and the message) from the ring. This technique is prone to an addressing fault similar to the rotating slots method, except in the source field instead of the destination field. If a bit error alters the source address, the source BIU will not recognize its own message and cannot take the shift register out of the ring until the ring is known to be idle.

A ring using register insertion is under development at Ohio State University. Originally referred to as the Distributed Loop Computer Network (DLCN),[31] more recent publications by the authors have renamed it the Distributed Double-Loop Computer Network (DDLCN).[32] This latest design employs two rings for fault tolerance. The advantages of register insertion

---

[30] E.R. Hafner, Z. Nenadal, and M. Tschanz, "A Digital Loop Communication System," IEEE Trans. Commun., Vol. COM-22, No. 6, June, 1974, pp. 877-881.

[31] M.T. Liu and C.C. Reames, "The Design of the Distributed Loop Computer Network," Proc. of the 1975 International Computer Symposium, Vol. I, pp. 273-283, August, 1975

[32] D. Tsay and M.T. Liu, "Interface Design for the Distributed Double-Loop Computer Network (DDLCN), Proceedings of the 1979 National Telecommunications Conference, pp. 59.3.1-5, December, 1979.

over the control token method are not immediately obvious. It is claimed that the waiting time to get a message onto the bus is shortened, and that simultaneous transmissions are possible. However, the total length of the ring can grow, making the transit time longer. Simulations by the architects of the DDLCN[33,34] are claimed to point to superiority of register insertion over other methods.

4.1.1.3 Conclusions

Although other distributed ring control systems, such as free contention,[35] have been postulated, the three described above (rotating slots, control token, and register insertion) are the most widely analyzed. Of these, only control token and register insertion can be made totally distributed. These two can also be seen as offering higher efficiencies. The register insertion method is inherently more complex than control token, and the degree of performance improvement is not too clear. Based on the proven performance of control token as evidenced by the Irvine ring and the commercial product Ringnet, control token is recommended as the control mechanism for the ring candidate architecture for the 21(V) application.

4.1.2 Redundancy Considerations

A single non-redundant network suffers from the likelihood that a failure in any BIU will disable the network. For networks having a large number of BIU's, the design of a fail-safe mechanism is, therefore, of paramount importance.

---

[33] M.T. Liu, R. Pardo, and G. Babic, "A Performance Study of Distributed Control Loop Networks," Proc. of the 1977 International Conference on Parallel Processing, pp. 137-138, August, 1977.

[34] M.T. Liu, G. Babi, and R. Pardo, "Traffic Analysis of the Distributed Loop Loop Computer Network (DLCN)," Proc. of the 1977 National Telecommunications Conference, pp. 31.5.1-7, December, 1977.

[35] Op. Cit., Number 21.

For purposes of reliability analysis, a BIU can be broken into two machines, M1 and M2, as shown in Figure 4.1.2-1. All components whose failure would disrupt operation of the ring are included in M1. These generally include fiber-optic drivers and receivers, bit synchronizers, ring access control circuitry, and all associated power supplies. All other components are included in M2. A failure in M2 will disrupt service to the local user, but will not cause a catastrophic failure of the system.

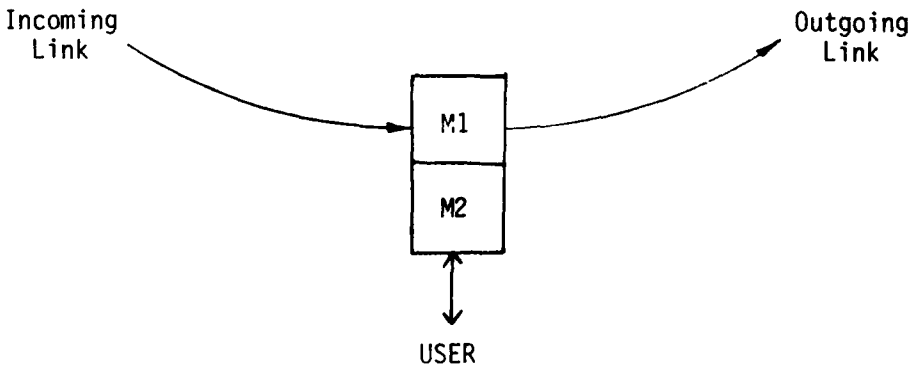

Figure 4.1.2-1. Ring BIU Fault Model

A minimal fail-safe mechanism consists of fault isolation circuitry which can detect failures in the regular data flow paths and control functions of M1. Upon detection of a failure, this circuitry directly connects the receiver to the transmitter, thus bypassing the BIU electronics. The reliability improvement is only minimal, since such circuitry cannot protect against failures in the receiver, transmitter, or power supplies.

This problem has been solved for coaxial cable rings by using a mechanical relay which directly couples the incoming and outgoing cables, thus bypassing all active components. The relay is normally closed, so that loss of power will also result in a bypass condition.

An optical bypass switch, which can operate in an analogous manner, has been reported by Mitsubishi.[36] Its operation is illustrated in Figure 4.1.2-2. In the power-on state, an electromagnet attracts an assembly having mirrors on each end. These mirrors divert light from port 1 to port 2 (and on to the receiver in the BIU), and divert light entering port 3 (from the BIU transmitter) to port 4. This assembly is spring-loaded so that, upon power failure, it is withdrawn allowing light to pass directly from port 1 to port 4. Inquiries to Mitsubishi revealed that this device is not yet commercially available.

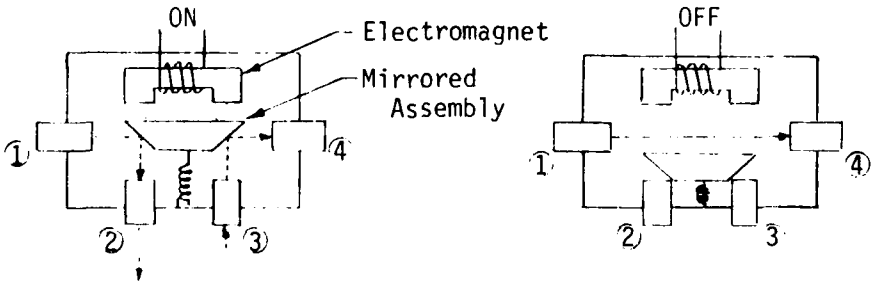

Figure 4.1.2-2. Optical Bypass Switch (Mitsubishi)

A problem with the mechanical bypass is that it is difficult to isolate faults in transmitters and receivers to the extent that such a bypass would be useful. For example, if a BIU detects a missing incoming data stream, it is virtually impossible to determine if the malfunction is in its receiver or in the upstream transmitter.

[36] M. Nunoshita and Y. Nomura, "Optical Bypass Switch for Fiber-Optic Data Bus Systems," Applied Optics, Vol. 19, No. 15, 1 August 1980, pp. 2574-2577.

The use of redundancy can significantly improve the network availability. The most obvious form of redundancy is the use of dual links between each pair of BIU's. The BIU transmits its data on both the primary and secondary links. At the receive end, the BIU normally receives on the primary, but switches to the secondary when detecting a signal loss on the primary. As a minimum, the transmitters and receivers are duplicated. Other candidates for duplication are the bit synchronization circuitry, power supplies used by these components, and control circuitry. The extensive use of redundancy can, however, significantly increase the cost of the BIU.

A second dual-link configuration employs primary and secondary links operating in opposite directions[37,38] as shown in Figure 4.1.2-3. The secondary link may carry an "I am healthy" message, or may actually be used to carry data in a load sharing arrangement. Upon failure in a BIU, or even a break in a fiber, the resulting configuration is a loop which bends back on itself at either side of the failure, as in Figure 4.1.2-3. Zafiropulo[39] has suggested making the redundant link bidirectional, allowing either of the two previous fallback modes.

Both of the previous redundant-loop arrangements require significant additional components to provide a substantial reliability improvement. A simpler, yet apparently more effective, method is that of the interlaced ring shown in Figure 4.1.2-4. In this arrangement, the secondary link leapfrogs over the immediately-downstream BIU to the next one in line. Outgoing information from the BIU is thus transmitted simultaneously to the next two downstream BIU's. Each BIU normally receives

---

[37] H.K.M. Grossen and F.J. Schramel, "Data Transmission and Switching Equipment for the Seat Reservation System of the United Airlines," Philips Telecommunication Rev., Vol. 24, February, 1963.

[38] J.H. McNeilly, R. Kitajewski, U.S. Patent 44396, March, 1972.

[39] P. Zafiropulo, "Performance Evaluation of Reliability Improvement Techniques for Single-Loop Communications Systems," IEEE Trans. Comm., Vol. COM-22, No. 6, June, 1979, pp. 742-751.

on the primary link, but upon detection of a failure, switches to the secondary link, thus bypassing the immediately-upstream BIU. Like the reverse redundant fail-safe, this technique can compensate for any failure within a BIU which would normally disrupt the ring.

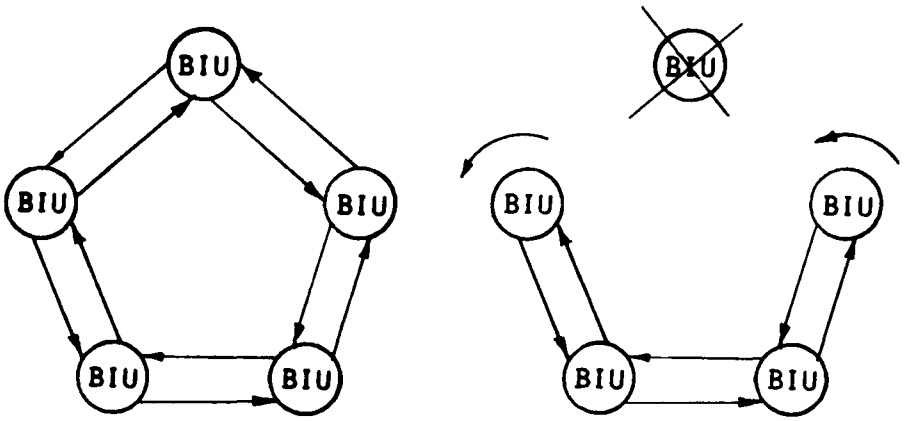

Figure 4.1.2-3. Reverse Redundant Link

The interlaced ring concept provides fault tolerance for any number of failed BIU's in the ring as long as no two failed BIU's are adjacent on the ring. In contrast, multiple failed BIU's in the reverse redundant approach result in segmenting the network unless the BIU's are adjacent. For a ring containing a large number of BIU's, the probability of adjacently-failed BIU's is much lower than the probability of nonadjacently-failed BIU's. Further, the interlaced ring concept can be implemented less expensively as described below.

Figure 4.1.2-4 implies that each BIU contains two drivers and two receivers. The redundant link may best be routed (passively) through the downstream BIU, with the three necessary fibers contained in a single cable. This facilitates adding or deleting BIU's from the system and simplifies cabling of the system by not requiring a separate cable for the redundant links.

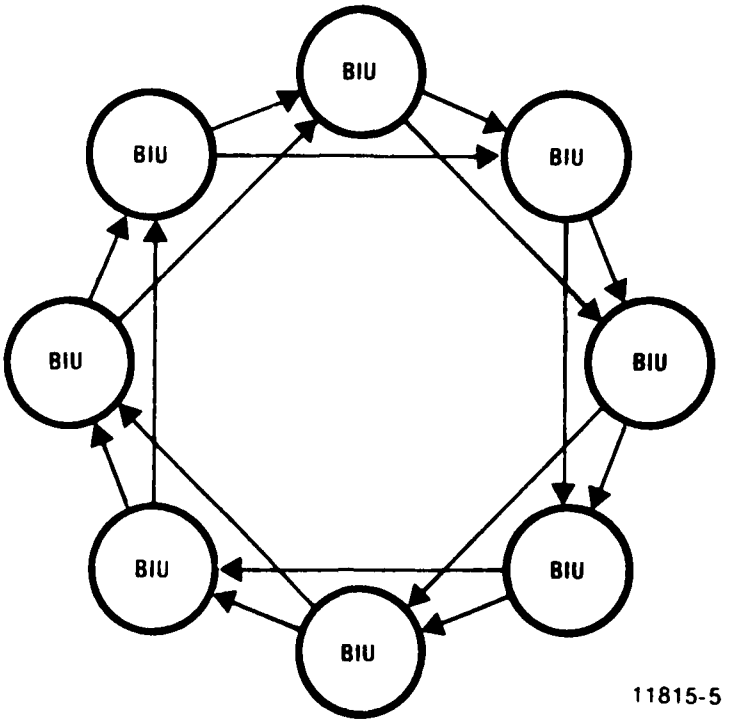

Figure 4.1.2-4. Interlaced Ring

A savings can be realized by using a single transmitter driving the two outgoing fibers through an optical splitter, as shown in Figure 4.1.2-5(a), rather than two transmitters. A further savings is realized by moving this splitter to the other end of the primary link, as shown in Figure 4.1.2-5(b), thus requiring only two fibers per cable. The configuration of Figure 4.1.2-5(b) is the recommended fail-safe approach for the ring candidate architecture.

The monitor mechanism for the interlaced ring must detect some fairly regularly occurring event in order to diagnose a fault. Under the control token access scheme, this event could be the occurance of either the control token or a message separater. A maximum time can be determined during which a token or message separater should occur in a normally functioning ring. Since the token can vanish due to bit errors, the fault detection scheme must be combined with token management to prevent false

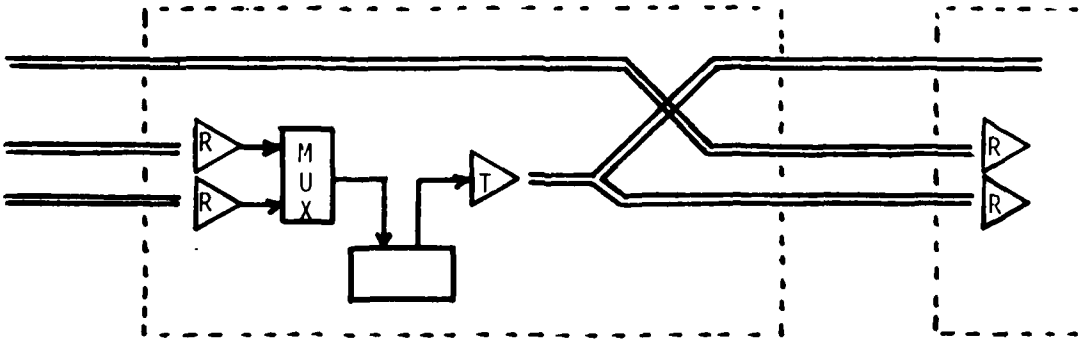

(a). Three-Fiber Cable

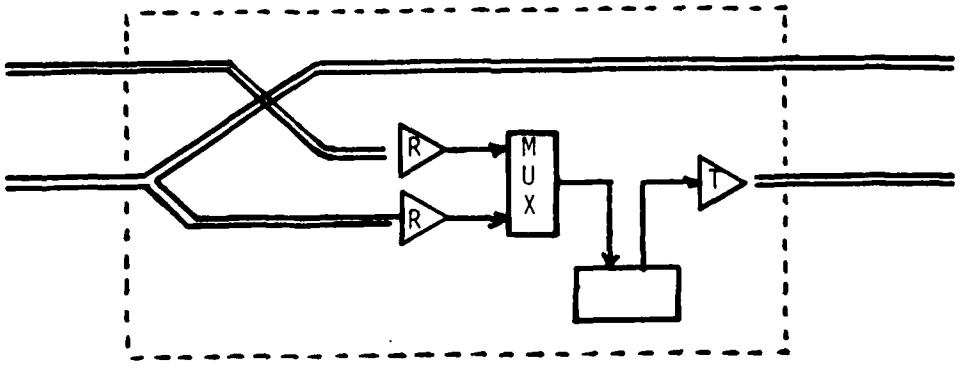

(b). Two-Fiber Cable

Figure 4.1.2-5. Component Reduction for Interlaced Ring

bypassed conditions. Upon timing out, a BIU should launch a token and perform another timeout, after which it may conclude that switching to the secondary output is appropriate.

4.2 Multiaccess Bus

The multiaccess bus, or "multidrop", has been the most successful interconnect method for coaxial computer networks. A signal transmitted by one terminal, or node, travels along the bus and is received by all other nodes. The nodes are, in effect, connected in parallel, as opposed to the nodes in a ring which are connected in series. The primary motivation for a parallel-connected bus is the probability that a failed BIU will not disrupt the entire network. Examples of operational networks based on coaxial cable multidrop interconnects include Xerox's Ethernet,[40] Ford's LNA,[41] the National Bureau of Standards bus at Gaithersburg, Maryland,[42] and the commercially marketed HYPERCHANNEL[43] by Network Systems Corporation. Xerox has also reported a fiber-optic Ethernet-like bus employing a star coupler.[44,45]

---

[40] R.M. Metcalfe and David R. Boggs, "Ethernet: Distributed Packet Switching for Local Computer Networks," Communications of the ACM, Vol. 19, No. 7, July, 1976, pp. 395-404.

[41] R.H. Sherman, M.G. Gable, and G. McClure, "Concepts, Strategies, for Local Network Architectures," Data Communications, July, 1978, pp. 39-49.

[42] "National Bureau of Standards Implements Local Packet Data Network," Computer Design, October, 1979, pp. 18-23.

[43] Network Systems Corporation, "Systems Description: Hyperchannel Network Adapters," Publication No. A01-0000-02, 1976.

[44] E.G. Rawson and R.M. Metcalfe, "Fibernet: Multimode Optical Fibers for Local Computer Networks," IEEE Transactions on Communications, Vol. COM-26, No. 7, July, 1978, pp. 983-990.

[45] E.G. Rawson, "Application of Fiber Optics to Local Networks," Proc. of the Local Area Computer Network Symposium, May, 1979, pp. 155-167.

4.2.1 Control Schemes

As with the ring approach, there are many control schemes for the multiaccess bus which require a centralized controller. A fixed bandwidth allocation TDM frame can be employed, but is wasteful of bandwidth, as argued in Paragraph 4.1.1. A TDM frame with dynamically-assigned bandwidth (reservation system) can be quite effective if the delay time for making reservations can be tolerated. A reservation system, using a star coupler, may use a form of Priority Oriented Demand Assignment (PODA)[46] originally intended for satellite networks. In a PODA scheme, a BIU can anticipate its assigned slot and transmit early so that the slots are in alignment at the star coupler and thereby improve the network efficiency.

Another popular centralized control scheme is polling. A central controller sequentially polls each station on the bus to determine if it has a message to transmit. If a terminal has traffic it becomes the bus master, transmits the message, waits for an acknowledgment, then releases the control back to the controller which resumes polling. This scheme can become quite inefficient, especially if the network is unbalanced, that is, only a few stations generate the major portion of the traffic. Polling stations without message traffic represents inefficient use of the bandwidth available.

To reduce this inefficiency, Hayes[47] introduced a tree-structured polling scheme called "probing". In probing, the controller transmits an address which one-half of the stations recognize. All stations with messages place a signal on the bus in response. If the controller detects no signal, it probes the other half of the stations. If it does

[46] I. Jacobs, et. al., "CPODA-A Demand Assignment Protocol for SATNET," Fifth Data Commun. Symp., Snowbird, Utah, September 27-29, 1977, pp. 2.5-2.9.

[47] J.F. Hayes, "An Adaptive Technique for Data Distribution," IEEE Trans. Commun., Vol. COM-26, No. 8, August, 1978, pp. 1178-1186.

detect a signal, it transmits an address recognizable by one-fourth of the stations within the half where a signal was detected, and so on in a binary tree search until a single active station is found. If the network is balanced, that is, most stations are participating, or contributing message traffic, probing becomes much less efficient than straight polling. Hayes suggests an adaptive approach which uses polling, or probing, or something in between, depending on the network statistics.

As with the ring system, a distributed control mechanism is preferred for the multiaccesss bus for reliability reasons. Distributed control schemes applicable to the multiaccess bus were actually first applied to packet radio, and have since been adapted for use in coaxial bus systems. With few exceptions, these methods work exactly the same way in fiber-optic implementations.

The most primitive arbitration scheme is the ALOHA technique.[48] When a station has a packet ready for transmission, it transmits the packet with no regard for the present state of the bus. If it does not receive an acknowledgment after a reasonable delay, it "times out", assumes the packet collided with another, and retransmits the the packet.

An obvious enhancement over ALOHA is the CSMA (Carrier Sense Multiple Access) method[49] in which a sender listens for an idle channel before transmitting. Collisions still occur when two or more nodes begin to transmit simultaneously when the bus becomes idle. After no acknowledgment, a transmitter tries again after generating a random or unique delay to prevent recolliding.

---

[48] N. Abramson, "The ALOHA System: Another Alternative for Computer Communications," AFIPS Conf. Proc., 37, p. 281, November, 1970.

[49] L. Kleinrock, Queueing Systems Vol 2: Computer Applications, New York, Wiley, 1976.

A further refinement is to listen while transmitting. The transmitter may detect a collision as soon as it occurs and abort the remainder of the packet, thus saving time. The transmission is rescheduled as with CSMA. This refined scheme is called Carrier Sense Multiple Access with Collision Detection (CSMA/CD) and is used in Ethernet, and many of the more successful protocols. Many variations of CSMA exist (such as non-persistent, 1-persistent, and optimum p-persistent[50]) whose performance depends upon network conditions. Other random access schemes include slotted ALOHA[51] and a variation of slotted ALOHA advanced by Capetenakis[52] which uses a binary tree search to arbitrate between colliding stations.

Other contention schemes avoid collisions entirely. One such scheme is MSAP (mini-slotted access protocol)[53] which is a special case of BRAM (broadcast recognizing access method[54]). BRAM uses the transmission delay time, T, to separate transmission attempts. If two nodes schedule a tranmission at least T seconds apart, then the second one can always avert a collision by yielding to the first. In BRAM, each node waiting to transmit begins a delay of XT seconds when the channel becomes idle. The integer X is computed as X = (K - L + N) modulo N, where K equals index of node, L equals index of the last node which transmitted, and N equals number of

[50] F.A. Tobagi, "Multiaccess Protocols in Packet Communication Systems," IEEE Trans. Commun., Vol. COM-28, No. 4, April, 1980, pp. 468-488.

[51] L. Kleinrock and S. Lam, "Packet-Switching in a Slotted Satellite Channel," Nat. Computer Conf., AFIPS Conf. Proc., Vol. 42, Montvale, NJ, AFIPS Press, 1973, pp. 703-710.

[52] J.L. Capetanakis, "Generalized TDMA: The Multi-Accessing Tree Protocol," IEEE Trans. Commun., Vol. COM-27, No. 10, October, 1979, pp. 1476-1483.

[53] L. Kleinrock and M. Scholl, "Packet Switching in Radio Channels: New Conflict-Free Multiple Access Schemes for a Small Number of Users," Proc. ICC, Chicago, June, 1977, Paper No. 22.1.

[54] I. Chlamtac, W. Franta, and K. Levin, "BRAM: The Broadcast Recognizing Access Method," IEEE Trans. Commun., Vol. COM-27, No. 8, August, 1979, pp. 1183-1190.

nodes in the network. This creates a unique delay at each node, after which the node begins transmitting, providing the intervening nodes did not use their opportunities. This results in a "self-polling" effect with a rotating priority. Parametric BRAM allows the modulus of the above operation to be N/M, where M is some small integer. This results in M nodes computing the same delay, and thus M collisions can occur. When M = 1, the method is pure BRAM, or MSAP. When M = N, the method collapses to CSMA. For values in between, the method exhibits properties of both.

For an unbalanced system (few participients), MSAP (or simple BRAM) is inefficient for the same reason that polling is inefficient. Yet under these conditions, CSMA has its highest efficiency. Kleinrock[55] has suggested an adaptive system that uses M = N for highly unbalanced conditions, and gradually reduces M until M = 1 for a balanced system. Such a technique could prove highly efficient if the statistics of the network do not rapidly change. The complexity of such a technique, however, may not be warranted for this improvement in efficiency.

An access method, which combines a self-polling technique with CSMA in a more or less adaptive manner, is the HYPERCHANNEL protocol. Immediately after a transmitted packet, each station awaiting transmission executes a delay XT, where the integer X is preassigned to each node. This results in a fixed, as opposed to rotating, priority. After this delay, if no station has used the bus, the clocks are stopped and the bus reverts to CSMA. Transmission of a packet restarts the polling process. This solves many problems. The stations do not have to recognize the address of the last transmitter in order to maintain synchronism, since the poll always starts at the same place. Further, clock drift problems after the bus becomes idle for a long time are not a problem, since the system reverts to CSMA.

---

[55] L. Kleinrock, "On Resource Sharing in a Distributed Communication Environment," IEEE Communications Magazine, Vol. 17, No. 1, January, 1979, pp. 27-34.

Another property of the HYPERCHANNEL protocol can be used to advantage. The devices are inherently prioritized due to the unique delay which is predetermined for each BIU. By placing the processors and faster peripherals on the highest priority BIU's, the system can be optimized for maximum efficiency. Based on its simplicity, and apparent efficiency advantages, the HYPERCHANNEL protocol will be assumed for the candidate multiaccess bus architecture.

4.2.2 Interconnection Methods

The multiaccess bus is more difficult to implement with fiber-optics than with coax technology, because of the need for tee or star couplers. The implementation which places the least demands on the fiber-optic components is the so-called "active tee coupler" shown in Figure 4.2.2-1. The bus is implemented with two unidirectional fibers; one carrying data to the left, and the other carrying data to the right. At a BIU, both incoming fibers are terminated with receivers. The outputs of the two receivers are logically OR'ed to produce the input to the BIU electronics. The transmit signal from the BIU electronics is logically OR'ed with each received signal and transmitted on the corresponding fibers.

Note that although the BIU's are optically and electrically connected in series, they are logically connected in parallel, and operation is quite different from that of the ring. But, as with the non-redundant ring architecture, an active tee coupled bus is subject to catastrophic failure if any BIU fails. Further, redundancy techniques suitable for the ring would be less effective for the active tee configuation due to fault isolation difficulties. The active tee configuration is thus rejected based on reliability considerations.

The most practical implementation of a linear tee-coupled bus appears to be the dual unidirectional configuration shown in Figure 4.2.2-2. Each unidirectional bus is coupled to the BIU through a splitter/combiner pair (which may, in fact, be a single device). A practical tee bus is

limited by the number of such couplers which may be placed in series along the bus before a repeater must be used. A practical number has been calculated to be 4 or 5. Active repeaters placed this frequently along the bus result in serious reliability problems, as well as inconvenience of implementation. For this reason, tee-coupled buses will not be considered further.

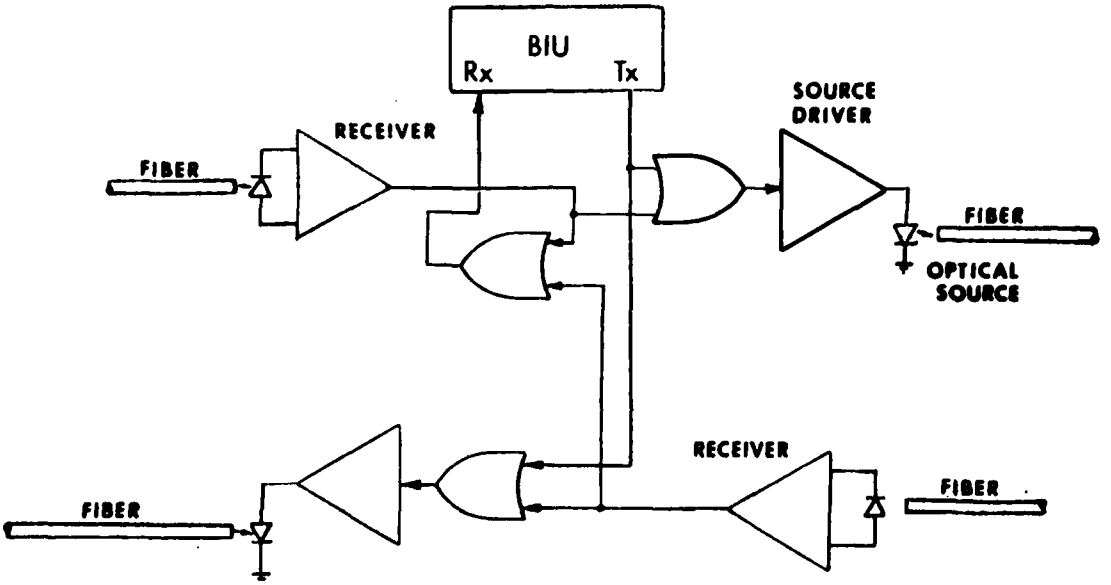

Figure 4.2.2-1. Active Tee Coupler

The star-coupled bus allows considerably more connections between repeaters than the tee-coupled bus. The only penalty is an increase in the total amount of fiber required in the network, since each terminal must connect to the central star. If N terminals are physically located in a circle of radius R, the amount of fiber-optic cable required is 2 X N X R, as opposed to $2\pi R$ for a non-redundant ring, or a tee-coupled bus. Thus for N greater than 3, and circular networks, the star configuration would require more cable. For the general case where BIU's are scattered randomly in two dimensions (or possibly three), this increase in fiber becomes much less significant and the tradeoff blurred.

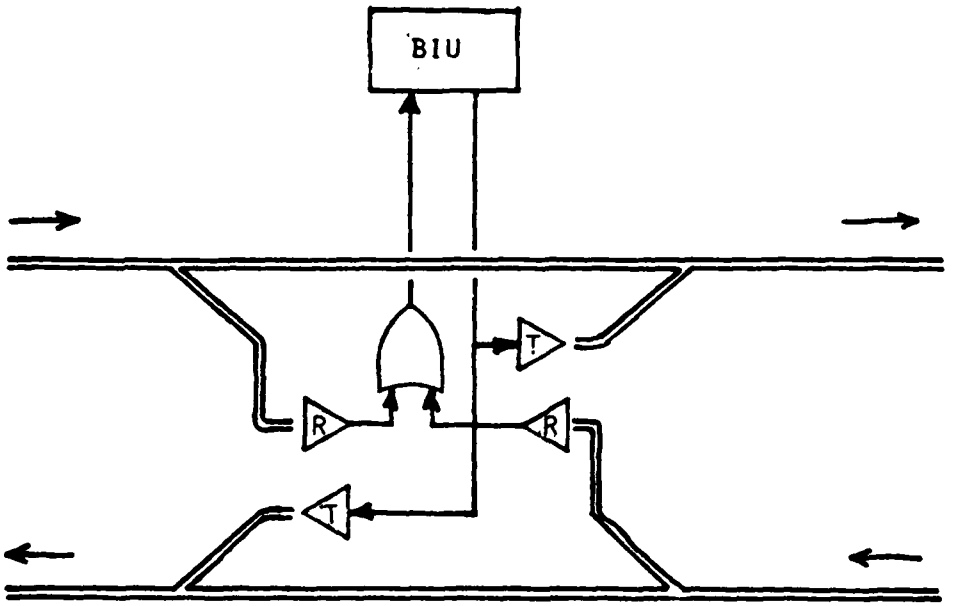

Figure 4.2.2-2. Dual Unidirectional Configuration

The star may be of the reflective or transmissive type. For the reflective star, used widely with fiber bundles, a single bidirectional fiber connects each BIU to the star. Light energy from the various links is mixed and reflected back to the BIU's on the same fibers. Each BIU must use a coupler to couple both its receiver and transmitter onto the same fiber. Losses can be expected to be higher with this approach than with the transmissive star, and the implementation of bidirectionality makes the approach more complex. Reflective stars are thus ruled out in favor of transmissive stars.

In the transmissive star configuration, each BIU interfaces to the star with a pair of fibers. Light energy transmitted by any BIU on its "Transmit" fiber is split within the star and is received by all BIU's via the "Receive" fibers.

Losses incurred in the transmissive star configuration include transmit fiber loss, splitting loss in the star (plus excess losses), and receive fiber loss. The transmit fiber loss may be compensated for by terminating each fiber with a repeater before entering the star. This requires many expensive repeaters. The same effect is achieved by placing a single repeater between the combiner and splitter portions of the star. The splitting loss can only be compensated for by placing a repeater on each outgoing link from the star. This again requires many repeaters and is not practical. The practical use of repeaters in a star is that of placing the repeater between the combiner and splitter functions. The use of an active star makes the network vulnerable to the repeater failure, but this activeness is concentrated in a single module and does not represent as great a threat as the numerous cascaded repeaters required in the tee-coupled approach or non-redundant ring. For this reason, both passive and active transmissive stars will be considered for candidate architectures.

4.3 Architectures for Further Analysis

Based on arguments presented in Paragraphs 4.1 and 4.2, three candidate architectures have been chosen for further analysis: 1) the interlaced ring, 2) the passive star, and 3) the active star. The following paragraphs describe these three approaches in more detail, and Section 5.0 presents an analysis of the ability of each approach to meet the program goals plus some other attributes deemed desirable.

As pointed out previously, the network operates in a packet-switched mode, with responsibility for bus control and link level protocol vested in the BIU's. The BIU is a programmable device which interfaces the fiber-optic bus to a processor or a peripheral. The "front end" of the BIU is a high-speed ECL-based design which transmits and receives packets on the bus at the burst rate. The "back end" of the BIU is a PDP 11/04-based design which transfers packets between the front end and the attached peripherals. This back end processor provides a UNIBUS interface to the peripherals, and executes the device handler programs. A device normally

connected to a 21(V) processor may be placed on the fiber optic bus for purposes of remoting or time sharing with multiple processors. The hardware retrofit consists of unplugging the device along with its UNIBUS interface from the host, and plugging it into a backplane slot within a BIU.

The PDP-11/04 backplane in the BIU provides multiple slots for device interfaces. Thus it is relatively straightforward to place more than one peripheral on a single BIU. Generally, a BIU can accommodate a single high-speed peripheral such as a disk or magnetic tape drive, or several low-speed devices such as card readers, paper tape units, or CRT displays. It is expected that, as an average, four peripherals may be placed on a BIU.

4.3.1 Ring Architecture

The first candidate architecture is the interlaced ring with passive bypass as in Figure 4.1.2-4, and using the control token access method. Although the number of BIU's in the ring has no theoretical limit, it will be desirable to avoid very long rings by breaking a large network into a few autonomously-operating rings connected with store-and-forward gateways. A gateway BIU in a ring recognizes a packet destined for another ring, and forwards it via a dedicated link to a similar gateway node on the other ring. Such an arrangement allows higher network rates in two ways; through simultaneous transmissions allowed by the autonomy of the rings, and higher efficiencies in each ring due to the shorter lengths.

4.3.2 Passive Star

The passive star approach assumes a 32-port biconically fused taper star in a central location connected to each BIU with a fiber-optic pair. The star is controlled with a variation of HYPERCHANNEL protocol which operates as a prioritized MSAP as long as transmissions are continuous, then reverts to CSMA/CD when the channel becomes idle for an extended period.

When more than 32 BIU's are required, star clusters may be tandemed in one of two methods. Figure 4.3.2-1 depicts a centralized repeater/arbitator. This device is "captured" by the first star which becomes active after an idle period and remains so for the duration of the transmission. The transmission from that star is broadcast to all other stars, but not back to the originator star. This repeater function illiminates the endless active loop encountered if the stars are connected with dumb repeaters. This repeater/arbitrator is a simple device, but presents a single point of failure.

The second star tandeming technique uses store-and-forward gateways as described for the ring approach. Figure 4.3.2-2 shows how all possible pairs of stars in the network might be joined resulting in only one store-and-forward delay between any two nodes in the network. This technique allows higher throughput due to the simultaneous transmissions made possible by autonomously-operating stars, plus increased efficiency due to the shorter bus in each subnetwork.

4.3.3 Active Star

The active star approach is no different from the passive star approach, except the star must have access to electrical power, and presents a point of failure or degradation. Section 5.0 documents the decrease in system availability due to the activeness of the star.

4.4 Signalling Requirements

4.4.1 Link Rates

The program goal is a network rate of 30 Mb/s. A general rule of thumb for this type of network is that an efficiency of 50 percent is achievable. With this in mind, a bus burst rate of 60 Mb/s is assumed, which degrades to an average effective rate of 30 Mb/s due to intermessage gaps, and necessary overhead.

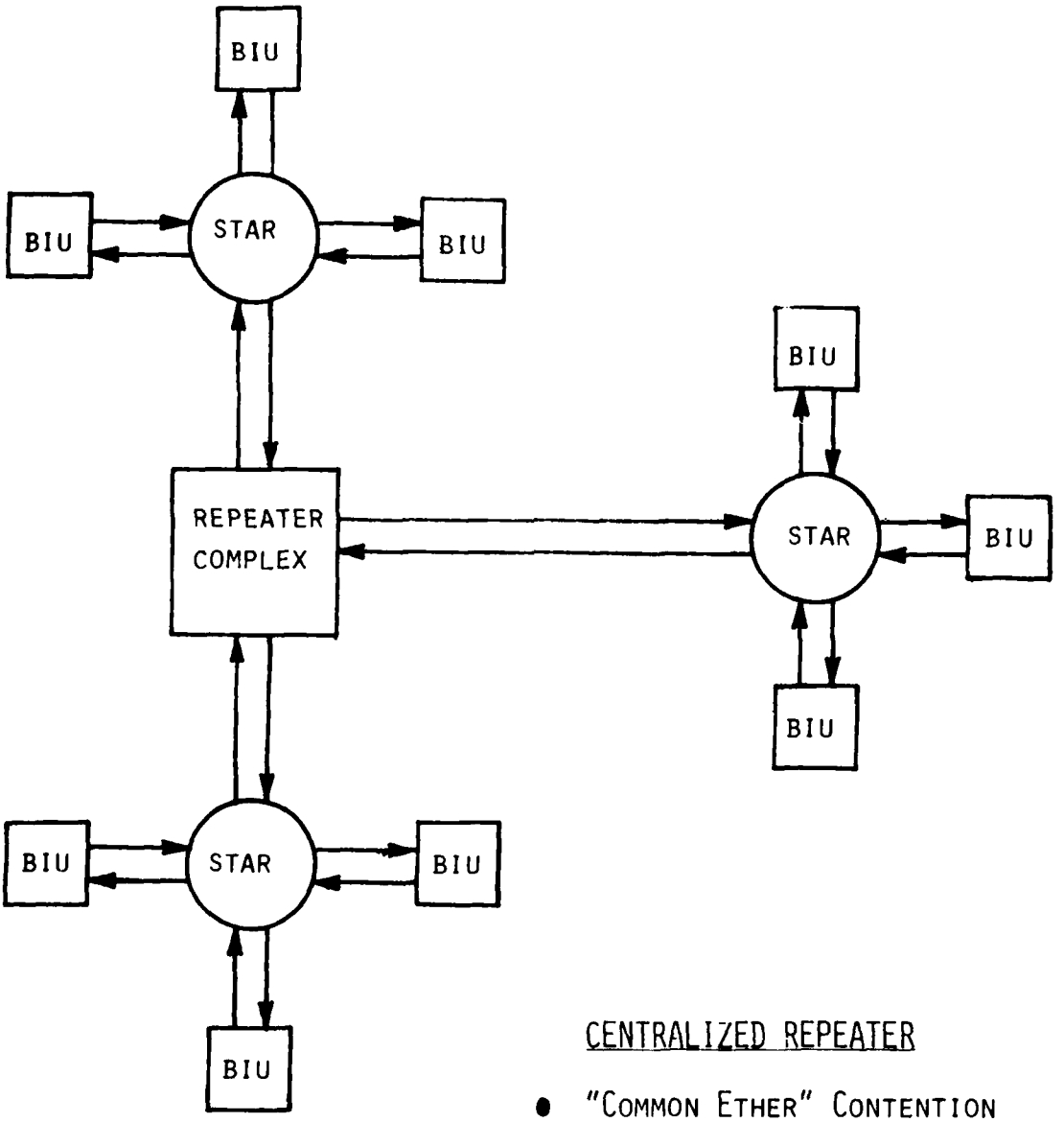

CENTRALIZED REPEATER

- "COMMON ETHER" CONTENTION
- ARBITRATER/ECHO CANCELLER
- SIMPLE ELECTRONICS
- SINGLE POINT OF FAILURE

Figure 4.3.2-1. Repeater Complex Tandeming

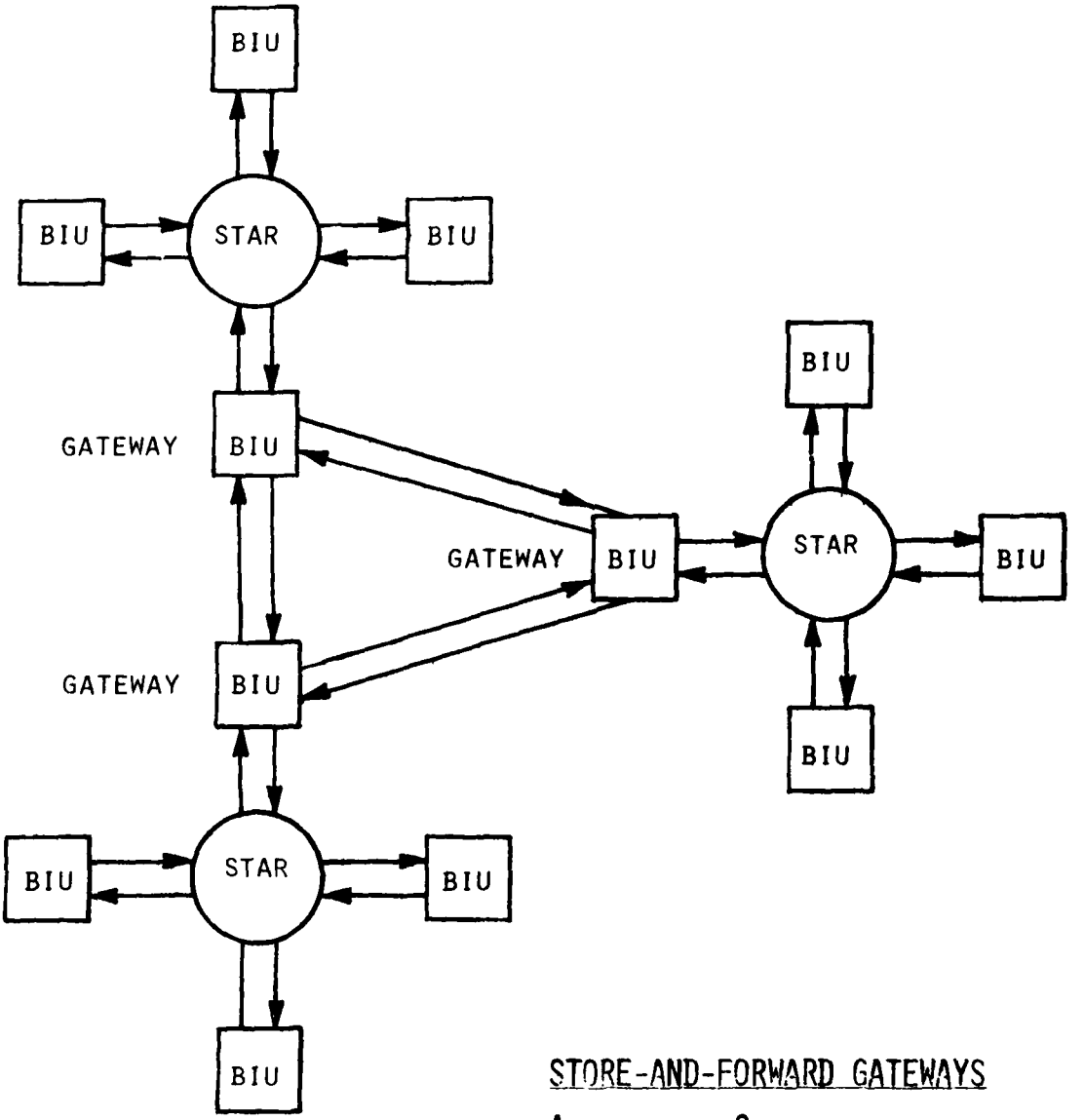

STORE-AND-FORWARD GATEWAYS

- AUTONOMOUS STARS
- GRACEFUL DEGRADATION
- COMPLEX PACKET-SWITCHED GATEWAYS
- STORE-AND-FORWARD DELAY

Figure 4.3.2-2. Gateway Tandeming

Paragraph 5.4 will analyze the architectures' relative abilities to provide the desired 30 Mb/s.

4.4.2 Protocol

In addition to the link access methods, namely CSMA/CD or control token, an end-to-end protocol must be established for a source BIU to communicate with a destination BIU. Currently, bit-oriented protocols such as HDLC, SDLC, or ADDCP are the most efficient protocols available, and are rapidly obsolescing byte-oriented protocols.

The assumed protocol for the remainder of this report will be the ANSI standard ADDCP, modified for Local Computer Network use by the inclusion of a source address. The format of a frame is, opening flag, source address, destination address, sequence number, information, Cyclic Redundancy Check (CRC), and closing flag. The flags in the Control Token Ring approach double as either message separater or token. The sequence number is necessary to preclude the possibility of the destination BIU receiving the same packet more than once. The deferred acknowledgement procedure used in Long Haul Networks is neither necessary or desirable in the Local Computer Network; the source BIU will not transmit a new frame until the previous frame is acknowledged.

4.5 Modulation Techniques

This section addresses considerations of the optical pulse formatting. Three basic types of line codes are available for optical fiber cable systems: the non-return-to-zero (NRZ) format where a transmitted data bit occupies a full bit period; the return-to-zero (RZ) format where a transmitted data bit occupies less than a full bit period; and the phase encoded (PE) format where both full width and half width data bits are present. All signals transmitted over an optical fiber must be unipolar. Multilevel signalling is feasible, however, the large bandwidth of single fibers overcomes the drawback generally associated with pulse code

modulation techniques, i.e., the use of "n" bit pulse code modulation requires a bandwidth of more than 2n times that of the original analog signal.

Although large bandwidths are attainable with optical fibers, signal-to-noise considerations of the receiver (addressed in Paragraph 3.1) require that larger bandwidths infer larger noise contributions. Another consideration is the availability of data timing from the bit stream, and the penalty associated with incorporating timing into the data stream. If no bit timing is available from the bit stream, the clock stability is an issue determined by the worst case message length.

The required optical power plots of this section use normalized noise bandwidth as the independent variable. To determine the required power the data required to enter these plots is the number of bits per Hertz of the particular line code (NRZ allows 2 bits/Hertz, Manchester 1 bit/Hertz, *and so forth*). A summary of these power spectral densities is shown in Figure 4.5-1 illustrating the normalized frequency content of each of the line codes discussed.

The discussion will first center on various line codes, beginning with NRZ to establish a baseline performance, followed by several of the RZ codes, and concluding with the Miller and Wood codes. With the discussion of line codes established, a review of the so-called "tri-level" modulation technique will be undertaken. At the conclusion of the section, the line coding techniques will be summarized and a tabulation of the pertinent characteristics presented.

Before discussing available coding schemes, a basis for comparison should be established. We will use the concept of an "eye diagram" to characterize the performance of the line codes. The "eye diagram," so-called because of the shape of the pattern generated on an oscilloscope, pictorially illustrates the effects of noise bandwidth, ac coupling of the receiver (baseline wander), and signal to noise (or "eye opening").

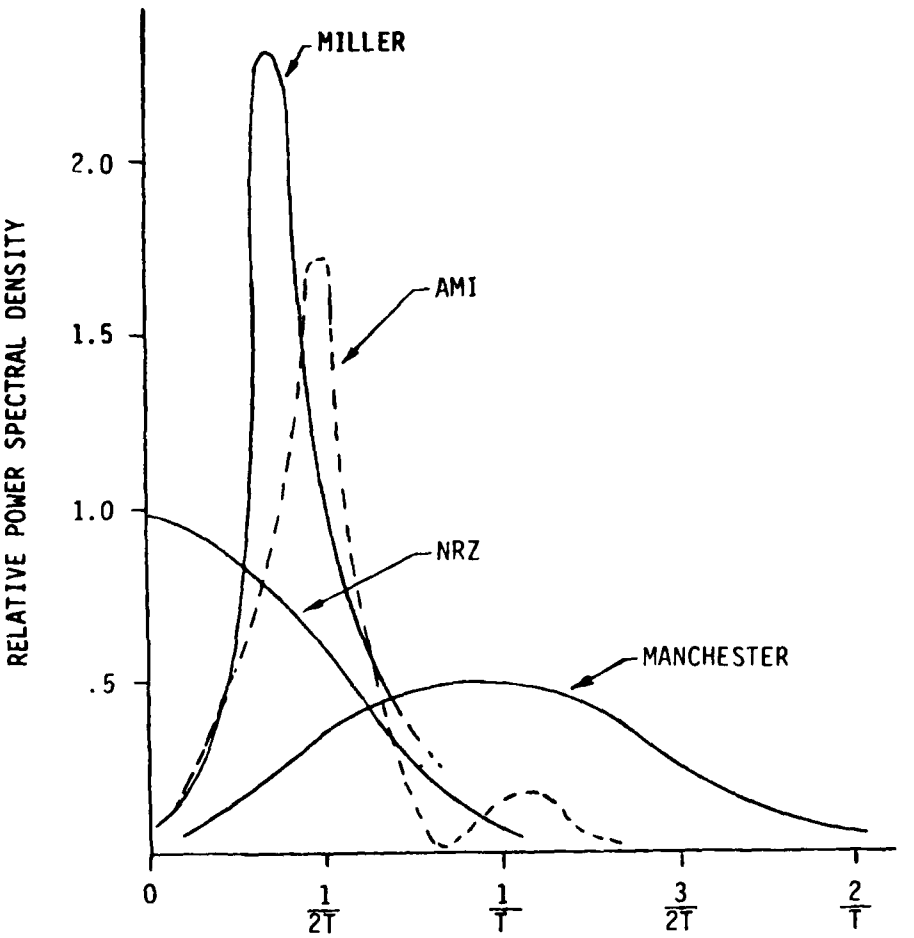

Figure 4.5-1. Plot of Power Spectral Density for Various Line Codes

Eye diagrams are used extensively in telecommunications systems to measure circuit or system performance. Briefly reviewing the concept, an eye diagram is an overlay of data sequences of ONEs and ZEROs. A 31 bit pseudorandom number sequence that is partitioned every three bit periods and each three bit period overlaid on a common set of axes generates an eye diagram such as that depicted in Figure 4.5-2(a). For this figure, the noise bandwidth is set quite large relative to the bit rate, allowing the

(a)

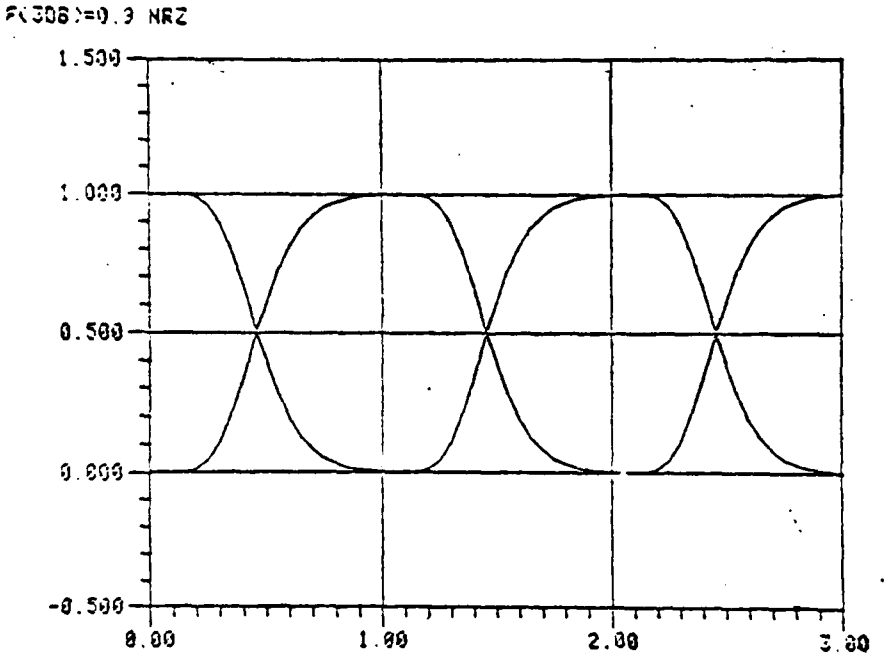

(b)

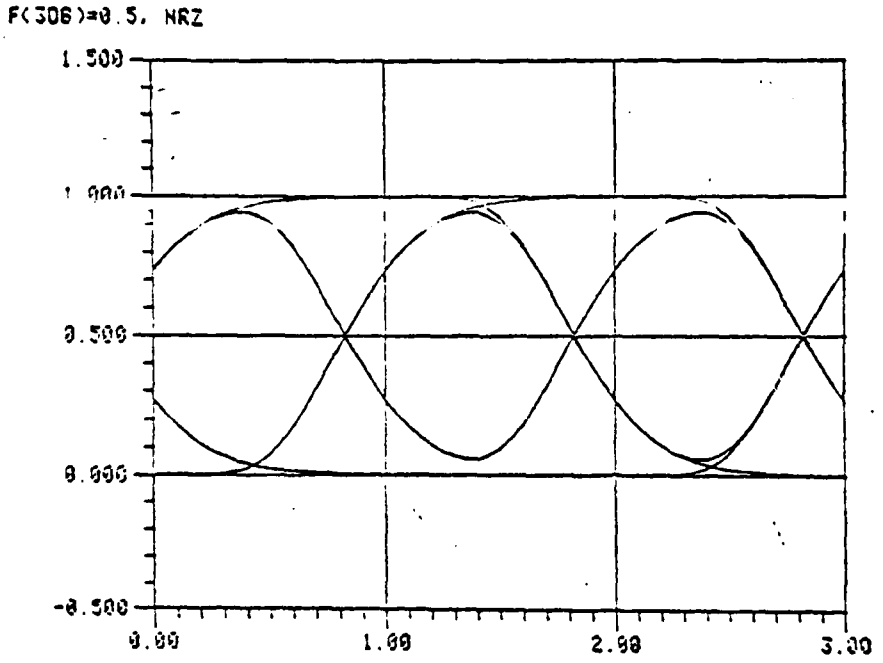

Figure 4.5-2. Eye Diagrams, NRZ Encoded Data, Noise Bandwidth Set at 0.9 and 0.5 of Bit Rate

"eye" to be "fully open" (e_m is maximized). By reducing the noise bandwidth to a value generally used in data transmission systems, another eye diagram is generated, shown in Figure 4.5-2(b).

The eye diagrams shown in Figures 4.5-2(a) and (b) illustrate the effect of reducing the noise bandwidth by reducing the upper frequency cutoff of the filter. Reducing the noise bandwidth by raising the lower frequency cutoff illustrates the impact of baseline wander and is shown in Figures 4.5-3(a) and (b) for two values of lower frequency cutoff (expressed as a fraction of the upper frequency cutoff). Baseline wander thus generates an effective eye closure and zero crossing jitter. Note that Figures 4.5-2(a) and (b) assume a lower cutoff frequency of essentially dc.

These eye diagrams illustrate the effects discussed using NRZ coded data. The basis for discussion of other coding schemes will be compared to NRZ, therefore the next discussion will outline some of the considerations of NRZ coding.

4.5.1 Non-Return-to-Zero Codes

The non-return-to-zero (NRZ) codes encompass several techniques of conveying serial data streams of ONEs and ZEROs. The simplest of the NRZ codes from the point of view of understanding is the NRZ-L. For a serial data stream encoded using NRZ-L, all data ONEs are encoded as a HIGH state, while all data ZEROs are encoded as a LOW state. The other two NRZ codes are known as NRZ-M and NRZ-S. NRZ-M is used in magnetic tape recorders and presents a change of state for each ONE (positive logic or a HIGH state is assumed). The change of state for each successive ONE for NRZ-M constitutes an "Invert on ONE" coding. The remaining code, NRZ-S is the complement of NRZ-M or invert on ZERO. These codes are shown in Figure 4.5.1.

F(3DB)=0.5, NRZ -- AC COUPLED RECEIVER @ 0.0001(0.00234).

(a)

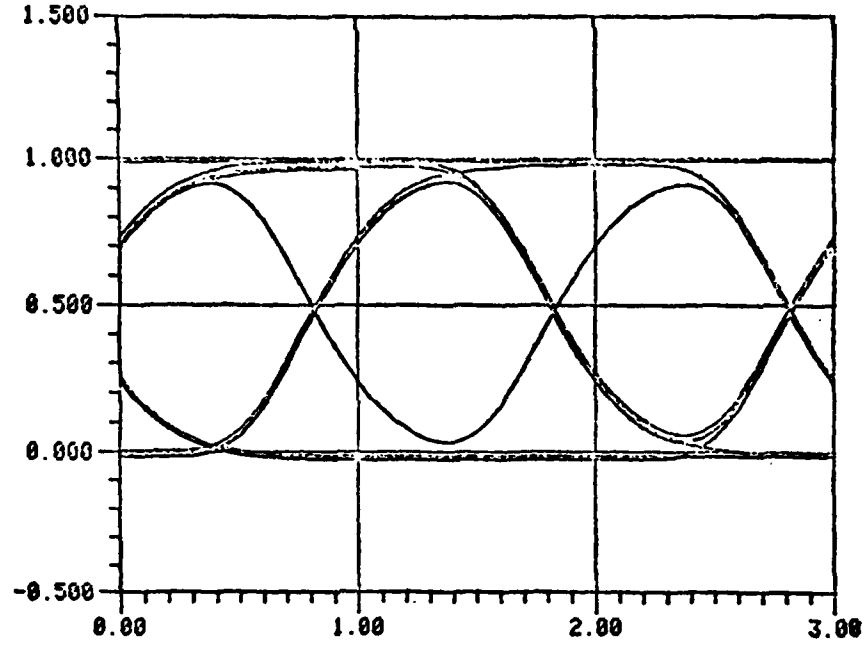

F(3DB)=0.5, NRZ -- AC COUPLED RECEIVER @ 0.001(0.02345).

(b)

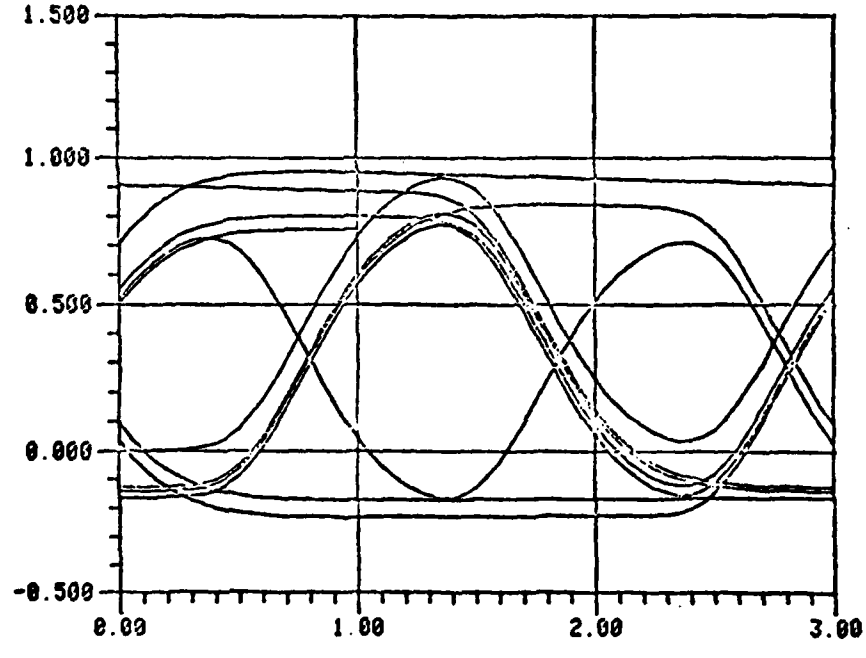

Figure 4.5.1. Eye Diagrams, NRZ Encoded Data, AC Coupled Receiver Performance for Various Coupling Factors

The selection of a particular NRZ code should be made with reference to the expected data stream characteristics. If no prior knowledge of the bit stream statistics is available, consideration should be given to scrambling techniques to assure reasonable transition density to maintain bit timing over long messages. However, if the expected probability of a ONE is significantly greater than that of a ZERO, the use of NRZ-M would be preferred. The same would apply to the selection of NRZ-S if ZEROs were more probable than ONEs.

A plot of the power spectral density versus normalized frequency was shown in Figure 4.5-1. Inspection of Figure 4.5-1 reveals the NRZ coding to require the least bandwidth of all the codes shown.

Although NRZ coding offers the minimum bandwidth requirement, the average power input to the receiver is data pattern dependent. Thus, for receivers exposed to different data sources with "short" intermessage gaps (as an example, less than two bit periods), a high level of received power coupled with a high percentage of HIGH data bits (again assuming that a ONE represents a HIGH signal state) in a message can result in the receiver threshold being raised to minimize the probability of error for a ZERO signal state (approximate threshold of half the signal height yields minimum error rate for equally probable ONEs and ZEROs and signal quantum noise negligible). This "adaptive threshold" receiver must then recover to the minimum threshold during the interword gap. If the succeeding message is a very low level and the threshold has not recovered, errors may be introduced if the preamble is not sufficiently long to allow synchronization. Protocol then impacts the receiver performance by defining the minimum intermessage gap length.

Alternatively, if the transit time through the network is sufficiently long, the dynamic range of signals may be of little consequence. For networks having a geographic distance between terminals of ~1000 meters the transit time is 5 μs (for protocols demanding a wait

for worst case propagation delay), allowing recovery of the receiver for data rates greater than 500 kb/s (assuming 2.5 bit periods are adequate to reach minimum threshold, and the receiver determines the end of message).

For NRZ coding schemes, the determination of the end of message poses a problem since NRZ is not run length constrained (i.e., there is no limitation on the number of successive ONEs or ZEROs). Several alternatives exist to the run length problem. One solution is to automatically invert one data bit every so many bits. This establishes a minimum transition density. Another technique is to employ a variant of the bipolar three zero (or six zero) substitution used widely in long haul telephone systems.

The use of bipolar three zero substitution (B3ZS) in a unipolar system requires some additional information to distinguish between substituted ZEROs and normal ONEs. To distinguish substituted ZEROs from ONEs parity can be used. For B37S a parity bit will be required such that two successive 3 ZERO lengths cannot occur without a parity bit. A 4 bit parity word length can also be used with a high probability of distinguishing ONE's from substituted ZEROs, however, this increases the data rate by 25 percent.

Alternatively, the unipolar receiver could be modified to establish a third level (mid-level). A simple inversion of every fifth or sixth bit would probably accomplish the same goal, but without the increase in data rate required for the insertion of the parity bit, or the establishing of three signal states. The use of zero substitution codes will therefore not be addressed further.

Since there are no guaranteed transitions in NRZ (without "n^{th}" bit inversion), the preamble length must also provide for the bit timing accuracy over the maximum expected length of no transitions. The use of "n^{th}" bit inversion can benefit the coding by allowing a shorter preamble, since timing accuracy is updated periodically.

Another alternative is to employ scrambling (modulo-2 addition of a known sequence with the data stream) to assure transition density. At the receiver, the data stream is again added to modulo-2 with the same sequence and the data recovered. The preamble can be fairly short when using this technique, since frame sync acquisition is the only requirement, bit timing having a high probability of being maintained by the scrambled data sequence.

The use of a preamble with a data scrambling technique allows the descrambling sequence to be generated from the preamble. This precludes resetting of each of the transmit and scrambling sequence generators each time a message is transmitted. The receiver descrambling circuitry must be resettable with each message however.

All the techniques discussed to constrain the run length of the coding have not altered the basic bit rate of the data stream (discounting parity bit insertion, which was dismissed). If adequate link margin exists, each incoming data bit can be encoded as two transmitted bits. These codes will be addressed next. The NRZ coding will be used as the baseline for comparison of these codes.

4.5.2 Return-to-Zero Codes

The use of NRZ coding minimizes the bandwidth requirement, but increases the complexity of the receiver to resolve the problem of run length constraints. The use of return-to-zero (RZ) coding substitutes a transition during either some or all bit periods to assure timing maintenance. Several RZ code types exist: half period RZ, where each data ONE is represented as a HIGH either during the first or second half of the bit period, and ZERO is represented by no signal during the bit period; biphase, where a ONE is represented by a HIGH in the first half bit period and a LOW in the second half of the bit period (a ONE is transmitted as "10") and the converse is true for a ZERO (a "01" is transmitted); and "short duty cycle" RZ, where the duty factor is less than 0.5 and either RZ

or biphase coding is used. Biphase is also called Manchester, although for optical systems the unipolar nature of the signal is differentiated from wire line systems, which generally employ bipolar Manchester signalling.

Several other line codes adapted from wire lines are also adaptable to a unipolar type of system. These other line codes include the Alternate Mark Inversion (AMI) codes. The RZ codes addressed are shown in Figure 4.5.2-1. There are three general classes of AMI codes (which we designate Classes I, II, and III for convenience). These three classes are defined based on the two bit code representing a ZERO, and are discussed next.

The AMI line codes all encode data ONEs alternately as two half periods in the HIGH state followed by two half periods in the LOW state, or as "11" and "00" in the notation previously mentioned. The AMI Class I line code employs a "01" code to represent ZERO, independent of the previous symbol. The AMI Class II line code represents a ZERO as "01" after a "11" (ONE), or as "10" after "00" (ONE). Consecutive ZEROs (either "01" or "10") are encoded the same until changed by a data ONE ("11" or "00"). The AMI Class III line code represents a ZERO by "10" following a "11" and as "01" following "00." Consecutive ZEROs alternately coded as "01" and "10" to maximize the distance between transitions. Figure 4.5.2-1 illustrates the RZ codes and the various conventions for each of the line coding schemes.

Each of these RZ coding schemes can be characterized in terms of minimum and maximum run lengths, timing component availability, and mean transition period. This characterization is shown in Table 4.5.2.[56] Also shown in Table 4.5.2 is the characterization of NRZ for comparison purposes.

[56] R. Petrovic, "New Transmission Code for Digital Optical Communications," Electronic Letters, Vol. 14, No. 17, 17 August 1978.

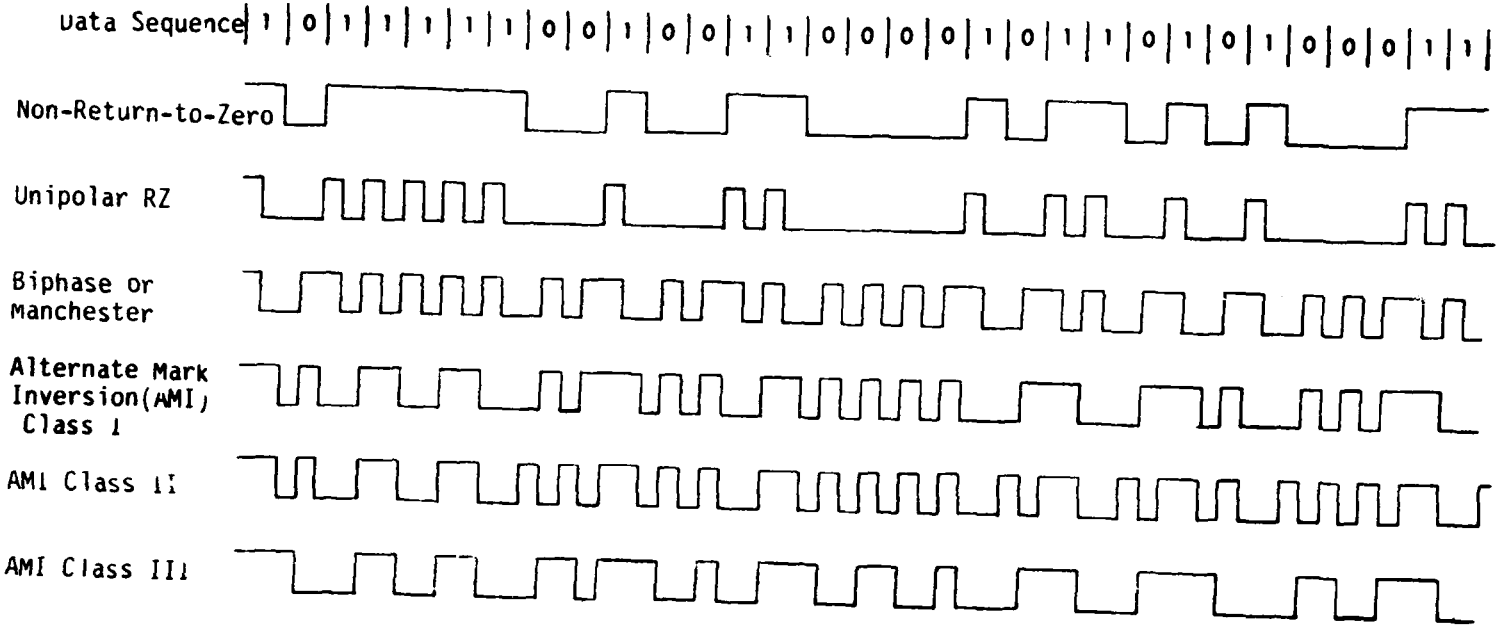

Figure 4.5.2-1. Return-to-Zero Line Codes (NRZ Shown for Comparison)

Table 4.5.2. RZ Line Code Characteristics

Type	Maximum Run Length	Minimum Run Length	Timing Component	Mean Transition Period	Minimum Bandwidth
NRZ		1T	No	T/2	1/4T
Half Period RZ		T/2	Yes	T	1/T
Manchester	1T	T/2	Yes	2T/3	2/T
AMI Class I	3T/2	T/2	Yes	4T/5	3/2T
AMI Class II	1T	T/2	Yes	2T/3	2/T
AMI Class III	2T	T/2	Yes	6T/5	1/T

As can be seen by inspection of Table 4.5.2, AMI Class III offers the lowest signal bandwidth (equivalently, the longest mean time between transitions) of the RZ codes discussed. The major difference between AMI Class II and Class III is the insertion of two transitions immediately following each ONE data bit for Class II, and the elimination of one transition for Class III. The use of AMI Class III minimizes the number of transitions and conserves bandwidth while AMI Class II maximizes the number transitions at the expense of increased bandwidth.

Since timing is available with AMI Class III, while bandwidth is conserved (to minimize noise bandwidth), this coding scheme offers the most benefits of the available RZ codes. The half period RZ code appears attractive; however, the significant dc content, which is data pattern dependent, coupled with the significant frequency content above the bit rate dictates some form of constraint of the run length (as in the case of NRZ). Before selecting AMI Class III line encoding a review of the time domain performance of these codes is appropriate.

To assess the performance of the various Alternate Mark Inversion Codes, eye diagrams for AMI Class II and Class III are illustrated in Figures 4.5.2-2 and 4.5.2-3. In both cases, a noise bandwidth of half the bit rate is assumed, and lower frequency cutoffs of 0.0001 and 0.001 times the upper frequency cutoff are shown. The same data is also shown for unipolar Manchester (biphase) in Figure 4.5.2-4. In all these cases, the lower cutoff frequency should be set at 0.0001 times the upper cutoff frequency for minimum baseline wander.

The eye diagrams thus indicate the maximum eye opening is available with AMI Class III of the RZ codes; however, there is a "short pulse" that creates a smaller eye opening (see Figure 4.5.2-3), which can introduce a significant bit error rate increase if the eye opening were set for the larger pulse width. In Manchester and AMI Class II, the "short pulse" is in the majority and the eye opening is readily apparent for this pulse width. Bit timing extraction will require two sampling points per bit period, and error detection of single bit errors can be accomplished by monitoring the received bit pattern for violations of the encoding rules.

Comparison of AMI Class II and Manchester indicate no basic difference in the noise bandwidth requirements. The eye diagrams indicate these codes are essentially the same from a channel bandwidth characterization viewpoint. Comparison of AMI Classes II and III indicates the more infrequent occurrence of the "short pulse" in the AMI Class III.

Between AMI Class II and Class III, the preferable line code from a signal to noise viewpoint is the line code that minimizes the noise bandwidth. Neither code exhibits any dc content (baseline wander induced from data pattern variations). Decoding of either code is simple and transition density is sufficient to guarantee timing maintenance. Detection of single bit errors is possible by comparison of the received data stream with the encoding rules to isolate violations.

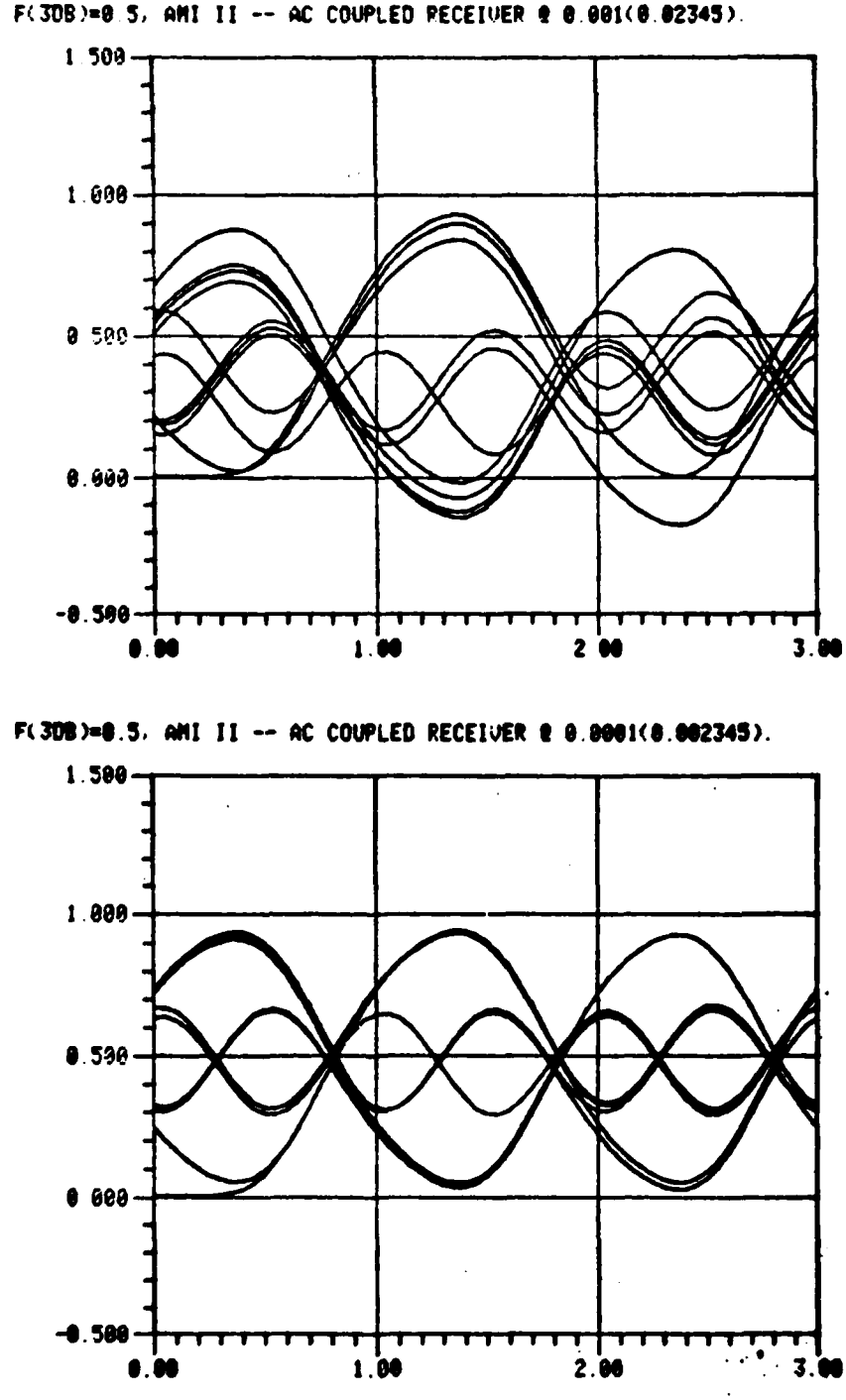

Figure 4.5.2-2. Eye Diagrams, Alternate Mark Inversion Class II Receiver Performance for Various Low Frequency Cutoff Values

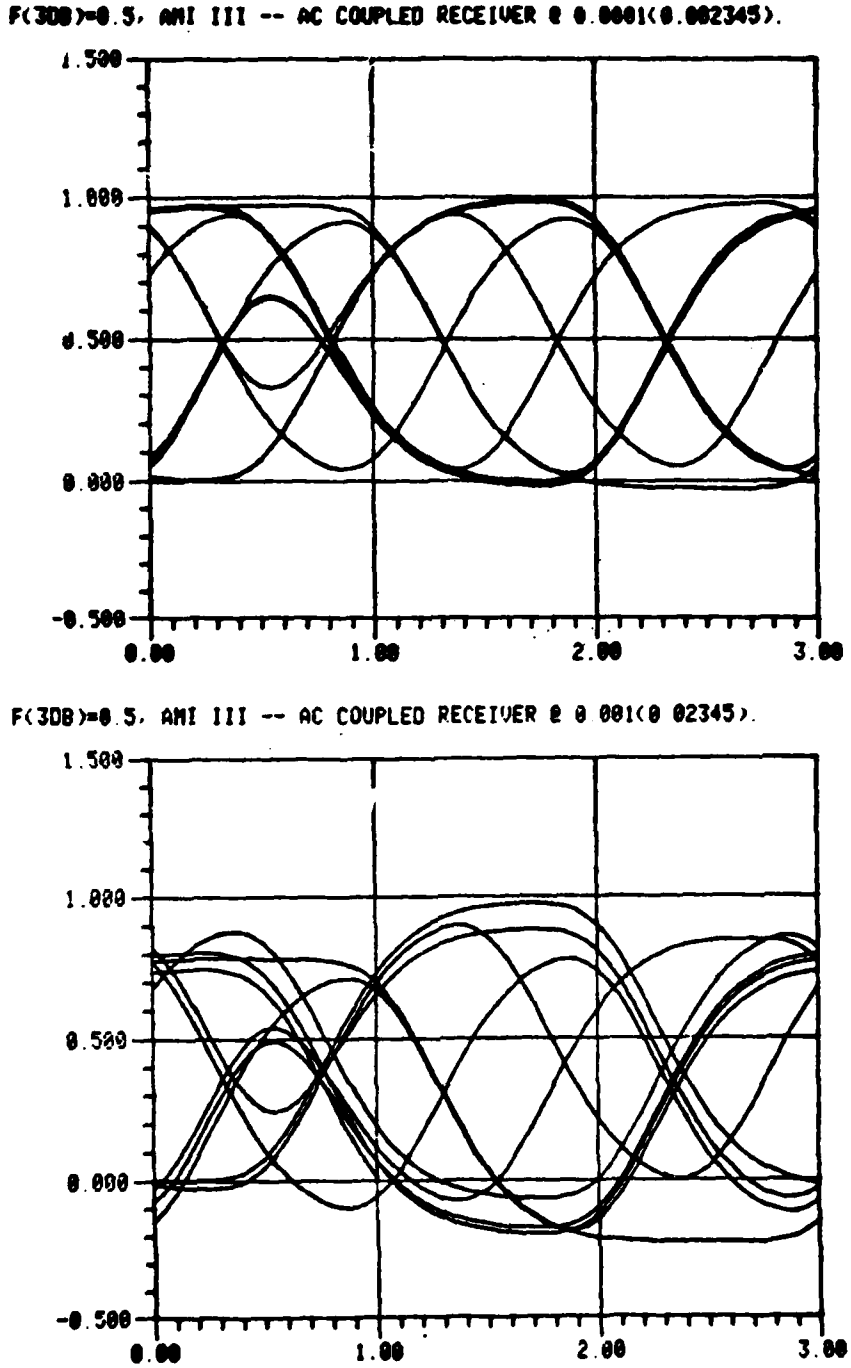

Figure 4.5.2-3. Eye Diagrams, Alternate Mark Inversion Class III Receiver Performance for Various Low Frequency Cutoff Values

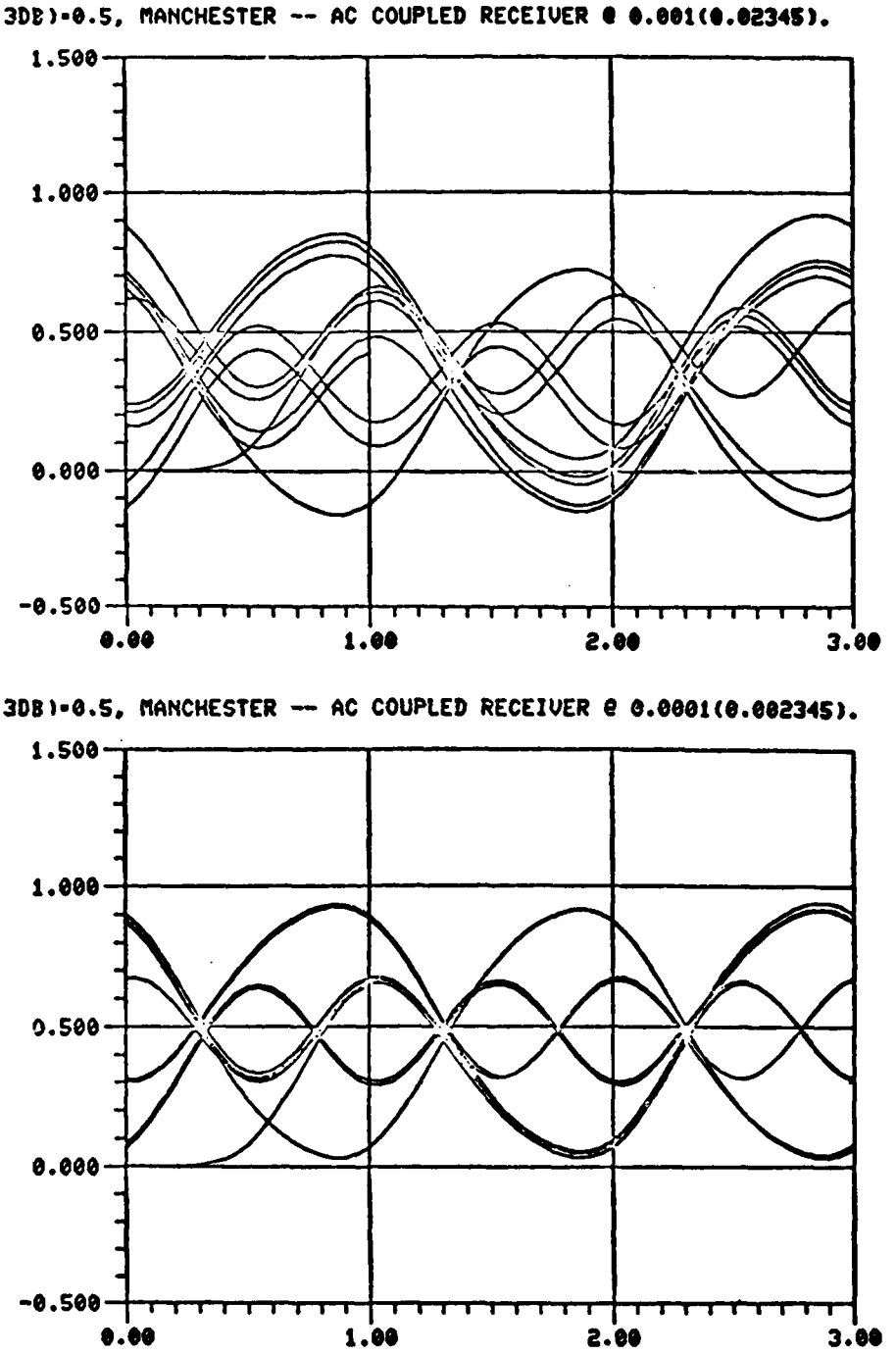

Figure 4.5.2-4. Eye Diagrams, Manchester Coded Data, Ac Coupled Receiver Performance for Various Low Frequency Cutoffs

For systems requiring the maximum received signal, the choice of encoding for RZ codes is AMI Class III, since bandwidth is minimized and it does not exhibit undesirable characteristics. Note that AMI Class III does have a larger bandwidth than required for NRZ, and the tradeoffs between scrambled NRZ and AMI Class III must be addressed. Prior to this tradeoff discussion, a review of phase encoding techniques is appropriate and addressed next.

4.5.3 Phase Encoding Techniques

The discussion of RZ codes above tentatively pointed to AMI Class III as the preferred RZ coding scheme. An alternative is to consider phase encoding, of which there are three commonly used codes: Miller code; Modified Miller code, in which the delay rule is changed; and Wood code, where ONEs and ZEROs are transposed from Modified Miller code. Figure 4.5.3-1 illustrates the three phase encoding schemes, as well as NRZ and AMI Class III for comparison purposes. All three phase encoding schemes have the same spectral density characteristics (see Figure 4.5-1).

As can be seen by inspection of Figure 4.5.3-1, the phase encoding (PE) techniques eliminate the "narrow pulse" condition seen in the AMI codes. Selection of a particular PE line code should be made in light of the data statistics. One factor that is determined by inspection of Figure 4.5-1 is the small, but finite, dc content of Miller (or Wood) codes. This is a result of a non-zero average for an odd number of ZEROs (or ONEs for Wood code) for Miller code. This dc content can be eliminated by the insertion of parity bits (with the attendant penalty of increased data rate). A review of the eye diagram performance is undertaken next.

The eye diagrams for Miller code are shown in Figure 4.5.3-2. Note that there are three possible sampling values at the point of maximum eye opening; HIGH, LOW, and transition. It is possible to sample successive transition points, potentially leading to ambiguous data. Consideration might be given to an oversampling technique (2x would be adequate) to avoid data ambiguity.

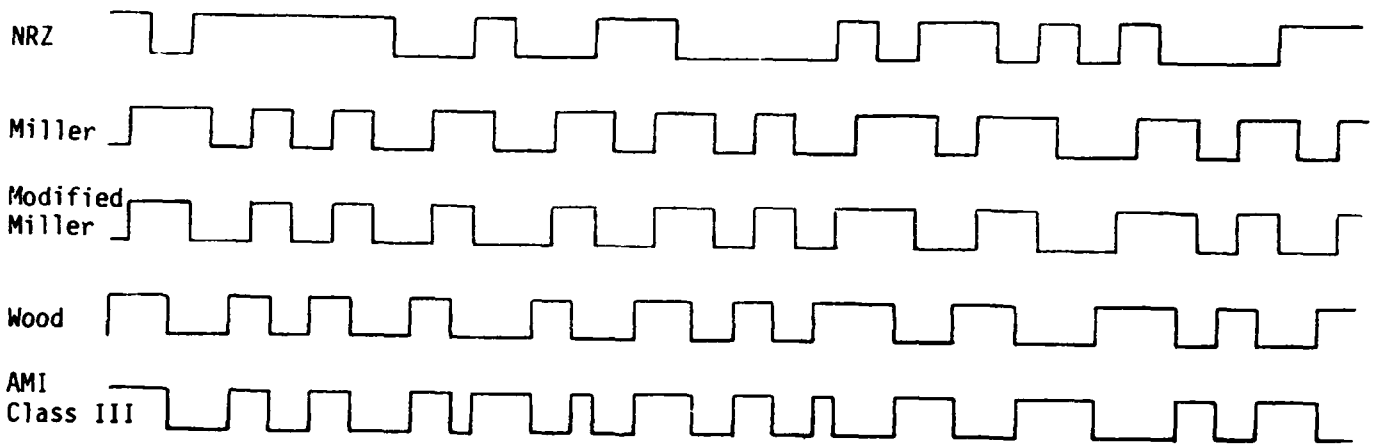

Figure 4.5.3-1. Data Sequences for Phase Encoding Techniques with NRZ and AMI Class III for Comparison

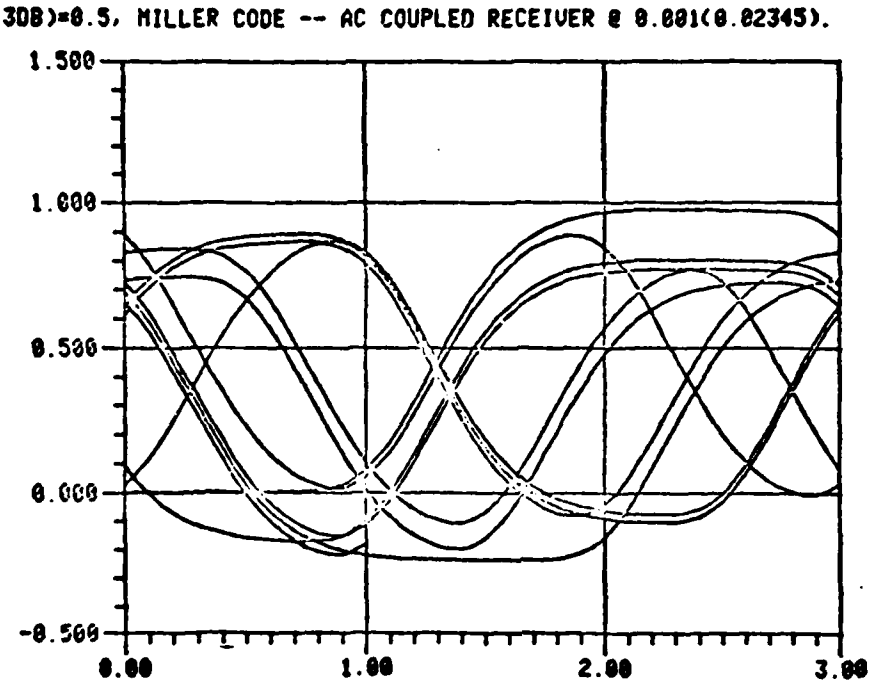

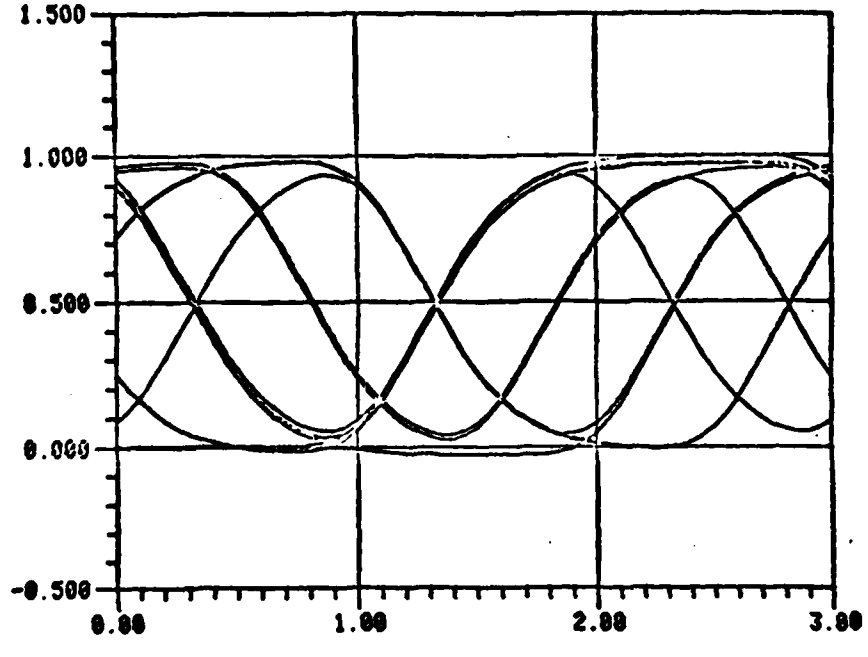

Figure 4.5.3-2. Eye Diagrams, Miller Coded Data, Ac Coupled Receiver Performance for Various Low Frequency Cutoffs

Comparing the Miller code eye diagram with that of NRZ encoding, Table 4.5.3 presents data concerning the phase encoding techniques as was done for the RZ codes. Note that the minimum time between transitions is greater than the RZ codes with the bandwidth correspondingly reduced.

Table 4.5.3. Phase Encoding Code Characteristics

Type	Maximum Run Length	Minimum Run Length	Timing Component	Bandwidth Required	DC Component
NRZ	∞	1T	No	1/4T	Yes
Miller Code	2T	1T	No	4/10T	Yes

4.5.4 Other Modulation Concepts

The previous discussions have assumed all coding is "two state," either ON or OFF. The use of "tri-level" has been proposed as a means of representing a bipolar signalling scheme over a unipolar transmission medium. In "tri-level," the "OFF" state is represented by "half power," and "+" and "-" states are represented by "full power" and "zero power," respectively. Another technique that has been advanced as a potential modulation format for fiber-optic data buses is a "short duty cycle" Manchester format. This signalling format uses a duty factor of approximately one-tenth of a pulse width, and increases the peak power from the source by tenfold to maintain a constant average power. These two techniques are addressed next.

The use of tri-level modulation offers a potential advantage in that a "zero level" is established and "+" and "-" signal transitions from the zero level can be generated from unipolar signals. For a bus network, where a receiver "sees" either more than one or all transmitters, a half power constant level signal from all inactive transmitters is translated into an effective increased "dark current" at the receiver. For a bus

network, where a receiver "sees" only one transmitter, the use of tri-level offers no "dark current" penalty since signal and quiescent states are orthogonal. The possible advantage offered is indication that the transmitter is functioning during periods of no message traffic.

Addressing tri-level in the case where more than one transmitter is seen by a receiver (Paragraph 3.1 goes into greater explanation of the signal power seen by the receiver), the number of terminals in the network and the network configuration determine the idle condition power seen by the receiver. If the same power is received from all transmitters, the constant value idle condition power will be:

$$P_i = \left[\frac{n-1}{2}\right] P_r \qquad (33)$$

where

P_i is the idle power seen at the receiver, in watts

n is the number of transmitters in the network

and

P_r is the received power from one transmitter, in watts.

Inserting this idle power into equation (13) of Paragraph 3.1, and comparing the performance to that of a single transmitter, a penalty of 6 dB is seen to exist (assuming JFET input receiver) from the effective increase in dark current for 15 terminals (1 terminal of the 15 is assumed to be transmitting data).

One question should be addressed before dismissing tri-level due to its penalty is that of operating at high data rates where the source is not fully extinguished in the OFF state for data ZEROs (assuming positive logic). For this case, (not tri-state, although similar) the source is commonly biased ON for a LOW level to prevent "ringing" for very fast rise time pulses. If a 10:1 ratio between ON and OFF is used, the idle power

seen by the receiver will be 1/5 of that given in equation (33). For this extinction ratio of the source (10 dB), the required power is increased by 4.5 dB. In either case, the presence of optical power during the LOW state degrades the receiver performance.

Another modulation concept that has been advanced[57] is that of a "short duty cycle" Manchester (we will abbreviate this modulation technique "SDC Manchester"). This technique employs low duty factor pulses (10% duty factor) with high peak power (10 X peak power) to maintain a constant average power. This modulation concept is applicable to average power limited devices (LED sources), but cannot be applied to peak power limited devices (ILD sources).

For LED sources employing the SDC Manchester modulation technique, the impact on the receiver performance is dependent on the limiting noise mechanism. For dark current limited receivers, the increase in bandwidth raises the noise power as the square root of the bandwidth. The power received then increases faster than the noise floor, and it is possible to achieve improved signal to noise performance. For receivers that are amplifier noise limited, the noise increases as the three halves power of the bandwidth, while the signal power increases linearly with bandwidth, degrading the receiver performance.

Also consider the associated rise time requirements for receivers supporting data rates greater than 20 Mb/s, the noise bandwidth must be opened to accommodate rise times associated with 100 MHz (or greater) analog systems. Were a monolithic receiver chip to be used, performance would suffer, since amplifier noise is the limiting factor. Receivers that are dark current limited are either low bandwidth (~1 MHz) or high temperature

[57] R. Betts, "An Aircraft 1553B Compatible Fiber Optic Interconnect System," Proc of 2d AFSC Mux Bus Conf, 10-12 October 1978

(100^{o} C) where dark current shot noise is significant compared to amplifier noise. These conditions are not anticipated for the AN/GYQ-21(V) data bus system and this modulation technique will not be considered for the AN/GYQ-21(V) network.

In summary, the use of tri-level imposes a 4-6 dB (or more) penalty in receiver performance. Similarly, the use of SDC Manchester offers no advantage to systems supported by receivers that are not dark current shot noise limited. The technical risk is also increased in the receiver design (designing a 250 MHz bandwidth to support a 50 Mb/s system represents significantly increased technical risk over a 25 MHz bandwidth design) even though dynamic range problems are eliminated with SDC Manchester (the receiver recovers to the baseline between pulses). With no significant advantage accruing to these modulation techniques, they are not considered as potential modulation techniques.

4.5.5 Line Code Performance Comparison

From the previous discussions, three candidate coding techniques appear as possible choices: Non-Return-to-Zero (NRZ); Alternate Mark Inversion (AMI), Class III; and Miller Code (or Wood Code). These candidate coding techniques have advantages and disadvantages. From Paragraph 3.1, increasing the noise bandwidth by a factor of two will increase the required signal power by more than twofold (see Figure 3.1.2.4-2).

A tabulation of the three line coding techniques is given in Table 4.5.5.

The advantages and disadvantages of each line code have been reviewed in the appropriate discussion, but are summarized here. Non-Return-to-Zero (NRZ) encoding without "n^{th}" bit inversion or scrambling does not guarantee sufficient transition density to guarantee timing recovery and is subject to baseline wander. The use of NRZ with scrambling increases the complexity of the encoders and decoders. The

Alternate Mark Inversion (AMI) Class III has a significantly smaller eye opening for the "short pulse." Miller code does not exhibit this "short pulse," but still requires two sample points per pulse to assure accurate data estimates. The decoder for Miller code is more complex than the AMI Class III decoder;[58] however, Miller code uses less bandwidth. Miller code also has a small dc component which results from certain code patterns, but this dc component is small.

Table 4.5.5. Line Code Comparison

Type	Maximum Run Length	Minimum Run Length	Timing Component	Noise Bandwidth
NRZ	∞	1T	No	1/4T
AMI Class III	2T	T/2	Yes	1/T
Miller	2	1T	No	1/2T

The use of NRZ with a scrambler offers the lowest bandwidth. The use of a scrambling sequence permits a high probability of maintaining timing, while minimizing baseline wander. The penalty to using scrambled NRZ is in encoder and decoder complexity. No error detection is available from either NRZ or scrambled NRZ from encoding violations.

[58] Op. Cit., Number 56

For high rate data bus networks, the minimum technical risk is to employ the minimum bandwidth coding scheme and maximize the received signal to noise ratio. If this criteria is used, scrambled NRZ offers the preferred alternative. If timing maintenance or a constant baseline value are of paramount concern, then either Miller Code or AMI Class III should be used, with preference to Miller code. During the discussion of network configuration analysis, the link margin available will be presented. This discussion will place the modulation analysis in the perspective of network (and link) margin requirements.

5.0 ARCHITECTURE FEASIBILITY

The previous discussion addressed the various configurations available for fiber-optic data bus networks that can support the AN/GYQ-21(V). With these network configurations characterized, the loss budgets of the candidate architectures can be reviewed. The loss budget of the particular network configuration can be applied against the receiver sensitivity to determine the required optical power that must be coupled by the source.

The required coupled power from the source compared with that available from sources commercially available determines the feasibility of the link. Each of the networks selected for further discussion are addressed in terms of the link loss budget available. After discussing the link budget a review of the network feasibility is undertaken. As part of the network feasibility discussion, a review of several of the timing and synchronization considerations is addressed.

The architectures considered in this section are the ring network (specifically the interlaced ring) and the star network (either passive or active stars). Each of these network configurations offers advantages and disadvantages and are discussed in the following paragraphs.

5.1 Link Loss Analysis

As discussed above, the two network configurations reviewed in this analysis are the interlaced ring and the star network. The first network discussed will be the interlaced ring. This configuration is a ring network configuration provided with redundancy to allow immunity to single point failure modes. The second network discussed is the star network, which also alleviates the single point failure mode of the ring network configuration. The star network also has a single point failure mode if physical destruction of the star coupler is considered, or if an active star without redundancy is implemented.

5.1.1 Ring Network Losses

The interlaced ring network, illustrated in Figure 4.1.2-4, can be modelled as a point-to-point link for loss calculations, with an additional loss for the coupler to accommodate the interlacing function. For the completely redundant configuration (additional transmitter at each network terminal) the additional loss for the coupler is eliminated.

With the constraints of 2-4 connectors per link, plus link lengths of 25 meters to 1000 meters, a tabulation of the loss contributors to the network can be compiled as shown in Table 5.1.1-1.

Table 5.1.1-1. Ring Network Losses

Loss Contributor	Minimum	Maximum
Fiber Losses*		
- Minimum length 25m	0.2 dB	
- Maximum length 1000m		8.0 dB
Connector Losses		
- Minimum 2 @ 1.0 dB each	2.0 dB	
- Maximum 4 @ 2.0 dB each		8.0 dB
Detector Coupling Loss	0.5 dB	0.5 dB
Detector Responsivity Improvement		
$10 \log \frac{0.65}{0.50}$	-1.2 dB	-
Total Losses		
- Minimum	1.5 dB	
- Maximum		16.5 dB

*Predicated on an 8 dB/km glass-on-glass fiber

The losses indicated in Table 5.1.1-1 lead to a source coupled power requirement of -35.1 dBm without any link margin (based on Figure 3.1.2.4-1). Comparing this requirement with the available optical power from light emitting diode sources having a bandwidth of ~40 MHz (see Table 3.2.3-1), adequate margin is available.

The data in Table 5.1.1-1 also indicates the receiver design must accept a range of optical signal power inputs. Although for this network configuration, the receiver "sees" only one transmitter (e.g., one detector can receive signals from only one upstream source), the receiver design must be capable of accepting a range of input signal levels, depending on source power, range of link lengths, variation in the number of connectors in the source-to-detector links and the loss of those particular connectors and other variations in link to link losses. This range of losses generates a bus dynamic range, which is also termed an optical signal range.

This optical signal range is a portion of the bus dynamic range since the variation in detector responsivity is not properly categorized as a variation in optical power seen by the receiver. The optical signal range added to the variation seen in detector responsivity is then one design constraint on the receiver. The other design constraint (other than minimizing the noise contribution) is the intermessage dynamic range, or the variation in signal levels between successive messages (or packets). Since the ring network always has the receiver addressed by the same source the intermessage dynamic range is essentially zero (0 dB). Some long term effects will change the received power, such as source aging and temperature effects on fiber and connectors. These long term effects are not significant in terms of intermessage intervals.

The ring network reliability was discussed in Paragraph 4.1 and the concept of an interlaced ring was broached as a means of improving the network reliability. The interlaced ring can be implemented by either separate transmitters for each of the two links emanating from the node, or one transmitter can be employed with an optical power splitter such as the CANSTAR TC-4C directional coupler.

If the separate transmitter approach is employed the data in Table 5.1.1-1 is applicable. If an optical power splitter approach is employed (less costly than a separate transmitter), the link budget is modified as that shown in Table 5.1.1-2.

Table 5.1.1-2. Interlaced Ring Network Losses (Passive Optical Splitter)

Loss Contributor	Minimum	Maximum
Fiber Losses*		
- Minimum length 25m	0.2 dB	
- Maximum length 1000m		8.0 dB
Passive Optical Splitter**	3.5 dB	4.5 dB
Connector Losses		
- Minimum 2 @ 1.0 dB each	2.0 dB	
- Maximum 4 @ 2.0 dB each		8.0 dB
Detector Coupling Loss	0.5 dB	0.5 dB
Detector Responsivity Improvement		
$10 \log \frac{0.50}{0.65}$	-1.2 dB	-
Total Losses		
- Minimum	5.0 dB	
- Maximum		21.0 dB

* Predicated on an 8 dB/km glass-on-glass fiber
** Predicated on CANSTAR Type TC-4C Coupler with 4.0 dB $\pm$0.5 dB insertion loss.

As in the case of the simple ring configuration adequate margin is available for the system. Two receivers are required at each node, thus there are no intermessage dynamic range requirements on the receiver. Some form of decision circuitry is required to evaluate the received signal and if it is invalid, switch to the alternate signal source. This decision circuitry requires some form of delay element to allow comparison between the two upstream terminal outputs. This decision circuitry impacts the network reliability, but discussion of this impact is deferred to the next section.

In summary, the loss budget for the interlaced ring network, either using separate transmitters for each downstream link or a single transmitter with an optical splitter, is easily achieved with simple receiver designs and low power light emitting diode (LED) sources.

5.1.2 Passive Star Network Losses

An alternative to the interlaced ring network is the star network, either passive or active depending on the network loss budget. The passive star network eliminates the requirement for retransmission of a message packet by any terminal in a particular cluster interconnected by a single star coupler. The use of a star coupler in the network does introduce additional connectors between a transmitter and a receiver (to allow the star coupler to be inserted or removed from the network) and also introduces a splitting loss. This splitting loss is generally the largest single loss contributor in the network and limits the number of ports a single star coupler can support (based on the receiver sensitivity).

Using the same per link constraints as was done for the ring network a tabulation of the minimum and maximum link losses can be projected. One additional network imposed loss is the addition of two connectors in all links to accommodate insertion or removal of the star coupler from the network. The star coupler losses are also introduced into all links, as indicated in Table 5.1.2-1.

Table 5.1.2-1. Passive Star Network Losses

Loss Contributor	Minimum	Maximum
Fiber Losses		
- Minimum length 25m	0.2 dB	
- Maximum length 1000m		8.0 dB
Connector Losses		
- Minimum 4 @ 1.0 dB each	4.0 dB	
- Maximum 6 @ 2.0 dB each		12.0 dB
Star Coupler Losses		
- Splitting loss 10 log (1/32)	15.0 dB	15.0 dB
- Implementation loss	2.5 dB	2.5 dB
- Port-to-port variance	-0.6 dB	+0.6 dB
Detector Responsivity Improvement		
10 log $\frac{0.65}{0.50}$	-1.2 dB	-
Detector Coupling Loss	0.5 dB	0.5 dB
Total Losses		
- Minimum	20.4 dB	
- Maximum		38.6 dB

The star coupler losses have been divided into two categories: the first being splitting losses, which are fixed once the number of ports is determined; and the second being implementation losses, accounting for losses incurred from the mixing process and for variances between output ports for a given input port. These implementation losses are representative

of those achieved on a 10 port coupler fabricated at Harris. Some improvement in these losses (particularly the port-to-port variation) should be achieved in the near future.

The total link losses of Table 5.1.2-1 lead to a source, coupled power requirement of -12.5 dBm coupled power and, as in the case of the ring network, with no margin, assuming an APD gain of 20 as shown on Figure 3.1.2.4-1. Increasing the APD gain to 100 allows the coupled power to be reduced to -15.7 dBm, or an approximate 3.2 dB gain in link margin. This link is feasible with any of the high radiance Burrus structure LED sources. These sources couple ~200 μW of optical power into fibers having numerical apertures (N.A.) of 0.25, which can support the bandwidth requirement for the AN/GYQ-21(V). The source coupled power of -7 dBm (200 μW) allows a link margin of approximately 5-8 dB, depending on the avalanche gain value.

The passive star network introduces a new requirement on the receiver that does not exist on the ring or interlaced ring networks. Since each receiver now can receive signals from all sources accessing a single star coupler, the received signal power will vary with the transmitting source. This varying signal power, termed intermessage dynamic range, requires that the receiver be capable of seeing a large signal from one source followed by a small signal from the next source transmitting. The receiver then must be capable of recovering between messages to be able to successfully detect the smallest signal seen.

The intermessage dynamic range imposed on any receiver is a subset of the bus dynamic range (also the optical signal range). In the passive star network that portion of the loss between the star coupler and the receiver is a fixed loss and imposes only long term variation (temperature, connector loss changes - such as unmating/mating - and other relatively slow variations). Thus the intermessage dynamic range is the variation in the source-to-star-coupler losses. These losses are tabulated as Table 5.1.2-2.

Table 5.1.2-2. Intermessage Dynamic Range Factors

Source power variation (ΔP_C)	3.0 dB
Variation in the number of connectors (1@ 2.0 dB)	2.0 dB
Temperature induced connector loss variance (source to star coupler, 2 connectors)	2.0 dB
Star Coupler port-to-port variation ($\pm$ 0.6 dB)	1.2 dB
Temperature induced fiber loss (1/2 maximum length Λ = 3 dB/km)	1.5 dB
Fiber length variation ((1/2 maximum)/(1/2 minimum))	2.5 dB
Total loss variation	12.2 dB

Thus, although the bus dynamic range is ~20 dB, any receiver will see a maximum of ~12.2 dB. Note that the detector responsivity variation is not included as part of the intermessage dynamic range, since a particular receiver is connected to only one detector. A similar argument can be made for the connectors and fiber between the star coupler and the receiver.

The intermessage dynamic range can be accommodated in two ways; one is to increase the intermessage gap, and the second is to design the receiver to accommodate a larger signal range. The first method is by far the easier method and offers no appreciable risk unless the increased intermessage gap impacts the bus throughput rate. To better quantify this 12.2 dB of intermessage dynamic range (16.6:1 signal power range), it is instructive to look at the response time of the post-detection filter.

The worst case intermessage dynamic range (IDR) situation for the receiver is the case of a maximum signal followed by a minimum signal after the minimum intermessage gap time. The residual signal remaining from the maximum signal level can be set at an arbitrary amount (some percentage of the minimum signal) and the filter bandwidth which will yield this arbitrary

signal level ascertained. Using a 3-pole Bessel filter characteristic and defining the maximum residual signal as 1 percent of the minimum signal level two bit periods after a maximum signal, the filter bandwidth can be determined.

The 3 dB filter bandwidth is a function of the bit rate and the filter characteristic. To achieve the 0.06 percent residual signal (of the maximum signal -0.01 X 16.6 = 0.06%) the 3 dB filter bandwidth can be determined by a successive approximation technique as:

$$B_{3dB} = 0.636\ f_{BR}$$

where

B_{3dB} is the half power filter bandwidth, in Hz

and f_{BR} is the data rate, or bit frequency in the case of full baud codes, in Hz

With this half power filter bandwidth, the modified noise bandwidth, B_n, is expressed as:

$$B_n = 1.075\ B_{3dB} = 0.54\ f_{BR}$$

These bandwidths are determined by using the time domain response of various 3 dB bandwidths to determine when the residual signal is below the specified amount after 2 bit periods. The use of a 3 dB bandwidth of 0.75 times the bit rate is adequate to assure a dynamic range of 12.2 dB. If a slightly greater intermessage gap is present, the 3 dB bandwidth can be reduced. Additionally, since the receiver uses a sampling technique to make bid decisions, the sampling point being at the midperiod point of the bit, the residual signal at 2 1/2 bit periods is the appropriate residual measurement point.

Using the 2 1/2 bit period as the measurement point, the same procedure yields a 3 dB filter bandwidth of:

$$B_{3dB} = 0.426\ f_{BR}$$

both quantities being defined as before. The discussion of filter bandwidths in Paragraph 3.1 indicated the potential difficulties of operating with a noise bandwidth near $0.4/\tau$ from parameter variations. The use of a 3 dB bandwidth of $0.426\ f_{BR}$ leads to a noise bandwidth of:

$$B_n = 1.075\ B_n = 0.458\ f_{BR}$$

The use of three decimal places is misleading, since component tolerance is more significant than the third decimal place. For this case a noise bandwidth of one half the bit rate is adequate to handle the dynamic range imposed. This noise bandwidth is consistent with that anticipated for normal receiver design considerations.

The passive star network offers an alternative to the interlaced ring configuration. There is no decision circuitry required at each terminal to select which upstream terminal is the proper source selection. The network losses are higher than for the interlaced ring network and there is not a significant link margin. Message retransmission is eliminated, since all receivers ran receive messages from all sources connected to the star coupler inputs.

The link margin is of concern in the passive star network, as the source coupled power is near the maximum achievable with most LED sources. One new source which has been developed under contract to the Air Force Avionics Laboratory* by Plessey offers coupled power near that achievable by

*Plessey LED Type Number C0045, developed under contract Number C0045 for U.S. Air Force Avionics Laboratories

injection lasers. This device couples ~ 850 μW of optical power into 0.3 N.A. fibers, with a rise time of 2.4 nsec and a fall time of 2.7 nsec. The device can therefore meet the data rate requirements of the AN/GYQ-21(V) network.

The use of the Plessey high speed LED thus permits significantly more coupled power (-0.7 dBm versus -7.0 dB for conventional Burrus devices). The use of this device allows a link margin of 11.8 dB, which is a significant improvement over the marginal ~4.9 dB previously attainable with the passive star network (APD gain set at 20).

Another alternative is to use an injection laser diode to achieve 1-3 milliwatts (mW) coupled into the fiber. This power level (0-4.8 dBm) increases the link margin further, albeit at the expense of "laser noise" discussed in Paragraph 3.2, and the additional circuit complexity of optical feedback, thermoelectric cooler, and bias stabilization requirements. The development of the Plessey LED is the first real alternative to the ILD offering substantial coupled power and concurrently short rise and fall times.

The star coupled network is thus marginally feasible with a Burrus LED. The use of a high radiance Plessey LED offers reasonable link margin, as does the use of an ILD, although with additional circuit complexity and design risk.

5.1.3 Active Star Network

An alternative to the passive network is the active star network, using a repeater at the central node of the network. To preclude a single point failure mode with the introduction of a repeater, a redundant repeater set can be paralleled at the central node. The introduction of one (or two) repeaters at the central node also eliminates intermessage dynamic range at all receivers except those at the central node. Additionally the link losses are reduced due to the shorter maximum link length and fewer connector insertion losses.

Using the same network parameters as has been assumed for the previous network types, a link loss budget can be constructed as shown in Table 5.1.3-1.

Table 5.1.3-1. Active Star Network Loss Budget

Loss Contributor	Minimum	Maximum
Fiber Losses		
- Minimum	0.2 dB	
- Maximum		4.0 dB
Connector Losses		
- Minimum 2 each @ 1.0 dB	2.0 dB	
- Maximum 3 each @ 2.0 dB		6.0 dB
Star Coupler Losses		
- 10 log 1/32	15.0 dB	15.0 dB
- Implementation loss	2.5 dB	2.5 dB
- Port-to-port variance	-0.3 dB	+0.3 dB
Detector Responsivity Variation		
10 log $\frac{0.65}{0.50}$	-1.2 dB	-
Detector Coupling Loss	0.5 dB	0.5 dB
Total Losses		
- Minimum	18.7 dB	
- Maximum		28.3 dB

*Maximum source-to-detector cable distance half the maximum link length

With these losses and maintaining the same receiver performance, the source coupled power requirement is reduced to -23.3 dBm, or comparable with the interlaced ring network source coupled power requirement. Using the same Burrus structure LED yields a link margin of 16.3 dB, resulting in a low risk approach.

Another factor that results from the repeater insertion is a reduction in dynamic range. The intermessage dynamic range is reduced to zero for all terminals (receivers at the terminals are always addressed by the source at the repeater) and the bus dynamic range is reduced with the reduction in the number of connectors and the shorter link lengths.

The intermessage dynamic range, seen only at the repeater at the central node, as theoretically 7.8 dB, but more probably will not be greater than ~6.8 dB. This lower expected intermessage dynamic range results from the low probability that one connector in the coupler array would exhibit excess loss induced by low temperature while another connector in the same array would not exhibit a similar low temperature induced excess loss.

The active star network essentially subdivides the technical requirements into two areas: one, of supporting an intermessage dynamic range, accomplished at the repeater; and two, supporting a sensitive receiver design, with essentially no intermessage dynamic range. These two requirements are associated with separate link loss budgets, tabulated as Tables 5.1.3-2 and 5.1.3-3.

In summary, the active star network offers improved performance over the passive star network, while simultaneously reducing the associated implementation risk in not being able to close the link. The active star network divides the technical requirements of the star network - intermessage dynamic range and receiver sensitivity - into two separate requirements, allowing separate receiver designs to be optimized for one of the two requirements, rather than requiring one receiver design to support both intermessage dynamic range and maximum sensitivity.

Table 5.1.3-2. Active Star Network Loss Budget Terminal-to-Repeater Link

Loss Contributor	Minimum	Maximum
Fiber Losses		
- Minimum 25 meters	0.2 dB	
- Maximum 500 meters		4.0 dB
Connector Losses		
- Minimum 3 @ 1.0 dB each	3.0 dB	
- Maximum 4 @ 2.0 dB each*		8.0 dB
Bifurcation Loss**	3.0 dB	4.0 dB
Star Coupler Implementation Loss***	1.0 dB	3.1 dB
Detector Responsivity Variation	-1.2 dB	-
Detector Coupling Loss	0.5 dB	0.5 dB
Total Losses		
- Minimum	6.5 dB	
- Maximum		19.6 dB

* Assumes connector between repeater and "Y" coupler
** Splitting loss for two repeater central node employing "Y" coupler at central node
***Implementation loss of 32:1 combiner (1/2 biconically tapered star coupler) may be one half of expected 2.5 dB for complete star coupler, plus splice loss of splicing "Y" coupler to combiner. Implementation loss includes any port-to-port variation.

Table 5.1.3-3. Active Star Network Loss Budget Repeater-to-Terminal Link

Loss Contributor	Minimum	Maximum
Fiber Losses		
- Minimum	0.2 dB	
- Maximum		4.0 dB
Connector Losses		
- Minimum 3 @ 1.0 dB each	3.0 dB	
- Maximum 4 @ 2.0 dB each*		8.0 dB
"Y" Coupler Insertion Loss*	0.5 dB	1.0 dB
Star Coupler Losses		
- Splitting losses	15.0 dB	15.0 dB
- Implementation losses**	2.2 dB	3.1 dB
Detector Responsivity Variation	-1.2 dB	
Detector Coupling Loss	0.5 dB	0.5 dB
Total Losses		
- Minimum	20.2 dB	
- Maximum		31.6 dB

* Includes splice loss to 1:32 power splitter
** Includes any port-to-port variation

The active star network does allow a single point failure mode (addressed more fully in the discussion of network reliability) unless a redundant repeater is employed. Dynamic range requirements on the active star network are substantially less than the passive star network and adequate link margin is achieved.

5.1.4 Summary

The three networks that have been addressed - the interlaced ring, the passive star and the active star - have been shown to be feasible with varying degrees of implementation risk. Of the three, the passive star network offers the greatest implementation risk and the greater receiver design problem, since the receiver must be designed for both maximum sensitivity and intermessage dynamic range. The interlaced ring network offers the least design and implementation risk and the active star offering slightly more design effort and implementation risk.

The use of the passive star will require either an injection laser diode source or less link operating margin must be accepted. A possible alternative is the Plessey high radiance source developed under contract to the Air Force Avionics Laboratories; however, manufacturing of this device has not been undertaken and no second sources presently exist.

The use of the interlaced ring allows simple PIN detector and LED sources with ample link margin. Additional circuitry is required at each terminal (additional receiver, more stringent constraints on the timing reconstruction, and decision circuitry) to assess the health of the upstream terminal.

The active star network has more worst case loss (longest links with greatest number of connectors) than the interlaced ring, but could potentially allow LED sources and PIN detectors (although the margin would be minimal - equivalent to that of the passive star network). The active star network requires repeatering at the central node of the network, but minimizes the dynamic range requirements and maximum sensitivity associated with the passive star network.

Of the three network types, the interlaced ring network offers the least implementation risk in terms of loss budget. The active star offers slightly more implementation risk. The most implementation risk is associated with the passive star network. The ring (noninterlaced) was addressed also but not discussed due to its susceptibility to single point failures.

5.2 Network Reliability and Test Considerations

At this point we have determined that three network types are considered for the AN/GYQ-21(V) network configurations - the interlaced ring network, the passive star network and the repeatered, or active, star network. Insight can be gained into the reliability tradeoffs of each of these networks by appropriate modelling of the network to analyze assembly and network failure rates. Availability can be determined, given the assembly failure rates and the mean-time-to-repair a failed assembly.

The network availability can thus be established as a measurement criteria to determine the relative merit of each network type. This relative merit is determined for nonredundant networks to preclude serious network shortcomings from being masked by "an alternate path". Redundancy is then not used to attempt to substitute for low failure rate components. The use of redundancy to compensate for poor component reliability creates a system that requires constant maintenance action, substantially higher operating costs, as well as a higher acquisition cost. The use of redundancy to mask poor design or component reliability thus seriously impacts life cycle cost.

To determine the merit of the three candidate architectures, a failure rate will be determined for the link, based on projected assembly failure rates. This link failure rate, coupled with a repair action estimate allows a link availability to be ascertained. Appropriate combinations of link availabilities then leads to a projected overall network availability. A tabulation of these projections is then presented for comparison of the three network types.

5.2.1 Link Reliability Projection

The reliability of a basic fiber-optic link can be calculated by review of the components for each assembly and then review the required assemblies for each link. A network reliability projection can be attained by investigation of the link interconnections. A basic fiber-optic link reliability projection then must review the components and assemblies.

Any fiber-optic link has a transmitter, including an optical source (be it a light emitting diode (LED) or an injection laser diode (ILD) source), an interconnecting fiber, and a receiver including a photodetector. The interconnecting fiber (including any splices, connectors, and passive couplers) is passive, and does not exhibit failures in the sense of a mean-time-between-failures, or lifetime expectancy. The electronics at the transmitter and receiver and the electro-optic transducers (source and detector) effectively represent the failure mechanisms of a fiber-optic link.

With the failures restricted to the active devices, it is relatively straightforward to compute an assembly failure rate for a given circuit with a specified level of component quality factors. Without the actual circuit, a like circuit can be employed to project the reliability. An illustration of a comparable receiver preamplifier is shown in Figure 5.2.1-1. A similar diagram for a simple timing extraction circuit shown in Figure 5.2.1-2, and a diagram of a comparable transmitter circuit is shown in Figure 5.2.1-3.

The bit timing extraction circuit shown in Figure 5.2.1-2 is not adequate for a bus network where data arrives in asynchronous, independent packets. For networks where a synchronization word precedes every frame and sequential frames are in synchronization such as with the ring, or interlaced ring, the timing extraction circuit of Figure 5.2.1-2 is appropriate. For asynchronous frames (or packets) the complexity of the timing extraction

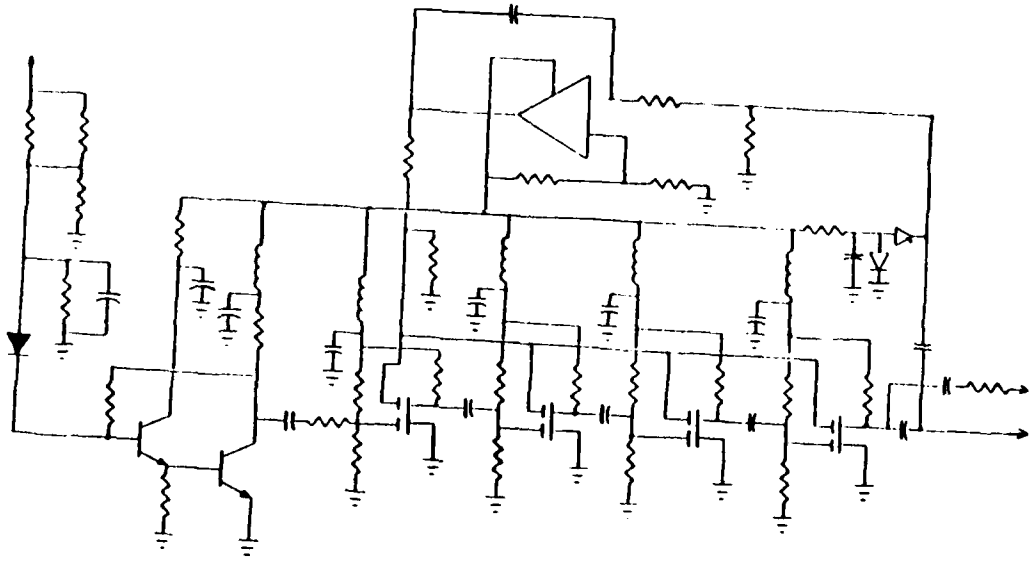

Figure 5.2.1-1. Typical Receiver Schematic

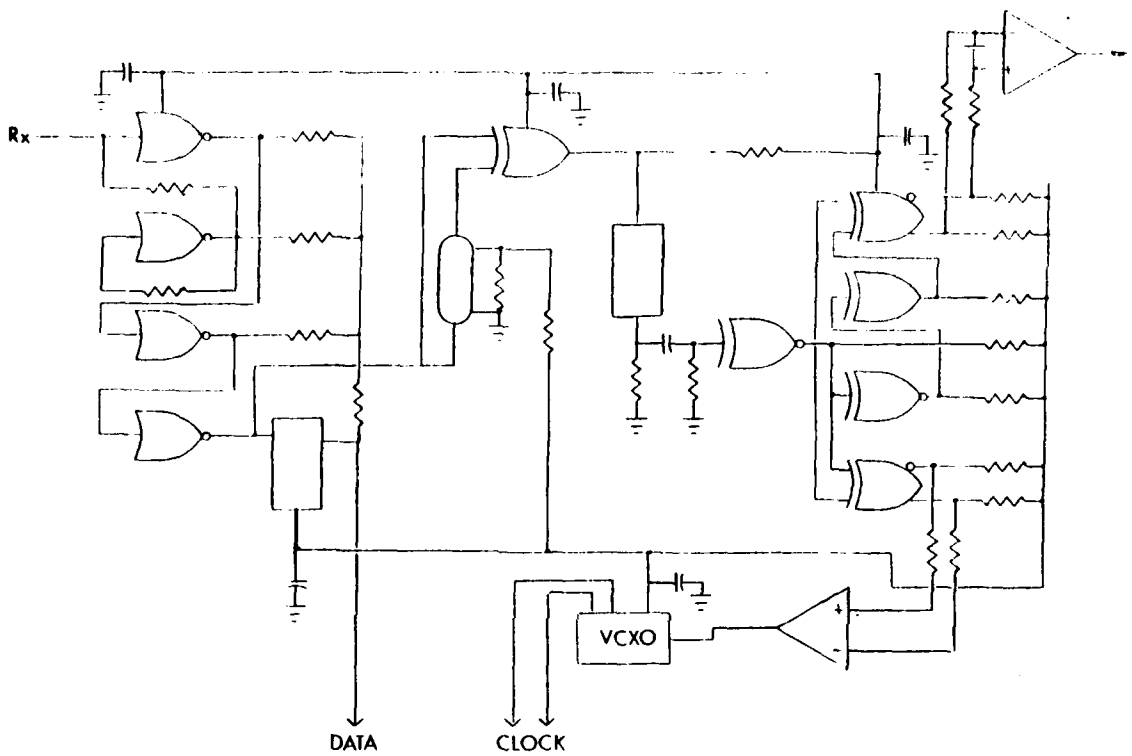

Figure 5.2.1-2. Bit Synchronizer Schematic (Partial)

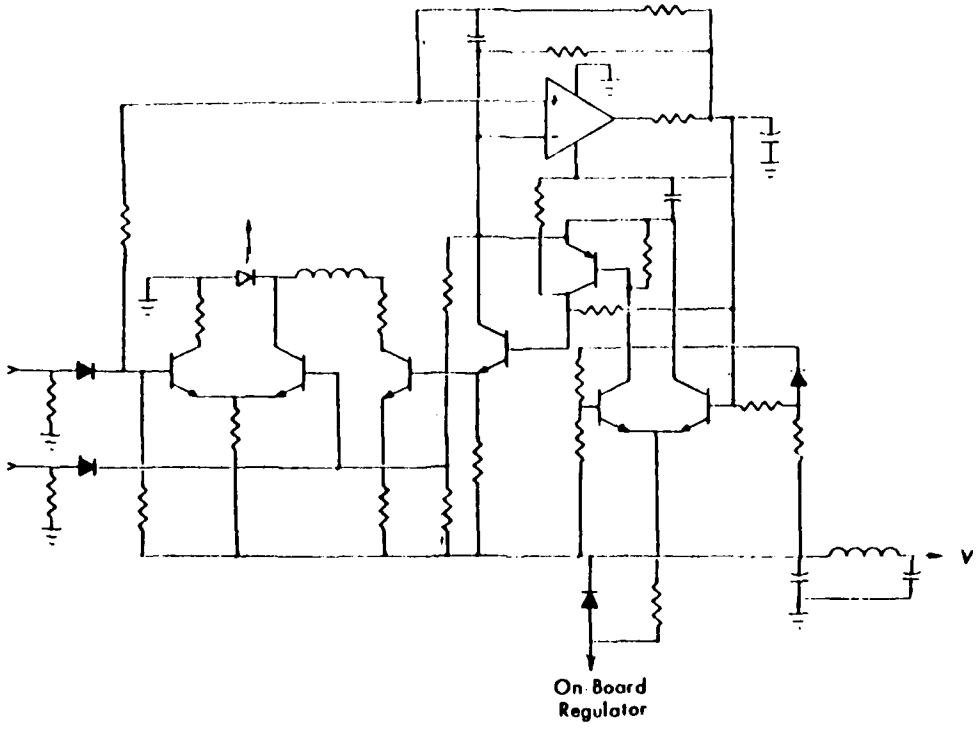

Figure 5.2.1-3. Typical Transmitter Schematic (Partial)

circuit could be as much as three to four times greater. As an approximation, a factor of four will be used to project a failure rate of an asynchronous timing extraction circuit.

Each of these circuit diagrams can then be reduced to a number of components, and a failure rate associated with component type. An assembly failure rate can then be computed from the tabulation of component failure rates, as shown in Table 5.2.1. The tabulation in Table 5.2.1 does not exactly match the component count of the schematic diagram, but allows for several additional components that may be required to achieve operation over a wider temperature range, larger dynamic range, or other different operating conditions.

The total failure rate shown for each of the assemblies is approximate, and is used only as an indicator of the order of magnitude of the assembly failure rates to be expected, but are adequate for comparative purposes. With this caveat, the failure rates shown in Table 5.2.1 are rounded to two places. These failure rates will be used in subsequent calculations to determine estimated network availability. These network availability calculations require estimates of the network maintainability, in terms of the time required to repair a failed terminal. These estimated times are addressed next.

5.2.2 Maintenance and Test Considerations

The time required to restore a link (or network) to service is a function of the number of diagnostic tests that must be performed and the complexity of (or equivalently, the time to complete) each diagnostic test. The time to complete each diagnostic test can be significantly reduced with Built-In-Test (BIT) performing monitoring functions of specified assemblies and components.

Table 5.2.1. Component Failure Rates by Assembly

Component	Number per Assembly	Component Failure Rate ($\times 10^{-6}$)	Total Failure Rate
Transmitter Assembly			
ILD (or LED)	(1)	4.000	4.000
PIN Detector	(1)	0.1470	0.1470
RF Transistors	(4)	7.038	28.1520
PNP Transistors	(1)	11.178	11.178
Differential Pair Transistor	(1)	8.4456	8.4456
Thermoelectric Cooler	(1)	0.8929	0.8929
Diodes	(8)	0.9450	4.7280
Integrated Circuit	(1)	0.69040	0.69040
Resistors	(30)	0.01265	0.3795
Capacitors	(10)	0.00172	0.0172
RF Chokes	(2)	0.05000	0.1000
Printed Circuit Board	(1)	0.00048	0.00048
RF Connectors	(2)	0.21736	0.43472
Multipin Connectors	(2)	0.34320	0.68640
		Total Assembly Failure Rate	59.85352

Table 5.2.1. Component Failure Rates by Assembly (Continued)

Component	Number per Assembly	Component Failure Rate ($X\ 10^{-6}$)	Total Failure Rate
Receiver Assembly			
APD Detector	(1)	1.5152	1.5152
Thermoelectric Cooler	(1)	0.8929	0.8929
Thermistor	(1)	0.1680	0.1680
Bipolar Transistors	(2)	7.038	14.076
MOSFETs	(4)	3.5250	14.100
Integrated Circuits	(2)	0.69040	1.38080
RF Chokes	(8)	0.05000	0.4000
Diodes	(4)	0.94500	3.7800
Resistors	(30)	0.01265	0.37950
Capacitors	(20)	0.00172	0.00344
Printed Circuit Board	(1)	0.00048	0.00048
Connectors, RF	(2)	0.21736	0.43472
Connectors, Multipin	(2)	0.34320	0.68640
		Total Assembly Failure Rate	37.82171

Table 5.2.1. Component Failure Rates by Assembly (Continued)

Component	Number per Assembly	Component Failure Rate ($X\ 10^{-6}$)	Total Failure Rate
Bit Synchronizer Assembly			
Emitter Coupled Logic IC's	(4)	0.39516*	1.58064
VCXO Circuit	(1)	1.850	1.850
Linear IC's	(2)	0.69040	1.3808
Transistors	(3)	1.0380	3.1140
Delay Line	(1)	negligible	negligible
Diodes (Zener)	(2)	1.2750	2.550
Filter	(2)	0.400	0.400
Diodes (Si)	(5)	0.94500	4.7250
Resistors	(35)	0.01265	0.44275
Capacitors	(15)	0.00172	0.0258
Printed Circuit Board	(1)	0.00048	0.00048
Connectors, Multipin	(2)	0.34320	0.68640
Connectors, RF	(3)	0.21736	0.65208
		Total Assembly Failure Rate	17.40795

The addition of activity monitoring circuits at board level offers the capability of functional testing during normal operation and fault isolation to assembly or module level on detection of a failure. An optical transmitter employing an injection laser source is an example of an assembly where addition of BIT is extremely simple and yields dividends in terms of early detection of degraded performance. Injection laser diodes generally use optical feedback to stabilize the diode over temperature, thereby avoiding the requirement to tailor threshold adjustment circuitry to each device. This optical feedback is derived from "back facet" emission and applied to a PIN detector to maintain the optical power output by adjusting the bias current level. Simple monitoring of this "automatic gain control" (AGC) circuit against bias current allows determination of the health of the ILD source.

The health of the ILD device can thus be determined by comparison of the optical power output (detector output) and the bias current level, for a given temperature and using some form of "look-up table" at the central test location. Similarly, a comparison of the bit stream input to the transmitter with output from the ILD source can ascertain function of the transmitter. Placement of this BIT circuitry on the transmitter printed wiring board minimizes the requirement for additional connector pins for access to the board and output from the board, but increases the complexity of the transmitter assembly. Additionally, failures in the BIT circuitry may go undetected and not generate early warning of maintenance action requirements.

The use of BIT circuitry for the receiver follows the same general principles as for the transmitter. It is not possible to test the photodiode without an external signal however, and without a known incoming optical signal input, it is only possible to test the later stages of the receiver. A known bit stream pattern can be injected into the receiver, but this requires the receiver to either be "off-line," or the network be inhibited from handling data while testing is in progress. The synchronization pattern can alternatively be compared with the correct

pattern in each successive digital frame in both synchronous and asynchronous networks. Again, on-board BIT circuitry increases the complexity of the receiver.

Test points can be brought out from the transmitter and receiver such that "remote" testing of the operation of the receiver and transmitter can be performed. "Remote" may simply mean a separate card plugged in adjacent to the receiver and transmitter cards which accesses various test points in a programmed series of test routines. The test routines could then be accessed separately to perform self-test functions as well as providing monitoring and testing of the transmitter, receiver and timing extraction circuitry.

If test routines to exercise various components in the network are possible, the test card potentially can reduce the optical power output from the transmitter as a means of verifying bit error rate performance of the receiver. Measuring bit error rate performance of the receiver is an indirect method of ascertaining the health of the photodetector. If avalanche gain is used the temperature, bias voltage and received signal must be used to determine photodiode performance.

The error rate measurement technique varies with the network architecture. This difference in measurement technique is due to the differing numbers of receivers addressable by a given transmitter in each network configuration. The larger the number of receivers addressable by a single transmitter the fewer the number of tests required to determine the bit error rate for each receiver and for the network. After determining the bit error rate for each receiver all networks will require at least one message per terminal not successfully tested to report the status of the terminal. No difference between networks for reporting status then exists. Each network testing procedure is reviewed in the following paragraphs.

The ring network test procedure requires testing of each individual link in the network, since one transmitter addresses one receiver. A test message will require decoding at each bus interface unit prior to the actual test sequence. To use the test a receiver without first instructing the receiver to not "pass the message" is to risk the receiver not detecting the message type (test) due to an error in the message instruction and the test message propagating around the network. This fault mode is modelled as an "endless loop" fault mode. The careful attention to test message protocol is thus imperative to avoid this fault mode.

The ring network thus requires that the test message be transmitted serially around the loop. Due to the link margin available in the ring network, some method of reducing the source coupled power of a "healthy" source will be required to accurately determine the status of a receiver. This reduction in power is necessary to generate a sufficient number of bit errors to achieve statistical significance. Thus the ring network requires each transmitter to reduce its output power to properly measure receiver performance.

An alternative to reducing the transmitter power is to manually insert an optical attenuator in each link, measure the received power at the receiver (to ascertain the particular link losses and source coupled power) then measure the receiver performance. This approach is totally unsuited for automated testing and although offering short term savings in acquisition cost, seriously impacts life cycle cost from an operating and support cost viewpoint. Manual testing of the terminals allows some insight into the number and types of tests that must be performed, but is inefficient and costly, except in the case of troubleshooting/fault isolation.

It is not possible to simultaneously test each individual link in the ring network, simply due to the propagation time for the command message to transit the loop. After each terminal receives an instruction to transmit a test message (and retransmits that instruction). The following

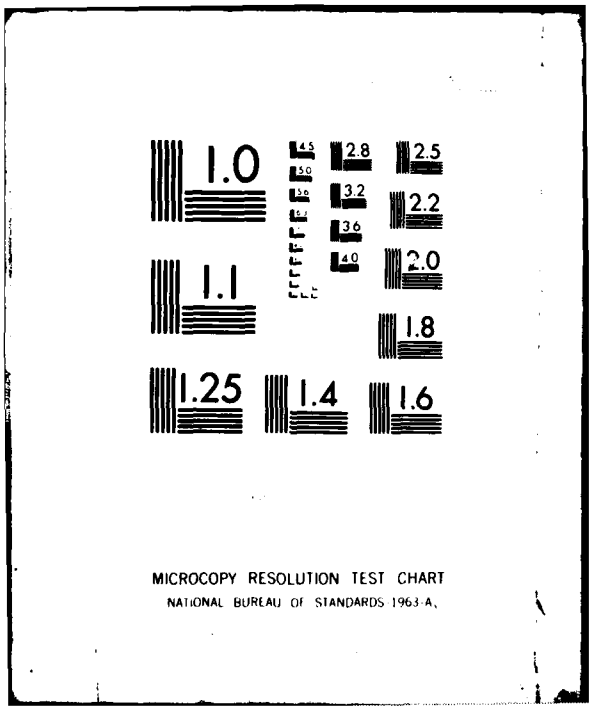
1.0
1.1
1.25
1.4
1.6
1.8
2.0
2.2
2.5
2.8
3.2
3.6
4.0
4.5
5.0
5.6
MICROCOPY RESOLUTION TEST CHART
NATIONAL BUREAU OF STANDARDS 1963-A

message can be the reduced output power test sequence. It is feasible to transmit the received test sequence by each terminal to a master test station to allow analysis of the performance of each bus interface unit at one location (assuming no errors are introduced during retransmission). Additional data concerning the optical source drive current and temperature is required by the master test station for each link in the network.

The interlaced ring may be treated as a simple ring in terms of testing sequences, since all terminals are assumed to be tested. The employment of decisionmaking circuitry at the downstream terminal alleviates the fault recovery action (a fault is overcome by the network) but may or may not indicate degraded performance. Catastrophic failures are thus readily identified and recovery action initiated, but degraded performance may or may not be detected and flagged by downstream terminals.

The passive star coupled network allows one transmitter to address all receivers "simultaneously." Theoretically one test message sequence (after an alerting message) could be employed to address all terminals. The problem of terminal reply sequencing presents itself and unless accommodated by a protocol, or some form of time slot assignment is employed, individual query messages will be required to each terminal followed by a response message. If time slot assignment is done, the alerting message could be followed by the test sequence, and all terminals not successfully decoding the sequence respond in their time slot.

The range of received signal power seen by the receivers in the passive star network is moderate (20.1 dB per Table 5.1.2-1), and more than one test sequence message would be necessary to allow receivers to see approximately the same received signal power level ($\pm$2-3 dB). A look-up table would be required to allow a master test station to evaluate the performance of the receivers, since knowledge of the topology is required to predict the expected performance of a given receiver to a given input signal level. One consideration of the star network configuration is that there is no requirement to inhibit the receiver from "passing the message," since that is not a function performed except in the ring network.

The repeatered star network again allows one transmitter to address all receivers in the network (although the caveat concerning transmitter reply sequencing is valid also for the repeatered star network configuration). The dynamic range is much reduced for the repeatered star network over that of the passive star network and one test sequence message could potentially be used for all bus interface unit receivers.

The above discussions concerning test sequences are independent of whether the test and maintenance actions are automated or manual. The obvious choice of network types if manual testing must be done is either the passive or repeatered star network, since single point network testing may be accomplished. If manual testing and maintenance actions are accomplished for the ring or interlaced ring network, 32 test stations are required per terminal cluster. The next discussion will address maintenance actions required to restore the network to service in the event of bus interface unit failure. The sequence of actions is similar to that required for testing.

To ascertain the time to repair a terminal all faults can be classified as either "major" or "minor." All "major" and "minor" faults can be summarized for display at all terminals in the network using indicators and/or alerting devices (buzzers, printout summaries, or other). To isolate a fault to a module or assembly, separate indicators, either labelled on the test card or on the module/assembly, can be used to identify the faulty module or assembly within a particular bus interface unit. Minor faults are those classified as not affecting network performance (i.e., a terminal may be non-operative, but the network remains functional). Only major faults are considered in this discussion.

With fault summaries at each BIU (or terminal), the time to repair becomes a function of the number of terminals, and the time required to access a faulty board, replace the board, and verify proper function of the replacement board (or module or assembly). If all terminals are manned, the fault isolation can be rapidly accomplished, and corrective action taken if spares are on hand at the failed unit's location.

If maintenance spares are stored at one location and all terminals are not manned, the probability of an unmanned terminal failing must be considered. If the network is nonredundant and a terminal fails, the time to isolate a fault becomes a function of the network topology and configuration. Each network then exhibits somewhat different time-to-repair characteristics (redundancy would allow transmission of fault data over the functioning spare path to the central location).

For the pure ring network a measure of network performance can be made by transmitting a test message through the network and comparing the received message with that transmitted. As discussed earlier, source power may have to be reduced to accurately measure receiver performance. In this network configuration all bus interface units in the network must be functional to have the network operational.

For the nonredundant ring network the failure of any optical detector or optical source constitutes a system failure, since a terminal may be able to send a message to another terminal but will be unable to receive a message from that terminal. Another system failure is when a message makes multiple transits around the loop. To minimize the time to isolate a faulty terminal the "successive division" technique may be used (i.e., proceed from the known good terminal to a terminal half way between two known good terminals; or, if thirty-two terminals comprise the network and only one terminal is known to be functional, move sixteen terminals around the loop and determine message receipt and/or transmission). The process is then repeated in the proper direction to isolate the fault.

Using the "successive division" fault isolation technique for a 32 terminal ring network the maximum number of terminals that must be tested is six and the minimum that must be tested is one. The successive division fault isolation technique then will average 3 testing locations per failure. This is a significant improvement over a successive testing technique where each terminal in the network is sequentially tested. This

technique would require an average of 16 X 3, or 48 tests per network failure to isolate the faulty terminal (assuming randomly distributed failures).

In addition to the average 3 test locations per network failure, the faulty terminal will then require testing (time) to determine the faulty module or assembly plus time to replace the failed unit and verify operation of the replacement unit. The tests to determine the fault of the terminal then consist of transmitter test routine, message inhibit (preclude a message addressed to the terminal from being retransmitted) routine, and synchronization word validation to determine proper function of the receiver. There are then three tests per ring network terminal to determine status of the terminal. The sequence of testing would preferably be based on testing the component and module (or assembly) having the highest likelihood of failure first, followed by testing of the next highest likelihood failure mode, etc.

For a mean of 3 test locations and three possible tests per location, the number of tests per network failure can then be estimated as a mean of 8.5 tests per network failure, with the maximum number of tests being 18 and the minimum number of tests being 1. Note that this fault isolation technique may not be the minimum time to repair if travel time is included, since for an average terminal spacing of 100 meters serially in a loop, the mean distance covered by a single maintenance technician (one assumed available) will be 3100 meters. This compares to a mean distance of 1600m for a serial testing sequence.

The passive star network offers the simplest fault isolation routine. The passive star network allows a minimum of one test location and a maximum of two locations with a simultaneous maximum of four tests at any one location. Since nonreply to a message may be either a fault in the sending terminal (failure to send the message - transmitter failure - or to receive the reply - receiver failure) or the receiving terminal's inability to receive or reply, the failure of a terminal to reply should be checked by

querying another terminal. Failure of the second terminal to reply may indicate a sending terminal transmitter or receiver fault. Reply of the second terminal verifies the operation of the sending terminal and thus fault testing of the inoperative terminal can be initiated to determine the failed module or assembly. A maximum of three tests and a minimum of one are then performed at the indication of a bus interface unit fault. These three tests are: query another terminal, the minimum required additional test; test the transmitter, on determination that the second terminal did not reply; and test the receiver if the transmitter indicates proper operation, and the second terminal did not reply.

The passive star network then supports a mean of 1.5 test locations and a mean of 3 tests per location. The mean number of tests performed to isolate a faulty assembly in the network is then 4.5. These estimates are based on equally likely failures, and as such can be significantly improved on by proper sequences of actions to weight the likelihood of failure into the restoral action sequence.

The repeatered star network adds to the testing requirements, although not significantly. The same routine is entered on indication of a fault (query a second terminal). The diagnostic sequence must then determine the function of the initiating terminal (2 additional tests), whether the test routine is initiated from the repeater or any other terminal in the network. If the initiating terminal is not the repeater, testing must then be performed at the repeater to determine its operation (2 tests). With this diagnostic sequence the maximum number of tests will then be 5 and the minimum 2.

With these network diagnostic steps discussed, a tabulation for each of the network configurations summarizes the above discussion. This tabulation is shown in Table 5.2.2.

Table 5.2.2. Network Configuration Diagnostic Steps

	Number of Tests to Isolate Fault (Maximum/Minimum)	Mean Number of Tests to Find Fault	Maximum Number of Tests/Repeater	Maximum Number of Tests/Terminal	Mean Distance per Repair Action
Ring Network	18/1	8.5	3	3	~3100m
Passive Star Network	3/2	2.5	-	2	~500
Repeatered Star Network	5/2	3.5	2	2	~ 250-500*

*Depends on starting point of repair action.

Table 5.2.2 indicates that if all tests were of the same length and travel time between testing locations is neglected, the passive star network has the minimum mean-time-to-repair (MTTR), followed by the repeatered star network. The ring network has the worst MTTR. If travel time between terminals is integrated into the MTTR, again the star networks would indicate lower MTTR values.

In summary, the three basic network configurations offer differing diagnostic sequences which can be quantified to ascertain a mean number of tests required to isolate a fault. The simplest network from a diagnostic viewpoint is the passive star network, followed closely by the repeatered star network. The most complex network of the three discussed is the ring network.

5.2.3 Redundancy Considerations

The previous discussion addressed test and maintenance considerations for non-redundant networks. Non-redundant network configurations were used to ensure that network problems were not camouflaged by the availability of an alternate path. With the network test and maintenance considerations in hand, the proper selection of redundancy can measurably improve both network availability and fault isolation capability.

It must be reiterated that the wholesale application of redundancy to solve basic network deficiencies and compensate for either poor network or component reliability results in a costly and suboptimal system. The system is not only costly from an acquisition cost (investment cost) standpoint, but also from an operating and support cost standpoint, due to frequent maintenance and substantial spares requirements. The system then impacts logistic requirements and life cycle costs become less manageable.

Each network type will be reviewed to see the impact of adding a redundant link and the improvement available from the addition of redundancy. The "yardstick" by which the improvement in system or network reliability is measured will be system availability. Several assumptions concerning mean-time-to-repair (MTTR) will be made to quantify this time value. Mean-time-between-failures (MTBF) based on the assembly and link failure rates projected in Paragraph 5.2.1 will be used in the network availability calculations.

The link failure rate projected in Paragraph 5.2.1 was not applied to any specific network configuration, but was applicable to a fiber-optic link consisting of a transmitter, receiver, and timing extraction circuit. Each of the three network types can be modelled as a combination of fiber-optic links. The ring network is a simple interconnection of fiber-optic links into a 32 terminal loop, as shown in Figure 5.2.3-1.

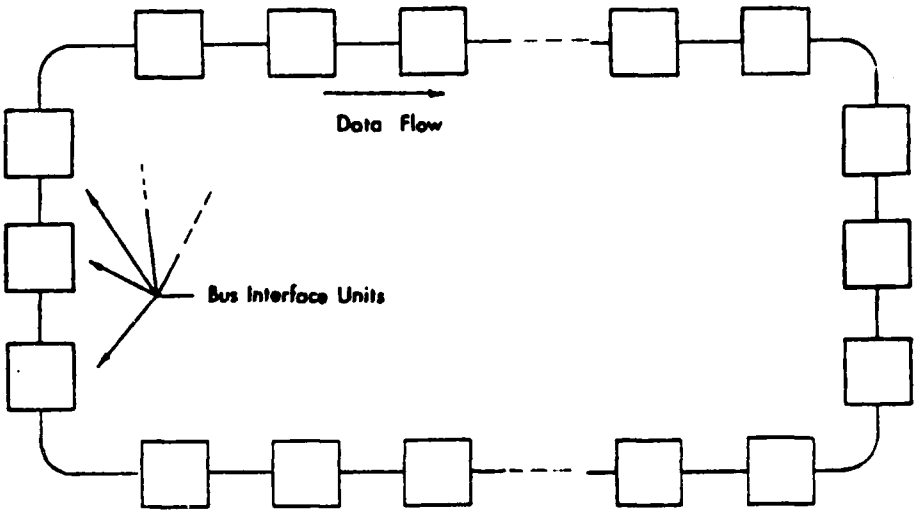

Figure 5.2.3-1. Ring Network Reliability Model

Each of the blocks in Figure 5.2.3-1 is composed of receiver, timing extraction circuit (bit synchronizer), possibly an "inhibit" module, terminal circuitry, and a transmitter, as shown in Figure 5.2.3-2.

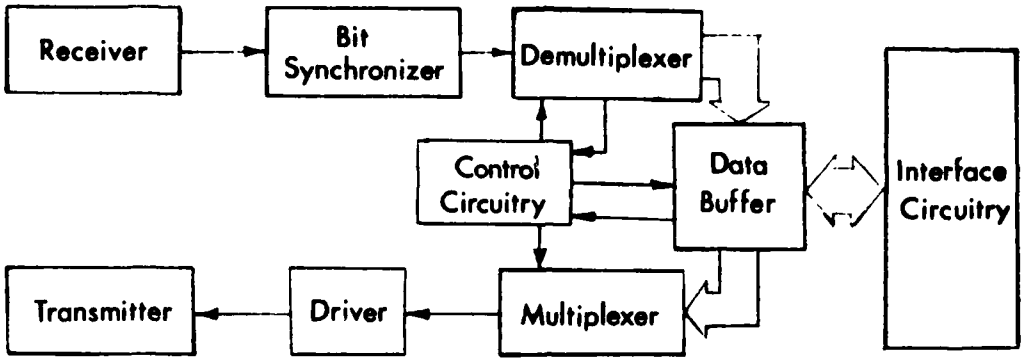

Figure 5.2.3-2. Terminal Reliability Model

For simplicity of modelling purposes, any inhibit circuitry can be assumed to reside in only one terminal. The bus model then consists of 32 transmitters, receivers, bit synchronizers, terminals, and (possibly) 1 inhibit circuit. Since the terminal equipment consisting of the multiplexer, demultiplexer and interface circuitry is the same, regardless of network type, these items can be removed from the model for comparison purposes (these additional items are present in all BIU's without changes). The network MTBF can then be computed from the network failure rate, where:

$$\lambda_{Ring} = 32\ (\lambda_{RCVR} + \lambda_{BS} + \lambda_{XMTR}) + \lambda_{inhibit} \qquad (58)$$

where

λ_{Ring} is the failure rate of the daisy chain network

λ_{RCVR} is the failure rate of the receiver

λ_{BS} is the failure rate of the bit synchronizer

λ_{XMTR} is the failure rate of the transmitter

$\lambda_{inhibit}$ is the failure rate of the inhibit circuitry and all failure rates are in hours^{-1}.

The estimate of the failure rate of the inhibit logic circuitry can impact the network failure rate significantly, or may be insignificant. If the message path inhibit logic resides in one (or possibly two) terminals, careful design can make this circuitry a minor contributor to the network failure rate. Alternatively, if a simple, highly reliable technique is devised at each terminal to inhibit retransmission of messages around the network more than once, the contribution to the bus interface unit failure rate can be considered insignificant. Also, if the protocol is properly chosen, the inhibit circuitry can potentially be eliminated. This case will be assumed. For this case, the network MTBF can be expressed as:

$$MTBF_{Ring} = \frac{1}{Ring} \quad \frac{1}{32\ (\lambda_{RCVR} + \lambda_{BS} + \lambda_{XMTR})} \tag{34}$$

or, inserting values (exclusive of power supplies, cable breakage, battle damage, etc.) for the assembly failure rates:

$$MTBF_{Ring} = 272 \text{ hours} \tag{34a}$$

This value can be combined with the MTTR to arrive at a value for the network availability, A, as:

$$A_{Ring} = \frac{MTBF_{Ring}}{MTBF_{Ring} + MTTR_{Ring}} \tag{35}$$

where A_{Ring} is the availability of the ring network. The value of the MTTR is thus required to determine the system availability.

Table 5.2.2 at the end of Paragraph 5.2.2 addressed the relative numbers of tests associated with each type of network. Also included was the comparative mean travel distance for each network; however, this was predicated on there being only a single repairman and a rough estimate of the geography of the network. These assumptions are probably valid only for a small minority of cases, and "travel time" will be excluded from MTTR to preclude unnecessary bias. The amount of time required to perform a test then becomes the central assumption in calculating the MTTR, and consequently in determining the network availability.

A comparative analysis can then use the same time for each test in each network type, provided the tests are approximately of the same complexity. Realistically, the "time-to-test" is insignificant if built-in test (BIT) with automated routines is considered. Access to the test board, interpretation of the results, replacement of the faulty assembly, and verification of network operation after replacement action then determine the MTTR. These considerations are relatively constant for each network type.

If an assumption of 5 minutes is used for test board access time and interpretation of the results, followed by 2 minutes for cases of the terminal not being faulty and an additional 5 minutes if the terminal is faulty, then an estimate of the relative MTTR for each network can be made. This estimate is predicated on only one terminal (repeater) location being tested at any one time, and no travel between locations considered. Also, only simple hand tools are used in the repair activity.

The ring network MTTR can then be estimated as 62.5 minutes to repair (1.042 hours), based on 8.5 being the mean number of tests (7.5 unsuccessful tests and the last test successful). Inserting this value into the availability equation leads to a network availability of:

$$A_{Ring} = \frac{543 \text{ hours}}{272 \text{ hours} + 1.042 \text{ hours}} = 0.996178 \qquad (35a)$$

This is the network availability, or approximately 33.5 hours of network "downtime" per year. The mean number of failures per year would be 32.1, or essentially one failure per year per bus interface unit. This figure is based only on the bus interface unit projected reliability and on the coarse estimates of repair time. Terminal failures associated with the multiplexer, demultiplexer, or interface circuitry are not accounted for, nor is cable breakage due to accident, battle damage, or other cause.

As a means of improving the ring network reliability, the interlaced ring has been advanced. For this network configuration two terminals must fail and the two failed terminals must be adjacent. This significantly improves the network availability, since the network now must have two failures the second occurring within the mean-time-to-repair and can create a network failure only if the second failure is at one of the two adjacent terminals to the first failed terminal. The probability of one of the two adjacent terminals failing during the MTTR of a given failure can then be calculated as:

$$P_{f_{2|1}} = \lambda_1 \cdot \frac{MTTR_1}{MTBF_2} \cdot \frac{2}{32}$$

where $P_{f_{2|1}}$ is the failure of a second terminal given one failure,

$MTTR_1$ is the mean-time-to-repair terminal "1,"

and $MTBF_2$ is the mean-time-between-failure of terminal "2."

This probability of a "double failure" is then:

$$P_{f_{2|1}} = 8.62249 \times 10^{-10}$$

which leads to a revised network availability of:

$$A_R = 0.99999997 = 0.9_7 7^*$$

where A_R is the availability of the interlaced ring.

This availability is slightly optimistic, since the interlaced ring has a second receiver at each terminal and some form of decision circuitry to ascertain which upstream terminal the received signal should be accepted. Both of these assemblies contribute to an increased failure rate and some reduction in the network availability. This increase in failure rate is not significant however, and may be neglected without materially increasing the error.

The system availability can be further improved if faults are reported allowing repair to be conducted before a second failure occurs such that the system remains operational during single failures. Since the probability of a "double failure" is significantly less than a single failure, the number of network failures are reduced several orders of magnitude.

With fault reporting, the failure rate of a redundant system can be modelled using the "redundancy with repair" equation or:

$$\lambda_{eff} = \frac{N!\lambda^{m+1}}{(N-m-1)!u^{-m}} \qquad (36)$$

*Where the notation $0.9_7 7$ defines seven "9's" after the decimal point followed by the remainder of the number.

where λ_{eff} is the effective failure rate of the redundant assembly, in hours^{-1}

N is the number of parallel assemblies

λ is the failure rate of the assembly without redundancy, in hours^{-1}

m is the number of assemblies allowed to fail before link failure occurs

and u is the mean-time-to-repair (MTTR) in hours.

Employing the interlaced ring and assuming the passive splitters have a negligible failure rate ($< 5 \times 10^{-9}$ hours), the effective failure rate of a modified interlaced ring (MIR) may be computed as:

$$\lambda_{MIR} = 1.379598 \times 10^{-8} \text{ hours}^{-1} \quad (36a)$$

If the MTTR is adjusted to delete unsuccessful testing to isolate faults, this effective failure rate then infers a redundant network availability, A_{MIR}, of:

$$A_{MIR} = 0.9999999984 = 0.9_8 84 \quad (37)$$

This corresponds to 0.09 seconds per year outage time, or an insignificant failure rate. Thus, if a interlacing ring network is used, the appropriate configuration is to provide redundant buses, as in Figure 4.1.2-4. The two ring configurations performance are summarized as:

Network Type	MTBF	Availability	Outage Yime/Year	MTTR (Hours)
Ring	272 hours	0.9_2 62	33.5 hours	1.041
Interlaced Ring	7.25×10^7	0.9_6 72	0.09 second	0.2

The star network has fewer assemblies per terminal than the ring network. A passive star network can be treated as a two terminal link with one transmitter and one receiver-bit synchronizer. No "inhibit circuitry" is required since there is no "loop" in the star network. The MTBF of the "network" for the passive star must be defined in terms of some arbitrary number of failed terminals (bus interface units), since there are no repeaters in the passive network.

Using the "redundancy with repair" model to represent independent failures of the star network bus interface unit (assuming four failures consititute a "system failure"), the effective failure rate of the network can be determined from equation (61) as:

$$\lambda_{STAR} = 2.1052 \times 10^{-14} \text{ hours}^{-1} \tag{38}$$

which constitutes an $MTBF_{STAR}$ of 4.75×10^{13} hours. Computing the availability using an MTTR of 12 minutes (employing the assumptions made in the discussion of the daisy chain network), the system availability is essentially unity ($> 0.9_{14}$).

This network then looks attractive from a reliability viewpoint. If a repeater is required to attain sufficient signal margin, the network availability would be expected to be essentially that of the repeater. This availability is then:

$$A_{RS} = 0.9_4 77 \tag{39}$$

where A_{RS} is the availability of the repeatered star network.

Employing redundancy to improve this availability can be achieved by providing a redundant repeater. Again, the availability of the remainder of the network is essentially unity, and the MTTR is assumed to be ~12 min; or, the availability may be computed as:

$$A_{RRS} = 0.9_7 7 \tag{40}$$

where A_{RRS} is the availability of the redundant repeatered star network.

Further improvement can be attained in the network availability if the central repeater is composed of three repeaters. For this case, the network availability is raised to greater than 0.9_{10}. An alternative method of improving the availability is to employ fault reporting with two repeaters.

Summarizing the star network in the manner of the two previous discussions, for passive star, repeatered star and redundant repeatered star networks, the following tabulation results.

Network Type	MTBF (Hours)	Availability	Outage Time/Year	MTTR (Minutes)
Passive Star	4.75×10^{13}	0.9_{14}	-	12
Repeatered Star	8.689×10^{3}	$0.99_4 77$	12 minutes	12
Redundant Repeatered Star	$7.55 \times 10_6$	$0.9_7 74$	0.95 second	12

Combining the tabulations for the ring, the passive, and the repeatered star, Table 5.2.3 illustrates the comparison.

Table 5.2.3. Comparative Performance of the Networks

Network Type	MTBF (Hours)	Availability	Outage (Time/Year)	Assumed MTTR (Hours)
Ring	272	$0.9_{2}62$	14.01 hours	0.9
Interlaced Ring	7.25×10^{7}	$0.9_{8}72$	0.9 second	0.2
Passive Star	4.75×10^{13}	0.9_{14}	-	0.2
Repeatered Star	8.689×10^{3}	$0.9_{4}77$	12 minutes	0.2
Redundant Repeatered Star	7.55×10^{6}	$0.9_{7}7$	0.95 second	0.2

Ordering these networks, the obvious choice is the passive star, followed by the interlaced ring network. In terms of the amount of equipment necessary to support each network, the passive star network requires the least, with the repeatered star next, followed by the interlaced ring. The interlaced ring network requires the most equipment, since each terminal (BIU) has an additional receiver and requires that the repeaters have additional logic to ascertain the health of the two upstream terminals. The star network may also require some additional logic to prevent a failure mode from generating source chatter. It is anticipated that this logic would be less than the logic required for the interlaced ring terminal.

5.2.4 Reliability and Maintainability Summary

This section has discussed reliability, availability, and maintainability of the different network configurations. Circuit diagrams of similar equipment to that anticipated in this network was used as a basis for projection of failure rates. These failure rates are not "hard and fast" numbers, but representative of the numbers expected for equipment of this complexity and function.

With the projected failure rates in hand, each link type was reviewed to assess the maintainability of the link configuration. Built-in-test (BIT) was reviewed, as was fault isolation techniques for non-redundant networks. The number of diagnostic tests required to isolate a fault was presented in Table 5.2.3 as a function of network type.

The next discussion combined the link failure rates, the number of diagnostic steps for fault isolation for each network type and several assumptions concerning the time to diagnose a fault and isolate the faulty assembly. These data, combined with several assumptions, allowed the projection of the network availability for each network type and the improvement attainable with redundancy.

The results of the comparative performance for the networks were that the passive star network offered the maximum availability and minimum mean-time-to-repair (MTTR). This network was closely followed by the interlaced ring in ordering of the networks by availability. The third network type, the redundant repeatered star network, offers an alternative of lower availability with a reduced receiver design requirement.

In summary, the passive star network offers the best network availability and the least maintenance cost. The estimated reliabilities of these networks were compared based only on the optical components, with the balance of the bus interface unit considered as common to all network types. The impact of these additional components and assemblies will reduce substantially the availability numbers presented in this discussion.

5.3 Data Integrity

Data integrity refers to the ability of the network to deliver error-free data from the source to the destination. Error-free in this context should be taken to mean incurring a bit error rate no higher than that experienced on a computer mainframe bus. Bit error rates as low as 10^{-15} are normally quoted for such internal buses, as well as for peripherals such as disk drives and magnetic tape units.

It was previously shown that a raw BER of less than 10^{-9} is practical for the worst case links in both star and ring approaches. Overall system BER's much less than the raw BER can be achieved by one of two methods in a packet-switched network. Error correction encoding may be used to correct a given number of errors per codeword at the receiving station. Such encoding requires a higher bandwidth (50 percent to 100 percent) due to the redundancy of the codes. This increase in bandwidth requirements results in a higher noise bandwidth in the receiver, and thus a lower signal-to-noise ratio, and a higher raw BER. Thus, the addition of redundancy for error correction results in diminishing returns on the improvement of the effective bit error rate. Such data encoding is judged inappropriate for this application. However, error-correction encoding on critical control variables such as the source and destination addresses could considerably reduce the occurrence of certain disrupting error conditions.

A much more effective means of error control is that of error detection followed by a request for retransmission of corrupted packets. This approach is used almost universally in packet-switched systems because of the low overhead (typically 1 percent to 2 percent) required. This error control procedure is a feature of the ADCCP protocol, and is accomplished by appending a CRC (cyclic redundancy check) sequence at the end of each packet. Occasionally, error-correction encoding is performed in addition to (externally of) this protocol. The following analysis is intended to show that the error control procedures built into ADCCP are sufficient, without further encoding to achieve practically error-free performance without incurring a significant overhead.

The CRC is computed in such a manner that, when appended to the end of the message, an n-bit frame is formed whose bits can be thought of as coefficients of an n^{th}-order polynomial, M(X). The CRC bits form the least significant coefficients of this polynomial, and are computed such that M(X) is exactly divisible by a generating polynomial P(X). If errors occur in transmission, the receiver encounters the polynomial M(X) + E(X)

where E(X) is the error polynomial. The received sequence is divided by P(X), and a zero remainder indicates that 1) either the transmission was error-free, or 2) the error polynomial E(X) is exactly divisible by P(X). The latter case represents the class of undetectable errors.

The generating polynomial, P(X), is chosen such that it will not divide into the most likely occurring error polynomials. The CCITT V.41 polynomial, used by most bit-oriented protocols, is

$$P(X) = X^{16} + X^{12} + X^5 + 1 = (X + 1)\, P_{15}(X). \qquad (41)$$

It can be shown[58] that this polynomial detects the following error patterns.

(1) Any combination consisting of an odd number of errors, since P(X) contains the term X + 1.

(2) Any combination of two errors, provided the frame length, n, is less than or equal to $2^{15}-1$, since P(X) contains the factor $P_{15}(X)$ which is a primitive polynomial of degree 15.

(3) Any burst of errors whose length is 16 or less.

(4) Any combination of two error events, each event consisting of two adjacent errors, providing that $n \leq 2^{15}-1$.

Property (4) is very important when employing the "invert on zero" modulation scheme selected in Paragraph 4.5. Errors, under this modulation scheme, always occur in pairs. The most probable undetectable error sequence when using this modulation scheme with the 16-bit CRC is that of 3 error pairs within a frame. The error analysis will be performed for both the ring and star configurations.

[58] W.W. Peterson and D.T. Brown, "Cyclic Codes for Error Detection," Proc. IRE, January, 1961, pp. 228-235.

5.3.1 Ring Error Analysis

It will be assumed that no more than 100 BIU's will be placed in a single ring. Larger networks may be constructed with smaller rings connected by store-and-forward gateways. The store-and-forward gateways will not forward faulty packets from one ring to the next, so errors do not propagate in this manner. The error analysis will be done for an autonomous ring.

Paragraph 5.1 indicated a BER of no more than 10^{-9} for the worst case point to point link in the ring. Assuming each link to have this BER, the effective error rate between the farthest-separated nodes in a 100 node network will be approximately 10^{-7}. Because of the modulation scheme, which doubles each error during decoding, this figure represents an average of 1 error pair in 10^{7} bits.

Assuming an average packet size of 1000 bits, the probability of the three error events in a frame is

$$P(3) = \frac{(1000)\ (999)\ (998)}{6}\ (10^{-7})\ (10^{-7})\ (10^{-7}) = 1.67 \times 10^{-13} \qquad (42)$$

Actually, a large percent of these triple error events will be detected, but the above figure will be pessimistically used as the probability of an undetectable error. Since such an event would result in 6 undetected bit errors in a frame of 1000 bits, the net uncorrected BER of the system is

$$\frac{6}{1000} \times 1.67 \times 10^{-13} = 10^{-15} \qquad (42a)$$

Note that Paragraph 5.1 indicates a comfortable link margin for the 10^{-9} raw BER, and the above analysis used worst case links for all 100 in the system. The 10^{-15} final BER is, therefore, overly pessimistic.

Another important parameter to consider is the overhead due to retransmission of frames. Assuming a 1000-bit frame and a 10^{-7} system error event rate, the percentage of frames which have to be retransmitted due to errors is $1000 \times 10^{-7} = 10^{-4}$. The retransmission overhead is, therefore, insignificant.

5.3.2 Star Error Analysis

In the star configuration, the BIU's are parallel-connected, so that the raw system BER is equal to the raw link BER. Paragraph 5.1 established a 10^{-9} raw link BER.

Assuming a 1000-bit packet and "invert on zero" modulation, the probability of the undetectable three error events is

$$P(3) = \frac{(1000)\ (999)\ (990)}{6}\ (10^{-9})\ (10^{-9})\ (10^{-9}) = 1.67 \times 10^{-19} \qquad (43)$$

Therefore, the net uncorrected BER of the system is

$$\frac{6}{1000} \times 1.67 \times 10^{-19} = 10^{-21} \qquad (43a)$$

The overhead due to the retransmission of corrupted packets is $1000 \times 10^{-9} = 10^{-6}$, for an insignificant retransmission overhead.

5.3.3 Error Performance Summary

The above analyses appear to indicate better system BER performance in the star configuration than in the ring. The underlying assumption was that the raw link BER for each approach was the same (10^{-9}). The cascading effect in the ring system, led to further degradation, resulting in 10^{-7} raw system BER. In a practical system, it is easier to achieve a lower raw system BER in the ring than in the star, as evidenced by the large link margin shown in Paragraph 5.1 for the ring system.

However, the 10^{-7} raw system BER calculated above for the ring proved to be satisfactory. In fact, by using sufficiently robust error control procedures, a raw system BER of 10^{-6} could be tolerated. The conclusion is that the raw BER performance predicted in Paragraph 5.1 for both approaches is sufficient for providing virtually error-free service to the users while incurring negligible overhead for error control.

5.4 Throughput Analysis

The purpose of this section is to determine to what extent the ring and star approaches meet the throughput requirements of the network. The usual methods for throughput analyses assume homogeneous sources (all nodes generating traffic at the same rate) and a constant packet size. The use of 1000 bits as an average packet size is appropriate for a computer system such as the one under study. This number has been established by several researchers who have collected statistics from typical systems. The assumption of a balanced system (homogeneous sources), however, is quite unrealistic.

A minimal AN/GYQ-21(V) system consists of one DEC Series 11 processor plus a number of peripherals. The DEC UNIBUS is capable of transferring a 16-bit word entry 400 nsec under ideal conditions (2.5M word/sec); however, the maximum transfer rate depends upon bus length, loading, interface design, and ultimately memory speed and the CPU's capability to process the information. A realistic goal to set for the processor bandwidth is one M word/sec (16 Mb/s), which would be typically divided equally into input and output rates of 8 Mb/s each. It will be assumed that the bus should support a sustained output rate of 16 Mb/s from any one processor in the system. For multiprocessor systems, the peak average data rate is assumed to be 30 Mb/s. Table 5.4 summarizes the assumed maximum transfer rates of representative AN/GYQ-21(V) system components.

Table 5.4. Representative Data Rates

Device	Data Rate
Processor	1 Mword/s = 16 Mb/s
CR11	185 cards/min = 3 kb/s
LP11	300 lines/min = 5.3 kb/s
TM11	36K char/sec = 2.88 kb/s
200 Mbyte Disk	Track/54 Msec = 4.3 Mb/s
300 Mbyte Disk	Track/33 Msec = 2.7 Mb/s

The disk throughput rates are based on an entire track transfer every two revolutions. Typically, a revolution is lost during head moves. If the disk drives are operated in a sector mode, as in most computer systems, these maximum rates are reduced by an order of magnitude. Table 5.4 shows that multiple peripherals such as card readers, line printers, and CRT displays may be placed on one BIU. The BIU design presented later should support at least 5 Mb/s, except for the processor BIU which can operate up to 16 Mb/s.

5.4.1 Ring System

In the Control Token access method, a BIU places a message on the bus and follows it with a token. As soon as this token reaches the next downstream BIU, that BIU May remove the token, place a message directly behind the first, and follow it with a token, and so forth around the ring. If all BIU's have messages to transmit, then each one in turn will place its message directly behind the previous BIU's message. This argument makes it sound as if the ring can be kept 100 percent utilizes. In fact, an omniscient observer will note a dead time as the token travels from the BIU that just inserted it to the next BIU in line.

Stated equivalently, an observer positioned immediately upstream from a BIU notes continuous traffic until the token reaches that BIU. Then the link is idle until the start of message from that BIU traverses the ring. The total active time consists of the transmission of N messages (from N BIU's) and the idle time consists of one round trip delay. The effective intermessage gap is, therefore, equal to the average transmission time between nodes on the ring.

For the case of N homogeneous sources, a packet length of 1000 bits (16.67 μsec at 60 Mb/s), and a round trip delay, τ, the average data rate is

$$\text{Data Rate} = \frac{1000 * N}{N * (16.67 \times 10^{-6}) + \tau} \qquad (44)$$

The round trip delay, τ , is equal to N times the average BIU to BIU delay, X. Rewriting (44) yields

$$\text{Data Rate} = \frac{1000 * N}{N * (16.67 \times 10^{-6}) + N * X} = \frac{1000}{16.67 \times 10^{-6} + X} . \qquad (44a)$$

Thus a 30 Mb/s rate is obtained if the average BIU to BIU delay is 16.67×10^{-6}, corresponding to approximately 3.3 kilometers. The maximum expected BIU to BIU separation is 1 kilometer and the average is probably 30 to 50 meters.

Consider the unbalanced case of a processor transmitting data to a large number of peripherals. The processor should be allowed to transmit 16 Mb/s as argued previously. For this case, the intermessage gap is the round trip delay, τ , and the maximum data rate is

$$\text{Data Rate} = \frac{1000}{16.67 \times 10^{-6} + \tau} . \qquad (45)$$

For a single processor rate of 16 Mb/s, solving for τ yields 46 μsec corresponding to about 9 kilometers. This is the most pessimistic computation of throughput for the ring system.

Thus far, the effect of acknowledgement traffic has been ignored. As previously assumed, a BIU will not transmit a new packet until the last packet has been acknowledged. The Ringnet System of Prime Computer, reserves a space at the end of each packet for the destination to insert an acknowledgement. The source receives the acknowledgement when its own message returns from the round trip. Thus the destination has an opportunity to return the acknowledgement immediately even if several other packets immediately follow the one addressed to the destination. An immediate acknowledgement is important, since it allows the source to deallocate the buffer in which the message had to be retained in case of a need for retransmission. Using this scheme, the acknowledgement process does not impact the ring throughput except for the small amount of overhead space required in each packet, which is estimated to be less than 1 percent.

The conclusion is that the ring operating at a burst rate of 60 Mb/s can provide more than adequate throughput rates under rather extreme ring length requirements and worst case loading conditions.

5.4.2 Star Throughput Analysis

The throughput analysis for passive and active star systems will be identical. It will be initially assumed that the length of all arms of the star are the same (namely 500m). This will simplify calculations, but is not a necessary condition. The delay in transmission, τ , from one node to any other node is, therefore, 5 μsec (one kilometer transit time).

Any carrier sense distributed control scheme depends upon detecting an inactive bus at the end of a transmission before initiating the next transmission. This results in a minimum intermessage gap of τ, the propagation time. Realizing that an acknowledgement is required of the

destination, an additional τ seconds are allocated for every message (assuming the acknowledgement duration is negligible). Reserving time at the end of each packet (which has advantages discussed previously) results in an effective minimum intermessage gap of 2τ. Arbitration among competing nodes degrades this minimum gap further. For free contention protocols, such as Ethernet, collisions will cause a degradation in efficiency. In collision-avoidance schemes used as MSAP/BRAM, unique deference delays at each node add to the 2τ minimum. For balanced systems, the MSAP approach with round robin priorities results in the minimum delay. For unbalanced systems, the probabilities of collision are low, and an Ethernet protocol results in higher efficiency. Also, on MSAP-type deference scheme which allows multiple slots for higher-speed users can minimize delay if the degree of imbalance is known a'priori, and is of a static nature.

The latter was chosen for analysis, since the statistical nature of the Ethernet protocol requires simulation capabilities which were not available.

We assume that all BIU's "eavesdrop" on a transmitting BIU and its destination, and that each BIU can distinguish a message from an acknowledgement. After a message, all BIU's will refrain from transmission until a positive acknowledgement is sent.

Consider first round robin priorities with each BIU using its slot (balanced system). After the transmission of a packet, it will be 2τ before the second BIU in realizes it can use the bus. We assume an additional wait of 0.2τ to "make sure"; then the next terminal begins. If all BIU's participate, the transfer rate is then

$$\text{Data Rate} = \frac{1000}{16.67 \times 10^{-6} + 2.2 * (5 \times 10^{-6})} = 36 \text{ Mb/s} \qquad (46)$$

If the second BIU above does not use its opportunity, the third will realize this after an additional 1.2τ and begin its transmission. If only one BIU is participating, the maximum rule for round robin in a 32 BIU system is

$$\text{Data Rate} = \frac{1000}{16.67 \times 10^{-6} + (2.2 + 1.2 * 31) * (5 \times 10^{-6})} = 4.7 \text{ Mb/s} \quad (46a)$$

Thus, a "self-polling" scheme which gives devices such as the processors more opportunities than the other devices is desired.

The Hyperchannel protocol uses fixed, rather than round robin "self-polling" cycles. A single transmitting processor placed in the highest priority thus can achieve a data rate of

$$\text{Data Rate} = \frac{1000}{16.67 \times 10^{-6} + 2.2 \times 5 \times 10^{-6}} = 36 \text{ Mb/s} \quad (46b)$$

which is more than sufficient. Note that this processor would have the capability of hogging the system to some extent by depriving lower priority devices of opportunities. The extent of the hogging, however, is limited by the processor's maximum bandwidth of 16 Mb/s.

For two processors of priority 1 and 2, (and no other traffic) the sequence is as in Table 5.4.2.

Table 5.4.2. Sequence of Actions

Action	Time (μsec)
1 Transmits	16.67
Acknowledge	11
Deferral to 2	6
2 Transmits	16.67
Acknowledge	11
1 Transmits	Beginning of new cycle

The total bus efficiency for the two high-speed users is then

$$\text{Data Rate} = \frac{2000}{(2 \times 16.67 + 28) \times 10^{-6}} = 33 \text{ Mb/s} \qquad (47)$$

The conclusion is that a suitable "self-polling" sequence can be formulated for a given system to permit adequate throughput for the 32-port star with 500-meter arms when operating at a burst rate of 60 Mb/s.

6.0 DESIGN AND COST ESTIMATES OF CANDIDATE ARCHITECTURES

The interlaced ring and star approaches were conceptually designed in sufficient detail to determine the approximate costs for each terminal type. This conceptual design allowed examination of the system partitioning, complexity, and generation of sufficient data to allow cost estimation of the final production models based on the use of computer modelling.

6.1 Bus Interface Unit Partitioning

A generalized block diagram of a Bus Interface Unit is shown in Figure 6.1. This block diagram illustrates both star and ring BIU configurations, with the interlaced ring network requiring an additional receiver and the star network requiring "echo check" circuitry to compare the "echoed message" with that transmitted to detect collisions. Although some protocols to not require this echo check circuitry for generality, it will be included in the model.

The design assumes a 10 inch by 14 inch four-layer printed circuit card capable of holding 150 to 200 digital integrated circuits. The front-end is primarily ECL-logic. The device controller is PDP-11/04 processor costing approximately $5,000. This processor executes the driver programs for the attached peripherals or processors.

Table 6.1 is a breakdown of the card types and quantity for each design. The fiber-optic card is different for the two designs; the ring design employs two receivers and a passive splitter for achieving a failsafe approach. The logic cards are packaged with power supplies and motherboards in a 19 inch rack-mountable chassis. This chassis and the PDP-11/04 processor are mounted in a mini-rack (approximately 4 inches high). Peripheral interfaces (not costed) are plugged into the PDP-11/04 or attached "expansion chassis". These are interfaces which already exist in the 21(V) mainframes.

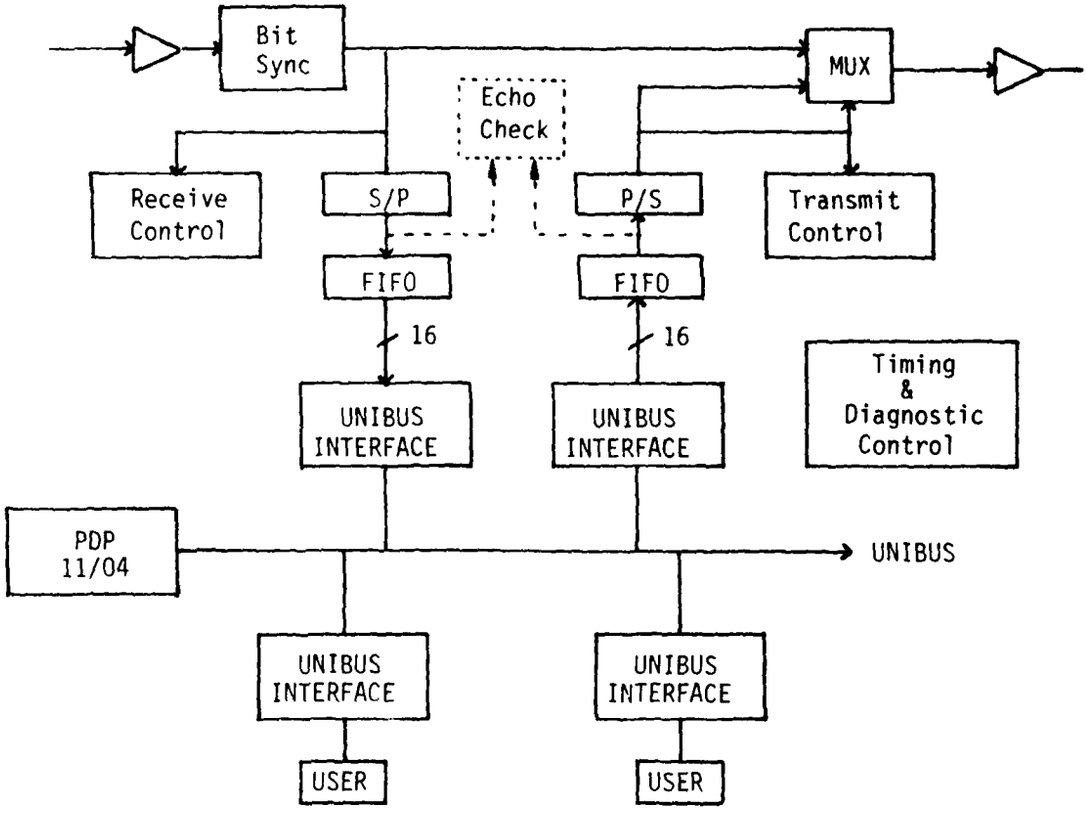

Figure 6.1. BIU Block Diagram

The pricing exercise assumed the typical system to consist of 32 BIU's and two gateway nodes. The gateway BIU is identical to the normal BIU but contains an additional fiber-optic card for the store-and-forward link between gateways. The total procurement was assumed to be 50 of the typical systems.

Table 6.1. Modules for Ring and Start BIU's

Modules	Star	Ring	Characteristics
Fiber Opt	1	1	
- Tx	1	1	Special
- Rx	1	2	
- Bit Sync	1	1	
Rx Cont	1	1	ECL
Tx Cont	1	1	ECL
Timing	1	1	ECL
Echo Check	1	0	TTL, Hs Ram
Interface	1	1	TTL, Hs Ram
PDP 11/04	1	1	Purchase $5K

6.2 Computer Pricing Model

The RCA PRICE program was used for cost estimation. Harris has extensive experience with this model and is one of its larger users. The following parameters are required as inputs to the model.

1. Qty - Total amount of production units.

2. Protos - Total amount of non-production units, i.e., EDM STM, Mockups, etc. Any equivalent units. including partial units, are included.

3. Wt - Total weight in pounds of the assembly to be priced. The weight is for each assembly. Weight includes both the enclosure and the electronics.

4. Vol - Volume in cubic feet of the subject unit. For electro-mechanical assemblies, the volume is a critical parameter and must be accurate.

5. Qtysys - How many of the subject items are required on a per system basis.

6. Integration - A description of the structural and electrical integration of the subject unit to the next higher assembly. Examples of types of integration:

   - Power furnished
   - Power furnished to assembly plus cabled output
   - Power furnished to assembly plus calibration and adjustment (tuning)
   - Power furnished to assembly, cabled output, calibration and/or tuning required plus possible parts assembly replacements including wiring and corrections
   - Physical mounting on one side only
   - Physical mounting on more than one side, no machining required
   - Physical mounting requiring considerable interface machining

7. Structure weight - Total weight of the enclosure, including the following items:

   - Metal sides

- Screws, nuts, bolts, etc.
- Connectors
- Magnetics
- Partitions
- Heat sinks
- Stiffening members
- Gears, relays, and electromagnetic devices

8. Structure Description - The description includes, but is not limited to, shape, type of material, environment, construction technique, i.e., costing, machining, etc.

9. Newness of Structural Design - The answer to this item should be indicated as a percent with 100 percent being a totally new design with no existing documentation or supporting analysis.

10. Electronic Description - Describe the electronic function of the subject item. Included in this description are card types, quantity and sizes. The circuitry and component type is also required. In addition to card quantity, the number of unique cards or functions are described.

12. Newness of Electrical Design - The percentage of new design required. This is a low number if some of the design has been done on another program. It is a high number for totally new design.

13. Expected power dissipation in Watts as it applies to the subject unit.

14. Component Quantity - The estimated total number of electronic components excluding relays and other electro/magnetic devices.

15. Development and Production Schedule Data

Engineering Development Schedule

- Calendar year in which program starts (Not FY Year).
- Name of month during first year in which design activity begins.
- Number of months ARO to completion of the first qualification tested unit.
- Number of months ARO to completion of testing of the last development or prototype unit.

Production Schedule

- Total number of months from the first month of the calendar year that significant production activity is initiated.
- Total number of months from the first month of the calendar that the last production unit will be delivered.

16. Engineering interpretation of design complexity - One of the PRICE parameters requires the users to catalog the design activity of the subject unit to be either, Second Generation, New, or Advance-in-State-of-the-Art.

17. Engineering Change Activity During Production - Values are inputted as a percent of documentation regeneration due to schedule legislation, testing or experience with customer redirection.

18. Tooling requirements are generated as routine, significant or nonexistent.

19. Production Methods - A description of the methodology to be employed in the assembly and fabrication of the subject unit is required. This data will determine the type of learning curve during production.

20. Systems Management and Data Management - A brief description of the System Management role and characterization of the CDRL items are required.

21. Platform is the variable that controls the environmental, reliability, impact and application impact on the design.

The PRICE outputs are development costs (including prototype builds) and unit production costs based on the total quantity in the build. Table 6.2 summarizes the costs for the two approaches. The slightly higher cost for the ring is because the redundant receiver costs slightly more than the echo check card in the star approach. This price differential is judged to be smaller than the accuracy of the pricing methods, leading to the conclusion that there is no significant difference in cost between the two approaches.

Table 6.2. PRICE Summary

50 Systems
32 BIU's/System
2 Gateway BIU's/System

	Star	Ring
Development	$1880K	$1765K
Average Recurring/System	$1243K	$1282K
Average Recurring/BIU	$ 37K	$ 38K

7.0 ARCHITECTURE TRADEOFFS

This discussion centers on the results of the previous sections of this study report. The discussion outlined in the early sections of this report centered on the basic network and component parameters that could be achieved. Later sections selected tentative network configurations that could meet the network performance requirements. These tentative candidates are then further analyzed to ascertain the advantages and disadvantages of each.

Section 3.0 addressed the baseline receiver performance achievable and the various optical components available and their parameters. Tentative component selections were made based on performance comparisons within component groups.

Section 4.0 addressed architecture available to meet the requirements of the AN/GYQ-21(V) assumed configuration. Tentative selection of the interlaced ring and star networks was made, and protocols and modulation formats to support each of these candidate networks for further evaluation were made.

Section 5.0 presented arguments that both the interlaced ring and passive transmissive star approaches will meet the 21(V) program requirements and are both satisfactory solutions in terms of data integrity and reliability.

Section 6.0 presented a costing exercise from which our conclusion is that there is no discernable difference in cost between the two approaches.

Other criteria should be examined before choosing a final solution. These additional criteria are flexibility, expandability, and development risk.

The flexibility metric indicates the responsiveness of the approach to changes in requirements. Such changes might include alteration of access protocols to allow higher priority for some classes of users, thus permitting them to operate at higher throughputs and lower latency times than lower priority devices. It may be desirable to power down all BIU's with attached devices which are not required at any particular time, or to remove or add BIU's without even momentary traffic disruption. In all such situations, the star approach appears more flexible than the ring.

Expandability is a measure of the difficulty (and thus expense) of accommodating an increasing number of users beyond the initial system requirements. In all approaches, such expansion must be anticipated by oversizing many parameters such as the number of bits in the address fields used to address the BIU's on the bus. Such oversizing of these parameters is normally done as a matter of course, and usually does not incur significant cost increases in the basic design.

There is no theoretical limit to the ultimate size of a ring, although there are practical limitations. Beyond a certain expansion point, reliability of a ring will degrade, and timing problems will be encountered in tandeming so many clock recovery circuits. The ring approach may, of course, be expanded beyond this practical limits through the use of multiple rings connected by store-and-forward gateways.

Expansion of the star network is straightforward until the capacity of the star coupler is reached. After this, expansion requires gateways or central switching complexes. The current practical limit for the star is 32 BIU's, and this is believed to be sufficient for the majority of 21(V) systems presently. Expansion beyond 32 is anticipated to be feasible in the future through substitution of larger star couplers as they become commercially available. Up to 128 ports per coupler with acceptable losses appear reasonable in the not-too-distant future. This number probably exceeds the practical limit for the size of a ring. The conclusion here is that the star and ring approaches will offer comparable expandability for future 21(V) systems.

The final evaluation criterion is development risk. The ring approach is judged as presenting very minimal risk. Coaxial ring systems based on control token have been operational for years, and commercial products based on this principle are available. The fiber-optic links for the ring are straightforward and present very minimal risk in receiver design.

The star approach presently presents a larger risk in terms of receiver design and star coupler performance. This risk is expected to decrease in the future as more experience is gained in the manufacture and use of star couplers. The feasibility of the star approach has already been demonstrated in the laboratory, and it is inevitable that the above mentioned risks will subside within one to three years.

Table 7.0 summarizes the results of Sections 5.0, 6.0, and 7.0.

Table 7.0. Comparison of Interlaced Ring and Star Approaches

Criterion	Preferred Approach
Throughput	No preference
Reliability	Star
Data Integrity	No preference
Relative Cost	No preference
Flexibility	Star
Expandibility	No preference
Design Risk	Ring

The conclusion is that if the development phase for a 21(V) fiber-optic network were to begin immediately, the ring would be preferred based on low development risk. This conclusion is expected to be reversed, however, within one to three years as experience is gained with star-coupled networks. At that time, the star would become the preferred architecture based on its superior flexibility.

8.0 DESIGN SUMMARY

The design requirements to meet the performance requirements of the AN/GYQ-21(V) are summarized in the following paragraphs. A brief summary of the system performance requirements is presented to outline the design requirements. Following the system performance requirements is a review of each of the elements required in the approach, including the BIU, the fiber-optic receiver and transmitter, the fiber-optic cable, connectors, and any couplers. Following the review of the elements of the approach is a synopsis of the interfaces required. A brief review of the advantages offered by the fiber-optic data bus and an incremental program outline complete this discussion.

8.1 System Performance Requirements

The number of distinct configurations of the AN/GYQ-21(V) is quite large. For purposes of performance requirements, a baseline network configuration was assumed. The baseline configuration was predicated on a maximum terminal-to-terminal separation of 1000 meters. A peak data rate of 60 Mb/s was assumed with a 50 percent bus efficiency yielding an average throughput rate of 30 Mb/s. An uncorrected bit error rate of $\leq 1 \times 10^{-9}$ was used as a design criteria. The nominal maximum number of terminals of 128 was assumed, grouped in clusters of no more than 32. Clusters are interconnected by gateway repeaters to achieve expansion capability.

Any link may have between zero and two in-line connectors, in addition to connectors for input and output from the Bus Interface Unit (BIU). The total number of connectors for interlaced ring networks can vary from two to four connectors. For the star network, the number of connectors can vary from four to six. A temperature environment of 0 to 50^{o} C was assumed, consistent with the temperature range anticipated for a computer environment.

8.2 Elements of the Approach

The elements of the fiber-optic bus and interface equipment are examined in the paragraphs below. The various elements include the BIU, the fiber-optic cable, the connectors, any couplers used, and the various interfaces. A discussion of fiber-optic receivers and transmitters is also presented. The interface discussion includes both the UNIBUS interface and the optical data formats on the fiber-optic waveguide.

8.2.1 Network Concepts

The proposed fiber-optic bus provides a common high-speed "data highway" for intercommunication of processors and peripherals within a 21(V) configuration. A processor or group of peripherals interfaces to this fiber-optic bus via a Bus Interface Unit (BIU). The BIU is an intelligent programmable machine which makes the operation of the fiber-optic bus transparent to the attached device. Data is transmitted between BIU's on the fiber-optic bus in the form of packets. A packet generally corresponds to a physical record such as a card image or disk sector.

Current AN/GYQ-21(V) systems employ a significant amount of peripheral sharing among multiple processors, as well as interprocessor communications. Devices such as the DEC UNIBUS switch, UNIBUS window, and UNIBUS link are used for these purposes. The UNIBUS switch is essentially a circuit-switched device which allows a peripheral or group of peripherals to be connected to the UNIBUS of one of two processors.

The bursty nature of computer traffic makes packet switching a natural and efficient means for resource sharing. Packet-switched communications between processors in a long haul network (such as ARPANET) is a well-established procedure. High-speed packet-switched communications between processors and peripherals on a local basis has become feasible within recent years due to decreasing digital component costs and to network design innovation.

Such an interconnection of processors and peripherals has been termed a Local Area Computer Network. The network architecture recommended for near-term development is that of a ring in which BIU's are connected in a closed loop with simple point-to-point fiber-optics between BIU's. Each BIU has the capability to pass the information it receives, or "break" the ring to transmit its own message. A passive optical bypass in each BIU allows ring operation to continue if a BIU fails.

8.2.1.1 Bus Control

BIU's achieve bus mastership via a distributed control mechanism known as the control token method. This approach has received widespread acceptance in industry as evidenced by several experimental ring systems, the PRIME Computer product Ringnet, and the inclusion of Control Token in the evolving IEEE Local Area Network Standard.

A control token is passed sequentially around the ring. Upon receiving the token, a BIU intending to transmit a message must modify the token to make it a message separator, transmit the message, and place a new token after the transmitted message. The initial generation of the token, as well as deletion of spurious tokens, is a cooperative effort among the BIU's.

The control token is identical to the flag character used in bit-oriented protocols (01111110). The message separator (01111111) is formed by inverting the last bit of the token, thus requiring only one bit of delay through a BIU. Zero-insertion logic prevents these two bit patterns from occurring randomly in the data stream.

8.2.1.2 Formats and Protocol

Data is transmitted from a source BIU to a destination in the form of packets. Generally, a packet will have a one-to-one correspondence with a physical record such as a card image, one line entered on a CRT, or a disk sector. An average packet length for a computer system such as the AN/GYQ-21(V) is 1000 bits. This packet communication is necessary because of the relatively long distances encountered in the expanded network.

Bit-oriented protocols such as ADCCP, HDLC, and SDLC are preferred for such a packet-switched network. They are much more efficient than older byte-oriented protocols, and can work in synergism with the control token access method. There are only minor differences between these three protocols; ADCCP, the ANSI standard, is assumed for incorporation into the ring network.

A modification to the usual ADCCP protocol is the inclusion of the source address. The resulting format of a packet is: message separator, source address, destination address, sequence number, data, CRC, and control token (or message separator). Each packet transmitted by a source must receive a positive acknowledgement from the destination before another packet is transmitted. A negative acknowledgement or a timeout results in retransmission of a packet.

8.2.1.3 BIU Implementation

The BIU design is depicted in Figure 8.2.1.3. The BIU "front-end" interfaces to the fiber-optic bus. This front-end implements the fiber-optic transmit and receive functions, as well as the access-control mechanism and the lowest levels of the ADCCP protocol. The BIU "back-end" is based around a DEC PDP-11/04 processor. This processor performs the higher levels of the ADCCP protocol and executes the device control software for the attached peripherals.

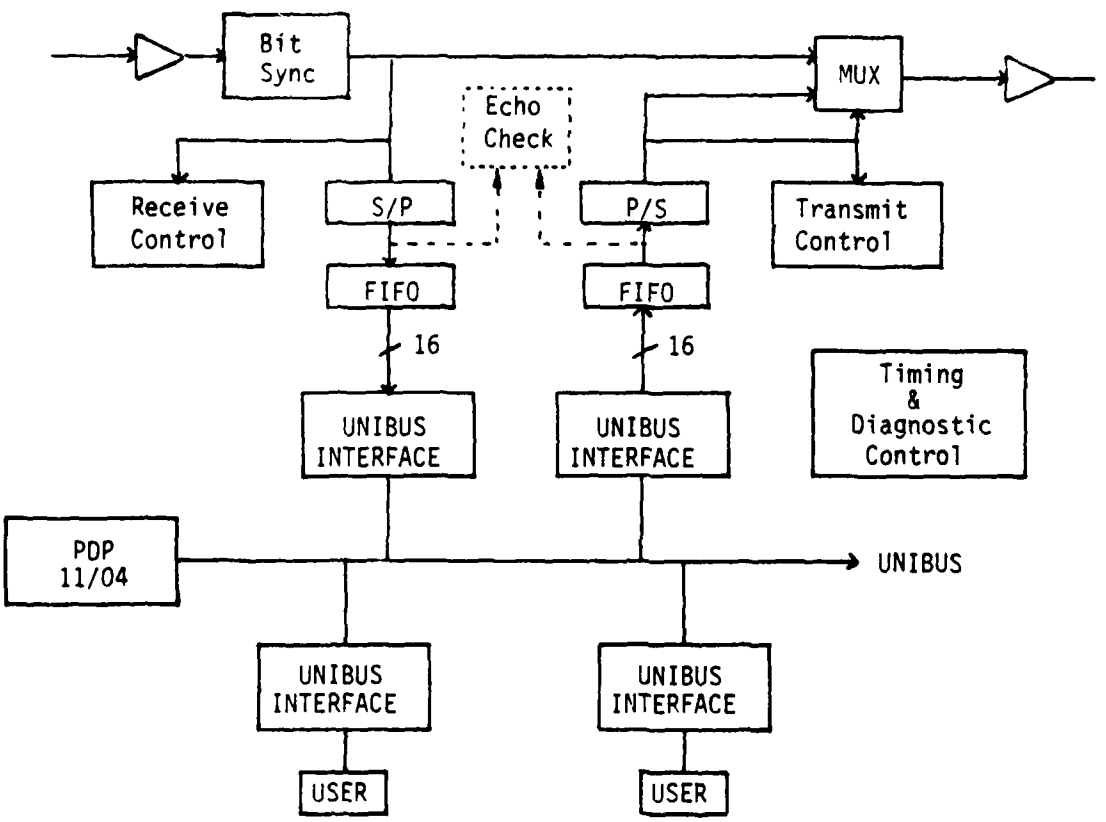

Figure 8.2.1.3. BIU Block Diagram

Peripherals such as card readers, line printers, CRT's, etc., with UNIBUS interfaces are remoted by unplugging them from the AN/GYQ-21(V) mainframes, and plugging them into a UNIBUS slot in the BIU's 11/04 processor. Thus, a single BIU can service a single fast peripheral (such as a disk drive) or several slow peripherals (such as card readers and CRT's).

The UNIBUS connection to a processor will be referred to as an active UNIBUS port, while the UNIBUS interface to a peripheral will be referred to as a passive UNIBUS port. The UNIBUS connection to the BIU's 11/04 provides an active port to which several passive ports (peripherals) can be tied. The BIU which connects one of the main processors to the network must contain a special interface to connect the 21(V)'s active port to the 11/04's active port. This interface contains a high-speed RAM buffer through which the two processor's communicate.

8.2.2 An Example

As an example of retrofitting a 21(V) system, consider the CMOSS Standard Configuration of Figure 8.2.2-1. The four 11/45 processors each have dedicated disk drives, tape units, and programmer consoles (DL-11). The two top processors share a bank of peripherals (card reader, line printer, and tape drives) via a DT07 UNIBUS switch. Additionally, these two processors share a bank of disk drives through the use of dual ports and dual interfaces. The same configurations can be seen in the bottom two processors. Finally, communications among the four processors is accomplished via the DA-11 devices. Separation of these peripherals and processors is limited, and peripheral sharing and interprocessor communications lack flexibility.

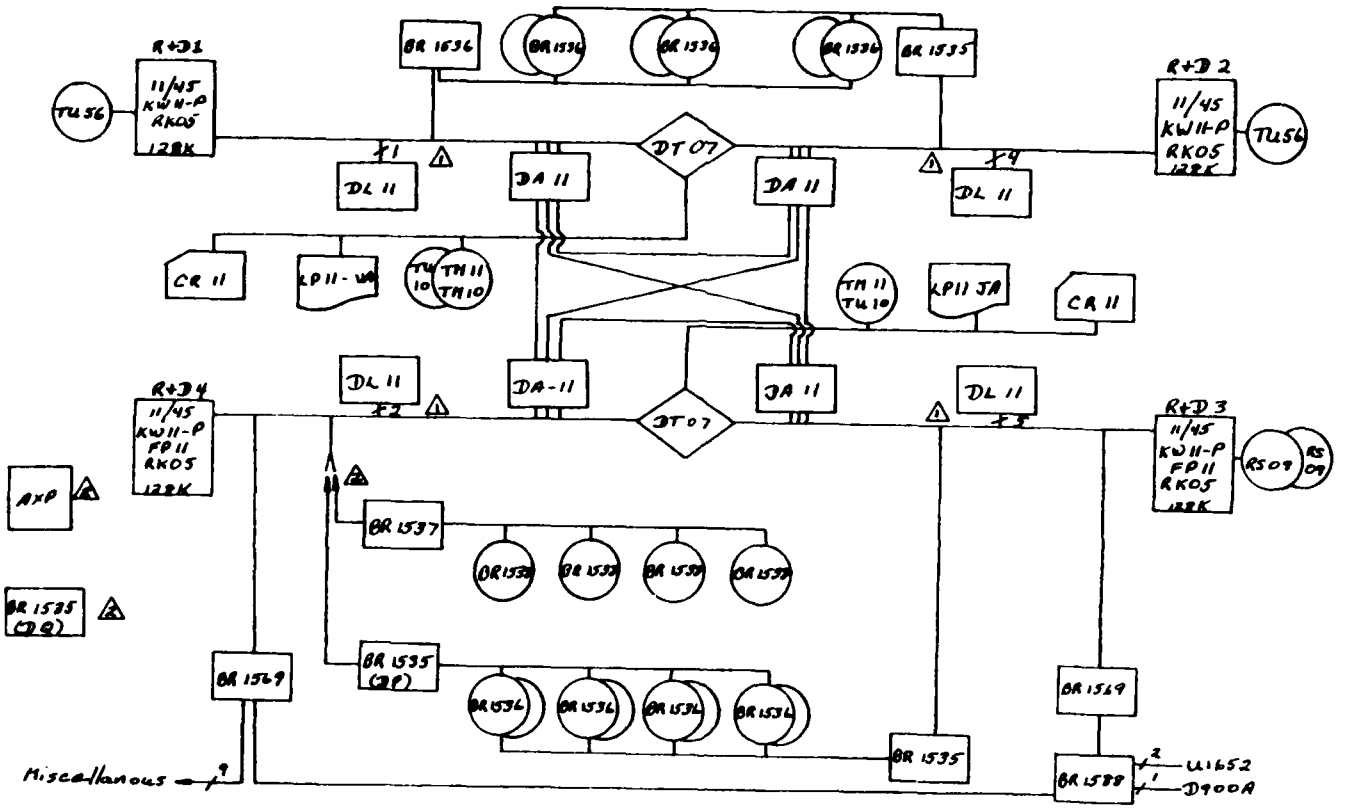

⚠ The number of DL11 interfaces represents the number of programmer consoles on the system.

⚠ Items noted indicate hardware not normally connected but available for incorporation to support special configurations.

Figure 8.2.2-1. CMOSS Standard Configuration

Figure 8.2.2-2 shows the CMOSS configuration retrofitted with a ring-coupled fiber-optic bus. This is only an example of many possible strategies. Each processor is shown retaining some peripherals on its local UNIBUS, although these peripherals could be remoted if desired. Devices have been placed on BIU's according to a general rule that a BIU can control one high-speed device (such as a processor) or several low-speed devices (such as consoles or card readers). The clusters of devices enclosed by dashed lines are typical of remote stations at which one may initiate jobs, input programs via cards, receive listings, and backup programs on magnetic tape. Any peripheral or group of peripherals attached to a BIU may be operated with one of the four 11/45 processors.

Distances up to one kilometer may be achieved between BIU's, allowing considerable freedom of device separation. Expandability in a ring configuration is accomplished simply by unplugging the fiber-optic cable from a BIU, and inserting a new BIU in series, or small rings may be connected via store-and-forward gateways.

8.2.3 Fiber-Optic Receiver Performance

The fiber-optic receiver performance is predicated on the use of an avalanche photodiode detector (APD) with the gain set at ~100, which is maintainable over a temperature range of 0 to 50^{o} C by varying the bias voltage from ~205 V to ~240 V, using an RCA C30902E APD. Given a gain of 100, the receiver is predicted to have an input referred noise current spectral density of $\leq 5 \times 10^{-12}$ A/$\sqrt{Hz}$, employing a 3-pole low-pass filter to bandlimit the noise. A 3-pole Bessel filter characteristic was assumed for the report, although comparable performance may be obtained with the Butterworth filter characteristic, or with some of the "transitional" filter characteristics.

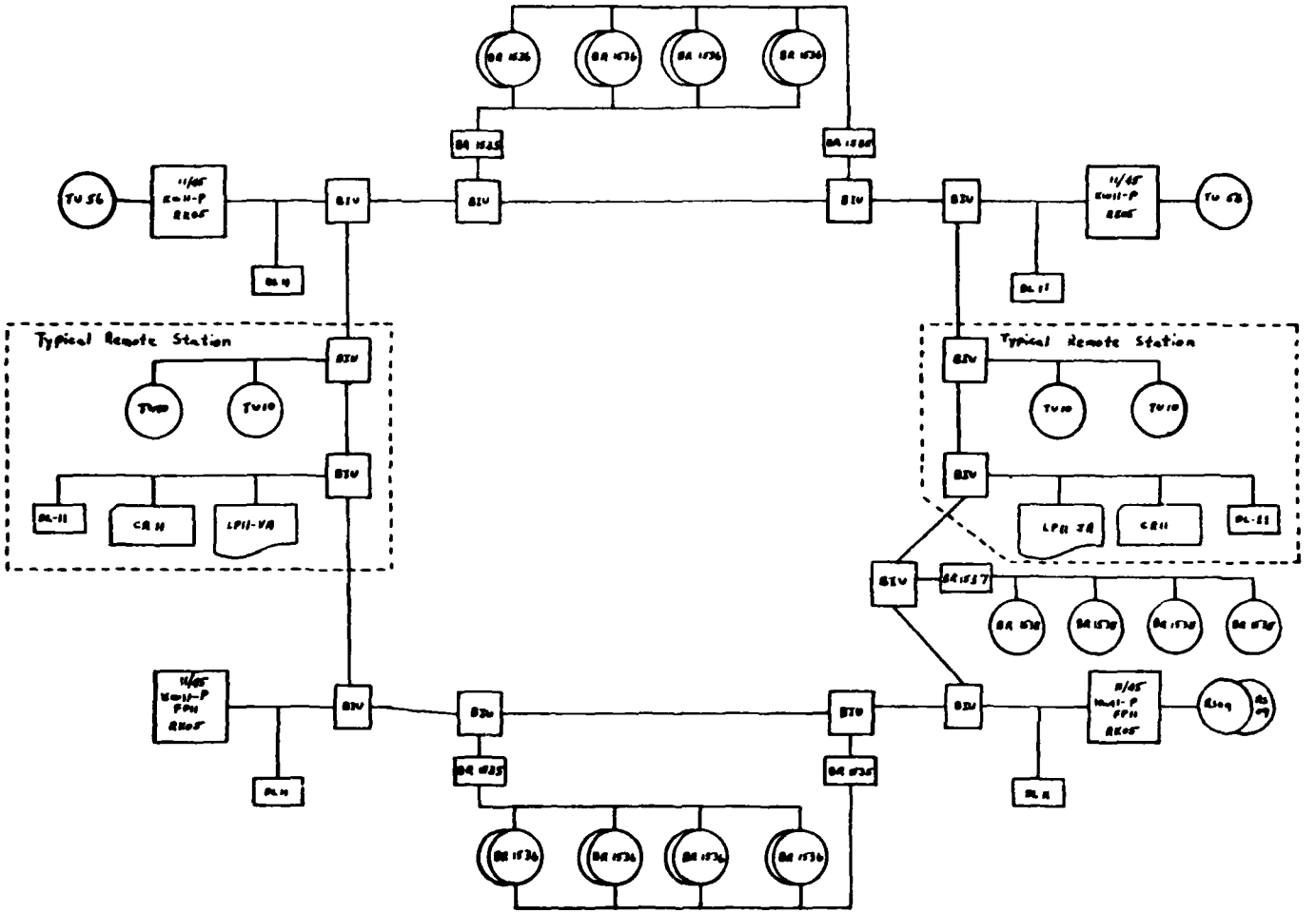

Figure 8.2.2-2. CMOSS Configuration Employing Ring Bus Topology

With the noise current spectral density assumed, the required optical power predicted at a data rate of 60 Mb/s (assuming 2 bit/Hertz encoding) is 3.6 nanowatts (nW), or -54.5 dBm, using equation (13) and assuming a JFET input transistor, per Figure 3.1.2.2-1. At this optical power input level for a "ONE" bit, a bit error rate of $\leq 1 \times 10^{-9}$ will be achieved, using a minimum responsivity (unity gain) of 0.5 Amperes/Watt (of optical power) for the photodetector. An excess noise factor of $G^{0.3}$ for the avalanche photodiode was assumed.

The achieving of this performance from the receiver assumes an optimized receiver, i.e., the noise bandwidth is set properly, the card layout of the receiver minimizes stray capacitance at the input of the receiver, the gain of the APD is well controlled, and the temperature is properly maintained. Inattention to these layout and design criteria will degrade the receiver performance rapidly from this minimum optical power requirement.

The receiver performance could be improved if the requirements were not to operate in a data bus environment. If the receiver were to see a constant data stream from a single transmitter, the noise bandwidth could be reduced to lower the noise floor, and with a constant signal-to-noise ratio, the signal can be reduced also. For a data bus environment, however, the receiver sees a range of input signals, and data arriving in bursts or packets. For a ring network, the receiver "sees" only two transmitters (primary and alternate). For a star network, the receiver "sees" all the transmitters in a cluster, imposing a intermessage dynamic range.

Setting the noise bandwidth at 0.5 times the bit rate allows the intermessage dynamic range of ~20 dB to be accommodated by the receiver without special design measures. Some design room thus exists to improve the receiver sensitivity for the ring network, as well as for the star network.

Summarizing the receiver performance criteria, a JFET trans-impedance preamplifier design using an avalance photodiode with a gain of 20 and a 3-pole low-pass filter set at 0.5 times the bit rate meets the receiver design requirements. Again, 20 to 100 can be used by the APD to set the receiver sensitivity between 6.9 and 3.6 nW.

8.2.4 Fiber-Optic Transmitter Performance

The fiber-optic transmitter used in the AN/GYQ-21(V) data bus application can be implemented with either a light emitting diode (LED) or an injection laser diode (ILD) optical source. The use of an ILD requires an increased transmitter complexity due to the requirement for optical feedback and (potentially) thermoelectric cooling to preclude thermal runaway of the source and consequent destruction. The use of a light emitting diode reduces the amount of available optical power coupled into the fiber, but the worst case link for either the interlaced ring network or the passive star remains feasible.

The use of an ILD not only requires some increase in the transmitter complexity, but also requires the receiver design to allow for the "laser noise" phenomena discussed in Paragraph 3.2.3. The recommended emitter for this application is a high radiance Burrus structure LED. The available devices meeting the source coupled power requirements are:

- Northern Telecomm NT 40-3-15-2
- Plessey HR982F
- Laser Diode Laboratories IRE161
- RCA C30133
- Plessey (Developmental) C0045

Of the available devices, the Plessey C0045 offers coupled powers near those attainable with ILD sources. Reliability data of this device is anticipated to be comparable with high reliability ILD sources. The source coupled power attainable from these devices allow a link margin for the star coupled network ranging from 4.9 to 11.8 dB and a link margin from 24.5 to 32.8 dB for the interlaced ring.

The transmitter design is predicated on full band optical pulses from the LED using NRZ data. All optical sources are assumed to be coupled into a 100 μm core "quasi-step" index fiber having a numerical aperture of 0.3. As in the case of the receiver, the transmitter environment is anticipated to be benign with temperatures not exceeding the 0 to 50^{o} C range. High temperatures exceeding this range will proportionately reduce the source coupled power available.

The data rate output from the transmitter is a maximum of 60 Mb/s, corresponding to a maximum bit period of $\geq$30 ns. Source rise and fall times are less than this bit period, assuring the source achieves maximum output power during the bit period. Special charge injection or sweep-out circuitry is not anticipated for the transmitter at these data rates (bit periods), based on the sources selected as candidates. The drive circuitry for the transmitter is anticipated to be Emitter Coupled Logic (ECL) combined with discrete transistors as the actual source drivers.

8.2.5 Fiber-Optic Cable

The fiber-optic cable selection criteria for the application were fiber bandwidth and large numerical aperture. The large numerical aperture (~0.3) allows substantially greater amounts of power to be coupled into the fiber by LED sources ($\leq$2.25 times greater than graded index fibers). This selection criteria yields two candidate fibers, which are available in cable form from several companies:

- Corning Short Distance Fiber (SDF) Type 1505
- Galite Type 5050

The Corning SDF fiber is available in cabled form from several companies, including Belden, Valtec, Siecor, and others. Galite Type 5050 is available from Galite. Some screening of both cables may be necessary to achieve the fiber bandwidth, since the data sheets indicate a "typical" bandwidth-length product of 50 MHz-km, but a "minimum" bandwidth-length product of $\sim$25 MHz-km.

Fiber loss for the network was set at a maximum of $\leq$8 dB/km, which is above that specified for both Galite and Corning, which specify a loss of 7 dB/km. If low temperature operation of the system is anticipated ($\leq 20^{0}$ C), the link margin may be degraded due to additional temperature induced fiber losses. This additional loss is predicted to be minimal for glass-on-glass fibers selected.

8.2.6 Fiber-Optic Connectors and Couplers

The fiber-optic connectors recommended for this network are either the Hughes 2-fiber connector or the Amphenol 801/906 connectors. The connector loss for the network (per connector) is set at a maximum of 2 dB per connector. The connector must accommodate the fiber selected (140 μm cladding diameter) and be sufficiently rugged to withstand repeated mating/unmating cycles.

The Hughes connector has a lower reported nominal loss than the Amphenol connector and would be initially selected. New connectors introduced into the marketplace may improve on these quoted losses and this initial selection may vary with time.

8.3 Interfaces

The introduction of a fiber-optic data bus to support a distributed AN/GYQ-21(V) system has two interfaces. The electrical interface seen by the user at the BIU UNIBUS® is identical to that interface now used. No changes are required in the application software to incorporate the fiber-optic data bus. A replacement of the existing channel extender with the fiber-optic BIU is accomplished by standard ribbon cable interface.

The optical interface on the bus side of the BIU is a standard 2-fiber interface accomplished at the BIU. The receiver design is capable of handling a sufficiently large dynamic range such that no "optical pads" (or attenuators) are required to interface the fiber-optic bus, i.e., custom engineering of each installation is not required. The PDP-11/04 assumed as part of the BIU is programmed to function as a standard BIU, or in the case of large networks, as a gateway between clusters.

8.4 Advantages

The use of a fiber-optic data bus to support a distributed AN/GYQ-21(V) offers a substantial operational advantage over a metallic implementation of the same system. The current "channel extender" operates at a maximum line rate of 50 kb/s. Remote locations for disk storage facilities, interactive graphic video terminals, and additional processors are severely limited since data must be buffered and sent at transmission rates much less than the access rates available.

The implementation of multiprocessor systems is also hampered by the lack of high-speed interprocessor communications. The use of a fiber-optic data bus allows a group of terminals to be clustered at distances of up to 1 km from the main processor without long delays between the request for processing time and the receipt of processed data.

Achieving a comparable data bus with a metallic cable system would require either RG-318/U or RG-319/U of diameter 2.2 cm or 4.1 cm, respectively. The use of these high quality coaxial cables would increase the volume requirements for shipment by a factor of 12:1 to 41.7:1 over a 0.64 cm diameter fiber cable. Simultaneously, the fiber cable offers superior handling qualities in terms of ruggedization, temperature performance, and installation, as well as lower weight.

For protected (physically secured) deployment areas, the fiber cable can be employed without the requirement for encryption devices, while metallic cables must either have encryption equipment or be placed in conduit that has been tested for suppression of radiated electromagnetic energy not normally accomplished in a tactical deployment situation.

Since the fiber-optic BIU unit electrical interface is a UNIBUS® physical interface, no changes to the equipment cluster attracted to a remote BIU is necessary; the fiber-optic data bus becomes transparent to the network, except for transit time delays. The fiber-optic data bus thus offers employment advantages in addition to weight and bulk savings over the equivalent metallic implementation.

8.5 Incremental Program Outline

To achieve a fiber-optic data bus implementation to improve the AN/GYQ-21(V) operational capabilities, a two-phase program is outlined. The first phase of the program is to fabricate a set of prototype BIU equipment. This phase would also include the integration of the PDP-11/04 (and associated software) such that the UNIBUS® interface is preserved and software within the current systems remain intact. The second phase of the program is the selection of a test bed and operational/development testing of the prototype equipment in the test bed.

The first phase of the program is anticipated to be 18 to 24 months in length, followed by 6 months of testing for the second phase. On completion of the testing, a 3 month analysis of the test results minimizes the program risk in application of the fiber-optic data bus to other systems. The total of the two phases of the implementation program is then 27 to 33 months in length.

APPENDIX A

FIBER-OPTIC STAR COUPLER INVESTIGATION

A.0 FIBER-OPTIC STAR COUPLER INVESTIGATION

Optical fiber is an attractive transmission medium for use in data buses and signal processing networks because of its low loss, broad bandwidth, and immunity to electromagnetic interference. The two commonly considered fiber-optic data distribution systems are the star coupled system and the T-coupled networks. Practically, the semi-star couplers and T-coupler are also the essential components for any wavelength division multiplexer/demultiplexer and signal transmission system employing duplex transmission over a single fiber.

The fabrication and performance of the directional T-coupler may be considered as a special case of the transmissive directional star coupler. The star configuration of data distribution possesses several advantages over the serial configuration in terms of reduced connector losses and dynamic range. In light of these factors, the investigation of star couplers became an objective in the AN/GYQ-21(V) data bus study.

A.1 Existing Star Couplers and Performance

Several types of fiber-optic star couplers have been reported using fused tapered (biconical) fibers, a mixing rod, graded-index rod lenses, (an angular scrambling of rod for brevity) and a kaleidoscope rod. Either a transmissive or a reflective star coupler can be fabricated from the fused tapered fibers configuration or from the mixing rod approach. The mixing rod star coupler has disadvantages of larger implementation loss and poor distribution uniformity. The kaleidoscope transmissive star coupler has low insertion loss (0.8 dB), good temperature stability (0.3 dB of coupling loss changes from -25^{o} C to 50^{o} C), and fabrication simplicity; however, it is difficult to implement more than 8-ports. By contrast, the biconically tapered fiber-optic star couplers with more than 100 ports is

realizable if the fabrication is well controlled. A 100 fiber channel star coupler has been fabricated and demonstrated by Rawson and Bailey[1] with excess insertion losses of 0.56 dB and normalized standard deviations of output power of 4.4 percent (0.2 dB).

Table A.1 summarizes the performance of different reported star couplers for fiber-optic data bus applications. The excess insertion loss of these couplers are the best insertion loss achieved. Presently, the coupler fabrication quality control still has difficulties. For instance, the 100-port couplers have insertion losses varing from 0.56 to 2.4 dB with statistical mean of 1.5 dB loss at six samples.

Table A.1. Reported Star-Couplers for Fiber-Optic Applications

Configuration	Number of Port	Best Insertion Loss (dB)	Reporting Country and Year
3-Rod Guided	3	0.5	USA 1977
	7	0.5	USA 1977
Kaleidoscope	4	0.8	Japan 1980
	8	2.2	Japan 1980
Bitaper (Transmissive)	100	0.56	USA 1979
Bitaper (Transmissive)	19	1.6	USA 1978
Bitaper	8 100 (realizable)	0.66	Canada 1979
Bitaper (Transmissive)	4	2.0	Canada 1976
Mixing Rod (Transmissive)	4	0.5	USA 1977

[1] E.G. Rawson and M.D. Bailey, "Bitaper Star Couplers with up to 100 Fiber Channels," Elect. Lett. 5th July 1979, pp 432-433.

A.2 Biconical Star Directional Coupler

Both fusing and adhesion techniques have been utilized to fabricate the multi-port directional star couplers. To make a coupler using adhesive approach, the biconical tapers are fabricated by pulling and then joining side-by-side by a clear optical adhesive (Aremo Crystalbond 509). The surface tension of adhesive before hardening draws the individual fibers together and causes the adhesive to form a smooth surfaced layer that fills the spaces between the biconical tapers. Unlike the stripped-cladding directional coupler which uses the cladding modes, the biconical star coupler converts the propagating modes at the taper section into radiating modes. The radiated light is launched preferentially into the adhesive since it has a higher refractive index than the surrounding material (air). This light is then guided by the taper sections of the coupler. The fabrication process of this adhesive approach requires a precision assembly skills and long curing time. Recently, a fusing technique was introduced to fabricate biconical tapered couplers and this report deals with this method.

A.3 Fabrication Method of Biconical Star Coupler using Thermally Fusing Technique

A number if different fiber types were tried, including 50 μm fused silica. Ultimately, (for handling ease and best performance) the fused silica fibers supplied by Valtec, Incorporated were chosen. These fibers are of the multimode graded index type. The first step in the process is to cut the fiber into appropriate lengths then strip the protective silicone jacketing from the fiber in the region to be tapered and fused using a hot sulfuric acid bath. These bare fibers are then inserted through special fiber holders spaced two inches apart and retained in a fixture of our design. With one of the holders held in a fixed position, the other was rotated 1-3/4 turns to give a tightly packed twisted section in the center of the bundle (Figure 5). The fibers were then cemented to the holders using photopolymer adhesive (NOA-61) which was cured for five to seven minutes under a 350 watt ultraviolet light source. This adhesive was

chosen because its refractive index provides a cladding mode stripping action at the input and output ends of the star. Once fixed in place, the twisted fiber bundle was heated to fusing temperature using an Oxy/Butane Micro-Torch and specially adapted tip for minimum flame dispersion. After the fibers had softened, one of the fiber holders was pulled axially and rotated in the direction of the twisted section to provide the biconical taper. The rotational motion was necessary to preclude air bubbles in the fused section. Once the fused taper was achieved, it was heated again from all sides to insure a uniform melt. The fiber holders were then fixed to their aluminum carrier with quick set epoxy to add rigidity to the assembly.

A.4 Star Coupler Measurement and Measurement Parameter Definition

Each fiber end of the star coupler had been cleaved before the measurement. All power measurements were performed using a Spectra-Physics model 120 He-Ne laser in conjunction with a precision 3 axis adjustment and 40X microscope objective to focus the beam and launch as many modes as possible into the fiber. Output power was measured with a Coherent Radiation model 212 Optical power meter and corresponding power sensor. An adapter designed by Harris was used to exclude all ambient light from the power sensor suring the measurement procedure. Both input and output cladding modes were stripped by passing the fiber through matching fluid reservoirs which absorbed the light energy of cladding modes.

It is debatable whether the removal of cladding modes is necessary. The cladding light energy is useful for many short-distance data bus or communication applications, and in may cases the cladding modes should not be removed.

Before the measurement results are presented, some measurement parameters are needed to be defined as follows:

- Excess insertion loss (db)

$$= 10 \log \sum_{i-1}^{n} (P_i/I_j)$$

Where P_i = the power coupled from output port i
I_j = power coupled into input port j
n = the number of ports (input or output)

- Coupling ratio, C_{ij}, in percent (%)
  Where C_{ij} = fraction of power coupled from port j to port i

- C_o = average coupling ratio

- The uniformity of the star coupler is the dispersion in coupling ratios

$$\Lambda = \left[\frac{1}{n-1} \sum_{i=1}^{n} (C_{ij} - C_o)^2 \right]^{1/2}$$

- Standard deviation, $\left(100 \times \frac{\Lambda}{C_o}\right)$ expressed as a percentage

A.5 Measurement Results

Two ten fiber stars have been successfully fabricated using the previously mentioned techniques and fully characterized. All of the techniques used are step-by-step refinements of earlier concepts which failed to produce the desired result. Actually, 28 stars were fashioned but problem areas had to be overcome along the way. Results of the evaluations to data are presented in matrix format on Table A.5-1 and Table A.5-2. The power input data was taken just prior to fusing the fibers.

Table A.5-1. Coupler F Loss Characterization

COUPLER "F" INPUT POWER IS 3.0 mW ALL CASES

	1	2	3	4	5	6	7	8	9	10	Average Insert Loss
Input Number	P_{out}*	P_{out}*	P_{out}*	P_{out}*	P_{out}*	P_{out}*	P_{out}*	P_{out}*	P_{out}*	P_{out}*	dB
1	140	160	200	160	190	155	145	150	170	190	12.5
2	147	152	175	146	176	165	147	200	137	141	12.77
3	170	170	159	164	125	133	157	143	162	145	12.96
4	BROKEN AT INPUT										
5	100	130	175	180	280	160	110	182	195	180	12.49
6	164	155	164	161	129	186	191	151	163	154	12.68
7	165	205	270	170	170	210	150	190	240	220	11.78
8	BROKEN AT INPUT										
9	145	175	210	270	260	230	110	170	110	141	12.3
10	190	150	188	164	169	145	184	159	155	171	12.54

* All power outputs in microwatts

Table A.5-2. Coupler G Loss Characterization

COUPLER "G" INPUT POWER IS 3.0 mW ALL CASES

	1	2	3	4	5	6	7	8	9	10	Average Insert Loss (dB)
Input Number	P_{out}*	P_{out}*	P_{out}*	P_{out}*	P_{out}*	P_{out}*	P_{out}*	P_{out}*	P_{out}*	P_{out}*	dB
1	125	170	90	110	175	150	160	150	160	170	13.12
2	130	235	290	250	200	230	160	270	180	220	11.4
3	340	160	105	170	155	190	245	220	285	230	11.5
4	120	580	110	220	190	240	190	390	180	200	10.93
5	110	160	110	500	180	180	180	220	190	220	11.65
6	195	195	195	350	155	140	290	123	175	240	11.63
7	BROKEN AT INPUT										
8	120	160	120	140	170	150	125	200	125	215	12.9
9	100	195	185	190	145	190	135	120	115	190	12.8
10	BROKEN AT INPUT										

*All power outputs in microwatts.

A.6 Discussion of Biconical Star Coupler Excess Loss Mechanisms

To improve the future biconical star coupler performance, one must understand the loss mechanisms and then minimize them. The excess insertion loss of the coupler may be caused by the following possible factors:

- Energy transfer loss: The light energy transfer from propagation modes to radiation modes and vice versa in the tapered sections due to changes of size, reflection index, and core/cladding configuration.

- Radiation: The light energy radiates into the surrounding medium (such as air or packaging material) from the tapered section.

- Scattering: caused by

  - air bubbles

  - irregular shape of tapered sections

  - impurities or nonuniformity of the glass in the taper section

  - reflection index mismatching.

- Reflection

- Absorption: OH molecules and other impurities are introduced into the coupling during the fusing process. OH modecules are the major source of absorption loss.

- Mode of coupling loss.

- Numerical aperture changes.

- Bending and microbending loss due to fiber twisting.

Reviewing these possible loss mechanisms, a minimum loss can be achieved by:

- Minimize fiber bending or twist

- Smooth tapering

- Fusing process performed in dehumified clean room

- Phase separation of the constituent glasses to retain waveguiding action.

MISSION
of
Rome Air Development Center

RADC plans and executes research, development, test and selected acquisition programs in support of Command, Control Communications and Intelligence (C^3I) activities. Technical and engineering support within areas of technical competence is provided to ESD Program Offices (POs) and other ESD elements. The principal technical mission areas are communications, electromagnetic guidance and control, surveillance of ground and aerospace objects, intelligence data collection and handling, information system technology, ionospheric propagation, solid state sciences, microwave physics and electronic reliability, maintainability and compatibility.

END

DATE
FILMED

1-82

DTIC